Technical Report Documentation Page

1. Report No. FHWA/TX-08/0-5179-1	2. Government Accession No.	3. Recipient's Catalog No.
4. Title and Subtitle DEEP SOIL MIXING TECHNOLOGY FOR MITIGATION OF PAVEMENT ROUGHNESS		5. Report Date October 2007 Published: August 2008 6. Performing Organization Code
7. Author(s) Anand J. Puppala, Raja Sekhar Madhyannapu, Soheil Nazarian, Deren Yuan, and Laureano Hoyos		8. Performing Organization Report No. Report 0-5179-1
9. Performing Organization Name and Address Department of Civil Engineering The University of Texas at Arlington, Arlington, Texas 76019-0308 Department of Civil and Environmental Engineering The University of Texas at El Paso, El Paso, Texas 79968		10. Work Unit No. (TRAIS) 11. Contract or Grant No. Project 0-5179
12. Sponsoring Agency Name and Address Texas Department of Transportation Research and Technology Implementation Office P. O. Box 5080 Austin, Texas 78763-5080		13. Type of Report and Period Covered Technical Report: September 2004 – August 2007 14. Sponsoring Agency Code

15. Supplementary Notes

Project performed in cooperation with the Texas Department of Transportation and the Federal Highway Administration.

Project Title: Deep Mixing Technology for Mitigation of Pavement Roughness
URL: http://tti.tamu.edu/documents/0-5179-1.pdf

16. Abstract

The effectiveness of Deep Soil Mixing (DSM) treatment method was evaluated in terms of reducing heave movements of underlying expansive soils. Several binder types were used to treat expansive soils and these methods are considered in a laboratory investigation to select the appropriate binders for field DSM studies. Laboratory studies indicated that a combined binder treatment approach of using lime and cement was the appropriate method for field studies. Two pilot scale test sections were then designed and installed on DSM soil columns. Anchor rods were used to fasten a biaxial geogrid to the DSM columns. Surcharge equivalent to loads from base and surface layers was placed on top of the DSM-geogrid sections through a fill placement. These treated test sections along with control sections on untreated soils were instrumented and monitored. Monitored results showed that soil shrink-swell related movements and pressures in both vertical and lateral directions were considerably less than those recorded in the untreated soil sections. Non-destructive studies using seismic methods showed the enhancements of shear strength in the treated zones. Overall, this research resulted in the development of a design methodology for stabilizing expansive clayey soils at considerable depths using DSM column treatment.

17. Key Words	18. Distribution Statement
Deep Soil Mixing, Expansive Soils, Transverse Cracking, Longitudinal Cracking, Pavements, Cement, Lime	No restrictions. This document is available to the public through NTIS: National Technical Information Service 5285 Port Royal Road Springfield, Virginia 22161, or http://www.ntis.gov

19. Security Classif.(of this report)	20. Security Classif.(of this page)	21. No. of Pages	22. Price
Unclassified	Unclassified	342	

Form DOT F 1700.7 (8-72) **Reproduction of completed page authorized**

DEEP SOIL MIXING TECHNOLOGY FOR MITIGATION OF PAVEMENT ROUGHNESS

by

Anand J. Puppala, Ph.D., P.E.
Professor

Raja Sekhar Madhyannapu
Graduate Research Assistant

Department of Civil Engineering
The University of Texas at Arlington, Arlington, Texas 76019

Soheil Nazarian, Ph.D., P.E.
Professor

Deren Yuan, Ph.D.
Research Engineer

Department of Civil and Environmental Engineering
University of Texas at El Paso, El Paso, Texas 79968

and

Laureano R. Hoyos, Ph.D., P.E.
Associate Professor

Department of Civil Engineering
The University of Texas at Arlington, Arlington, Texas 76019

Technical Report 0-5179-1
Project Number 0-5179
Project Title: Deep Mixing Technology for Mitigation of Pavement Roughness

Performed in cooperation with the
Texas Department of Transportation
and the Federal Highway Administration

October 2007
Published: August 2008

The University of Texas at Arlington
Arlington, Texas 76019-0308

DISCLAIMER

The contents of this report reflect the views of the authors, who are responsible for the facts and the accuracy of the data presented herein. The contents do not necessarily reflect the official view or policies of the Federal Highway Administration (FHWA) or the Texas Department of Transportation (TxDOT). This report does not constitute a standard, specification, or regulation. The researcher in charge was Anand J. Puppala, P.E., Department of Civil and Environmental Engineering, The University of Texas at Arlington, Arlington, Texas.

ACKNOWLEDGMENTS

This project is currently being conducted in cooperation with TxDOT and FHWA. The authors would like to acknowledge Mr. David Head, P.E. (Project Coordinator); Mr. Richard Williammee, P.E., Project Director (Project Director); Dr. German Claros, P.E.; Mr. Stanley Yin, P.E.; and Dr. Zhiming Si, P.E., TxDOT for their interest and support of this study. The authors would also like to acknowledge the assistance of the TxDOT Fort Worth District personnel for their help in the construction of test sections.

EXECUTIVE SUMMARY

Expansive soils are well known for their cyclic shrink-swell behavior due to seasonal moisture changes. These cyclic movements of expansive soils are due to physico-chemical changes at particle level that are dependent on mineralogical composition of these soils. The soil depths susceptible to moisture changes are known as active depths and based on previous studies vary from shallow to deep depths. Movements from these depths reflect to the surface leading to considerable damage to overlying infrastructures. Therefore, it is necessary to improve the expansive soils prior to any construction activity. However, the available methods are found ineffective for deep soil stabilization due to lack of appropriate design methodology. Since the chemical modification is a preferred method for stabilizing expansive soils, the researchers proposed deep soil mixing (DSM) technique using chemical binders.

The effectiveness of the DSM technique in minimizing shrink-swell behavior of expansive soils up to considerable depths was verified in the present research by conducting comprehensive laboratory and field studies. Results from laboratory studies revealed that all combinations of lime and cement binders reduced shrink and swell potentials based on linear shrinkage and free swell tests, respectively, to less than 0.5 and 0.1%, respectively. The strength properties of soils treated with binder compositions containing more than 75% lime and those with more than 75% cement are about 1.8 to 5.2 times and 5 to 12 times the untreated soil strength, respectively. Simplified linear ranking analysis yielded that a binder combination of lime (25%) and cement (75%) at a binder quantity of 200 kg/m^3 and a water-binder ratio of 1 was one of the best performing stabilizers. Therefore, it was adopted in the construction of the two pilot test sections.

Quality assessment studies conducted during construction of the DSM test sections indicated that both field stiffness and strength values are 40% and 20 to 30% lower, respectively, than those obtained in the controlled laboratory treatment conditions on small scale specimens. Non-destructive studies performed at both the treated test sections recorded average stiffness properties of 1.3 to 1.5 times those recorded in the untreated sections. Field monitoring studies revealed an overall vertical movement of less than 1 in. and more than 1.2 in. in the treated and untreated sections, respectively. Overall, the performance of the DSM treated sections as compared to the untreated sections was successful in minimizing shrink-swell movements due to seasonal moisture changes.

The analysis of the test results with field monitored data indicated that the analytical model provided reasonable predictions of soil movements for both control and treated soil sections. Numerical methods using the existing material models did not capture the realistic response of the treated sites. This might be possibly due to the limitations in the material models available, which do not account for physical and chemical behavioral changes and unsaturated soil response of treated expansive soils. Nevertheless, the present research has shown that the deep soil mixing columns along with the use of grids and anchor rods have effectively stabilized the expansive soils with active zones up to considerable depths at both test sections.

TABLE OF CONTENTS

LIST OF FIGURES

LIST OF TABLES

CHAPTER 1

INTRODUCTION

1.1 General

Expansive subgrades are commonly found in soils of various Texas Department of Transportation (TxDOT) districts in Texas (Fig. 1.1). Due to seasonal related moisture fluctuations, swell and/or shrinkage related soil movements commonly occur in these subgrade soils lying beneath infrastructures such as pavements, embankments and light to medium loaded residential buildings. These non-uniform soil movements in expansive soils often cause distress to structures resting on them. In case of pavements, these movements result in surface cracking thereby leading to pavement roughness and rider discomfort. Like all other Department of Transportation (DOT) agencies, this type of pavement distress is a major challenge faced by TxDOT, mainly due to two reasons: a) road users' discomfort and safety, and b) rehabilitation and maintenance costs of these effected pavements at millions of dollars annually. There have been continuous efforts from TxDOT to mitigate subgrade swell/shrinkage related pavement distress. TxDOT and The University of Texas at Arlington (UTA) as well as The University of Texas at El Paso (UTEP) research teams worked together to find suitable ground improvement techniques to stabilize expansive soils extending to depths greater than 10 ft below the ground surface.

The research team at UTA proposed the application of the deep soil mixing (DSM) technique to stabilize expansive soils beneath pavements to mitigate the distress caused by cyclic shrink-swell movements. This method is expected to improve the long-term performance of these pavements. DSM is a commonly adopted technique to stabilize very soft to soft clays,

organic soils, and loose sands and is widely applied in Japan, Scandinavian countries, and in some parts of the United States (Porbaha 1998).

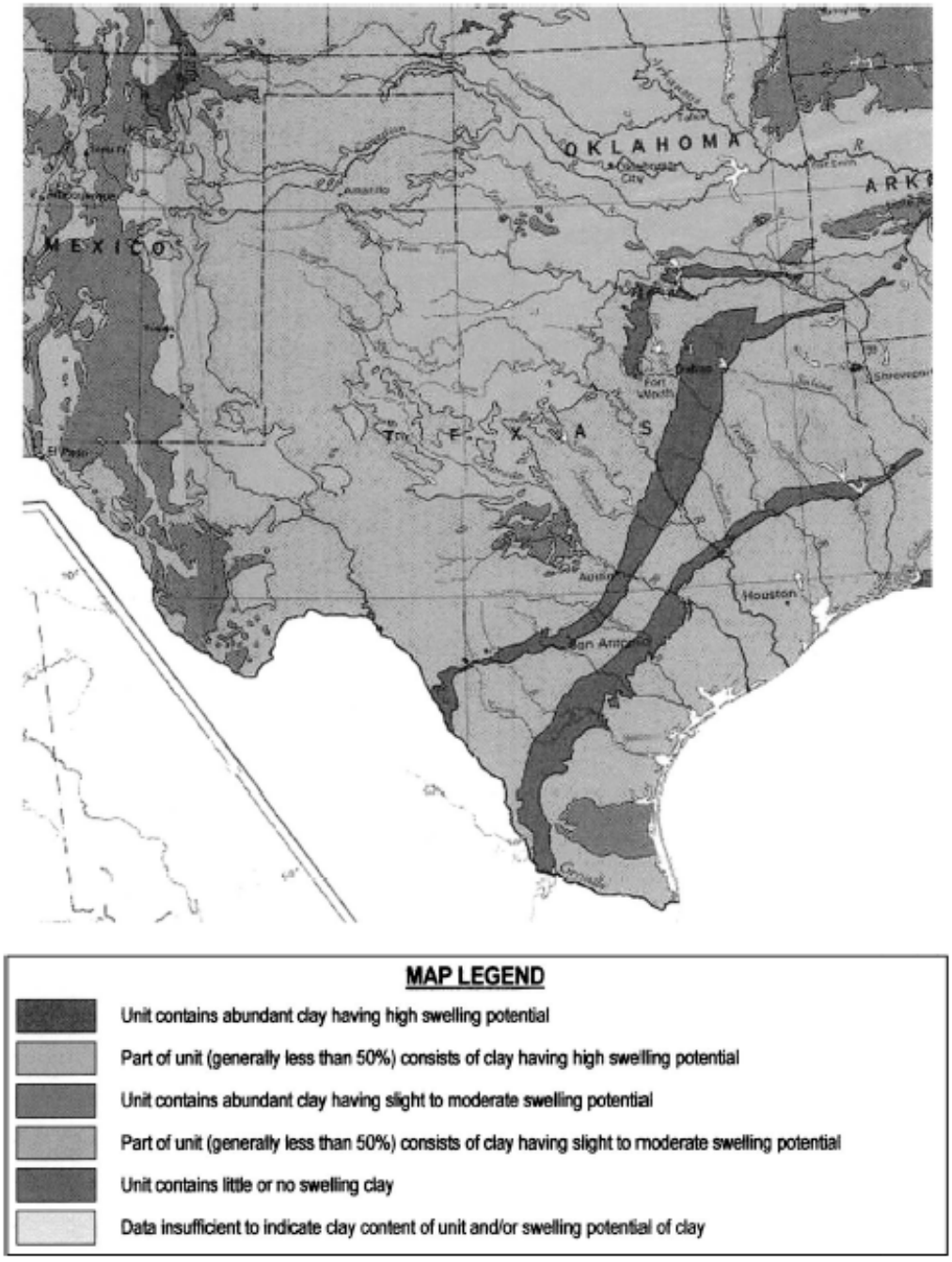

Figure 1.1 Distribution of swelling clays found in Texas (Olive et al. 1989).

1.2 Research Objective

The objective of this research study is to evaluate the effectiveness of the deep soil mixing technique in stabilizing expansive soils of considerable depths supporting infrastructures including highways, embankments and other earth and residential structures. The deep soil mixing method has proven to be an effective method in stabilizing soft soils and studies confirming this can be found at the Swedish Geotechnical Society (Porbaha 1998). However, no studies were found evaluating this technique in stabilizing expansive soils.

Since chemical stabilization is a preferred method for expansive soil improvement, the proposed study would lead to a new treatment technology, if proven effective, in stabilizing expansive soils with active zones extending to depths greater than 10 ft. This would help in minimizing the stress applied on infrastructures resting on these soils due to shrink-swell behavior related to moisture changes. The research is accomplished by following several tasks as outlined in Fig. 1.2.

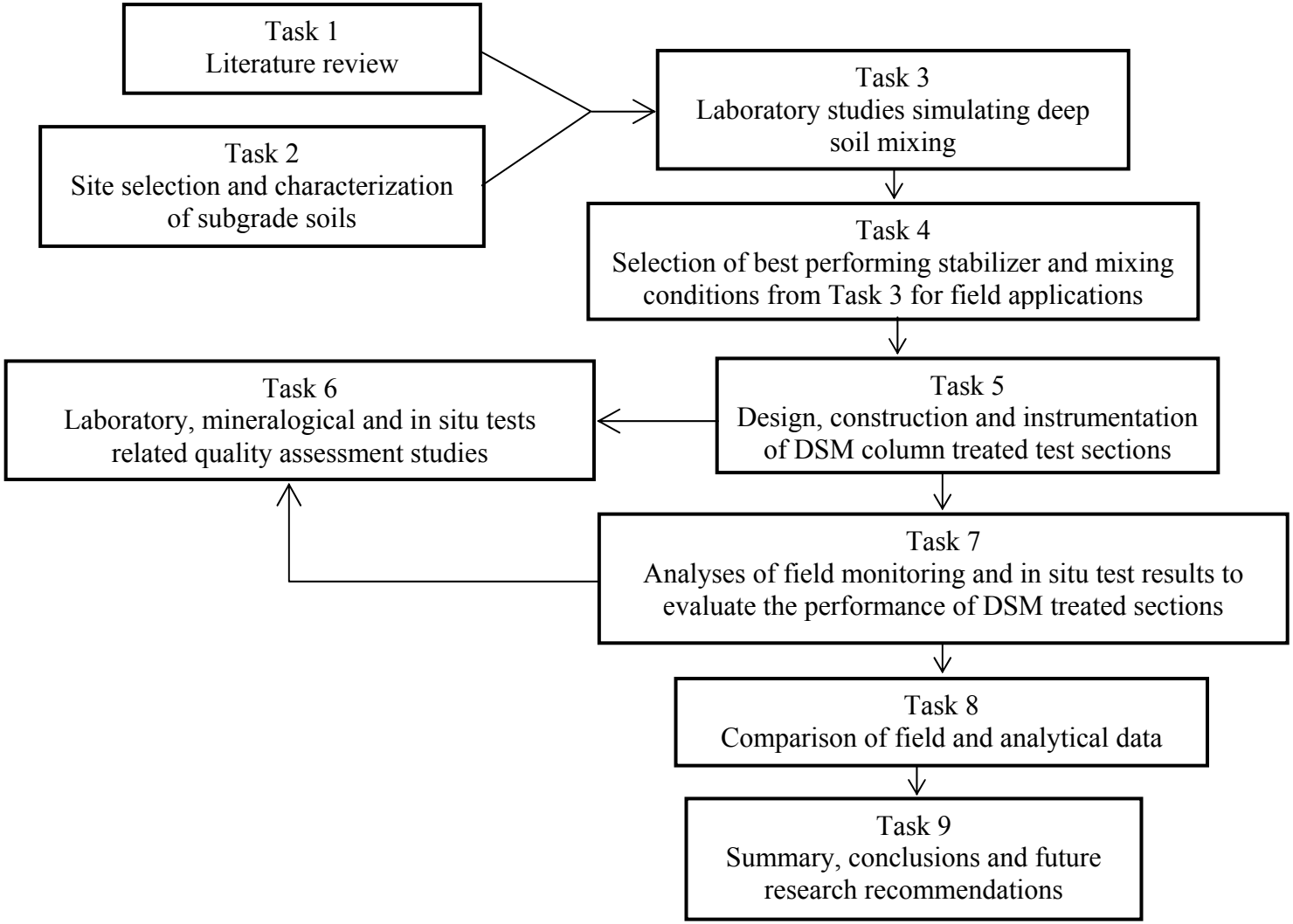

Figure 1.2 Schematic of tasks performed in this research.

1.3 Report Organization

This research report consists of eight chapters. The first two chapters present the background, objective and tasks involved in carrying out the research work and detailed review of available literature addressing the factors affecting deep soil mixing (DSM) treatment, design, construction procedure and quality assurance and quality control (QA/QC) aspects.

A stepwise laboratory procedure for preparation of soil-binder mixture followed by specimen preparation simulating deep soil mixing in the field was developed in Chapter 3. Calculations involving estimation of soil and binder quantities and amount of water required to prepare one set of specimens for unconfined compressive strength (UCS), free swell and shrinkage tests are also presented here. This chapter also presents the laboratory procedures pertaining to tests conducted on control and treated soil specimens.

Results obtained from laboratory studies were analyzed and discussed in detail in Chapter 4. This includes shrink-swell and strength-stiffness properties of both control and treated soil properties. Effects of factors such as soil type, binder type, binder dosage and proportion, water-binder ratio and curing time on these properties were also addressed. Empirical relationships for strength as a function of water-binder and stiffness as a function of strength and curing time were also developed here. Finally, this chapter presents the degree of strength improvement achieved through laboratory mixing of soil and binder with respect to control soil and ranking analysis procedure for selecting best performing binder combination for subsequent field studies.

Chapter 5 presents the design procedures based on analytical formulations for determining the length, diameter and spacing of DSM columns given the targeted heave of a DSM treated composite section. This chapter also presents the stepwise procedure explaining the construction of two DSM treated pilot test sections followed by instrumentation of these sections

with inclinometers, pressure cells, moisture probes and settlement plates. This chapter also presents the plan and sectional details of DSM treated sections and design charts for moderate to high swelling soils based on their swell index.

Quality assessments of the construction of DSM treated sections based on laboratory and in situ tests are presented in Chapter 6. Comparisons of strength and stiffness properties obtained from laboratory tests on specimens prepared in a controlled environment and in the field were made to address the effect of variations in the mixing process. Following this, empirical correlations were developed relating strength with shear wave velocity based on laboratory results. This chapter also presents the details of field monitoring studies including data collection procedures and the procedure followed for simulation of high precipitation during Phase II monitoring. Finally, mineralogical studies were discussed here to provide qualitative understanding of the degree of mixing in laboratory and field environments, cementitious and pozzalonic reactions in soil-binder mixtures at particle level.

Chapter 7 presents a comprehensive analysis of the results from the field studies. This includes results obtained from moisture probes, vertical and horizontal inclinometers, pressure cells and settlement plates. The performance evaluation of treated sections based on in situ testing is presented in this chapter. Finally, comparison of field data with analytical formulations is presented here along with some numerical simulation in the PLAXIS 3D Foundation software.

Summary and conclusions from this research study, significance of the findings from both laboratory and field studies, and future research needs are addressed in Chapter 8.

CHAPTER 2

LITERATURE REVIEW

2.1 General

As mentioned in Chapter 1, the deep soil mixing technique involving in situ mixing of existing soil with cementitious materials like lime, cement, or in combination was proposed for stabilization of expansive soils of depths greater than 10 ft. Not much previous work was noticed in the literature in this direction, except until recently. Tonoz et al. 2003 and Hewayde et al. 2005 reported prototype studies on stabilization of expansive clays using soil-lime mixed columns. As a part of the current research, a detailed literature review was conducted to gain a comprehensive understanding about: i) the behavior and problems related to expansive soils, ii) the treatment methods commonly adopted for stabilization with focus on deep soil mixing, and iii) the present research work based on previous studies. The following sections present elaborated discussions addressing the above-mentioned topics.

2.2 Expansive Soil Behavior and Associated Problems

Clay minerals are basically formed by different arrangements of the silica tetrahedral and alumina octahedral sheets and most common configurations of these sheets are 1:1 and 2:1. Minerals with a 2:1 sheet arrangement, i.e alumina sheet sandwiched between silica sheets (Fig. 2.1), belong to a group known as Smectite. These Smectite minerals are unstable and very plastic when they come in contact with water (Little 1995 and Mitchell and Soga 2005). Due to isomorphic substitution, these minerals possess high negative surface charge and these negative surface charges are satisfied by van der Waal's forces and adsorption of cations present in the pore water. Van der Waal's forces between adjacent layers / clay particles are weak and can be easily broken by the adsorption of water or any polar liquids. In this process, the minerals are

capable of accommodating water of seven times their dry weight (Little 1995 and Mitchell and Soga 2005). Soils with moderate to high percentages of Smectite minerals undergo the above-mentioned physico-chemical changes resulting in heave or swell at a macrostructural level causing distress to the infrastructure built on these soils. These soils also exhibit shrinking when subjected to drying due to loss of adsorbed water. Soils exhibiting shrink-swell behavior due to changes in moisture levels are generally termed as expansive soils.

Even though the expansive soils exist in almost every state of the United States, these soils are predominately encountered in the West than in the East (Website: www.hazmap.nctcog.org) as can be seen in Fig. 2.2. Over-consolidated clays and weathered shales are the expansive soil types commonly encountered in the north-central and Rocky Mountain regions (Nelson and Miller 1992).

Though expansive soils are rated less suitable for urban construction, the growth in population in the last decade and the associated urbanization led to construction in areas prone with expansive soils (Williams 2003). As a result, expansive soils-related damages to engineering structures have increased exponentially and these damage costs were estimated ranging from $2 to $9 billion annually (Jones and Jones 1987; Chen 1988; Keller 1996; Pipkin and Trent 1994). It is considered the most costly geologic hazards areas compared to all other natural hazards combined, including earthquakes, floods, tornadoes and hurricanes (Williams 2003; FEMA 1982; Rollings and Rollings 1996; Montgomery 1997 and Hudak 1998).

In southwestern parts of the US the expansive soil problems are considered to range from moderate to severe (Chen 1988). The soil problems in these regions are mainly attributed to volumetric changes; i.e., alternate shrinking and swelling due to long dry periods and subsequent periodic rains for short duration (Chen 1988, Hudak 1998, Bowles 1996, and Nelson and Miller 1992). This volume change and/or cyclic shrink-swell behavior of expansive soils cause severe

distress to engineering structures including foundations, buried utilities, airport runways, pavements and canal linings, etc. However, the most extensive damage can be seen in terms of 'roughness' values of pavements and streets, which indicate the ride quality of the pavement. Swell potential of these soils depends on various factors such as clay mineralogy, availability of moisture, geologic and climatic conditions and thickness of expansive soil layer (Hewayde 1994 and Hudak 1998).

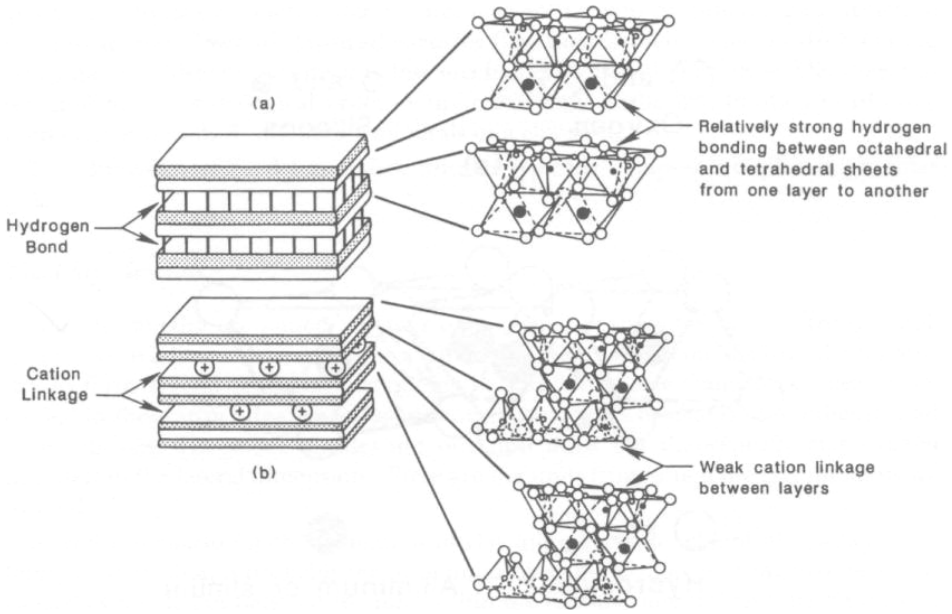

Figure 2.1 Arrangement of silica and alumina sheets in (a) 1:1 mineral (Kaolinite) and (b) 2:1 mineral (Smectite).

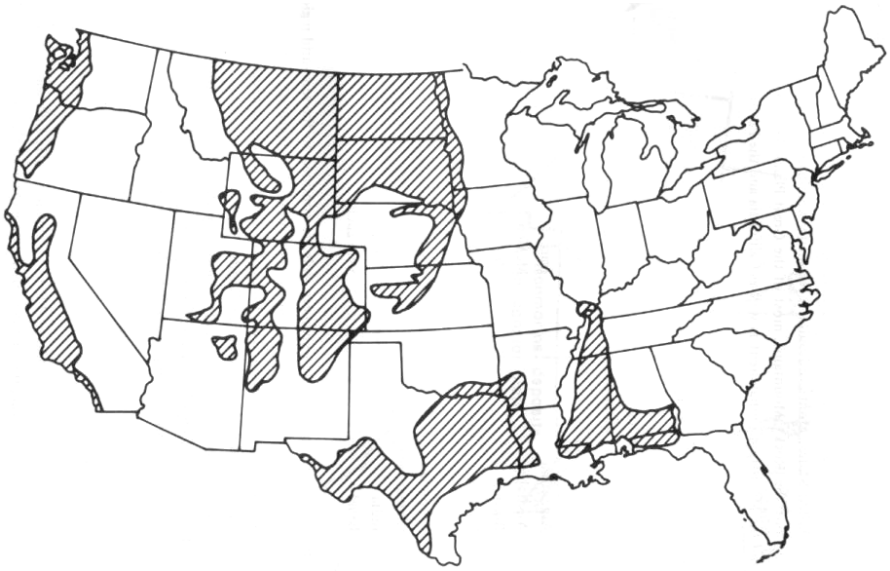

Figure 2.2 Distribution of expansive soil (shaded area) over the United States (Chen 1988).

2.3 Pavement Roughness in Expansive Subgrades

The analogy of moisture variations in slab-on-grade foundations over expansive soils can be applied to highway pavements. Highway pavements are designed as impervious shallow foundations which experience moisture variations at the center and at the edges of the pavement. These variations in moisture are a result of elimination of the subgrade center from, and continuous exposure of edges to, environmental elements such as rainfall and evapotranspiration (Nyangaga 1996, Picornell and Lytton 1989, and Nelson and Miller 1992). Expansive subgrades beneath the pavements subsequently undergo swelling or shrinking, depending on wet or dry conditions, respectively, causing distress to the pavements through differential movements. Also, when expansive soils are exposed to environmental changes, they develop a wave-like pattern on the surface known as "gilgai" (Lytton et al. 1976). Differential movements associated with formation of wave-like surface pattern result in the development of pavement roughness (Gay 1994 and Nyangaga 1996). Roughness is generally described as a distorted or irregular surface that leads to poor ride quality, increased fuel consumption and vehicle maintenance (Hudson 1981, http://training.ce.washington.edu). According to ASTM E867 (2006), pavement roughness is defined as "the deviations of a pavement surface from a true planar surface with characteristic dimensions that effect vehicle dynamics and ride quality." Fig. 2.3 depicts the deformed shape of pavement due to the effects of expansive subgrade.

Irrespective of the type of subgrade, pavement roughness is also caused over a period of time with uneven distribution of traffic loads, climatic changes and surface wear. A poor subgrade soil associated with these factors will enhance the pavement roughness and thus affect the pavement service life resulting in incurring large sums of maintenance costs. According to Jayathilaka (1999) the most common types of distress modes noticed in pavements built over expansive subgrades are as follows:

- surface unevenness distributed over a considerable length,
- longitudinal cracks, and
- excessive deformations near pipe culverts and trees.

Figure 2.3 Pavement overlying expansive soils and subjected to distress due to shrink-swell movements. (Source: www.surevoid.com).

Considering the influence of a poor subgrade soil in pavement performance, one finds that it is important to include the parameters defining the subgrade behavior in pavement roughness predictive models for use in pavement analysis, design and rehabilitation. Lytton et al. (1976), Velasco and Lytton (1981), Steinberg (1980 and 1985), Rauhut and Lytton (1984), McKeen (1985), Gay (1994), Nyangaga (1996), Jayathilaka (1999) and Hong et al. (2006) studied the pavement roughness associated with expansive subgrades. In the process, they developed several roughness predictive models which are capable of considering subgrade properties; treatment type – effect of barriers, lime – or cement stabilization; climatic conditions, traffic conditions; and pavement type. Several roughness indices were defined by researchers through various methods of analysis using different instruments. The most commonly used

current indices are Present Serviceability Index (PSI) and International Roughness Index (IRI) (Jayathilaka 1999). The following sections present brief details about these indices.

2.3.1 Present Serviceability Index (PSI)

The AASHTO (American Association of State Highway Transportation Officials) road test defined the serviceability performance concept in terms of present serviceability rating (PSR) based on individual observations (Carey and Irick 1960). PSR is the average of subjective ratings made by individuals of a panel based on the current ability of a pavement to provide intended service to the traffic (Nyangaga 1996 and Jayathilaka 1999). PSR ranges from 0 (very poor condition) to 5 (excellent condition). The limitation of PSR is that it solely depends on the ride quality of some individuals in an automobile and therefore is not practical to use for large-scale pavement networks (http://training.ce.washington.edu/WSDOT/). As such, a predictive model known as present serviceability index (PSI) was then developed based on physical pavement characteristics such as cracking, patching, rut depth, slope variance and others of a road surface and is linked to a subjective index, PSR, to develop PSI equations. The relationship between PSI and PSR is given below and the index goes beyond a simple assessment based on the ride quality (Gay 1994, Nyangaga 1996, Jayathilaka 1999 and http://training.ce.washington.edu/WSDOT):

$$PSR = PSI + E \quad (2.1)$$

where E is the error.

In order to predict the pavement roughness in expansive soils, AASHTO (1993) presented a procedure to estimate serviceability loss, ΔPSI, based on the following expansive soil parameters – swell rate constant, potential vertical rise, and swell probability. The swell probability indicates the percent of the project length that is subject to swell and the expression for serviceability loss due to expansive subgrades is as follows (Jayathilaka 1999):

$$\Delta PSI = 0.00335 \times PVR \times P_s \times (1\text{-}e^{-\theta t}) \quad (2.2)$$

where PVR = potential vertical rise (in), P_s = swell probability, θ = swell rate constant and t = time in years.

Similar correlations developed for serviceability index of pavements due to expansive clay activity using various methods of analysis and measuring procedures are reported in detail in Gay (1994), Nyangaga (1996) and Jayathilaka (1999).

2.3.2 International Roughness Index (IRI)

IRI is a product of the International Road Roughness Experiment in Brazil in 1982, initiated by the World Bank, to standardize roughness measurement in order to exchange roughness information at an international level without difficulties (Sayers et al. 1986). IRI is a mathematical function or profile statistic of a longitudinal profile of a traveled single wheel track and has units of slope (m/km or in/mile). There is no specified range for IRI as there is no theoretical upper limit but a value of '0' means a perfectly smooth surface (Jayathilaka 1999). The IRI is highly compatible to be estimated from various measurement methods (Sayers et al. 1996 and Nyangaga 1996) and is correlated to subjective index as below. Paterson (1986) reported:

$$PSR = 5e^{-0.18(IRI)} \quad (2.3)$$

Similar correlation was also reported by Al-Omari and Darter (1992) and Hong et al. (2006)

$$PSR = 5e^{-0.26(IRI)} \quad (2.4)$$

$$IRI = 8.4193\exp(-0.4664PSI) \quad (2.5)$$

where PSR = present serviceability rating and IRI = international roughness index. Hong et al. (2006) developed roughness predicting models based on both subgrade movements and traffic. The models are developed using the roughness measurements collected over 15 years by the Texas Transportation Institute (TTI). The indices, IRI and PSI, are estimated processing these data using the computer program WinPRES that relates with predicted vertical movements together with projected traffic. The predicted indices are then plotted against time and the models are developed by employing a nonlinear regression technique. Thus, the pavement performance can be estimated using these models, which are as follows:

$$PSI = PSI_0 - (PSI_0 - 1.5)\exp[-(\rho_s/t)^{\beta s}] \quad (2.6)$$

$$IRI = IRI_0 + (4.2 - IRI)\exp[-(\rho_i/t)^{\beta i}] \quad (2.7)$$

where as PSI_0 is initial present serviceability index; IRI_0 is initial roughness index (m/km) and ρ_s, β_s, ρ_i, β_i are roughness parameters obtained through regression analysis. Estimation of parameters ρ_s and ρ_i accounts for both expansive behavior of subgrade soils and projected traffic load.

2.4 Stabilization Methods for Expansive Soils

The problem of expansive soils was first recognized by engineers as early as the late 1930s (Chen 1988). Since then, the increase in population and subsequent urbanization pressure encouraged the use of problematic soils, including soft and expansive soils, for construction purposes. This initiated researchers and practitioners to find structural alternatives to minimize the distress caused to superstructure due to differential expansive soil movements. Other approaches include soil treatment alternatives such as chemical additives, prewetting, soil

replacement and compaction control, moisture control, surcharge loading and thermal methods (Nelson and Miller 1992). All these approaches except chemical additives and thermal methods mechanically stabilize the expansive soils without modifying their properties. These mechanical stabilization methods have severe limitations in their applications and might incur large maintenance costs in long-term performance (Nelson and Miller 1992 and Punthutaecha 2002).

Stabilization through chemical additives such as lime, cement and fly ash etc. modifies the soil properties offering a better foundation base for pavements (Hausmann 1990). Modifications in physico-chemical properties of expansive soils prove to be more effective on a long-term basis due to reduction in the maintenance costs that increased their applications in the last two to three decades. The following sections address the details on some of the structural and soil treatment alternatives.

2.4.1 Structural Alternatives

The most commonly used alternatives are drilled piers - grade beam and slab-on-grade foundation systems. The former system has been widely used in the Rocky Mountain region, while the latter one in the southern and southwestern regions of the United States (Nelson and Miller 1992 and Chen 1988). A brief schematic of a drilled pier – grade beam system is shown in Fig. 2.4. The main principle of this system is to balance the uplift forces exerted by the swelling of the surrounding soil in the active zone by withholding forces along the pier shaft below the active zone plus the dead load. It is also necessary to leave enough void space beneath the grade beams in order to prevent any uplift pressures from the soil on the superstructure (Nelson and Miller 1992).

The design of slab-on-grade foundation systems on expansive soils is based on slab and swelling soil modeled as a loaded plate or beam resting on an elastic continuum (Nelson and

Miller 1992). This system combined with vertical barriers to control moisture beneath the structure would be more effective in minimizing the swelling behavior. These systems offer a logical solution to some extent for construction of residential, and light to moderately loaded structures on expansive soils. However, one of the major disadvantages with drilled pier-beam systems are the construction costs and difficulty in areas with deep active zones (Chen 1988 and Nelson and Miller 1992). Also, both systems are vulnerable to uplift movements in areas where the soil has high swelling potential. More details on the design and applications of these systems and continuous and mat type foundations on expansive soils can be found in Chen (1988) and Nelson and Miller (1992).

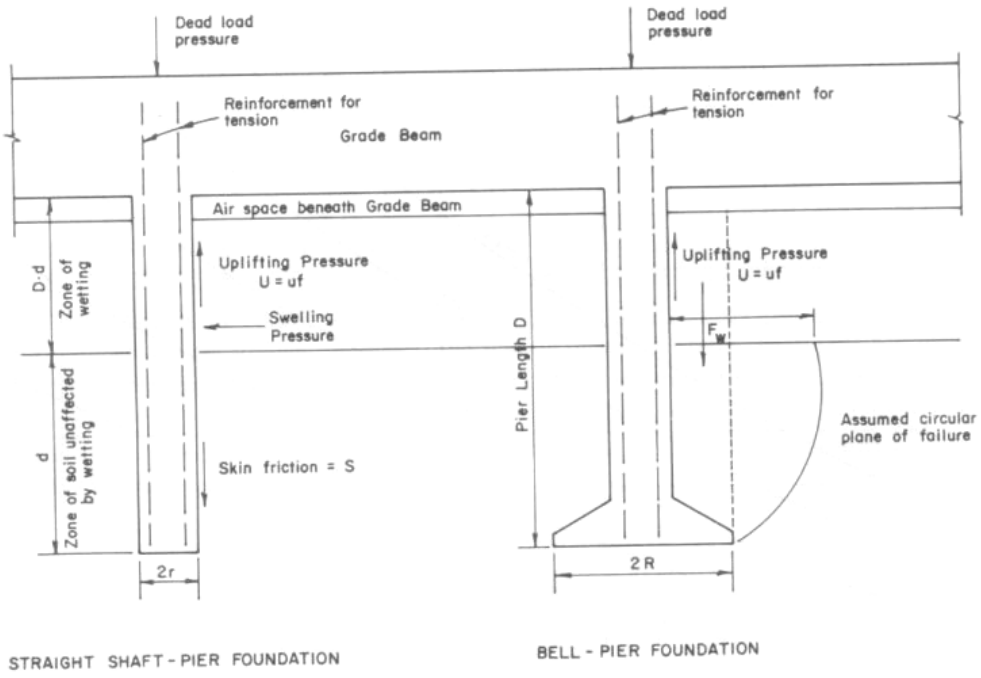

Figure 2.4 Schematic of drilled pier-grade beam system (Chen 1988).

2.4.2 Soil Treatment Alternatives

In this section, the authors emphasize an understanding of soil treatment through chemical additives and present a brief review of literature on the existing mixing methods used to stabilize expansive soils. Details regarding mechanical stabilization and thermal methods can be found in Nelson and Miller (1992) and Punthutaecha (2002).

2.4.2.1 Lime Treatment

Lime is the most widely used stabilizer in engineering practice since early times and has applications over a wide range of soils (Little 1995 and Petry and Little 2002). It is considered to be very effective for reducing swell potential, plasticity, and increasing workability of expansive soils. It also provides considerable strength gain of treated soils with time (Chen 1988 and Nelson and Miller 1992). Lime reacts with soils at physico-chemical and microstructural level (Wilkinson et al. 2004a) altering the properties as mentioned above. These soil-lime reactions are complex in nature and occur in two phases (Chen 1988, Nelson and Miller 1992, and Little 1995).

In the first phase, as soon as lime is added to the soil the divalent Ca^{2+} ion replaces weaker ions such as Na^{+} and Mg^{2+} adsorbed on the surface reducing the affinity for water and thereby decreasing the diffused layer thickness. This is followed by flocculation and agglomeration (Fig. 2.5) of clay particles causing a change in clay texture and reducing percentage of fine particles (Little 1995, Chen 1988). The result of these reactions can be seen in terms of improved workability, reduced plasticity and some strength gain (Little 1995) in lime treated soils.

Second phase reactions take place between Si^{2+} and Al^{3+} ions present in clay and Ca ions present in lime resulting in the formation of cementitious products including calcium silicate hydrate (CSH) and calcium aluminate hydrate (CAH). These reactions are known as pozzolanic reactions that occur in a high pH environment and contribute to strength gain with time (Little

1995, Nelson and Miller 1992, and Petry and Little. 2002). Due to successful implementation of the technique in numerous projects, most of the DOTs adopt it. It is reported by Chen (1988) that the Texas State Highway Department used nearly ½ million tons of lime for stabilization in 1969. Quick lime and hydrated limes are the most commonly used lime types in practice.

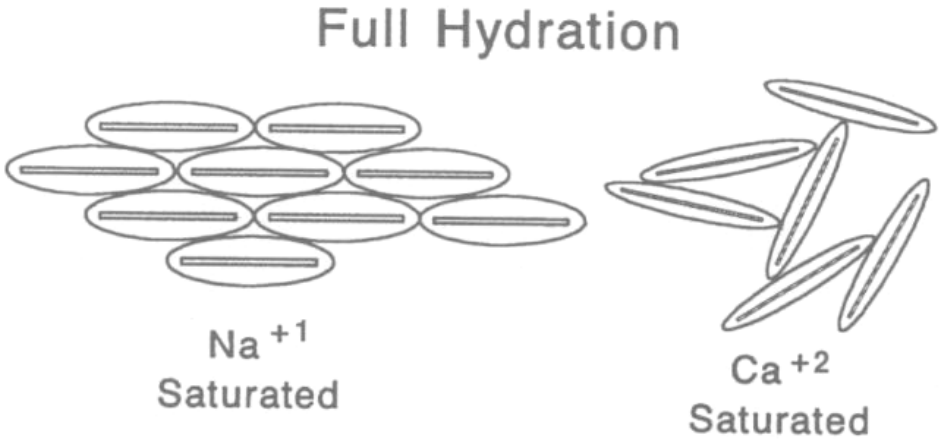

Figure 2.5 Schematic showing cation of weak soil exchange followed by flocculation (Little 1995).

2.4.2.2 Cement Treatment

Ordinary Portland cement is the most commonly used stabilizer, after lime, in practice, for the last two to three decades. The reactions between cement and expansive soil are almost similar to those that occur in lime treatment (Chen 1988 and Nelson and Miller 1992). Upon addition, cement immediately reacts with pore water and results in cation exchange and formation of cementing product, CSH, along with $Ca(OH)_2$. CSH helps in binding the soil particles together and increases the soil strength. The subsequent formation of $Ca(OH)_2$ contributes to long-term strength gain through secondary reactions (pozzolanic) in later stage, though to a lesser extent compared to those in lime treatment. These physico-chemical changes result in reduced plasticity and volume change potential, and increase of shrinkage limit and shear strength (Gromko 1974, Chen 1988, and Nelson and Miller 1992). However, the amount of

heat released in soil-cement mixture during hydration is high and might lead to cracking (Nelson and Miller 1992 and Punthutaecha 2002).

Other limitations include that cement treatment alone may not be as effective as lime in stabilizing highly plastic clays because of their high affinity for water, short setting time, high cost of the material and brittle failures formed during pozzolanic reactions (Nelson and Miller 1992 and Punthutaecha 2002). But from literature, it is noticed that with time the use of stabilizers such as lime, cement and fly ash in combination was increased to overcome some of the limitations. The changes in the reaction and structure of lime and cement with time are reported by Rathmayer 1997 and Ahnberg 2006 (Fig. 2.6). The mixing operations or application methods that are used in practice are the same for both lime and cement treatments and are presented in detail in the following section.

2.4.2.3 Mixing or Application Methods

The most widely accepted mixing method for lime stabilization by highway departments is in situ mass mixing and recompaction. This is a shallow treatment technique; therefore, limits of the depth of application are considered successful where active zones are not deep (Nelson and Miller 1992). In this method, the surface of expansive subgrade is scarified and loosened to the required depth of stabilization and then thoroughly mixed with the designed percent of lime and water and compacted to the corresponding density. Other methods of stabilization include drill hole/lime piles and lime slurry injection (LSI) techniques.

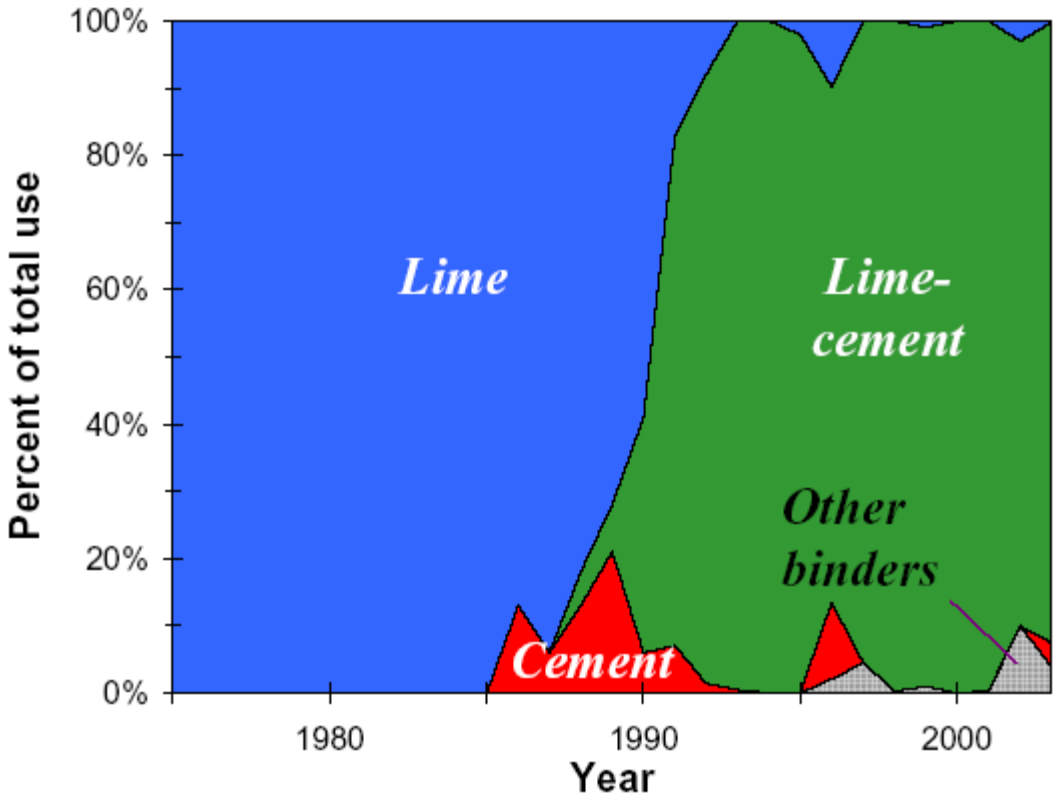

Figure 2.6 Changes in binder usage with time in deep soil mixing (Rathmayer 1997 and Ahnberg 2006).

In the drill hole/lime pile technique, small diameter holes are drilled at closer spacing (4 to 5 ft) and are filled with lime slurry. The effectiveness of this method depends on the diffusion of lime into the surrounding soil. This limits its application as the permeation rate in expansive soils is low. Nelson and Miller (1992) reported that the results of this technique were found to be erroneous and do not encourage its application. Recent prototype studies using lime piles in expansive soil beds revealed that the effective radius of lime migration / zone of influence is about 1.6 to 2 times the pile diameter (Rao and Venkataswamy 2002, and Tonzo et al. 2003). In the case of soft soils, a radius of six times the diameter is reported as the effective zone of influence for lime migration (Rajasekharan et al. 1997). However, these studies also revealed that lime migration did not help in increasing the pH level of the surrounding soil

beyond 12, which is considered favorable for pozzolanic reactions. Therefore, this limits the strength gain of the surrounding soil as compared to that in intimate mixing soil with stabilizer (Rao and Venkataswamy 2002). It is also observed that intimate mixing of lime and soil resulted in swell potentials < 0.5 % as compared to 2 to 5 % through lime migration (Basma et al. 1998, Nalbantoglu and Tuncer 2001 and Rao and Venkataswamy 2002). These observations reveal that the performance of intimate mixing of soil and lime is recommended for both strength gain and reduction in swell potential compared to the lime pile technique.

The use of the LSI (lime slurry injection) technique was first reported in the late 1960s, and Lundy and Greenfield (1968) were the pioneers to apply this in cohesive soils. Later, the process was extended to expansive soils, due to economic reasons, as an alternative to pier and beam foundations and slab-on-grade foundations (Baker 1992) and considered as an extension of the modified drill hole method to increase the permeation of lime slurry into the surrounding soil (Nelson and Miller 1992). The process involves injection of lime slurry under high pressures at design spacing intervals until the surface begins to fracture or no additional slurry can be pumped (Nelson and Miller 1992 and Wilkinson et al. 2004a). The maximum pressures applied are in the range of 800 to 1000 kPa (Wilkinson et al. 2004a and www.haywardbaker.com). This method is more effective in clays with maximum desiccation cracks/fissures formed due to shrink-swell behavior (Nelson and Miller 1992). This injection technique can be considered as both a pre- and post-construction treatment method. However, it is difficult to estimate the degree of improvement in this technique (Wilkinson et al. 2004a) and this may lead to secondary treatment in case the primary treatment fails to produce the expected results. Baker (1992) reported that the failure for widespread application of LSI is because of lack of specific acceptance criteria and developed the same parameters based on the data collected from previous projects. Also, from the researcher's current viewpoint, application of LSI in cases involving

moderately stiff to stiff expansive soils may require very high pressures, making its implementation in the field difficult because of their less permeable and stiff nature.

In general, most of the chemical stabilization of expansive soils includes subgrades under the pavements and soil under footings and slabs for lightly loaded structures. In all these cases, the treatment depths are limited and therefore considered as shallow stabilization. But, in the case of construction on deep expansive soils it is necessary to stabilize deeper layers to prevent distress to structures in response to seasonal variations (Rao and Venkataswamy 2002). The methods of treatment considered until now for deep stabilization of expansive soils are the lime pile technique and slurry injection methods. But applications of these methods for deep stabilization in expansive soils have certain limitations, as mentioned above. However, there are several ground improvement techniques using chemical additives for stabilization of soft soils at deeper depths and details of their history and development can be found in Moseley (1993), Bergado et al. (1996), Kitsugi and Azakami (1982), Rathmayer (1996), Holm et al. (1981) and Porbaha (1998). The most successful of these methods for deep stabilization is in situ soil mixing or deep soil mixing (DSM). The concept involved in this technique is mixing the soil with designed amounts of stabilizers (lime and/or cement) in situ using an auger to required depths. The first applications of DSM were found in Japan in the early 1970s for port and harbor structures (Moseley 1993). A detailed review on the development and applications of this technique are presented in the next section.

Considering the success of DSM in deep stabilization and chemical stabilization being a preferred technique for mitigating shrink-swell behavior, researchers suggested the application of DSM to expansive soil treatment. However, the authors noticed that not many studies on the application of in situ mixing in expansive soils were reported in the literature. Porbaha (1998), and Puppala and Porbaha (2004) discussed the idea of applying DSM to expansive soils.

A prototype study on model foundations resting on untreated, reinforced and unreinforced lime column treated expansive soil beds was reported by Hewayde et al. (2005) (Fig. 2.7). This study closely simulates in situ mixing of expansive soils. The composite expansive soil beds with reinforced and unreinforced lime columns exhibited a reduction of 33% and 69%, respectively, in swell potential as compared to the untreated expansive soil bed. These swelling reductions in composite expansive soil beds are due to both the physico-chemical changes at the particulate level and mobilization of mechanical forces (resisting) at the interfaces of the lime column and surrounding soil and the reinforced bar. Hewayde et al. (2005) also noticed that the reduction in heave of composite soil bed is a function of ratios of the length of column to the reinforced bar, length of column to expansive soil layer thickness, length to diameter of columns, and adhesive coefficients at the interfaces. Therefore, the above discussion of studies by Rao and Venkataswamy (2002), Tonoz et al. (2003), Hewayde et al. (2005) further support the idea of applying DSM to expansive soils but it is necessary to evaluate this technique in field settings preceded by some laboratory studies before considering for implementation in actual field projects.

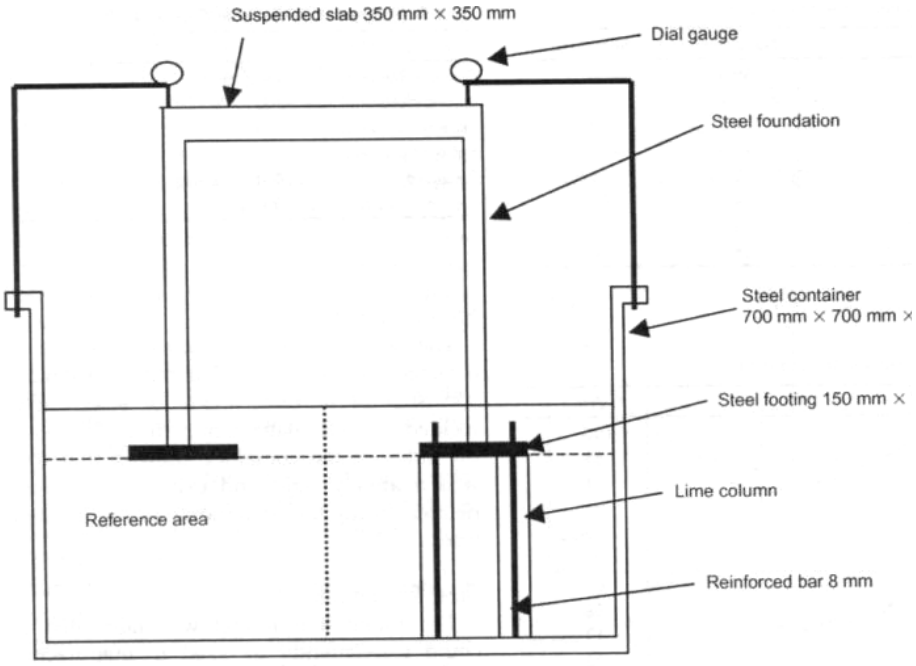

Figure 2.7 Schematic of model foundations resting on untreated and lime column treated expansive beds (Hewayde et al. 2005).

2.5 Background and Historical Review of DSM

Deep soil mixing (DSM) techniques, which were developed in the 1960s, were first reported in literature during the early 1970s (Broms and Boman 1979; Holm et al. 1981; Rathmayer 1997; Okumara 1996; Kamon 1997; Porbaha 1998). DSM technology involves the auger mixing of soils extending to large depths with binders such as cement, lime, or other types. The deep soil mixing method is a ground modification technique that improves the quality of soil by in situ stabilization of soft soil or by in situ fixation of contaminated ground (Porbaha 1998). In a broad perspective, the main objectives of improvement are to increase strength, to control deformation, to reduce permeability of the loose or compressible soils, or to clean a contaminated site. Fig. 2.8 presents a typical DSM operation and resulting columns in the field.

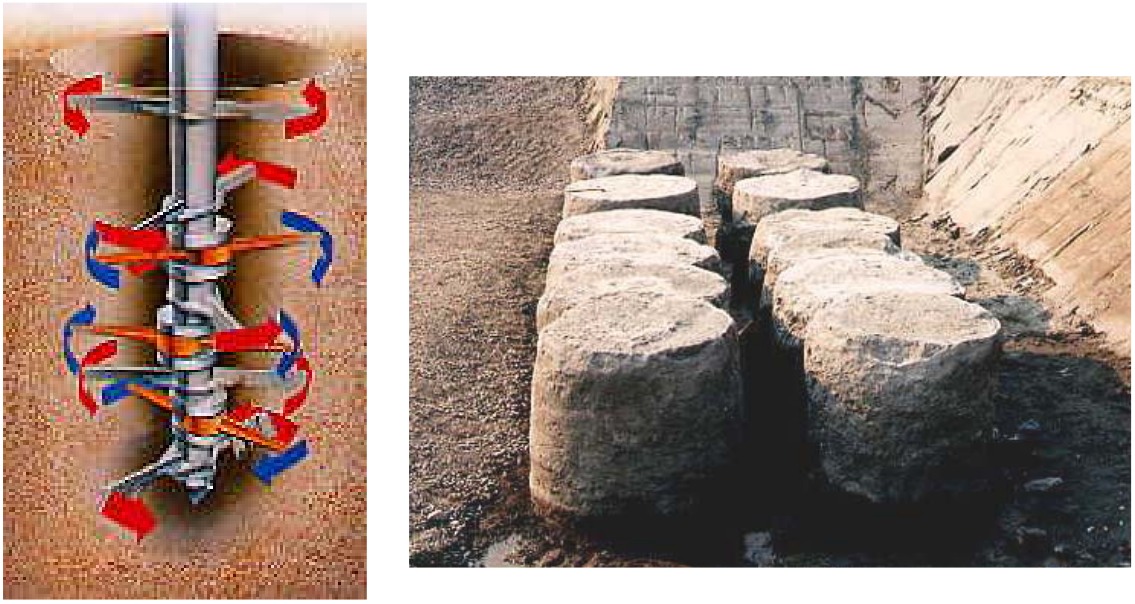

Figure 2.8 Deep Soil Mixing (DSM) operation and extruded DSM columns.

The choice of additives to be used in the field depends on the requirements of the project. For example, if the strength of soil is the main consideration, as in the case of structures built on loose sandy soils, reclaimed soils, peats and soft clays, the use of deep cement mixing is normally preferred. Cement stabilization provides substantial strength increase in a short time frame, due to cement hydration and pozzolanic reactions, cementation and agglomeration, as well as ionic exchange and flocculation mechanisms (Sherwood 1995; Hosoya et al. 1996). This stabilization technique is quite effective on soft clays, peats, mixed soils, and loose sandy soils (Rathmayer 1997; Porbaha 1998; Halkola 1999; Porbaha 2000; Bruce 2001 and Bruce 2002).

In projects where soil compressibility properties need to be enhanced to reduce undesirable settlements, either lime or combinations of lime with cement or other additives are typically used in the DSM treatments (Puppala 2003). Industrial waste stabilizers including slags and ashes could be used as co-additives for property enhancements. Usually, the chemical

stabilizer dosages used in DSM projects are reported in the ranges of 9.4 to 12.5 lb/ft^3 (150 to 200 kg/m^3), which usually represent 8 to 12% by dry weight of soil.

The stabilizing process typically takes place by mechanical dry mixing, by wet mixing or by grouting (Rathmayer 1997; Porbaha 1998; and Holm 1999). Dry mixing is usually preferred in project sites where the water tables are high and close to the ground surface. Wet mixing is recommended for dry and arid environments or sites with deep water tables. Grouting with or without jets has been used for ground strengthening, excavation support and ground water control in construction projects (Kamon 1997; Porbaha 1998; and Bruce 2001).

Deep soil mixing columns are formed in different configurations such as isolated columns, compound columns, panels, and grids (Fig. 2.9). All these configurations are used in different site conditions based on site soil characteristics, project requirements, load transfer mechanisms and settlement characteristics (Puppala 2003). For example, isolated columns are used in areas where the design improvement ratio (ratio of treated soil to an untreated soil) is low (less than 40 to 50%). Compound columns are used when the design improvement ratio at the site is high (higher than 50%). Panels and grids are also used in high ratio environments and when superstructures are large in size such as embankments, dams and retaining wall structures. In highway applications, typically single (Fig. 2.9a) or multiple columns (Fig. 2.9b,c,d) are used to stabilize soils (Esrig et al. 2003 and Lambrechts et al. 2003).

Due to the success of these DSM based ground treatment methods, several advances have been made in deep soil mixing technology. This has led to improved processing and novel installation technologies with the use of different additives incorporated as either dry or wet forms to stabilize soils. As a result, several new methods were introduced and labeled with various terminologies. Currently, there are more than eighteen different terminologies used to identify different types of deep soil mixing methods (Porbaha 1998 and 2000). Irrespective of

these terminologies, the stabilization mechanisms are similar and their enhancements to soil strength and compressibility properties are considerable.

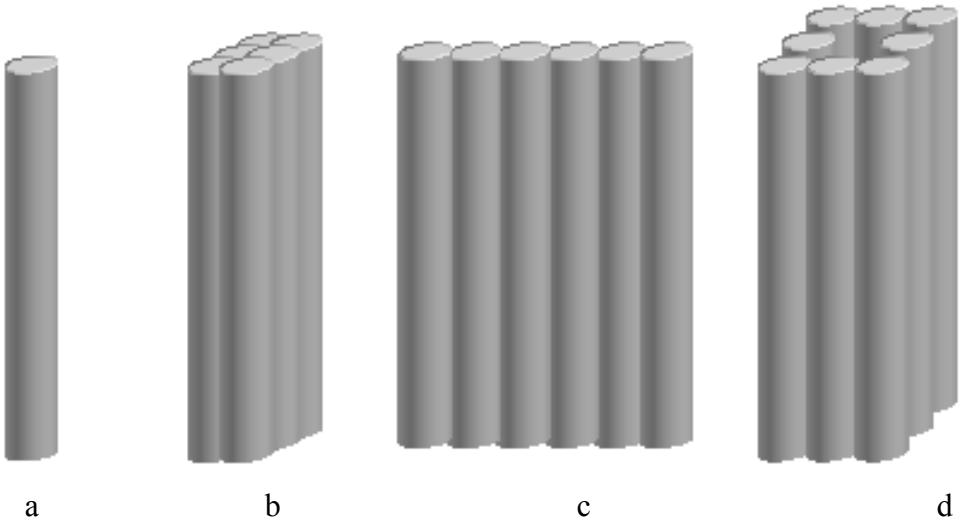

Figure 2.9 Different configurations of DSM columns (a) Single column (b) Compounded columns (c) Panel and (d) Grid types.

Fig. 2.10 presents different infrastructure projects where the DSM has been used. The DSM technology has been used in these projects for the following specific applications:

- Increasing bearing capacity of soft soils
- Reduction of settlement of compressible soils
- Prevention of sliding failure of slopes and embankments
- Protecting structures surrounding the excavation site
- Controlling seepage and cutoff barriers
- Preventing shear deformation (liquefaction mitigation)
- Remediation of contaminated ground and vibration impediment

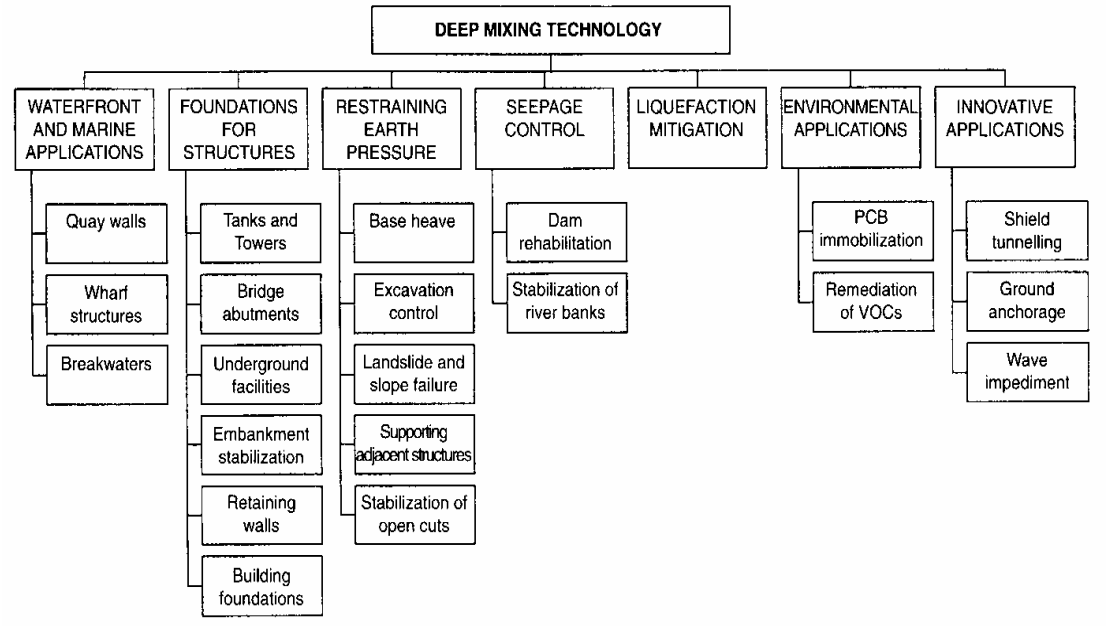

Figure 2.10 Specific application areas (Porbaha 1998).

The development of new applications should take advantage of the unique characteristic of DSM in which rapid stabilization is possible in a short period of time, which will lead to accelerated construction in the field. Although the initial demand for DSM was to gain higher strength at lower cost, the recent complex construction dilemmas in expansive soils and other problematic soils have led to a greater need of evaluating this technology for expansive soil modification in field settings (Porbaha and Roblee 2001). Since the chemical modification is a preferred method for stabilizing expansive soils, the proposed DSM method utilizing chemical treatments will have a high potential of success in the real field condition. This has been the main impetus behind the proposed research. This initiates the need for conduct laboratory prototype studies to get a thorough understanding about the merits and limitations of applying DSM technology in expansive soil treatment. These studies will also help in developing procedures and methodologies for analysis, design and specifications for construction of DSM columns in expansive soil settings. The following section presents the review of previous laboratory studies on deep soil mixing.

2.6 Laboratory Studies on DSM Technique

The authors noticed extensive literature being published on laboratory studies of DSM with respect to its application in soft and/or organic soils. This is evident from the international conferences on deep soil mixing held in Tokyo and Sweden during 1996, 1999 and 2005, respectively. Recently, a prototype study (Hewayde et al. 2005) related to lime or cement mixing of expansive soils imitating DSM was reported. However, several studies can be found on intimate mixing of stabilizers such as lime, cement, fly ash, salt etc. with few studies on lime pile and slurry injection in expansive soils in the literature.

Extensive application of DSM in soft soils helped in identifying several factors affecting the performance of lime/cement columns. Babasaki et al. (1996) classified these factors in the following groups: characteristics and conditions of soil, characteristics of stabilizer, mixing conditions and curing conditions. As a part of the present study, effects of some of these factors including stabilizer type, stabilizer dosage and proportion; water–binder (lime/cement or both) ratio and curing period in stabilizing medium stiff to stiff expansive clays were studied in the laboratory. The following sections present a thorough review of past research on the effects of these factors on soil improvement and simulation of DSM in the laboratory environment.

2.6.1 Simulation of DSM Technique in Sample Preparation

The success of any deep soil mixing project is dependant on several parameters as mentioned by Babasaki et al. (1996). This initiates a need to evaluate these parameters through detailed laboratory testing program simulating field procedures to obtain optimum design values. Despite considerable advances in laboratory studies simulating DSM procedures (Japanese Geotechnical Society [JGS] 2000, EuroSoilStab 2002, Al-Tabba et al. 1999, Shen et al. 2003a, and Jacobson et al. 2003), no standardized procedure was reported in the literature and/or in the

ASTM (American Standard Testing Materials) standards. Therefore, an attempt was made to come up with a standard procedure by summarizing the differences in various sample preparation procedures proposed by different researchers from different parts of the world.

Table 2.1 Review of existing laboratory standards for sample preparation and testing simulating DSM technique.

Preparation standards	**Field sampling and storage**	**Sample preparation molds**	**Type of soil mixer**	**Sample preparation procedure**	**Curing conditions**
Japanese Geotechnical Society, JGS 0821-2000, Section 7.2	Thin walled sampling, store the specimens at original water content	The standard size of the mold is defined to create a specimen with a 5 cm diameter and 10 cm height.	Domestic dough mixer with 5,000 to 30,000 cm^3 mixing bowl and hook type paddle, capable of 120 to 300 rpm planetary motion (Fig. 2.11)	Mixing duration: 10 minutes with occasional hand mixing, compacted in 3 lifts with poking using a 5 mm metal rod and light tamping to exclude air voids	The sample ends are properly sealed with specified sealants and stored at 20±3°C for the specified time at 95% relative humidity
EuroSoilStab, CT97-0351. (Project No. BE 96-3177)	Tube, piston or Delft samplers, stored at in situ conditions	Plastic tubes or plastic coated cardboard, 5 cm diameter and 10 cm height coated with oil or wax on the inner side	Dough mixer or kitchen mixer with sufficient capacity and rpm for all soil types	Mixing duration: 5 minutes and is a variable depending on the soil type. Circular steel stamp 10 mm thick and 45 mm diameter, attached to a 50 mm long rod. Static load of 100 kPa may be used for 2 seconds on each layer	No mention of humidity, store samples at a constant temperature of 18-22 °C in properly sealed conditions

Table 2.1 Review of existing laboratory standards for sample preparation and testing simulating DSM technique (continued).

Preparation standards	**Field sampling and storage**	**Sample preparation molds**	**Type of soil mixer**	**Sample preparation procedure**	**Curing conditions**
Al-Tabba et al. (1999) and Shen et al. (2003)	N/A	50, 100 and 150 mm diameter soil mixed columns are prepared in test pits with same principle as the DSM column installing machine in field	Sensor controlled speed and rpm of the augers. The equipment mainly consists of slurry injection part, a mixing device and a controlling panel pressure control (Fig. 2.12)	Control panel operated and is dependant on soil type. Injection pressure can be adjusted from several kPa to several hundred kPa. Consolidation pressure can be simulated through air pressure	Cured at room temperature for a specific curing period
Jacobson et al (2002), Virginia Tech and VDOT, United States	Bulk samples with minimized exposure to air and stored at 100% Relative humidity at 20°C	50 mm diameter and 100 mm tall one time use plastic molds which can be easily tearable during sample extraction	Kitchen Aid dough mixer with dough hook. Outer spindle rotating at 155 rpm and inner spindle at 68 rpm to mix sufficient sample to form a batch of eight samples	Mixing duration of 5 minutes with intermittent hand mixing. 25 mm (1 inch) thick lifts in molds, poking with 5 mm brass rods evenly 25 times. 100 kPa pressure for 5-10 seconds using a 48 mm aluminum piston.	Cured at 100% relative humidity and 20±3 °C for 7, 14, 28 and 56 days

NOTE: VDOT- Virginia Department of Transportation

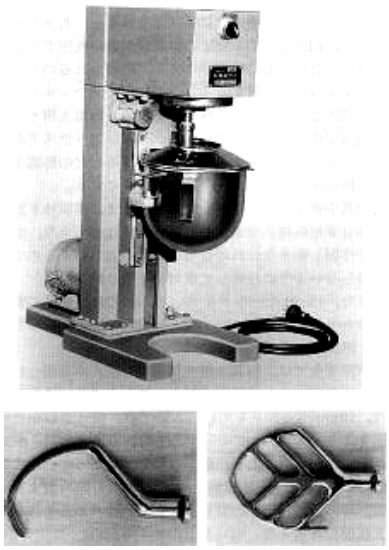

Figure 2.11 Domestic dough mixer and mixing blades (JGS 0821-2000).

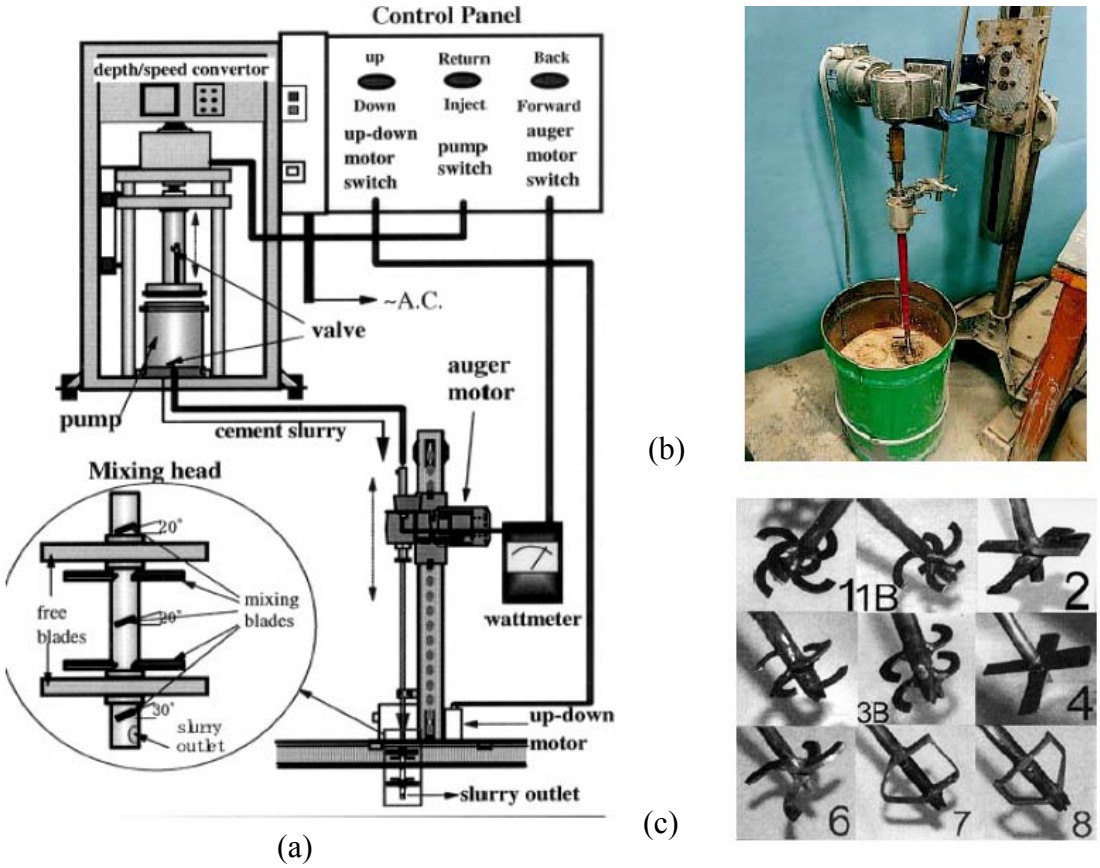

Figure 2.12 (a) Schematic of prototype soil-binder mixing device (b) Experimental setup and (c) Various blades for soil-binder mixing (Al-Tabba et al. 1999 and Shen et al. 2003).

The specimen preparation procedure for stabilized peat samples is different from that of clayey soils, as they differ in their structure and compressibility behavior (Pousette et al. 1999). In the process of establishing a standard method for peat, the authors studied several factors - size of specimens, mixing time, mixing device, curing time and applied load during this time and different peat qualities. The steps proposed by the authors (Pousette et al. 1999) in specimen preparation include:

1. Mixing peat for about a minute to homogenize prior to adding stabilizer.
2. Specimens of 50 mm and 68 mm dia. were tested and a slight scatter in the results of 50 mm dia. results was noticed. However, this variation was in acceptable limits and therefore either of the sizes can be selected based on the research requirement.
3. Two different kitchen mixers were used to simulate DSM in the laboratory environment. The dough mixer shown in Fig. 2.11 is found to be effective in mixing the soil and stabilizer uniformly.
4. Mixing times of 1, 2 and 5 minutes were tried and it was found that 2 minutes is good enough for mixing peat and stabilizer uniformly. Mixing times of 1 minute is too small to achieve uniform mixing and 5 minutes is too long and break the fibrous structure of peat, respectively.
5. The stabilized peat sample is packed in 0.79 to 1.18 in. (2 to 3 cm) layers up to a height of 5.9 in. (15 cm). For each layer, the mass is placed into the tube and distributed and packed with a small rod to avoid any cavities. This can be done in several steps to achieve uniform packing. A rod of about 40 kPa is then placed on the layer for 5 to 10 seconds to pack the whole layer.

6. Curing conditions - the specimens prepared in tubes are placed in a consolidation box and loaded with a rod equivalent to 40 kPa. This load corresponds to an embankment in field.

2.6.2 Effects of Type, Characteristics and Conditions of Soil to be Improved

Deep soil mixing is applicable over a wide range of soil types including clays, clayey silts, sands, sandy silts, organic clays and peat (Hausmann 1990; Ahnberg et al. 1995; Rathmayer 1997; Porbaha 1998; Japanese Geotechnical Society 2000; and Bruce 2001). But, in the case of organic soils the degree of improvement is less likely to be in the same order as that for inorganic soils at practical dosages of stabilizer. The major soil properties observed to have significant influence on strength development are pH, I_L (ignition loss), w_n (natural water content) and F_c (fines content) (Gotoh 1996 and Babasaki et al. 1996). The parameters pH and I_L showed significant effect on strength development compared to w_n and F_c. Soils with low pH values exhibited low strength gains even though there is a tendency of increase in strength with stabilizer content.

The correlations between unconfined compressive strength (UCS) and I_L and pH also indicated low strengths for soils with $I_L > 15$ % and pH < 5 even at high stabilizer contents (Babasaki et al. 1996). This is primarily due to the absorption of some of the calcium ions from the stabilizer by organic material in the soil to satisfy its cation exchange capacity (Arman and Munfakh 1972). The subsequent reduction in calcium ions for pozzolanic reactions results in very low strength enhancements. This behavior was noticed in recent studies of Babasaki et al. (1996) and Jacobson et al. (2003).

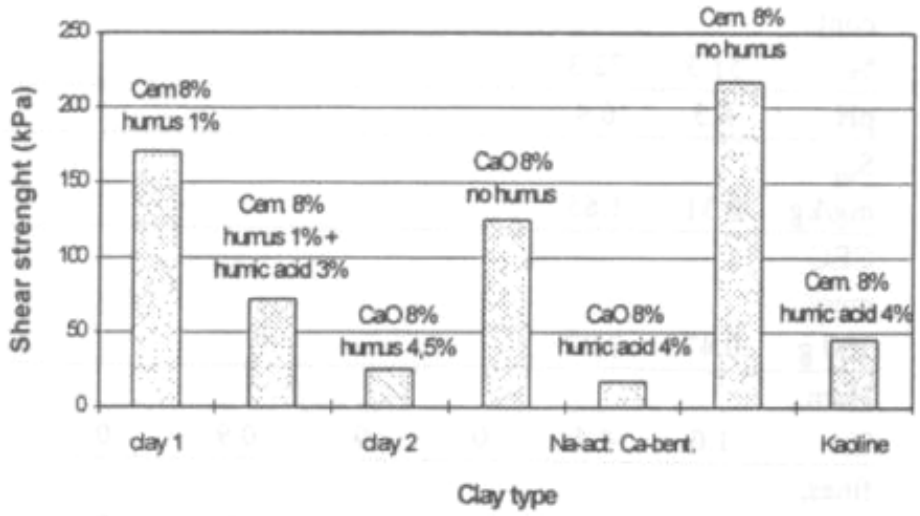

(a)

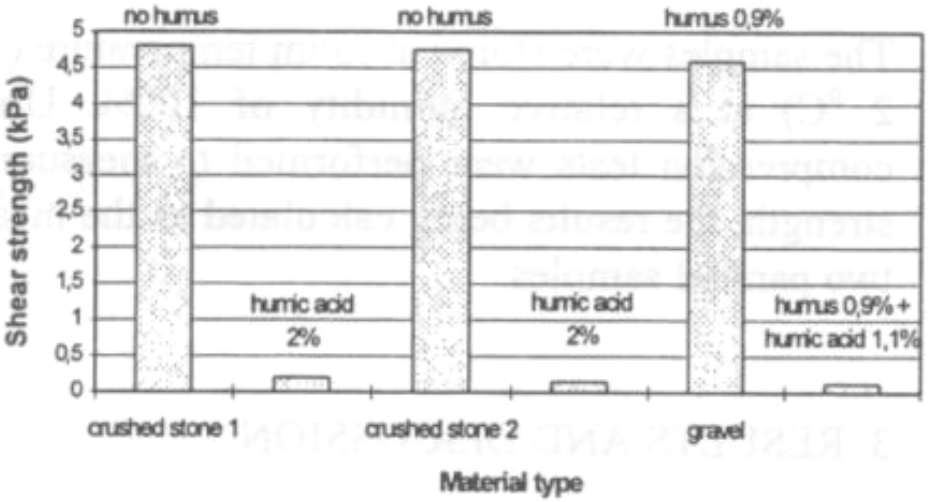

(b)

Figure 2.13 Effect of organic matter on strength gain of treated (a) Fine grained soils and (b) Coarse grained soils (Kujala et al. 1996).

The strength development of treated soils was also related to the degree of decomposition of organic matter present in the soils. In general, as the decomposition increases the achievable strength decreases as it alters both chemical and physical properties of the soil (Huttumen and Kujala 1996, and Hampton and Edil 1998). A significant portion of organic matter in soils contains humified material, i.e., humus, and has detrimental effect on strength properties, even

when I_L is below 15 % (Kujala et al. 1996 and Babasaki et al. 1996). Kujala et al. (1996) reported the effect of humus content on strength properties of various treated soil types. Results from laboratory tests revealed that coarse grained soils scarcely showed any increment in strength and the effect was similar in the case of fine grained soils also, even though not so pronounced (Fig. 2.13).

The presence of organics content, in considerable amounts, in soils also affects the initial conditions (Atterberg Limits and pH) based on the method of sample preparation for subsequent laboratory treatment and testing (Jacobson et al. 2003). The sample preparation methods followed include sealed (in situ), air-dried and oven dried conditions. Soil characterization tests on these soil samples revealed a decrease in pH and Atterberg Limits, upon drying, making the soil more acidic and less plastic. Strength tests on treated samples indicated low strength gain for soils subjected to drying and was primarily attributed to a decrease in Atterberg Limits rather than a change in pH (Fig. 2.14).

Most of the studies mentioned above used cement as the stabilizing agent but those involving lime showed a detrimental effect on strength enhancement (Kujala et al. 1996; Hebib and Farrell 1999; Axelsson et al. 2002; and Jacobson et al. 2003) as lime increases the solubility of organics. The increase in solubility allows uniform distribution of organics, which interferes with soil-lime reactions retarding the rate of and overall strength gain. They also reported the reverse trend in the presence of sulfates, i.e., decrease in organic solubility and thereby less interaction with lime-soil reactions. In cases of treatment involving a combination of stabilizers, low strengths were noted with an increase in the lime proportion (Hebib and Farrell 1999, and Jacobson et al. 2003).

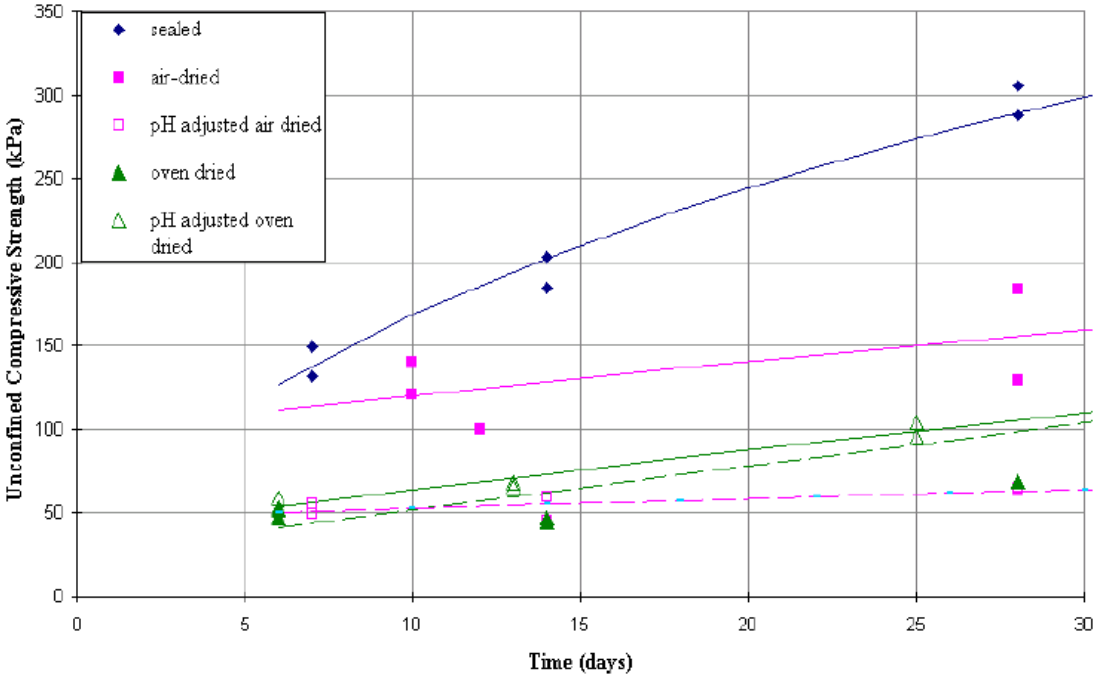

Figure 2.14 Effect of soil preparation on strength after treatment (Jacobson et al. 2003).

The parameters of soil other than organic matter that affect improvement by in situ mixing include soil characteristics such as type of clay minerals, soil consistency, percent of fines etc. (Babasaki et al. 1996). Earlier, Taki and Yang (1990) reported extensive data on 7- and 28-day compressive strengths of various cement treated sands and silts. Analysis of the data indicated the presence of fines in cohesionless soils play a major role in the degree of improvement. Silty sand with 42% of fines has recorded the highest unconfined compressive strength (Fig. 2.15). Later, Chen et al. (1996) reported similar results based on statistics of laboratory tests on several hundred samples from different locations in Shanghai. A maximum increase in strength was noticed in the case of sandy soil.

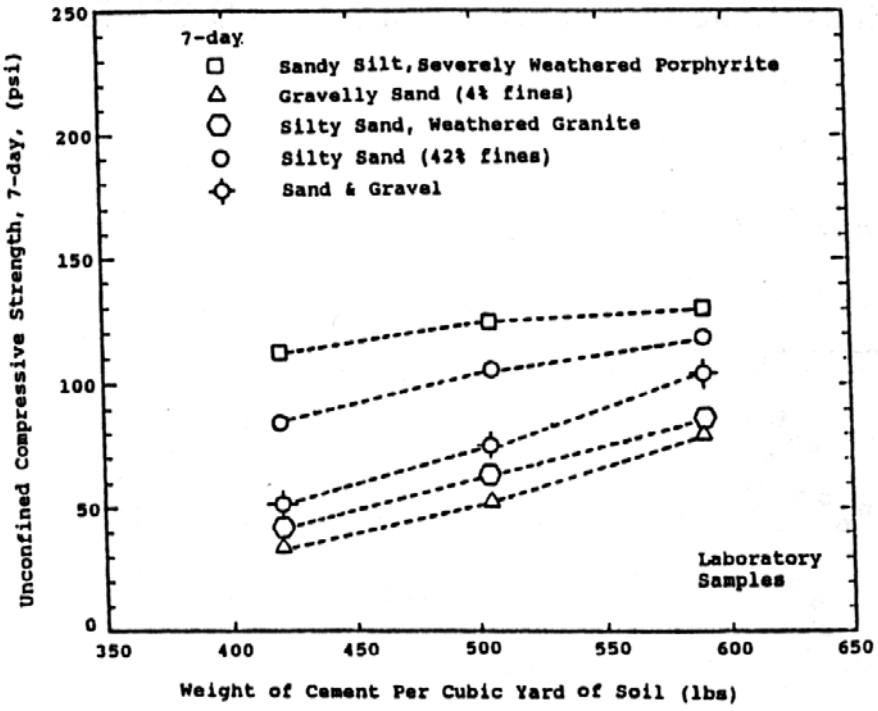

Figure 2.15 Effect of soil type on 7-day unconfined compressive strength of cement stabilized soils (Taki and Yang 1990).

2.6.3 Effects of Stabilizer Type and Dosage Rate

The selection of stabilizer type and amount is one of the major steps involved in the design of deep stabilization. The effectiveness of improvement varies based on type and amount of stabilizer, as different stabilizers build up strength in different ways, and the effect is more predominant in peat and organic soils than in clays (Babasaki et al. 1996; EuroSoilStab 1997 and Axelsson et al. 2002). The most widely used stabilizers for improvement of soft and expansive soils behavior include lime and cement. Other newly developed binders include industrial byproducts such as gypsum, different types of slags and ashes including fly ash and bottom ash. These stabilizers are modified to suit soil stabilization and are used in combination with lime, cement or both to enhance the pozzolanic reactions, retard the setting time for construction convenience or as a low-cost substitute (Babasaki et al. 1996, and EuroSoilStab 1997). The

following sections briefly present the interaction of these binders with soil and later on the strength as a function of stabilizer quantity.

Lime is one of the oldest and most versatile chemical stabilizers used in practice (Little 1995). Most commonly used and successful forms of lime in soil stabilization are quick lime [CaO] and calcium hydroxide or hydrated lime [$Ca(OH)_2$]. On addition to the soil to be treated, quick lime reacts immediately with pore water in the soil, forms hydrated lime and generates high hydration temperatures. These high temperatures contribute to faster reactions and subsequent strength gain of treated soil (Ahnberg et al. 1995 and EuroSoilStab 1997). Jacobson et al. (2003) reported, based on previous research, that quick lime produces a better stabilization effect than hydrated lime. The chemical reactions accountable for strength development and/or mitigation of shrink-swell behavior of treated soils with both forms of lime are identical except for heat of hydration, which is high in the case of quick lime. The details of soil-lime reactions are presented in section 2.3.2.1. However, these reactions and subsequent effects on treated soil can be summarized as follows (EuroSoilStab 1997):

- hydration of lime → drying of soil
- ion exchange reactions → modifies soil structure

} Phase I reactions

- increase of pH → release of Si and Al from soil
- pozzolanic reactions → Ca ions react with Si and Al ions forming cementitious products including CSAH, CSH and CAH resulting in strength gain with time.

} Phase II reactions

Cement is another stabilizing agent that is widely used, mostly in combination with lime, for soil improvement after lime. Cement is a hydraulic binder; i.e., self-setting upon contact with water and is formed by adding gypsum to cement clinker and then grinding it to powder. The reactivity of cement increases with a decrease in grain size (EuroSoilStab 1997; Babasaki et al.

1996, and Axelsson et al. 2002). The commonly used forms of cement based on soil conditions are Type I, Type II, Type I/II and Type V. Type I is ordinary Portland cement for general use. Type II and Type V are modified in their chemical composition from Type I to obtain moderate and high sulfate resistant cements, respectively, while the cement Type I/II offers the combined characteristics of both Types I and II.

The physico-chemical changes involved and subsequent improvement of soil properties in cement treatment were discussed in section 2.3.2.2. However, it should be noticed that the reaction products produced in the long term are the same as in the lime stabilization and approximately $1/5^{th}$ in the quantity. Also, because of the hydraulic nature of cement, cementitious reactions take place faster than pozzolanic reactions and help in early strength gain (Ahnberg 2006; Axelsson et al. 2002; EuroSoilStab 1997; Babasaki et al. 1996).

Other stabilizing agents such as fly ash and ground granulated blast furnace slag (GGBFS) are used in combination with lime and/or cement based on the mix design and economic aspects of the project. Fly ash and GGBFS are fine powdered materials produced as residual products in thermal power plants and from iron smelting, respectively. Based on the percentage of major oxides (Al_2O_3+SiO_2+Fe_2O_3), fly ash is classified as Class F (≥70%) and Class C (<70%) (ASTM C618). Class F fly ash is low in CaO content and possesses pozzolanic properties, whereas Class C fly ash is rich in CaO content and has self-cementing properties along with a pozzolanic nature. GGBFS is a latent hydraulic material and requires an activator such as $Ca(OH)_2$ from lime or cement to initiate reactions with its own lime content (Janz and Johansson 2002, and Ahnberg 2006).

The reactivity of fly ash and GGBFS depends on their source and the process of formation. As such, quality assessment of these materials prior to their use in deep stabilization is necessary (Janz and Johansson 2002). Overall, fly ash, also being low in CaO content, needs an external source of $Ca(OH)_2$ from lime or cement for pozzolanic reactions. Therefore, both fly ash and GGBSF are recommended not to be used solely as binders but only as additives to lime or cement (Janz and Johansson 2002). The principle chemical reactions involved and the resulting reaction products were almost similar for all these binders in soil stabilization (Fig. 2.16).

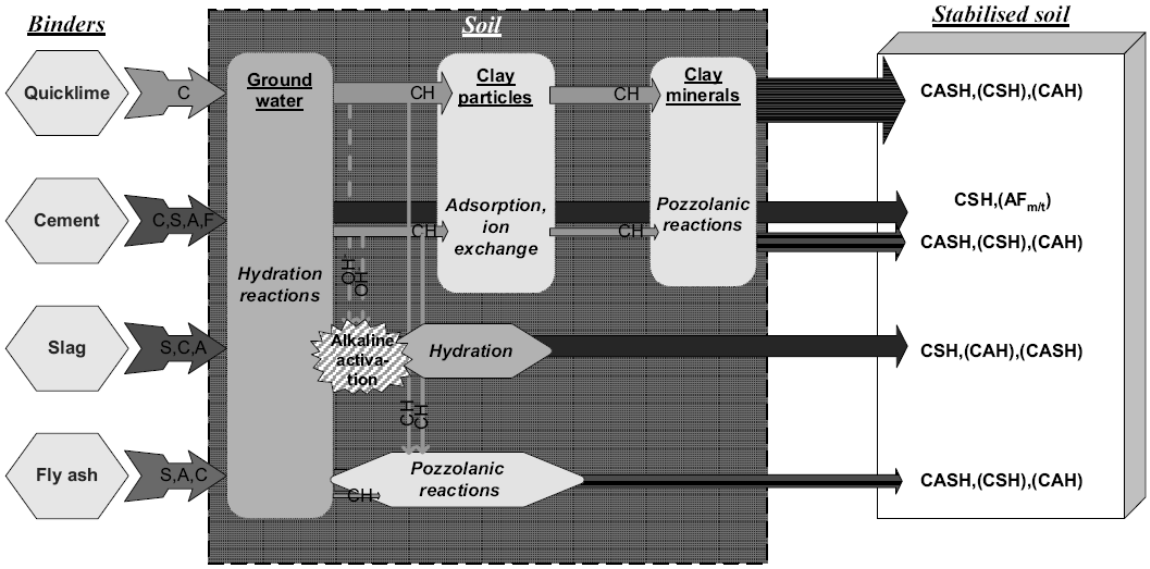

Figure 2.16 Principal chemical reactions and subsequent products formed in soil by different binder types (Ahnberg and Johansson 2005).

Based on the above discussion, it can be expected that the process of strength development, which involves ion exchange, cementitious reactions and secondary pozzolanic reactions of treated soils differs depending on the type of binder. The rate of these reactions is strongly dependent on the surface area of binders and hydration temperatures, which are high in the case of cement and lime, respectively. The strength development is also associated with the amount of reaction products formed during and after stabilization of soil (Ahnberg et al. 1995,

and Ahnberg 2006). As shown in Fig. 2.17 the highest amount of reaction products were produced in lime treatment as compared to others, in the long term. However, cement treatment results in early strengths due to the formation of cementitious product, CSH, within a few hours of treatment as compared to lime treatment. The delay in strength development of lime treated soils is attributed to the slow rate of pozzolanic reactions (Fig. 2.18).

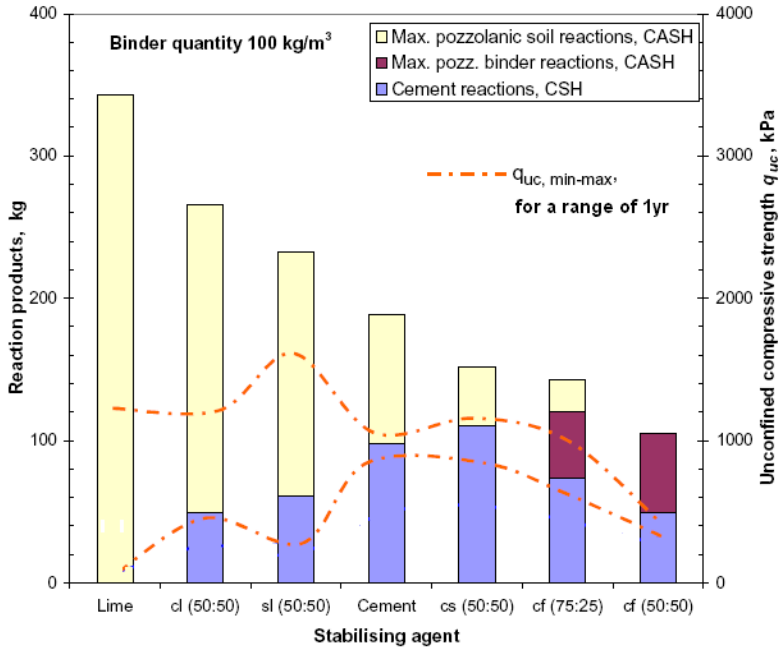

Figure 2.17 Production of reaction products in soil treated with different binder types (Ahnberg and Johansson 2005)

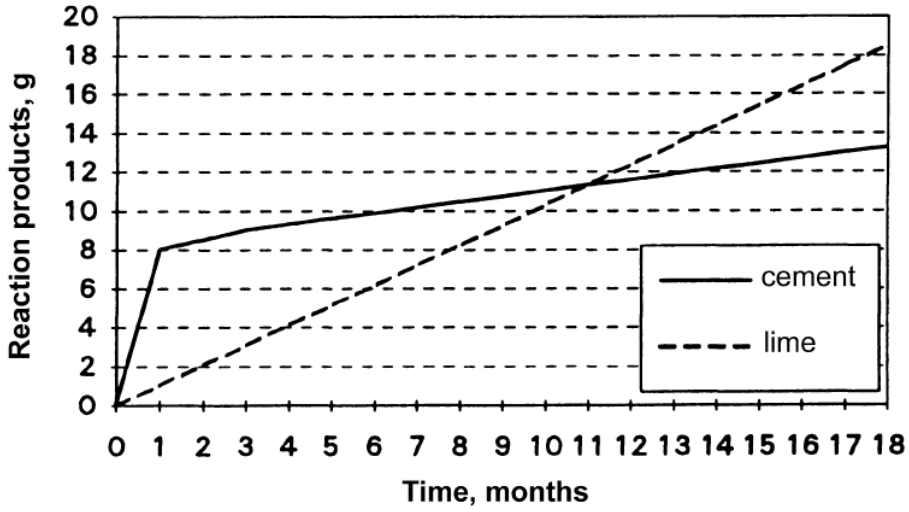

Figure 2.18 Production of reaction products in lime and cement treatments with time (Ahnberg et al. 1995).

Along with the type of binder, the optimum amount of binder is also important to achieve the target strength as per the project requirement. The more the quantity of binder, the weight of reaction products formed will be high, provided that the soil or additive has enough pozzalon, resulting in higher strengths. In this case, all the pozzalonic in the soil mass is consumed, and then addition of more quantity of stabilizer doesn't give an increase in strength. The general relationship between strength and binder quantity is as shown in Fig. 2.19. It reveals that a minimum quantity of binder is necessary to produce a load-bearing soil skeleton. For a given type of soil and stabilizer, the increase in binder content results in increased strengths (Ahnberg et al. 1995; Asano et al. 1996; Babasaki et al. 1996; Chen et al. 1996; EuroSoilStab 1997; Jacobson et al. 2003; Taki 2003; and Huat et al. 2006) (Fig. 2.20a) and reduced swell and shrink of expansive soils (Basma et al. 1998; Nalbantoglu and Tuncer 2001) (Fig. 2.20b). The increase in strength is high in the case of coarse grained soils compared to those with fine grained soils as noticed in studies reported by Haut et al. (2006); Taki (2003) and Chen et al. (1996), (Fig. 2.20a). Although an improvement of 250 % is observed in the case of organic soils at 10% cement content, it is found to be insignificant as compared to the improvement in the inorganic soils.

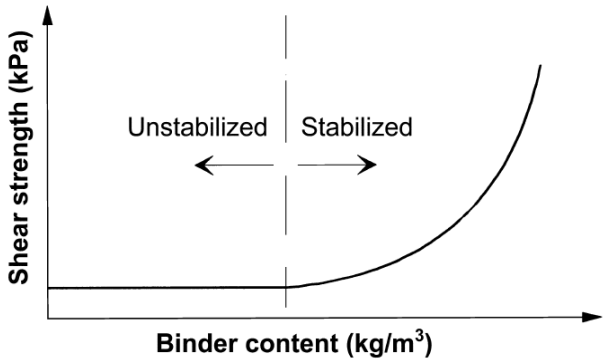

Figure 2.19 General relationship between binder content and strength gain (Janz and Johansson 2002).

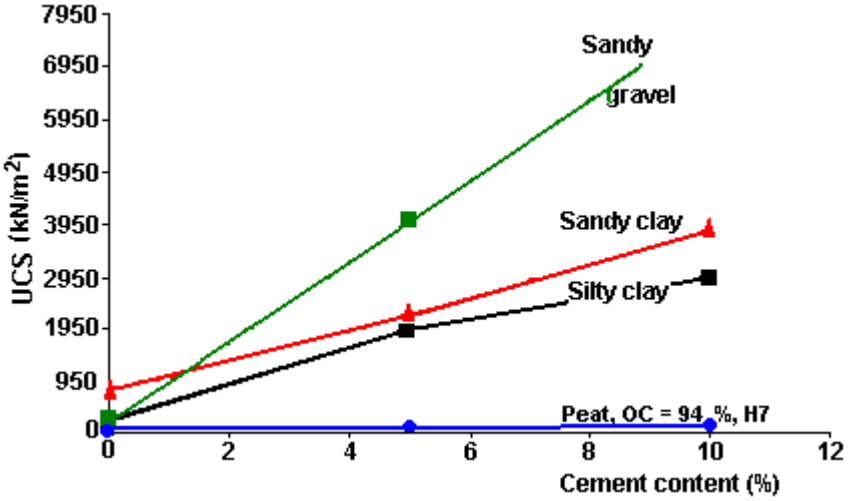

(a)

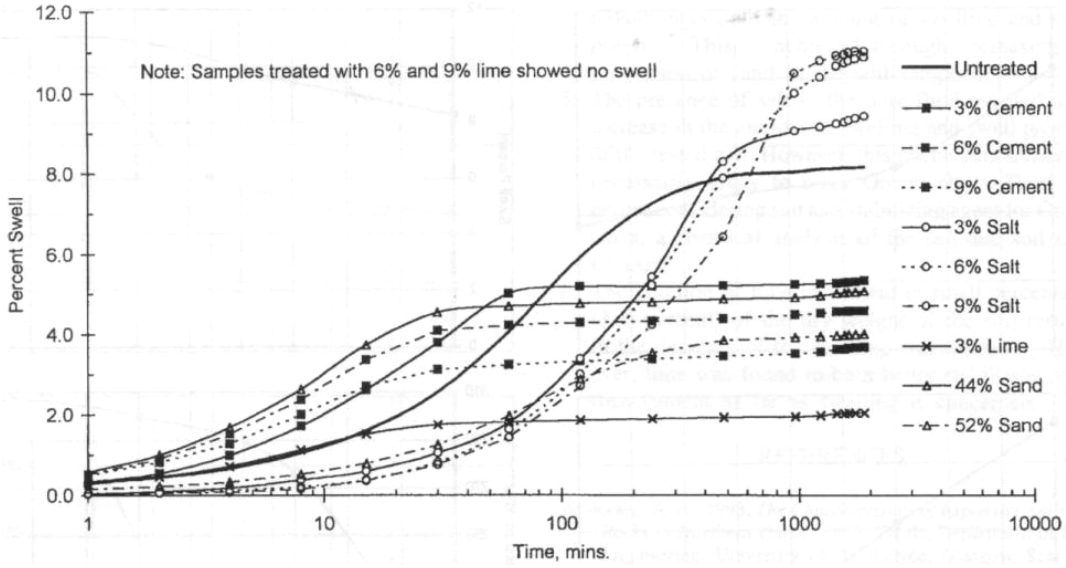

(b)

Figure 2.20 Effect of binder content on (a) 28-day strength of various soils (Huat 2006) and (b) Shrink-swell properties (Basma et al. 1998).

This shows that the organic matter significantly inhibits the chemical reactions between the stabilizer and soil minerals. The same has been reported in the studies performed at the Swedish Deep Mixing Research Centre.

From the previous studies mentioned above, it is noticed that a combination of cement and lime would provide better or even higher strengths than cement alone. Hydration of cement produces cementitious gel (CSH) that binds soil particles together, thereby resulting in early strength gain. At the same time, hydration of lime generates high temperatures, which enhance cementitious reactions, and large amounts of $Ca(OH)_2$ useful for pozzolanic reactions and ion exchange. The optimum mix of lime and cement is in the range of 60 to 90% (Cement) and 40 to 10% (Lime) (Ahnberg et al. 1995). The effect of binder quantity on inorganic soils is as mentioned above. But in the case of sulphide soil and organic soils (gyttja and peat) the effect of lime and lime-cement is not as pronounced as that of cement. The ineffectiveness of lime in these soils is explained in section 2.4.2. Similar results were reported by EuroSoilStab (1997) based on laboratory tests on different soils using various binder combinations (Table 2.2). This can be used as a guideline for the selection of binder type depending on the soil type to be treated.

Table 2.2 Relative strength increase based on laboratory tests on Nordic soils with various binders (unconfined compressive strength after 28 days) (EuroSoilStab,1997).

Binder	Silt Organic content 0-2%	Clay Organic content 0-2%	Organic Soils, e.g. Gyttja Organic Clay Organic content 2-30%	Peat Organic content 50-100%
Cement	xx	x	x	xx
Cement + gypsum	x	x	xx	xx
Cement + furnace slag	xx	xx	xx	xxx
Lime + cement	xx	xx	x	-
Lime + gypsum	xx	xx	xx	-
Lime + slag	x	x	x	-
Lime + gypsum + slag	xx	xx	xx	-
Lime+ gypsum + cement	xx	xx	xx	-
Lime	-	xx	-	-

xxx very good binder in many cases
xx good in many cases
x good in some cases
- not suitable

2.6.4 Effect of Water-Binder Ratio

One important constituent necessary for soil-stabilizer (lime/cement) reactions in chemical stabilization is water, which is available either in the form of in situ water content or stabilizer slurry. Water is essential for hydration of stabilizer and also for good and efficient mixing (Bergado and Lorenzo 2005). It is reported that in the conventional design of DSM columns, stabilizer content is used as the controlling parameter at a given curing time since it is considered as the sole factor affecting strength development (Kamon and Bergado 1991; Bergado et al. 1996 and Lorenzo et al. 2006). However, subsequent and some recent literature showed that strength development is also a function of water content in the treated soil matrix for a given soil type and mixing conditions. A unique relationship is obtained between water/binder (w/b) ratio and strength from unconfined compression tests on treated specimens (Rathmayer 1997; Asano et al. 1996; Saitoh et al. 1996; Miura et al. 2001; Janz and Johansson 2002; Jacobson et al. 2003; Lorenzo and Bergado 2004; Horpibulsuk et al. 2005; Bergado and Lorenzo 2005; Lorenzo et al. 2006; Lorenzo and Bergado 2006). It should be noted here that some of the studies mentioned considered the water quantity added from stabilizer slurry only, i.e., wet mixing method, in the ratio. Others, including most recent studies, emphasized the free water quantity present in the treated soil matrix to take into account the variations in situ water content at the time of actual construction. Also, according to Abram's Law in concrete technology, it is the ratio of free water content to stabilizer content that determines the strength of the mix and is independent of their absolute quantities. Therefore, as an analogy to soil-stabilizer-water mix, it is the ratio of total clay water content to binder content (w_c/b) that controls the engineering behavior of treated soils (Miura et al. 2001). The following paragraphs discuss some of the recent studies on the role of water to stabilizer ratio on the behavior of treated soil.

The total clay water content (w_c) is the sum of remolding or the in situ water content of the base clay (w^*) plus water in the stabilizer slurry. The parameter, w_c, is defined by Lorenzo and Bergado (2004) as follows:

$$w_c = w^* + \left[\frac{w}{b}\right](A_w) \tag{2.8}$$

where, w/b is the ratio of weight of water to the binder weight of the slurry and A_w is the stabilizer content in percent, defined as the ratio of weight of stabilizer to dry soil. Miura et al. (2001) and Horpibulsuk et al. (2005) revealed that the w_c/b ratio is the primary factor governing the deformation and compressibility characteristics of the treated soil. The changes that occur in the treated soil matrix are at a particle level and related to the soil structure. The clay water content of the matrix reflects the microfabric of clayey soil and stabilizer content reflects the level of cementation of that fabric (Horpibulsuk et al. 2003). It is the combination of these two factors that represents the structural state of treated soil governing the strength and deformation behavior. Therefore, the ratio w_c/b is an integrated parameter representing the structural state of the treated soil and yields a unique relationship with strength for a given curing time (Fig. 2.21) (Miura et al. 2001; Horpibulsuk et al. 2003; and Lorenzo and Bergado 2006).

Based on Abram's law, Horpibulsuk et al. (2003) developed a generalized relationship between strength, w_c/s, and curing time as follows:

$$\frac{q_{(w_c/b)_{1,D}}}{q_{(w_c/b)_{28}}} = 1.24^{[(w_c/b)_{28}-(w_c/b)_D]}(0.038+0.281\ln D) \tag{2.9}$$

where $q_{(w_c/b)_{1,D}}$ is the strength of stabilized clay at a clay water content to binder ratio of $(w_c/b)_1$ after a curing period of D days and $q_{(w_c/b)_{28}}$ is the strength at a ratio of (w_c/b) after

28 days of curing. Using this relationship, one can predict strength for different combinations of (w_c/b) and curing time from the data of only one trial mix after 28 days of curing.

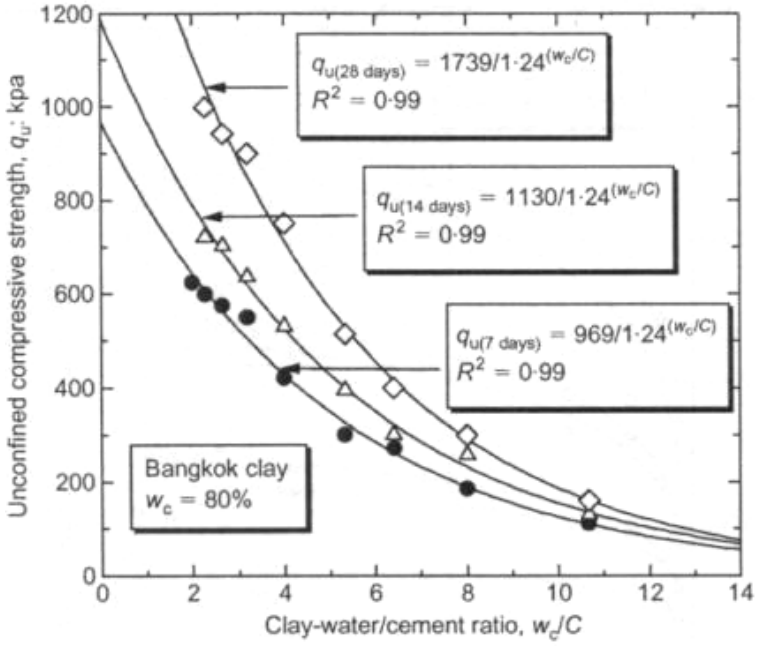

Figure 2.21 Variation of strength as a function of total clay water to binder ratio for different curing periods (Horpibulsuk et al. 2003).

Laboratory tests, including unconfined compression tests, consolidated undrained (CU) and consolidated drained (CD) triaxial tests and oedometer tests on treated Ariake clay exhibited identical behavior as long as the w_c/b ratio remains the same irrespective of various combinations of w_c and s (Horpibulsuk et al. 2005). Based on these experimental observations and clay microstructure Horpibulsuk et al. (2005) proposed the following identity:

$$\left\{\frac{w_{c1}}{b_1}\right\} = \left\{\frac{w_{c2}}{b_2}\right\} = \text{constant} \qquad (2.10)$$

where w_c and b are the clay water content and binder content in the treated soil matrix, respectively. In deep in situ mixing, after fixing the target strength ($q_{(w_c/b)_D}$) required with due considerations from field parameters and laboratory studies the required clay water-binder ratio (w_c/b) can be estimated using Eq. (2.9). Once the ratio is fixed in the field, Eq. (2.10) can be used to calculate modified cement content for any possible changes in clay water content during construction to achieve the specified target strength. Validation of the above relationship between strength and clay water-binder ratio with experimental data given by Soralump (1996) was reasonable and can be found in Horpibulsuk et al. (2003).

A new parameter, e_{ot}/s, as an extension to the one, w_c/s, proposed by Miura et al. (2001); Horpibulsuk et al. (2003) and Horpibulsuk et al. (2005), was developed by Lorenzo and Bergado (2004) to take into account the effect of curing time for the characterization of treated soil. The variables e_{ot} and s are after curing void ratio and binder content of stabilizer admixed soil, respectively. Along with curing time, the ratio, e_{ot}/s, also accounts for both before and after treatment conditions of the soil (Lorenzo and Bergado et al. 2004). Results from UCS tests on both laboratory and field specimens revealed that the ratio, e_{ot}/s, yielded a unique relationship with strength, q_u, (Fig. 2.22) combining the effects of clay water content, cement content, curing time and pressure (Lorenzo and Bergado 2004 and Lorenzo and Bergado 2006). The following empirical correlation has been proposed by these researchers based on their study:

$$q_u = Ap_a e^{B\left(\frac{e_{ot}}{s}\right)} \qquad (2.11)$$

where p_a is the atmospheric pressure; s is the stabilizer content; A and B are dimensionless constants depending on type of admixture and base clay, respectively. A simplified expression for estimating after curing void ratio, e_{ot}, based on unit weight and specific gravity of base clay, cement content, clay water content and curing time can be found in Lorenzo and Bergado (2004).

From Fig. 2.22, it can be noticed that the strength increase as the ratio, e_{ot}/s, decreases. Other laboratory tests including CU and oedometer consolidation exhibited the effectiveness of the parameter, e_{ot}/s, in characterizing the strength and compressibility of stabilized soils at high water content. In the process a number of empirical correlations related to strength, compressibility and elasticity were developed (Lorenzo and Bergado 2006).

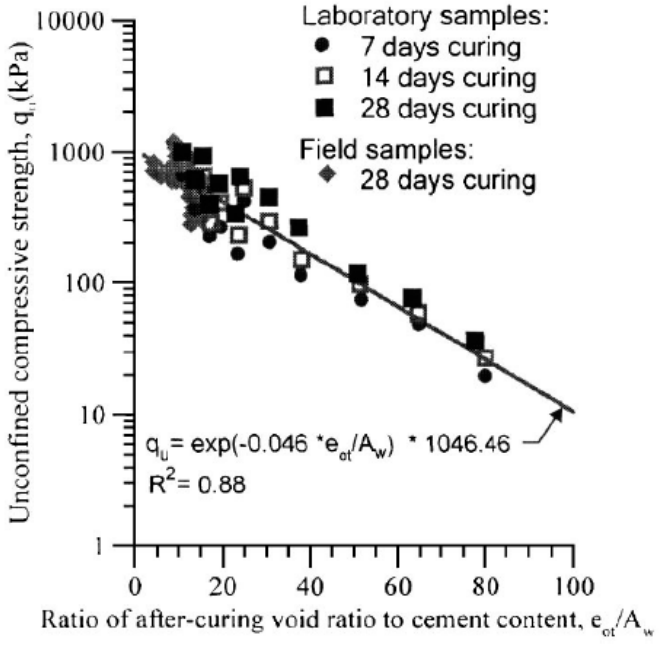

Figure 2.22 Strength as a function of after curing void ratio to binder content (e_{ot}/A_w).

Results from UCS and oedometer tests (Fig. 2.23) further revealed that there exists an optimum mixing clay water content ($C_{w.\ opt}$) at which the treated soil exhibits optimum improvement in engineering properties after the curing time (Lorenzo et al. 2006). The authors further confirmed the existence of $C_{w,\ opt}$, through a strength curve (Fig. 2.24) and schematic diagrams (Fig. 2.25) depicting the state of the treated soil matrix at different mixing clay water contents. High mixing water content results in reduced number of clay to clay contacts to be bonded due to the loss of electrostatic attraction of clay particles (Fig. 2.25b). This leads to

increased void ratios and subsequent low strengths, as indicated in strength curve $C_w/LL > 1.1$. The case of low mixing water content results in an unsaturated condition, i.e., some portion of the voids is occupied by air, and suppresses the dispersion ability of cementing ions. Therefore, some portions of the soil-stabilizer matrix may remain unmixed resulting in a non-uniform mixture (Fig. 2.25[d]) and low strengths, as reflected in strength for $C_w/LL < 1.0$. This illustrates that the range of $C_{w,\ opt}$ is from 1.0 to 1.1 time the liquid limit (LL) of the base clay. Thus, optimum mixing clay water contents provide an efficiently and economically mixed DSM column along with the highest improvement in its engineering properties.

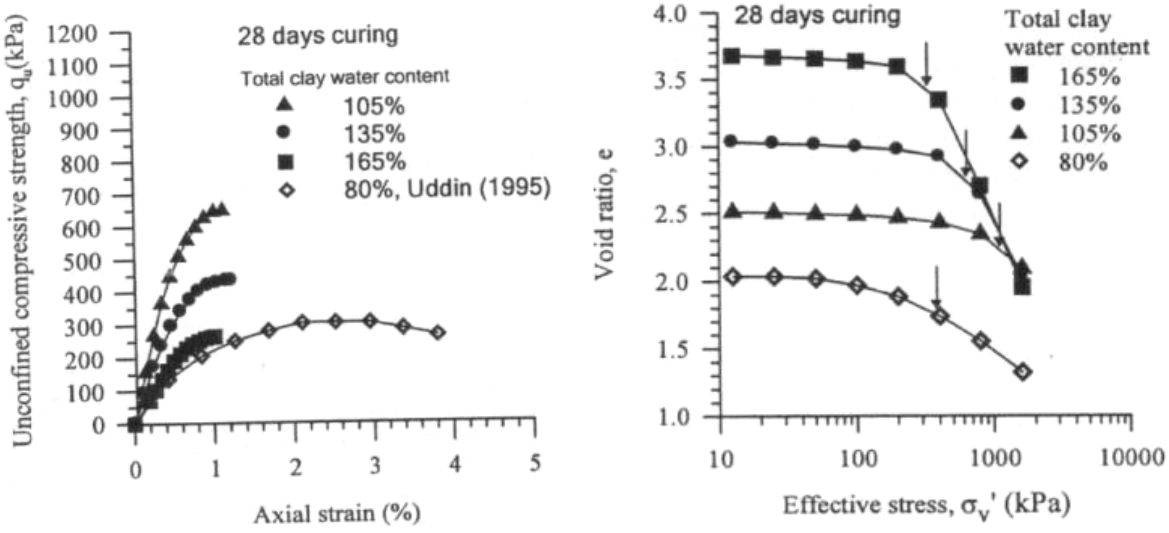

Figure 2.23 Typical Results from UCS and oedometer tests confirming the existence of optimum mixing clay water (Lorenzo et al. 2006).

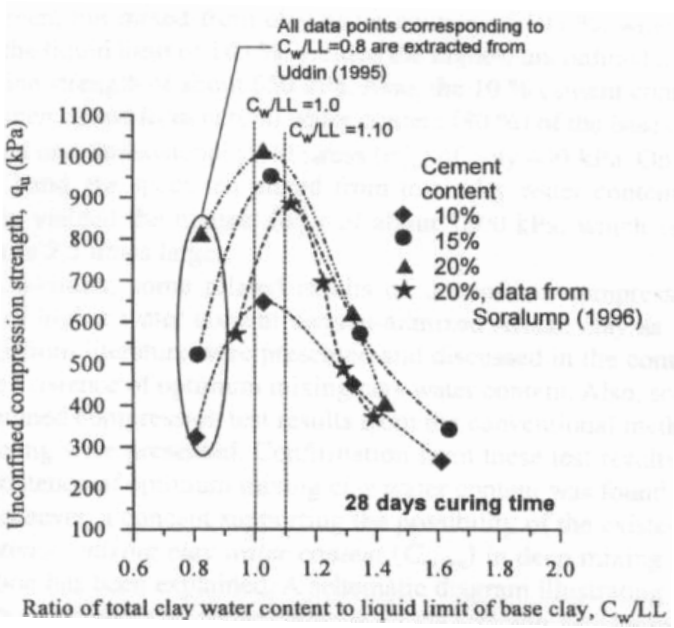

Fig 2.24 Strength curve of cement treated soil (Lorenzo et al. 2006).

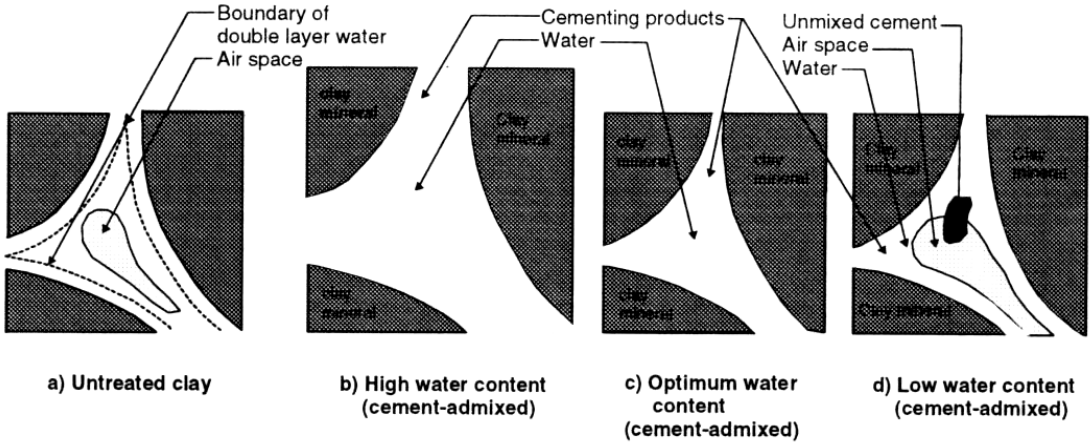

Figure 2.25 Schematic of cement admixed clay skeleton showing the effect of total water content (Bergado and Lorenzo 2005).

2.6.5 Effects of Curing Conditions

Curing conditions that effect the improvement of treated soils include curing temperature, time and environment (Babasaki et al. 1996). The rate of soil-binder reactions is dependent on the temperature. Stabilizers such as lime and cement release heat raising temperatures of treated soil matrix within the range of 15 to 50°C (Rathmayer 1997; and Babasaki et al. 1996). This helps in accelerating the rate of soil-binder reactions and thereby enhances the short-term strength gain. The increase in early strength gain is associated with increased amounts of cementitious products formed. However, variations in heat evolution can be found based on the type of binder (Fig. 2.26). This implies that binders with high heat evolution (lime and cement) are less dependent on the temperature of ambient soil than those with low heat evolution (GGBFS) (Axelsson et al. 2002). Therefore, in the case of soil stabilization with low exothermic agents, low early strength gains result if the temperature of the ambient soil mass is low.

Babasaki et al. (1996) presented a linear increase in strength with temperature for a given curing time (Fig. 2.27). Therefore, it becomes imperative to cure laboratory specimens at temperatures that closely represent those produced during in situ mixing — to reduce its influence in the selection of stabilizing agent through comparison of relative effectiveness of different binders. Few methods suggested in the literature to maintain temperature and humidity representative to in situ include insulating specimens using polystyrene casings, curing under water or sealing specimens in airtight tubes (Den Haan 2000).

Fig. 2.28 also depicts the effect of curing time on strength at a given curing temperature. Similar results were reported in the literature by several researchers based on their studies, of which typical results on Ariake and Bangkok clays were shown in Figure 2.28. The stabilizer used in these cases is cement with liquidity index of clay varied from 1.0 to 2.0. From Fig. 2.28(a) and 2.28(b), it is clear that most of the strength development in cement stabilization

is achieved during the first month. Whereas, in case of lime stabilization strength gain continues for several months depending on the rate of pozzolanic reactions between soil and lime. The same has been noticed by EuroSoilStab (1997) in their laboratory studies with different binder types – cement, lime, GGBFS and fly ash and at varying proportions with soil. Therefore, it is practical to assess the strength of treated soil as a function of clay-water content, curing time and temperature for the given improvement process.

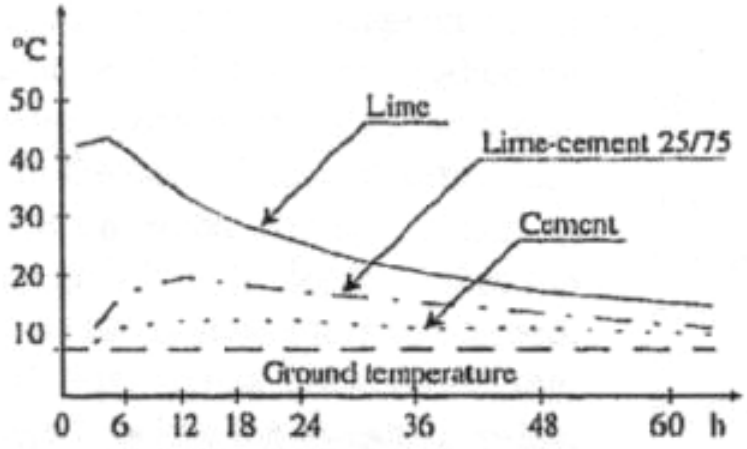

Figure 2.26 Evolution of heat during soil-binder reactions (Rathmayer 1996).

Babasaki et al. (1996) expressed the following relation, similar to that in concrete technology, between strength, curing temperature and time based on the experimental data of five different treated soil types from previous research (Enami et al. 1985; Horiuchi et al. 1984; and Babasaki et al. 1984):

For any given curing temperature and time,

$$q_u = A \log M + B \qquad (2.12)$$

$$\text{and } M = \int_0^t 2x \exp \frac{T+10}{10} dt \qquad (2.13)$$

where M is maturity in days.^{0}C; T is curing temperature and t is curing time in days. The constants A and B are dependent on soil type.

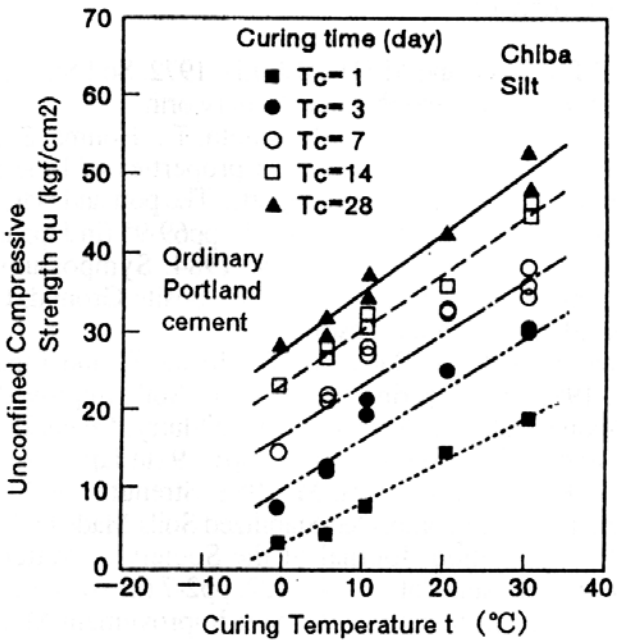

Fig. 2.27 Effect of curing temperature on strength gain (Babasaki et al. 1997).

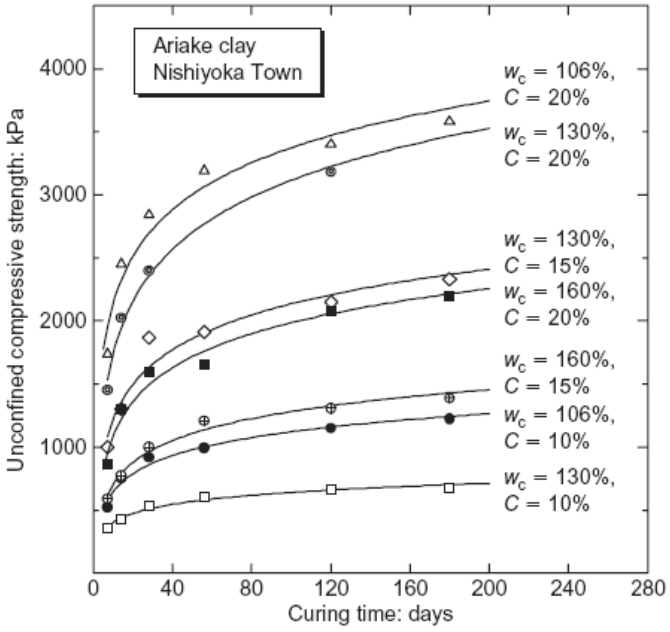

(a)

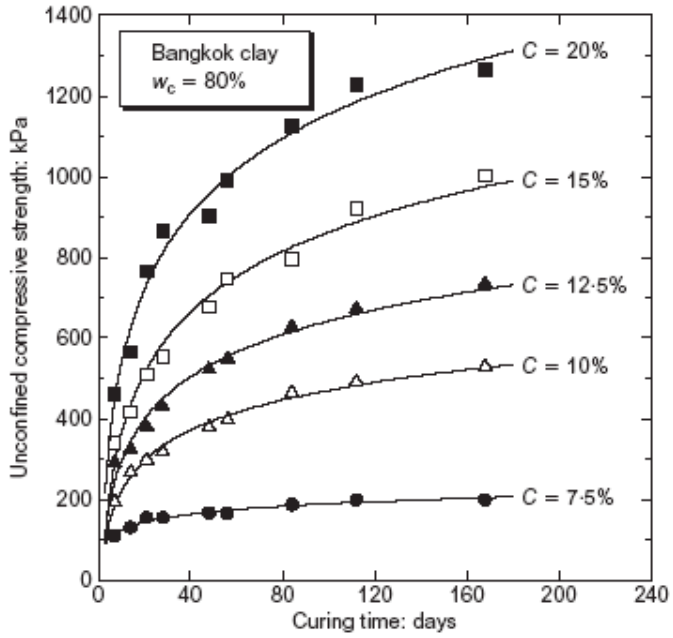

(b)

Fig. 2.28 Effect of curing time on strength for cement contents (Horpibulsuk et al. 2003).

In the process of developing a more generalized relationship, Eq. (2.9), among strength, total clay water content and curing Horpibulsuk et al. (2003) studied the pattern of strength

development with time. It is noted from their investigation of extensive experimental data that q_u varies linearly with the logarithm of curing time (Fig. 2.29) leading to the following empirical relationship for soils with liquidity index of 1.0 to 2.0 and at a particular value of w_c/s:

$$\frac{q_{u,D}}{q_{u,28}} = 0.038 + 0.281 \ln D \qquad (2.14)$$

where $q_{u,\ D}$ and $q_{u,\ 28}$ are strengths of the treated soil at D and 28 days, respectively. Normalization of $q_{u,\ D}$ with $q_{u,\ 28}$ resulted in a unique relation taking into account the effects of variations in clay type, total clay water content, cement content and temperature. Finally, a combination of the above expression (Eq. 2.14) with Abram's law resulted in a more generalized expression, Eq. 2.9, presented in the previous section.

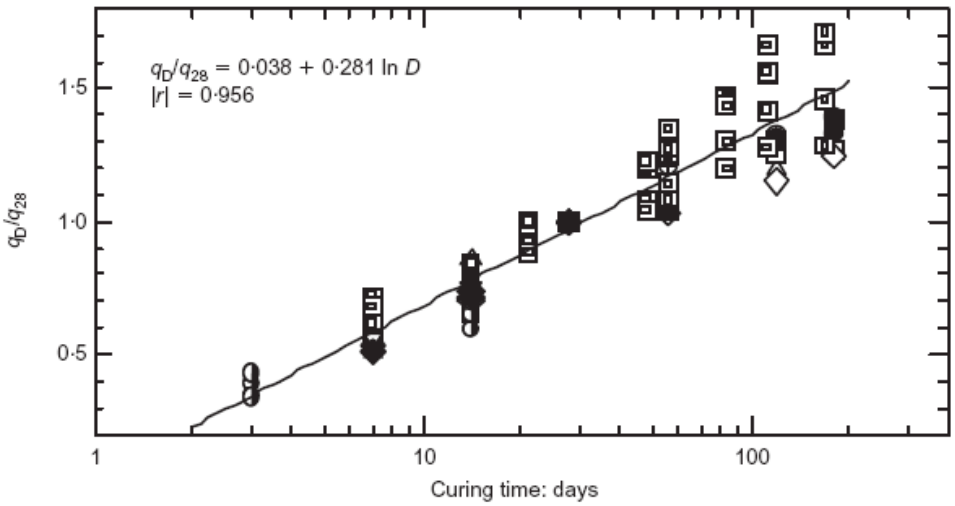

Figure 2.29 Relationship between curing time and strength (Horpibulsuk et al. 2003).

However, the author presents a review of previous research related to the installation effects on DSM columns and surrounding soil; configuration, geometry and spacing of soil-stabilizer (lime and/or cement) columns; studies related to lime piles and/or columns in expansive soils.

2.6.6 Effect of Installation Parameters

Several other factors such as installation rate (both penetration and withdrawal), revolution speed, mixing energy, mixing time and even shape of mixing blades during installation of DSM columns affect the degree of mixing and also the strength gain of treated soils. All these factors along with quantity of stabilizer and water to stabilizer ratio are grouped under mixing conditions by Babasaki et al. (1996). However, not much research has been carried out addressing the effects of these factors on treated soil until recently as it is complex to imitate them in a laboratory environment. Dong et al. (1996) reported an experimental apparatus (Fig. 2.30) simulating in situ mixing conditions and later Shen (1998) developed a small-size soil-stabilizer mixing device referred as model device (Fig. 2.12) for making model columns in the laboratory environment. These developments in testing apparatus at the laboratory level lead to the study of some of these parameters mentioned above.

Dong et al. (1996) constructed model cement columns 40 cm diameter and 100 cm high in a soft clay bed varying rotary speed, withdrawal speed, number of blade revolutions, slurry injection velocity and mixing blade shape and thickness. Results revealed that uniform degree of mixing was achieved at high mixing rotary speeds and subsequently in high strengths. Increase in strength was also noticed with an increase in the number of blade revolutions. Further, in all these cases for the same shape of mixing blades the ones with thin blades resulted in higher strengths. The specifications of the mixing apparatus and various shapes of the blades used in the investigation can be found in the above reference.

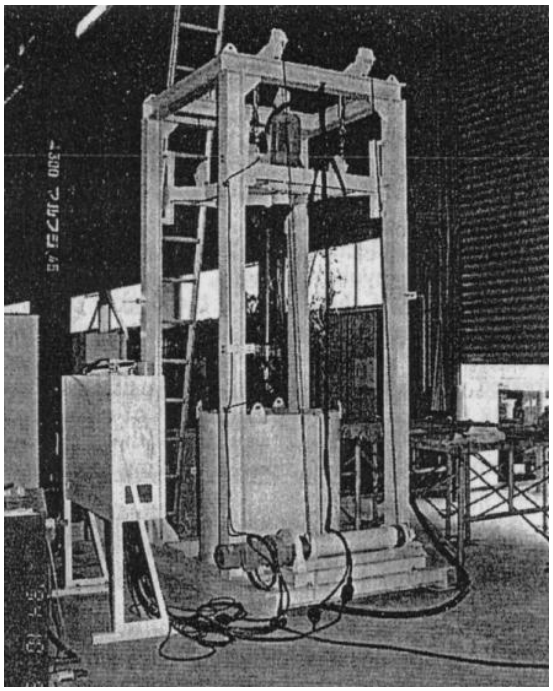

Fig 2.30 Soil mixing apparatus developed by Dong et al. (1996).

Horpibulsuk et al. (2004) performed laboratory studies alongside of a field investigation on Ariake clay to study the effects of installation rate (penetration/withdrawal) on strength development of DSM columns at high water contents. Columns were installed in the laboratory using a model device developed by Shen (1998) by varying the installation rate (0.3 to 1.0 m/min); cement content (54 to 139 kg/m^3) and adjusting w/c to obtain the liquidity index (LI) and w_c/C (clay-water to cement ratio) in the ranges of 1.25 to 1.75 and 7.5 to 15, respectively. The rotational speed of the mixing blade was maintained at 60 rev/min throughout the testing. In order to assess the effects of installation rate, UCS tests were conducted on soil specimens extracted from these columns and cured for 28 days.

Results showed that even though the clay water to cement ratio are the same, the strengths varied with penetration rates and with clay water content (Fig. 2.31). Based on liquidity index, which reflects the state of water content, the mixing states are classified into workable and bleeding states. Experimental results reveal that clay water contents corresponding to LI = 1.5 indicate a workable state that seems to be effective for both low and high cement content

columns at high and low penetration rates. For high clay water contents with LI = 1.75, the mixing conditions at high penetration rates lead to the separation of additional water from the mixed clay. At low water content states (LI = 1.25) high strengths were achieved for both low and high penetration rates for low cement content columns as compared to high cement content columns. Finally, it can be concluded that in order to achieve target strength in the field it is necessary to choose an adequate installation rate along with suitable clay water to stabilizer ratio and the quantity of stabilizer.

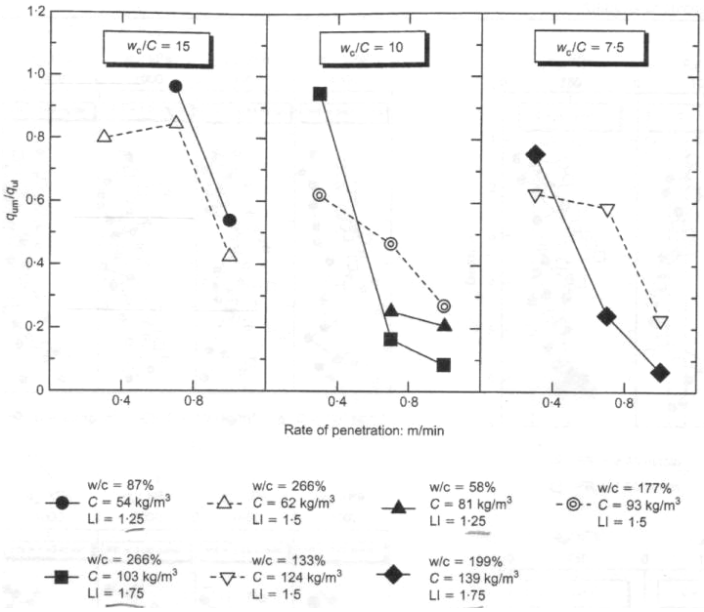

Figure 2.31 Effect of penetration rate on strength for a given total clay water to binder ratio (Horpibulsuk et al. 2004).

Laboratory and theoretical studies by Shen et al. (2003a and 2003c) revealed that mixing conditions such as slurry injection pressure, mixing time and rotation speed of blades affect the properties of the surrounding soil during installation. A total of 9 model columns of 10 cm diameter and 30 to 40 cm deep are installed in a remolded Ariake clay bed. The installation parameters adopted for column construction are a penetration rate of 0.5 m/min, withdrawal rate of 1.0 m/min and a rotation speed of mixer at 30 rpm. Mixing conditions include a w/b of 0.6 to 1.0 and binder (cement) quantity of 200 to 350 kg/m^3.

Results indicated that installation of DSM column resulted in an expanded zone and an influential zone. Expanded zone is the area formed beyond the designed diameter of the column (i.e., mixing blade diameter) by cylindrical expansion due to injection volume of slurry. However, the properties of the surrounding soil are affected much beyond this expanded zone due to shearing action of the mixing blades. The shearing action from rotation of the mixing blades results in fractures around the column in the surrounding clay. These fractures then act as drainage channels for injected slurry and faster diffusion of cations. The consequence of this phenomenon is the change in properties of the surrounding clay in short duration after DSM column installation. In the long term, these property changes are attributed to thixotropy recovery, consolidation and cementation due to ion diffusion. The zone in which properties of the surrounding clay change is referred to as the influence zone. The influence zone due to ion exchange varies based on the type of binder and is reported to be 4 times the column diameter for lime columns (Rajasekaran and Rao 1997) and is limited to the zone of soil fracturing for cement columns (Shen et al. 2003a). Shen et al. (2003a) also noticed that prior to these changes, mentioned above, the undrained shear strength of the surrounding clay decreased during installation of the DSM columns but regained after a short curing period. The decrease in properties is attributed to the disturbance caused during mixing. Based on the laboratory studies,

Shen et al. (2003c) was able to model the above observed interaction between the DSM column and the surrounding clay as the shearing-expanding process of a cylindrical cavity. Analytical results were verified against the laboratory data and indicated that shearing force from rotation of the mixing blades has a significant effect on clay fracturing in the range of 2 to 3 times the column diameter.

Later Shen et al. (2004) extended his laboratory testing to study the influence of mixing energy on strength development of treated Ariake clay. Results of this research led to the following observations:

1. The energy consumption depends on the type of binder, the method of deep mixing (wet or dry), in situ conditions of the untreated soil, rotation rate and mixing sequence.
2. Water in the water-cement ratio reduces the consumption of mixing energy during the first mix down.
3. In the repeated mixing, more energy is consumed as the augers need to break more cementation bonds during the second and subsequent flights. This effect is more obvious in slow mixing rates. The required energy also increases with the duration of mixing operation.
4. Higher mixing energy is found to produce greater strength. However, a threshold value for the unconfined compressive strength is observed with an increase in mixing energy (Fig. 2.32).

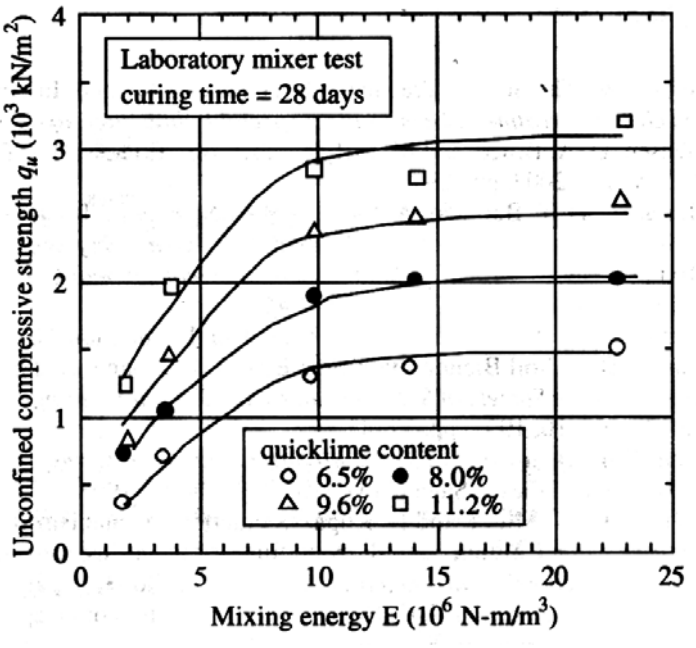

Figure 2.32 Relationship between strength and consumed energy in soil-quicklime mixing (Shen et al. 2004).

The mixing energy induced during installation of the deep soil mixing columns also significantly influences the properties of the surrounding soils. The same has been addressed by Shen et al. (2005) by conducting UCS tests on specimens collected from the DSM treated ground. DSM columns were installed into Ariake clay near Rokkaku River, Saga, Japan, in a triangular pattern following three different mixing methods (HJM – high jet mixing; PJM – powder jet mixing; and SLM – slurry mixing method). The three mixing methods are classified based on their binder injection pressure and type of binder mixing. The mixing energy of these methods varied from 100 kPa to 20 MPa with SLM applying the least. SLM and PJM methods involve vibration from the installation machine, shearing action from the rotation blades and lateral squeezing from the binder injection pressure, whereas HJM involves only high pressures which are 40 to 200 times more and slow installation speed, 1/20 to 1/10, compared to the other two methods. Other details of the in situ mixing parameters are presented in Table 2.3. The

improvement in strength $q_u(t)$, in t days after deep mixing of the surrounding clay is measured as a ratio with respect to the strength $q_u(0)$ before treatment. The results indicated that the strength ratio of SLM treated ground was higher than those of HJM and PJM and ranged from 1 to 1.4 after 35 days (Table 2.4). A similar trend was noticed for the modulus ratio ($E_{50}(t)/E_{50}(0)$), but the recovery rate is slightly lower than the strength of the soil. The study also concluded that SLM has the lowest degree of disturbance (D_D) and highest degree of strength recovery (D_R) of the surrounding clays from the cone penetration tests conducted at the center of the three columns.

Table 2.3 Installation parameters for DSM columns (Shen et al. 2005).

Method	Description	Injected Binder Volume	Injection / Jet Pressure	Installation Speed (m/min)	Rate of Rotation (rpm)
HJM	High pressure jet grouting	0.186	20MPa	0.05	20
PJM	Dry mixing with intermediate pressures	0.028	600kPa	0.5	30
SLM	Wet mixing with low injection pressures	0.186	100kPa	0.7 and 1.0	60

Table 2.4 Strength, stiffness, average disturbance and recovery in clay surrounding DSM column (Shen et al. 2005).

Method	Strength ratio (qu(t)/qu(0))	Modulus ratio (E50(t)/E50(0))	Time (t)	CPT results	
				D_D (%)	$D_{R(30)}$ (%)
HJM	0.7-1.0	0.5-1.0	60	41	65.8
PJM	0.72-1.02	0.75-0.95	30	21	62
SLM	1-1.4	1-1.3	35	15	153

Note: CPT – Cone Penetration Test

2.7 Design Aspects of DSM Columns

In general, the design of DSM treatment involves the following steps:

1. Selection of the binder type and optimum binder dosage levels following the laboratory mix design and subsequent analysis.
2. Selection of the water-binder ratio at which the maximum performance of DSM columns can be achieved.
3. Determination of the geometrical parameters (length, diameter and spacing between columns) of the DSM columns based on the properties of the treated and untreated soil obtained from laboratory testing, installation pattern (isolated - triangular; square or hexagonal), configuration (compounded, panel and grid) of columns and improvement area ratio (a_r) defined as the area of the columns to the total area of the treated ground.

The first two steps can be referred to as "geomaterial" design and the last one as "geometrical" design. The geometrical design of the DSM columns depends on the following considerations (Porbaha 2000):

- choice of the analytical framework (i.e., allowable-stress design or limit state design approaches, effective/total-stress analysis, drained/undrained conditions and 2D/3D analysis), numerical simulation and design optimization, and margin of safety (i.e., load factors and partial or global factors of safety);
- loading conditions during the lifetime of the project (i.e., inertia due to earthquakes in seismically prone areas, cyclic load due to traffic load) and load transfer mechanisms (i.e., floating versus bearing);
- relative stiffness of the treated and surrounding soil with respect to the function of the improvement and the loading condition; and

- soil-structure interaction, and displacement (vertical and lateral) as well as rotation of the stabilized ground.

2.8 Summary

This chapter successfully presents a thorough review of available literature on expansive soil behavior, their distribution in the United States and the related stabilization techniques. Major focus was given to the evaluation of DSM in stabilization of problematic expansive soils. Several laboratory and sample preparation procedures for soft soils simulating the DSM technique, derived by various researchers, were reviewed rigorously to develop a laboratory protocol suitable for expansive soil mixing in the following chapter. The influence of mixing conditions such as binder dosage, total clay water to binder ratio, soil type and mixing speeds on strength enhancements were also reviewed and presented in detail. Empirical correlations of strength as a function of total clay water content and curing time derived from previous research were understood and reproduced here. Finally, aspects involved in the design of DSM columns were studied and presented in detail.

CHAPTER 3

PRELIMINARY INVESTIGATION AND MIX DESIGN PROGRAM

3.1 General

As mentioned in Chapter 1, the main objective of this research study was to evaluate the effectiveness of DSM technology in stabilizing deep seated expansive soils. Based on the thorough review on the DSM technology and its design procedures, a successful execution of the DSM process in the field involves laboratory material mix design and geometrical design. The mix design includes appropriate selection of binder type, binder quantity and proportion, and water-binder ratio to achieve full benefit of ground improvement through DSM technology. In order to achieve this, it is necessary to study various factors, as mentioned in Section 2.5, which affect the stress-strain and shrink-swell behavior of treated expansive soil. This initiates the requirement for evaluation of untreated soil properties and an initial laboratory mix design to measure treated soil properties.

Following the laboratory mix design, this chapter describes the details of tests performed on untreated and treated soils, test equipment and procedures used, soil-binder mixing and specimen preparation procedure simulating DSM technology. The research variables and their ranges, procedures for calculating binder quantities and amount of water are also discussed in this chapter in detail. The flowchart in Fig. 3.1 depicts the detailed laboratory mix design carried out in this research. Also, all the engineering tests performed here are in compliance with the Texas Department of Transportation (TxDOT) and the American Society of Testing Materials (ASTM) standards, wherever applicable.

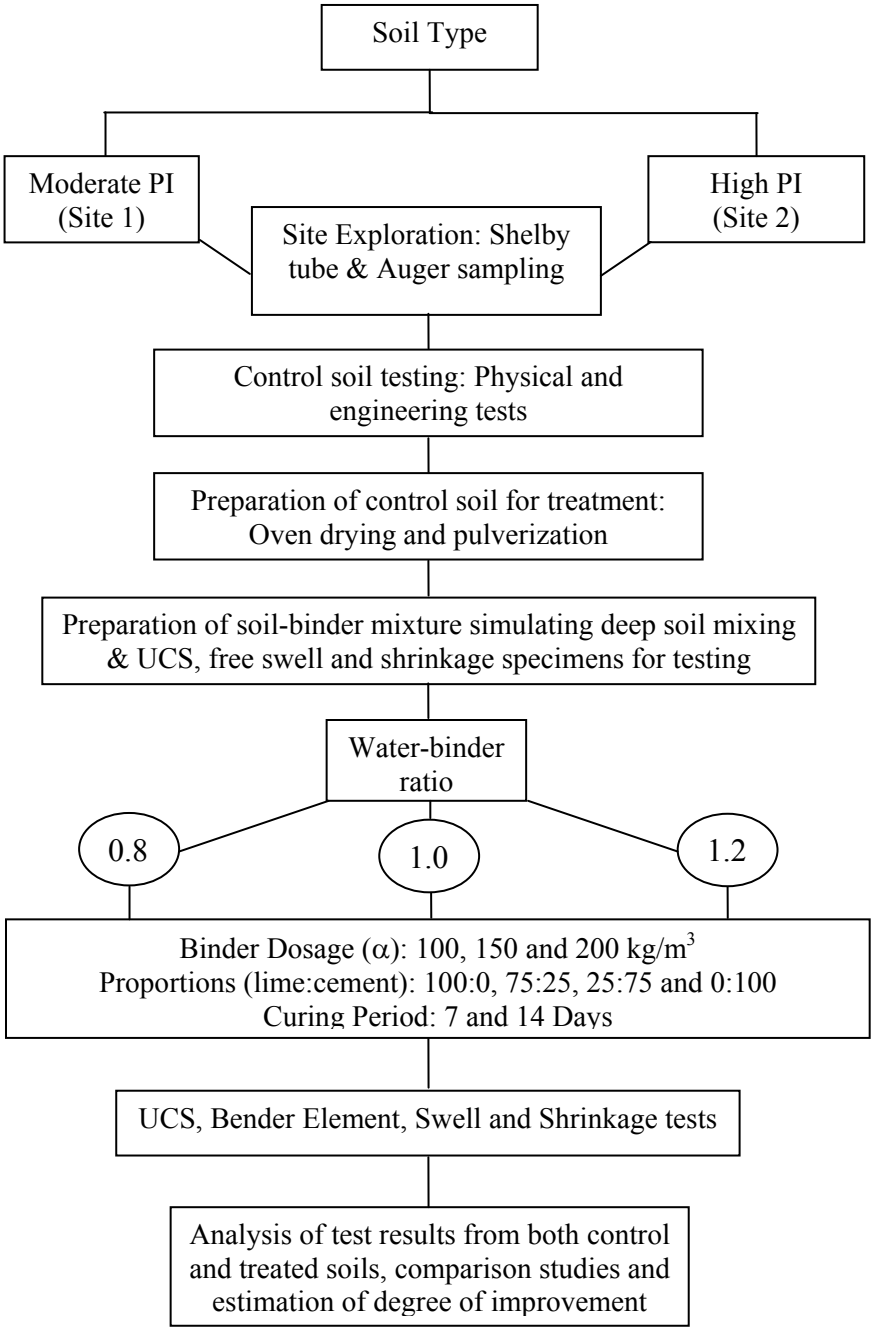

Figure 3.1 Flow diagram of laboratory mix design.

3.2 Site Selection, Characterization, Field Sampling and Storage

In this task two pilot test sections were selected for implementing the DSM technology for treatment of expansive soils. The selected sites were in the median of the North Loop Interstate 820, near the Beach Street exit, Haltom City and the east of IH 35 W, Fort Worth. This interstate is underlain by expansive soils resulting in increased pavement roughness with time. Initially, TxDOT proposed expansion of this highway from the existing two lanes to four lanes. The current preliminary design includes the reconstruction of the four lane divided highway to a six lane divided highway with four additional toll lanes planned for the inside area. This will provide a pavement width of 10+ lanes and a much greater need to suppress the future vertical pavement movement.

As a part of earlier geotechnical investigations, the project site contained expansive soils of considerable depth (20 ft or more), 12 ft needing remediation, which led to some discussions regarding various ground treatment methods that will provide enhanced performance and reduced construction costs as well as rapid construction in the field. This current research was performed to study one of the ground improvement methods, DSM, which was selected from the research discussions due to the potential for soil improvement, less disturbance to traffic during construction and less expensive. An attempt is made to evaluate the select improvement method in prototype construction in real field conditions and hence the field test sections selected here represent the actual soil conditions.

The parameters considered for selection of the two pilot test sections along the highway are plasticity index (PI) and PVR of the soils. The existing PVR calculations of these sections by TxDOT were also used to determine the heave potentials of both test sites. It was reported that the heave potentials at both sites were well above a PVR of 1 in. from the underlying clay layers

that contributed to the overall surface heaving. Based on the variations in heave amounts, two sites were selected and regarded as medium and high expansive soil sites.

Prior to construction of the DSM columns in the field test sections and laboratory mix design, it was necessary to evaluate the physical and engineering properties of the representative soils that relate to shrinkage cracking and heaving following standard laboratory tests. Engineering tests including sieve and hydrometer analysis (TxDOT Tex-110-E and Tex-111-E), standard Proctor compaction (Tex-113-E), soluble sulfate measurements (Tex-145-E and a modified UTA method), free swell strain and pressure swell tests, bar linear shrinkage (Tex-107-E) tests, unconfined compression tests and bender element tests were performed on soils from both sections. These soils were then treated with different chemical stabilizers in order to select the appropriate treatment for field studies. Evaluation of shrink-swell, strength and stiffness properties of untreated soils also helped in estimating the degree of the improvement of expansive soils through DSM technology.

The soil sampling was conducted at the two proposed pilot test sections along the Interstate mentioned above. The proposed test sections are to support a highway pavement over deep mixing columns which are intended to reduce the shrink-swell movements in the underlying expansive soil. The active depths at these sites extend beyond 15 ft (4.5 m) as per the calculations of TxDOT's (Texas Department of Transportation) recommended method of Potential Vertical Rise (PVR), Tex-124-E (1999).

The soil conditions beneath the site were explored by drilling six borings, three at each test site to depths of about 15 to 20 ft (4.5 to 6 m) below the existing grade using a 3.071 in. (76 mm) outside diameter and a 2.875 in. (73 mm) inside diameter thin-wall Shelby tube sampler. Shelby tube samples were preferred to obtain a relatively continuous stratification and an accurate estimate of the dry unit weight of the in situ soil. Bulk soil samples were also

collected by auguring the upper 9 ft (3 m) of soil adjacent to the boring locations. The undisturbed clayey samples were stored in polyethylene bags and were sealed in air-tight bags such that the in situ moisture content was retained. The samples were then carefully transferred to a 100% relative humidity room. Fig. 3.2 depicts the push tube sampling operation, sample identification and sealing of undisturbed cores into polyethylene bags.

The soil stratum along the depth of boring was classified and identical layers were then grouped. Representative soil specimens were obtained for each group from the undisturbed cores. These specimens were then subjected to tests as specified in the following sections to determine their engineering properties. The field moisture content and bulk unit weight and subsequently the dry unit weight of the soils with depth at both sites were determined by measuring the volume, and bulk and dry weights of the undisturbed specimens.

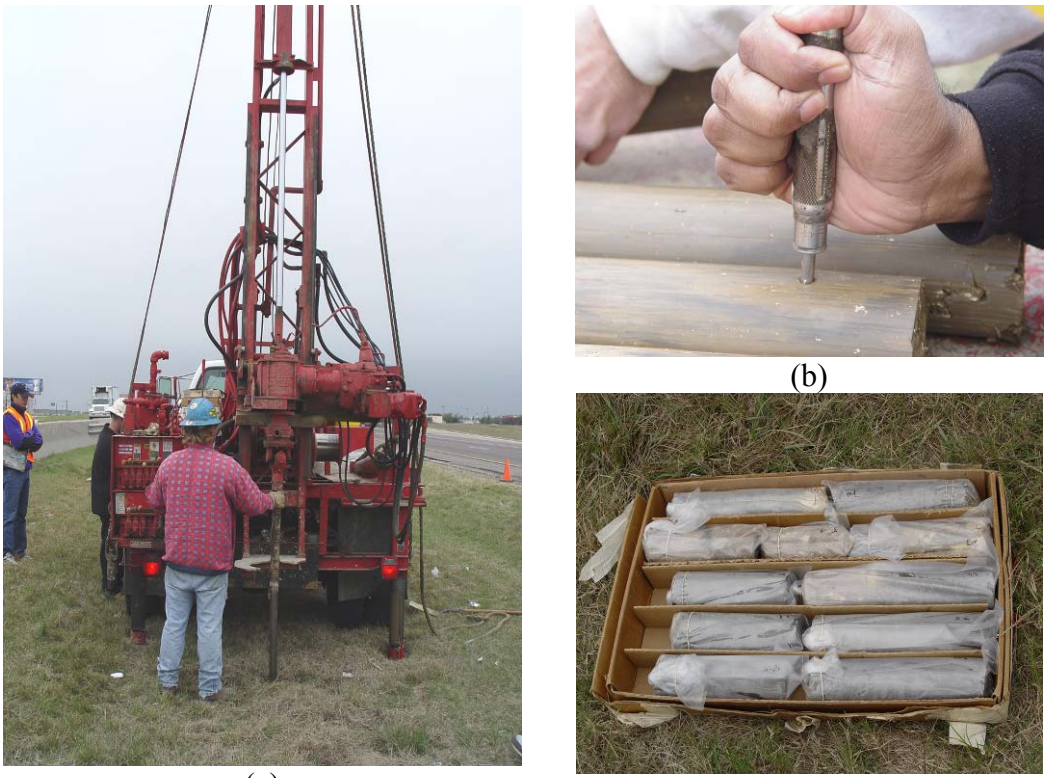

(a) (b) (c)

Figure 3.2 Pictures depicting (a) Field sampling (b) Recovered samples and (c) In situ sealing.

3.3 Details and Procedures of Engineering Tests Performed

This section presents the details and procedures followed to conduct engineering tests on the control soils. Sample preparation using the wet preparation method (Tex-101-E) for Atterberg Limits, linear shrinkage, particle size distribution, soluble sulfates, organic content and pH tests is also explained in detail.

3.3.1 Sample Preparation

In order to eliminate the effect of oven drying on the properties of the untreated soil, the wet preparation method (Tex-101-E) was followed to prepare soil samples for determination of Atterberg Limits, grain size distribution, soluble sulfate, organic content and pH. The procedure briefly includes soaking of the soil sample in tap water for a period of 24 hours (Fig. 3.3[a]) and then washing the sample through a No. 10 sieve (2 mm). The portion of the sample passing the No. 10 sieve was again washed through a No. 200 (0.075 mm) sieve until at least 95% of the material passed through the sieve. The soil samples were transferred into a Plaster of Paris bowl with filter and allowed to dry until the water content was below the liquid limit. To enhance the process of drying, an electric fan was used as shown in Fig. 3.3(b). When the sample was divided into wedges, it indicated that the soil was ready for the above-mentioned tests.

3.3.2 Atterberg Limit Tests

Atterberg limit tests reveal properties related to consistency of the soil. These include liquid limit (LL), plastic limit (PL) and shrinkage limit (SL) and are essential to correlate the shrink-swell potential of the soils to their respective plasticity indices (PI). Upon addition of water the state of soil proceeds from dry, semisolid, plastic and finally to liquid. The water content at the boundaries of these states are known as shrinkage (SL), plastic (PL) and liquid (LL) limits, respectively (Lambe and Whitman 2000). Therefore, LL is calculated as the water content at which the soil flows and PL is determined as the water content at which the soil starts

crumbling when rolled into a 1/8-inch diameter thread. These tests are somewhat operator sensitive and take time to perform. The numerical difference between LL and PL values is known as the plasticity index (PI) (Tex-106-E) and characterizes the plasticity nature of the soil.

(a) (b)

Figure 3.3 Sample preparation by wet analysis for soil classification and determination of Atterberg Limits (a) Soaking and (b) Drying.

Representative soil samples from different depths were prepared following the above-mentioned procedure and are subjected to Atterberg limit tests to determine the LL and PL following Tex-104-E and Tex-105-E, respectively. The water content of the samples during the tests were measured using the microwave drying method based on the repeatable data as reported by the Tex-103-E method.

3.3.3 Determination of Linear Shrinkage Strains

After performing the Atterberg Limit tests, the same soil samples were used to prepare specimens for shrinkage tests. Following TxDOT's method, Tex-107-E, the samples were given sufficient water, if necessary, to obtain soil slurry at the LL state. Subsequently, the soil slurry was placed into a linear shrinkage mold of dimensions, 4 in. long × 0.75 in. wide (102 mm long × 19 mm wide), as per the Tex-107-E method. The inner surfaces of the mold were greased sufficiently to reduce the friction between the specimen and inner surfaces upon subjecting them

to drying. Care was taken while placing the soil into the mold so that the entrapped air was removed. The surface was then leveled with the top of the mold using a spatula and the specimens were air dried at room temperature until a color change was observed. The mold was then transferred into an oven set at 110±5 ºC for 24 hours. The change in length was determined accurately using Vernier calipers and the linear shrinkage strain was calculated in percentage as follows:

$$L_s = \frac{\Delta L}{L_0} \tag{3.1}$$

where ΔL is change in length and L_0 is original length of specimen.

3.3.4 Particle Size Distribution

The grain-size distributions of soils from both test sections were determined following TxDOT's procedures mentioned earlier in Section 3.2. In this case, contrary to Atterberg Limit tests, a soil sample representative of the whole depth explored was prepared for each site as explained in Section 3.3.1. The distribution of particle size of the sample portion retained on the No. 200 sieve was determined by sieve analysis, while of the sample portion passed through No. 200 sieve was determined by the hydrometer analysis. The hydrometer analysis establishes the percentage of clay fraction in the soil samples. The detailed procedures for conducting both the sieve and hydrometer analyses can be found in the Tex-110-E and Tex-111-E test methods.

3.3.5 Determination of Soluble Sulfates, Organic Content and pH

The soluble sulfate content in the soil is an important test property that is known to affect the soil heaving process when stabilized with calcium based stabilizers. Hence, it was of importance to determine the sulfate levels of the control soils of both test sites before treatment. The modified University of Texas at Arlington method (2002) formulated by Puppala et al. (2002) which is a modified standard gravimetric procedure was used for measuring the amount

of soluble sulfates along with a calorimetric based TxDOT method (Tex 145 and 146-E). Further details on the sulfate gravimetric method can be found in Intharasombat (2003) and Wattanasanticharoen (2004).

From discussions in Chapter 2, it is clear that the presence of organics in soils inhibits the pozzolanic reactions of lime or cement treatment. Therefore, it is necessary to make sure that the organic fraction, if any, in the control soil is within the limits. In the current study, the amount of organics was determined as per ASTM D-2974. A known weight of oven dried soil sample (A) was placed in a muffle furnace and the temperature of the furnace was gradually brought up to 440 ºC. The specimen continued to dry until no further change in mass occurred. Finally, the mass of the dried sample after cooling was determined (B). The ratio [(B/A)*100] gave the ash content (%). The organic content (%) was then calculated as 100 - ash content in percentage.

The pH of the representative sample of untreated soils from both sites was determined based on ASTM D-4972 and Tex-128-E methods. A ratio of 1:5 soil to deionized water was used to prepare well-mixed soil samples. The pH of this solution was then determined using a pH meter calibrated in a buffer solution (pH=7.0). Proper care must be taken to ensure the electrode of the pH meter makes sufficient contact with the solution. Fluctuations in the readings of pH meter should be avoided and the electrode should be left in the solution for at least 5 minutes, allowing the value to stabilize.

3.3.6 Free Swell and Swell Pressure Tests

One-dimensional free swell and constant volume swell pressure tests were conducted on specimens collected from the undisturbed cores. A conventional oedometer steel ring of size 2.5 in. (64 mm) in diameter and 1 in. (25 mm) in height was pushed into the cores remaining after separating the specimen required for the UCS testing. The inner face of the consolidation ring was lubricated to minimize the friction during free swell. Two such specimens were

retrieved from core samples at regular depths. These specimens were then sealed in polyethylene bags and preserved in the 100% relative humidity room prior to testing.

One-dimensional free swell tests were conducted in accordance with ASTM D-4546. On the day of testing, the free swell specimens were removed from the humidity room and weighed along with the oedometer ring prior to testing. Porous stones were placed on both the top and bottom of the specimen to facilitate movement of water into the soil. The specimens were then transferred into a container and filled with water in order to soak the specimen under a no load condition. The amount of upward vertical movement (heave or swelling) of the specimens was recorded at various time intervals by placing a dial gauge on the top porous stone. Fig. 3.4 depicts a schematic sketch of the one-dimensional free swell and the test setup in the present study. The recording of readings was continued until no further movement was measured for at least one day. Soaked specimens were then carefully removed from the ring, weighed, oven dried, and weighed after drying in order to calculate the moisture content of the saturated specimen. The swelling of the expansive soil, measured as strain, is termed as the free swell index (FSI).

The constant swell pressure tests were conducted following the procedures reported by Sridharan et al. (1986) and Fredlund and Rahardjo (1993) and are defined as the amount of load that should be applied over the expansive soil to resist any volume change in the vertical direction. The setup for this test in the present study is shown in Fig. 3.5. Here, after soaking the specimen, whenever a change in height (Δh) was measured sufficient amount of load was applied to make $\Delta h = 0$. The process was continued until $\Delta h = 0$ under a constant load for at least one day. The load applied over the specimen at this point was termed as the swell pressure of the soil. Limitations of this test method and the corrections necessary to apply to the results can be found in Fredlund and Rahardjo (1993).

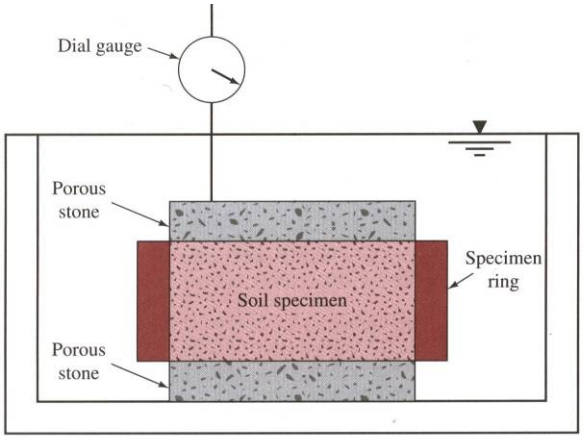

(a)

(b)

Figure 3.4 Free swell test (a) Schematic Sketch (Das 2002) and (b) Test setup.

Figure 3.5 Constant volume swell pressure test setup.

3.3.7 Bender Element (BE) Test – Stiffness Measurement

Bender element testing is a wave propagation based technique that has been successfully used in geotechnical engineering to estimate stiffness measurement and shear moduli of soils at very small shear strains (less than 10^{-3} %) (Thomann and Hryciw 1990; Viggiani and Atkinson

1995). The shear modulus, G, estimated at very small strains is considered as maximum and is nearly constant with strain at very low range of strains. Thus, the shear modulus is represented as G_{max} and is related to shear wave velocity as follows:

$$G_{max} = \rho \times V_s^2 \tag{3.2}$$

where G_{max} = small strain shear modulus,

V_s = shear wave velocity at small strains, and

ρ = mass density of soil specimen.

The bender element (BE) setup consists of piezoceramic bender elements (transmitter and receiver), signal generator, oscilloscope and a personal computer for data acquisition and processing reduction tasks. Both transmitter and receiver bender elements were then inserted into the protrusions made at both ends of the soil specimens ensuring proper contact. A typical BE test was conducted under unconfined conditions by sending a triggered single sinusoidal signal of ± 20 V amplitude to the BE transmitter was shown in Fig. 3.6(a). Further information on the BE test can be found in Kadam (2003) and Puppala et al. (2005).

The undisturbed cores were visually classified based on the material and color change along the depth of the bore log. Approximately 6 to 8 cores, each 2 ft (60 cm) long retrieved from different depths were separated for each test site for strength and stiffness measurements. The cores were then trimmed and the dimensions of the specimens were 2.75 in. dia. and 5.5 in. height (70 mm × 140 mm). Preliminary data including the site information, depth of retrieval, color of the sample, sample diameter at three different locations, sample height and bulk weight were recorded.

Two protrusions 0.07 in. wide × 0.47 in. long × 0.31 in. deep (2 mm × 12 mm × 8 mm) made at each surface of the specimen ends were used for preparing the bender element testing for

stiffness measurements. The weight of the sample was determined for measuring the bulk unit weight and mass density (ρ) of the soil specimens. The bender elements were then inserted into the protrusions ensuring proper coupling and isolation of the specimen and oscilloscope from the surrounding vibrations which might affect the shear wave velocities. A sinusoidal signal was

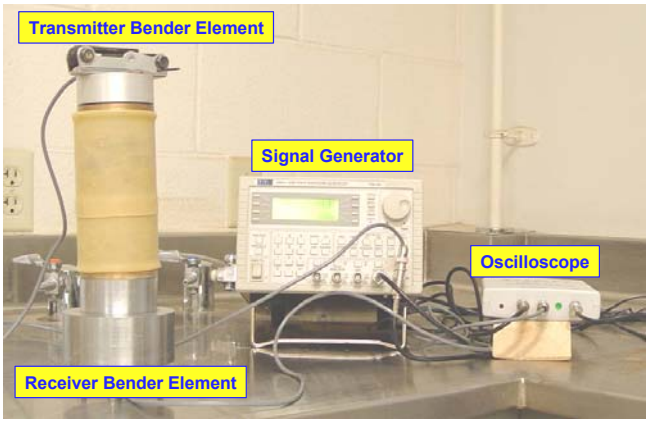

(a)

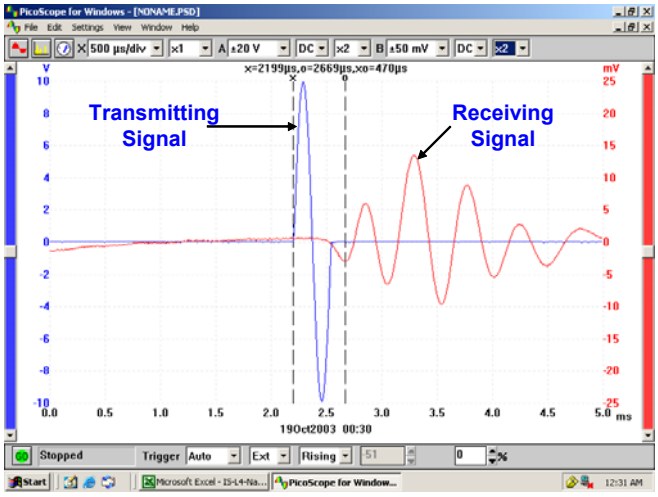

(b)

Figure 3.6 Bender Element test setup for stiffness measurements (a) Test setup and accessories (b) Real time capturing of shear wave (Puppala et al. 2006).

then sent through the specimen and the response from the receiving element was captured on the monitor. The start of the transmitter signal is marked by a vertical line 'x' on the monitor as shown in Fig. 3.6(b). The arrival of the shear wave is recognized through the first significant

inversion and a second vertical line 'o' is positioned there (Fig. 3.6[b]). The difference between the two readings provides the time of flight (Δt); i.e., the time taken by the shear wave to travel through the specimen length (l), excluding the depth protrusions. The shear wave velocity, V_s, is then computed as $V_s = l/\Delta t$ and the small strain shear modulus (G_{max}) of the soil specimen with a mass density of 'ρ' is calculated based on equation (3.2). BE tests on all untreated and treated specimens were performed under unconfined conditions.

3.3.8 Unconfined Compression Strength (UCS) Test–Strength Measurement

Bender element test being a non-destructive test, the same soil specimen was subsequently used to conduct unconfined compression tests for strength measurement. The UCS tests were performed as per ASTM D 2166. The specimen was first placed on a platform and then raised at a constant strain rate using the controls of the UCS setup until it came in contact with the top plate (Fig. 3.7[a]). Once the specimen was intact, it was loaded at a constant strain rate. As the load approached the ultimate load failure, cracks began to appear on the surface of the specimen. Both deformation and corresponding axial loads on the specimen were recorded using a data acquisition system feature of Labtech software. Fig. 3.7[b] depicts the shear failure of the specimen. The data retrieved from the computer program contain load (Q)-deformation (δ) and the same was analyzed for maximum unconfined compressive strength (q_u) in psi or kPa. The following expressions show the computation of stress (σ) and strain (ε) corresponding to the load-deformation data. After shearing, the specimens were placed in the oven to determine dry weights and thereby the water contents of the core specimens from different depths.

$$\varepsilon = \delta/L \tag{3.3}$$

$$\sigma = Q/A_c \tag{3.4}$$

$$\text{and } q_u = \sigma_{max} \tag{3.5}$$

Where δ = change in length, L = length of the specimen and A_c = Corrected area of cross-section of the specimen and equal to A/(1-e); A is the initial cross-section area.

(a)

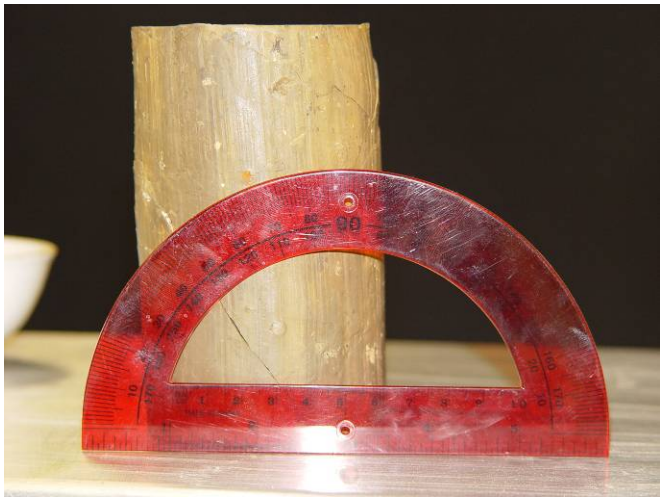

(b)

Figure 3.7 (a) UCS test setup and (b) Shear failure of specimen.

3.4 Research Variables

The strength and deformation behavior of DSM treated soils show a strong dependency on various factors as discussed in Chapter 2. Based on the literature review performed, variables such as soil type, binder type, binder contents, binder proportions, curing period, curing conditions and water-binder ratio are considered as the primary variables affecting the stress-strain and shrink-swell responses of the treated soil. To achieve maximum performance of the DSM technology in the field, it is necessary to clearly understand the behavior of treated soil for different combinations of these variables over a range. Consequently, the performance of treated soil in laboratory testing is optimized to arrive at the final mix design that is best suited for field implementation. Table 3.1 presents the ranges of these variables studied in this research.

Table 3.1 Research variables considered for the present research.

Variable Description	Range
Soil types	2 [medium and high PI]
Binder Dosage	3 [100 (6%), 150 (9%) and 200 (12%) kg/m^3)]
Stabilizer proportions (Lime:Cement)	4 [100:0, 25:75, 75:25, 0:100]
Curing time	2 [7 and 14 days]
Water binder ratio	0.8, 1.0 and 1.3
Curing conditions	1 [100% relative humidity, 20±3 ºC]

Before arriving at the above-mentioned ranges for binder dosage, the current researchers determined the optimum binder values for both lime and cement following the Eades and Grim (1966) and Tex-121-E methods.

Lime dosages in percentage by dry weight in the order of 0, 2, 4, 6, 8 and 10% were added to approximately 20 grams of air dried soil passing the No. 40 sieve. These lime-soil samples were transferred into a 250 ml plastic bottle with lid. Then 100 ml distilled water free of CO_2 in the ratio of 1:5 was added to these mixtures and the samples were shaken in an Eberbach shaker for 30 seconds. This process of shaking was repeated every 10 minutes and continued for at least one hour to ensure proper mixing of the binder and soil. The sample was then removed from the shaker and the pH was measured using the pH meter. The pH values versus the binder dosage in percentage were plotted and the threshold value was determined beyond which any further addition of the binder wouldn't change the pH of the soil-binder mixture. Even though this procedure is specifically mentioned for lime, this research extended the same procedure for cement also. Results reveal trends similar to those obtained for lime.

The optimum dosage of lime and cement for both sites was estimated to be 6% (100 kg/m^3). Also, from previous research studies, it was noticed overall that the binder dosages

varied from 80 to 400 kg/m^3 (Okumara 1997, Rathmayer 1997, EuroSoilStab 2002, Bruce 2001, Jacobson 2003, and Horpibulsuk et al. 2004). Hence, the dosage of the binders was fixed at 6% (100 kg/m^3) by dry weight of soil for both cement and lime. The conversion of percentage into kg/m^3 is discussed in the definitions section of this chapter. The other binder dosages were chosen as 9% (150 kg/m^3) and 12% (200 kg/m^3) to cover the above-mentioned range. In general, the water-binder ratio for DSM process varies from 0.6 to 1.3, with high values being chosen when field moisture contents are low (Okumara 1997). Therefore these three ratios were selected for the present study, which represent low, medium and high water-binder ratio values.

3.5 Specimen Notation

For easy identification of different soil types stabilized with different levels and proportions of binders, a simple notation system was followed throughout the study. Every specimen was assigned a notation; for example, in the form of S1-100-LC-100:0-7-1.0-1. The first letter of the notation indicates the site from where the control soil was obtained is S1 and S2 stand for Site 1 and Site 2, respectively. The second numerical symbol, 100, indicates the binder content in kg/m^3. The third symbol, LC, represents binder type; the letter L indicates lime and C indicates cement. The following ratio 100:0 indicates the proportions of these stabilizers (L and C) in the same order; i.e., lime is 100% and cement is 0% in this case. The numbers, 7 and 1.0, following the ratio represent the curing time in days and water-binder ratio. Duplicate specimens for each combination of variables were tested to ensure repeatability of test results. Consequently, the last part of the notation indicates the specimen No. 1 or 2. Table 3.2 depicts the detailed description of the notation used.

Table 3.2 Summary of specimen notation.

Symbol/Numerical	Description
S1	Site 1
S2	Site 2
100, 150 or 200	Binder content in kg/m^3
L:C	Proportions of stabilizers in the order lime and cement
100:0	100 % lime and 0 % Cement
75:25	75 % lime and 25 % cement
25:75	25 % lime and 75 % cement
0:100	0 % lime and 100 % cement
7 or 14	Curing period in days
0.8, 1.0 or 1.3	Water-binder ratio
1 or 2	Specimen No.

3.6 Glossary of Laboratory DSM Practices and Terminology

Deep soil mixing is one of the successful ground improvement techniques to stabilize soft and problematic soils. However, due to increased application areas and new installation techniques there is a wide variation in terminology and definitions of parameters with the same concept or idea. This diversity in the nomenclature creates confusion and causes miscommunication among the academia, designers and practitioners (Filz et al. 2005). This variation may be attributed to a lack of standard laboratory testing procedure simulating in situ mixing. Therefore, this section attempts to interrelate the various terms with the same idea, commonly used in the laboratory and field procedures.

An extensive literature review has not only provided insights into the factors that affect the performance of treated soil specimens, but also presented a comprehensive need to understand the differences in terminology and definitions used for various soil mixing

parameters. Based on the studies reported by the Japanese Geotechnical Society (2000), EuroSoilStab (2002), Lorenzo and Bergado (2004, 2006), Miura et al. (2001), Filz et al. (2005), Horpibulsuk et al. (2005), a glossary of various laboratory mixing terms commonly used in practice is presented in Table 3.3. It is recommended to follow the same notations to avoid further confusion.

Table 3.3 Glossary of laboratory deep soil mixing terms in deep mixing practice.

Reference	Definition	Notation
Filz et al (2005)	*Water to cement ratio of the slurry, w:c*: Weight of water involved in the slurry corresponding to weight of binder	$\frac{W_{w,slurry}}{W_c}$ (dimensionless)
	Cement factor, α: Weight of binder to volume of soil to be improved	$\frac{W_c}{V_{soil}}$ (kg/m^3 or pcf)
	Cement content, a_w: Ratio of weight of binder to weight of soil both reckoned in dry state	$\frac{W_c}{W_s}$ (percent)
	Total water to cement ratio, w_T:C: Ratio of total water of the mixture to weight of binder	$\frac{W_{w,mix}}{W_c}$ (dimensionless)
Miura et al (2001) and Horpibulsuk (2005)	*Clay water / cement ratio, w_c/C:* Ratio of initial water content of clay (%) to the cement content (%)	
	Cement content, A_w: Ratio of cement to clay by dry weight	
	Clay-water cement ratio identity:	$\left\{\frac{w_{c1}}{C_1}\right\} = \left\{\frac{w_{c2}}{C_2}\right\} = \text{Constant}$

Table 3.3 Glossary of laboratory deep soil mixing terms in deep mixing practice (continued).

Reference	Definition	Notation
Lorenzo et al. (2004) and Bergado et al. (2006)	*Optimum mixing clay water cement, $C_{w,opt}$* Total clay water content of the cement-clay-water mixture that would yield highest possible strength	
	Weight of remolding water, ΔW_w: Additional amount of water to be added in addition to cement slurry to reach the optimum	$\Delta W_w = \frac{W_T\left(w^* - w_0\right)}{\left(1 + w_0\right)}$ where:
	total clay water content ($C_{w,opt}$)	w^*: remolding water content w_0: in situ water content
	Total clay water content, C_w Total remolding water plus water in the cement slurry	$C_w = w^* + \frac{W}{C}\left(A_w\right)$ where W/C is the water cement ratio by weight of slurry
	After curing void ratio, e_{ot} *After curing water content, w_t* *After curing specific gravity, G_{st}*	

3.7 Preparation of Treated Soil Samples

The following section explains the steps involved in calculating the quantities of soil, binder and water followed by the procedures for preparing soil-binder mixture and UCS specimens.

3.7.1 Procedures to Determine Material Quantities

3.7.1.1 Soil Quantity

The in situ properties including bulk unit weight and water content of the soil should be estimated from undisturbed cores obtained from site exploration. In the present study, the same

have been determined from undisturbed core specimens as explained in earlier sections 3.3.6 and 3.3.7. Following are the expressions for both bulk unit weight and in situ natural water content.

$$\text{Bulk unit weight, } \gamma_b \text{ (kg/m}^3 \text{ or pcf)} = \frac{w_{w,core}}{v_{core}} \quad (3.6)$$

$$\text{In situ natural water content, } w_n \text{ (\%)} = \frac{w_{w,core} - w_{d,core}}{w_{d,core}} \quad (3.7)$$

$$\text{Dry unit weight, } \gamma_d \text{ (kg/m}^3 \text{ or pcf)} = \frac{\gamma_b}{1 + w_n} \quad (3.8)$$

where $w_{w,\,core}$ $w_{d,\,core}$ and v_{core} are wet and dry weights and volume, respectively, of undisturbed cores subjected to BE and UCS testing. The wet weights were obtained as soon as the cores were brought to the laboratory and the UCS specimens were extracted from the same cores. After shearing the specimens, the dry weights were obtained after placing them in an oven for 24 hrs. The weight of dry soil mass required for preparing a sample soil-binder mixture required for 2 UCS specimens, one free swell and a linear shrinkage specimen is as follows. Based on the standard dimensions of specimens subjected to these tests, the combined volume of a free swell and linear shrinkage specimen is about 0.22 times that of a UCS specimen.

Therefore, dry weight of soil for sample mix, $w_s = \gamma_d \times V \times N \times \eta$ (3.9)

where V is the volume of UCS mold, N is the number of specimens and η is the extra mass to account for any loss of material during preparation. The volume required for swell and shrinkage specimens is included in parameter N and therefore equal to 2.22 and η can be taken in the range of 1.1 to 1.2 (JGS 2000).

3.7.1.2 Binder Quantities

Following are the expressions for calculating the quantities of binder given the dosage or content in terms of kg/m^3 or percent and proportions, in case of binder containing more than one

chemical stabilizer. Binder content (a_w in %) is defined as the ratio of weights of binder to soil both in the dry state, whereas binder dosage (α in kg/m^3) is defined as the amount of dry weight of binder required for stabilizing 1 m^3 of soil in situ; i.e., bulk volume. The relationship between the two forms of definitions is as follows

$$\text{Binder factor, } \alpha \text{ (kg/m}^3\text{)} = \frac{a_w \times \gamma_b}{100(1+w_n)} \quad (3.10)$$

The amount of binder required to treat the soil quantity obtained from Eq. (3.9) is as follows:

$$w_b = \alpha \times V \times N \times \eta \text{ or } a_w \times w_s \quad (3.11)$$

If the binder is composed of more than one chemical stabilizer, as in the present study and given the proportions of these stabilizers, say lime and cement as L:C (0:100; 25:75; 75:25; 100:0), then

$$\text{Weight of lime, } w_L = \frac{L}{100} \times w_b \quad (3.12)$$

$$\text{Weight of cement, } w_C = \frac{C}{100} \times w_b \quad (3.13)$$

3.7.1.3 Slurry Mixing Water Content

The amount of slurry mixing water is calculated from the in situ natural water content (w_n) and water-binder (w/b) ratio as follows. The water-binder ratio is defined as the ratio of the weight of water required for slurry mixing to the dry weight of binder ($\frac{w_{w,slurry}}{w_b}$).

$$\text{Weight of water from w/b ratio, } w_{w,\,slurry} = w/b \times w_b \quad (3.14)$$

This ratio typically varied from 0.8 to 1.3 in the present study.

$$\text{Weight water from in situ water content, } w_w = w_n \times w_s \quad (3.15)$$

Therefore,

$$\text{Total amount of water for preparing soil-binder mix, } w_T = w_w + w_{w,\,slurry} \quad (3.16)$$

In some of the previous studies, the initial water content on treated soil behavior was studied by combining it with water-binder ratio and clay-water-binder ratio, which is the ratio of total water in the soil-binder mixture (w_T) to binder quantity (w_b).

3.7.1.4 Typical Example Calculations of Material Quantities

This section explains typical calculations, carried out in the present study, of required amount of materials per batch of soil-binder mix of notation S2-100-LC-75:25-1.0-X-X. A batch of soil-binder mix indicates 4 UCS specimens (2 for each curing time), two free swell and linear shrinkage specimens (one for each curing time). This is arrived at based on the capacity of the mixer which is capable of mixing soil and binder mass suitable to prepare 6 UCS specimens. As all the required number of specimens to study repeatability and curing time effect are prepared in one attempt, a symbol X is used in their place in the notation.

The in situ bulk unit weight and water content used in the present calculations are the average values derived from undisturbed cores of the control soil obtained from different depths. The subsequent calculations of dry soil, binder and water quantities are as follows and based on these average values.

From laboratory tests on undisturbed cores of 2.75 in. (7 cm) in diameter and 5.5 in. (14 cm) height:

Average in situ bulk unit weight, γ_b: 2050 kg/m^3

Average in situ water content, w_n (%): 24.14%

Average dry unit weight, γ_d (from equation 3.5): 1652 kg/m^3

Dimensions and volumes of UCS, free swell and linear shrinkage bar molds used for treated soils are as follows:

Table 3.4 Details of specimen molds used.

Mold, Dimensions, in. (cm)	Volume, in.^{3} (cm^3)
UCS, 2.75 (7) × 5.5 (14)	11.88 (538.78)
Free swell, 2.75 (7) × 1 (2.54)	5.94 (97.75)
Linear shrinkage mold, 4 (10.2) × 0.75 (1.9) × 0.75 (1.9)	2.25 (36.82)

The combined volume of free swell and linear shrinkage molds make 25% of the UCS and two specimens each would make about 50%. Therefore, N is taken as N = 4.5 for estimating the total dry soil mass with an extra of 10%; i.e., $\eta = 1.1$.

Dry weight of soil, w_s (from equation 3.6): 4.4 kg

Binder dosage, α or a_w: 100 kg/m^3 or 6%

Binder quantity, w_b (from equation 3.8) 0.264 kg

Lime-cement proportion (L:C): 75:25

Weight of lime (from equation 3.9): 0.198 kg

and weight of cement (from equation 3.10): 0.066 kg

Water-binder ratio(w/b): 1.0

Weight of water from w/b ratio for mixing, $w_{w,\,slurry}$ (using Eq. 3.11): 0.076 kg

and weight of water from in situ water content, w_n (from Eq. 3.12): 1.062 kg

Total water quantity for mixing (w_T): 1.138 kg

3.7.2 Laboratory Deep Mixing Protocol

The DSM protocol suggested in the present study for specimen preparation is presented here and is particularly applicable for medium stiff to stiff clayey soils. Attempts have been made to follow the testing procedure established for treatment of soft clays, but the researchers experienced difficulties in the soil-binder mixing process due to the stiff nature of the expansive

soils considered in this research. Therefore, in order to obtain a uniform soil-binder mixture, the bulk and undisturbed soil samples were first oven-dried (at 60ºC) and pulverized to obtain the fraction passing through the No. 40 (0.425 mm) sieve. The natural or in situ water content was added separately to the soil along with the weight of water from the water-binder ratio at the time of treatment. The intent of the protocol is to closely simulate the wet-mixing method for medium stiff to stiff clayey soils in the field. The apparatus used and their pertinent specifications are presented in Table 3.5.

Table 3.5 Apparatus used and specifications.

Equipment		**Specifications**
Mixing Apparatus	Soil Mixing	Kitchen Aid ®domestic mixer with 10 speed, 575 watt electric dough mixer, dough hook and beater with a mixing bowl approximately 5 Quart in volume (approximately 4700 cubic centimeters)
	Slurry Preparation	Commercially available blenders
Specimen preparation molds		Split type acrylic molds with three stainless steel hose clips and acrylic base plate. Dimensions: 2.75 in. φ and 5.5 in. ht. (UCS); 2.75 in. φ and 1 in. ht. (free swell); 4 × 0.75 × 0.75 in. (linear shrinkage)
Compaction equipment		0.2 in. φ poking rods and light rammer (4.41 lb base and 2 in. height of fall
Curing conditions		Temperature controlled, 100% Relative humidity chamber, Raymond 914 protective film (to be used as sealant) and plastic zip bags
Miscellaneous		US No. 40 Sieve, Weighing Scale, Moisture tins, hand gloves, sand paper, markers, straight edge, scale and vernier calipers

A detailed step-by-step procedure for soil-binder mixing and specimen preparation was developed based on previous research in laboratory DSM studies, presented in Chapter 2, and is explained in the following steps.

1. Obtain approximate quantity of representative ball-milled dry soil sample for preparing a batch (a batch is defined as a sufficient number of soil specimens to perform testing considering the variables such as curing conditions, number of tests and repeatability). In the present study, a batch includes 4 UCS, 2 free swell and 2 linear shrinkage specimens.
2. Weigh the appropriate amount of binders (lime and cement) based on the stipulated proportions and binder factor, α in kg/m^3. Subsequently, determine the total water content which includes the in situ water content and the amount of water from the water-binder ratio to prepare the soil-binder mixture as explained above in Section 3.7.1.4.
3. The quantities of lime and cement measured in the previous step should be mixed in dry conditions in a separate bowl prior to the addition of water. Lime-cement slurry is then prepared using a commercial blender (Fig. 3.8[a]) by adding total water content measured in Step 2 and mixing for approximately 2-3 minutes to ensure uniform binder slurry.
4. A commercially available dough mixer with a hook (Fig. 3.8[b]) is used in this study for mixing the soil and binder slurry. The dry soil collected in step 1 is transferred into the mixing bowl. The mixing rate of the outer spindle is preset at 60 rpm and the inner spindle rotated at about 152 rpm. These rates were arrived at by a trial and error process to facilitate sufficient mixing time without forming soil-binder lumps.
5. The binder slurry is slowly introduced with the mixer running at the preset speed. Care should be taken to avoid the soil from forming lumps which may be difficult to break after a certain period of mixing. A flexible spatula or beater can be used to prevent the soil from sticking to the sides and bottom of the mixing bowl.

6. Based on the recommendations from literature and on the experience in the present study, trial mixings were carried out to arrive at a mixing time that yields a uniform soil-binder mixture. The current procedure was found necessary, though not to simulate the field mixing, as a minimum to attain a homogeneous mix without lumps. After two minutes of initial mixing, the soil-binder mixture is transferred to a bowl to break the lumps formed and uniformly distribute the binder with the soil. The mixture is again transferred back to the dough mixer and the mixing is continued for 2 to 3 minutes. The total mixing time in this study is about 5 to 7 minutes. Finally, the soil-binder mixture is transferred into the bowl and used for the preparation of the UCS, free swell and linear shrinkage specimens.

(a) (b)

Figure 3.8 Apparatus for preparing (a) Binder slurry and (b) Soil-binder mixture.

Procedure for Making UCS Specimens

The steps involved in the preparation of the UCS specimen are as follows:

7. A split type acrylic mold, 2.8 in. (70 mm) in inner diameter and 6 in. (150 mm) in length with 10 mm thick acrylic base plate and three intermittent steel hoses is used for the UCS specimen preparation.

8. The empty weight of the mold with steel clamps fastened and excluding the base plate is recorded. A very thin layer of grease or similar material is applied to the inner surface of the mold and to the surface of the base plate (this can be done at an earlier time so as to minimize the time for sample preparation once the binder and soil are mixed).
9. As the soil is not in a consistency state to be poured into the molds, the soil mixture in semi-solid form is transferred into the mold using a spatula and then subjected to medium compaction in five equal layers. Each layer, after compaction is 1.18 in. (30 mm) in thickness. Care should be exercised so that the final height of the specimen shall not be less than 6 in. (150 mm) to preserve the aspect ratio for triaxial specimens. The final height of the specimen in this study is about 6 in. (150 mm). The steps necessary for the compaction of each layer are given in detail as follows:
    a. In this study, it was observed that in order to attain a lift thickness of 1.18 in. (30 mm) after compaction, the soil-binder mixture in the loose state has to be poured up to a height of 2.36 in. (60 mm) into the acrylic mold.
    b. Compaction should be done by poking using a 0.2 in. (5 mm) rod (Figure 3.9) for approximately 30 times spanning the entire surface of the specimen to remove the entrapped air voids within the specimen.
    c. It was observed that the clay is displaced in the direction opposite to that of the application of force forming hairline cracks along the surface and sides. This was resolved using slight tapping and compaction with a light hammer of 4.41 lb (2 kg) in weight and 2 in. (50 mm) height of fall (Fig. 3.9), imparting 25 blows. The blows are evenly distributed around the surface of the specimen to prevent any extrusion of soil through the edges and bottom of the mold. A collar was used during the compaction of the final soil layer.

Figure 3.9 Details of compaction rammer, poking rod, free swell mold, UCS mold, base plate and linear shrinkage mold.

d. Form grid type grooves at all intermittent layers using a spatula to ensure continuity in the specimen.

e. The final layer should be perfectly leveled to avoid bedding error during UCS testing (Tatsuoka et al. 1996). It is recommended using a slightly wetted spatula to obtain a flat surface. In the present study, two protrusions 2 mm (0.07 in.) wide, 12 mm (0.47 in.) long and 8 mm (0.31 in.) deep were made on either side of the specimen to facilitate bender element testing for stiffness measurements (Kadam, 2003, and Puppala et al. 2006).

10. The final weight of the mold without the base plate is recorded and the specimen, along with the mold, is sealed using a thin protective film (Reynolds 914 Film is commercially available for this purpose). The final setup is enclosed in a plastic airtight zip bag and is appropriately labeled. It should be noted that the air in the bag is excluded prior to sealing the bag.
11. The final assembly is stored in a 100 % relative humidity room with temperature control at 20±3 ºC.

12. Repeat Steps 9 through 11 within 20 minutes to prepare other specimens of the batch from the soil-binder mix; a total of four UCS specimens, two per each curing period (7 and 14 days) and two specimens per combination for repeatability of test results.
13. The specimens placed in the curing room are removed after 2 to 3 hours and the molds are stripped out. The specimens are then carefully sealed in the same plastic bags and transferred back to the curing room. The molds are used again for preparation of subsequent sets of specimens for further testing.

Procedure for Making Free Swell Specimens

The steps involved in the preparation of free swell specimens are as follows:

14. An acrylic mold, 2.75 in. (70 mm) diameter and 1 in. (25. mm) height are used for the preparation of specimens for free swell testing.
15. The empty weight of the mold is recorded and a thin layer of grease or similar material is applied to the inner surface of the mold.
16. The mold is placed on the base plate and the loose soil-binder mix is transferred into the mold in two lifts. Compaction of each lift is carried out as mentioned in step 9. A different swell mold of the same dimensions can be used as a collar for the final lift.
17. The weight of the swell mold along with the compacted specimen, excluding the base plate, is recorded. The mold is sealed using the protective film and placed in an airtight zip bag and appropriately labeled after excluding the entrapped air in the bag.

Procedure for Making Linear Shrinkage Specimens

18. A linear shrinkage bar mold with an assembly of six bars of dimensions 4 × 0.75 × 0.75 in. is used for this purpose. The empty weight of the bar is recorded and the inner surfaces are properly greased to minimize friction between the specimen and the inner surfaces during the drying process.

19. Place the soil-binder mixture into the first slot of the mold followed by slight tamping and poking randomly using a spatula to remove any entrapped air. The final weight of the mold with one slot filled is recorded.
20. The adjacent slot is filled with the same mix but at its liquid limit (Tex-104-E). For this purpose, a portion of the soil-binder mixture is wetted with sufficient water and placed in the Casagrande cup to determine the closure of the groove in approximately 25 blows. The slot is then filled with this mixture with the water content close to the liquid limit. The final weight is recorded with two slots filled with the mixture; one at the mixing water content and the other at the liquid limit. This is repeated at every filling of the mold to obtain the wet unit weight of the placed soil.
21. The slots in the mold are labeled at the bottom of the mold, covered with a wet geotextile and then placed in an airtight zip bag for curing in the humidity room. Thereafter, the molds are taken out of the curing room every two days and the geotextile is sprinkled with water to minimize the heat of hydration and subsequent shrinkage of the specimens even before drying.

It should be noted that all the specimens prepared in the current research were at compaction densities and will be different from proctor densities as the deep soil mixing is performed in the in situ conditions.

3.8 Laboratory Testing on Treated Soils

The test procedures, including linear shrinkage strain, free swell, UCS and BE explained in Section 3.3 with respect to control soil testing can be applied to test the above prepared treated soil specimens. This will determine the shrink-swell, strength and stiffness properties of treated soils and thereby the degree of improvement by comparing the results with those from the control soils. The tests are conducted at the end of the curing period and the data are recorded

accordingly. However, some of the steps involved prior to conducting the respective tests are outlined below:

1. The protrusions provided for bender element testing are adjusted to the required dimensions using a damp grooving tool to ensure proper coupling of the piezoceramic elements with the specimen. Any excess water is removed using a high absorbent paper.
2. The ends of the UCS specimens after the curing period are carefully made flat by rasping them with a sand paper to avoid bedding error that might create a large scatter in the strength results.

3.9 Summary

This chapter described various test procedures followed in the present research to determine the engineering properties of both the control and treated soils. The variables studied here are summarized and the specimen notation developed is explained for easier identification of treated soils.

A glossary of conventional DSM terms used in the laboratory DSM practice is discussed, followed by the definitions of various terms used in the current study. Detailed explanations on material calculations and control soil preparation for laboratory DSM treatment are presented. Finally, a laboratory DSM mixing protocol is suggested in a step-by-step procedure for the preparation of soil-binder mixture and subsequent making of UCS, free swell and linear shrinkage specimens.

CHAPTER 4

RESULTS AND DISCUSSION OF LABORATORY MIX DESIGN

4.1 General

This chapter presents comprehensive analyses of results obtained from laboratory tests on the control and treated soils of both test sections (Site 1 and Site 2). Specimen preparation of treated soils was based on the laboratory DSM protocol developed in an earlier chapter. The effects of binder dosage, water-binder ratio, proportions of lime and cement, curing time period on shrinkage-swell, stress-strain and stiffness properties of the treated soils are discussed. Finally, a ranking analysis is conducted to screen out binder alternatives and to select an optimum binder dosage and the proportions of lime and cement additives for field treatment.

4.2 Site Exploration, Physical and Engineering Properties of Control Soils

Results from site exploration and tests performed on subsequently obtained control soil specimens are analyzed and discussed in the following sections.

4.2.1 Soil Conditions

Based on the preliminary data provided by the commercial laboratory from the bore holes drilled at both pilot test sections, the soil profiles with depth are depicted in Figures 4.1 and 4.2. The bore logs also present the results from physical tests conducted subsequently on the control soils. From the bore log results, it is observed that the fill soils up to 5.4 to 6 ft (1.8 to 2 m) in thickness were encountered at both of the sites. The fill soils consist of medium plasticity clay and are characterized as medium to highly expansive from the free swell tests.

The natural soils consist primarily of clay with intermittent calcareous nodules and pieces of limestone. Weathered limestone was encountered at a depth of 14 ft (4.5 m) at Site 1 and was

not encountered within the depths explored at Site 2. Ground water was not encountered within the depths explored.

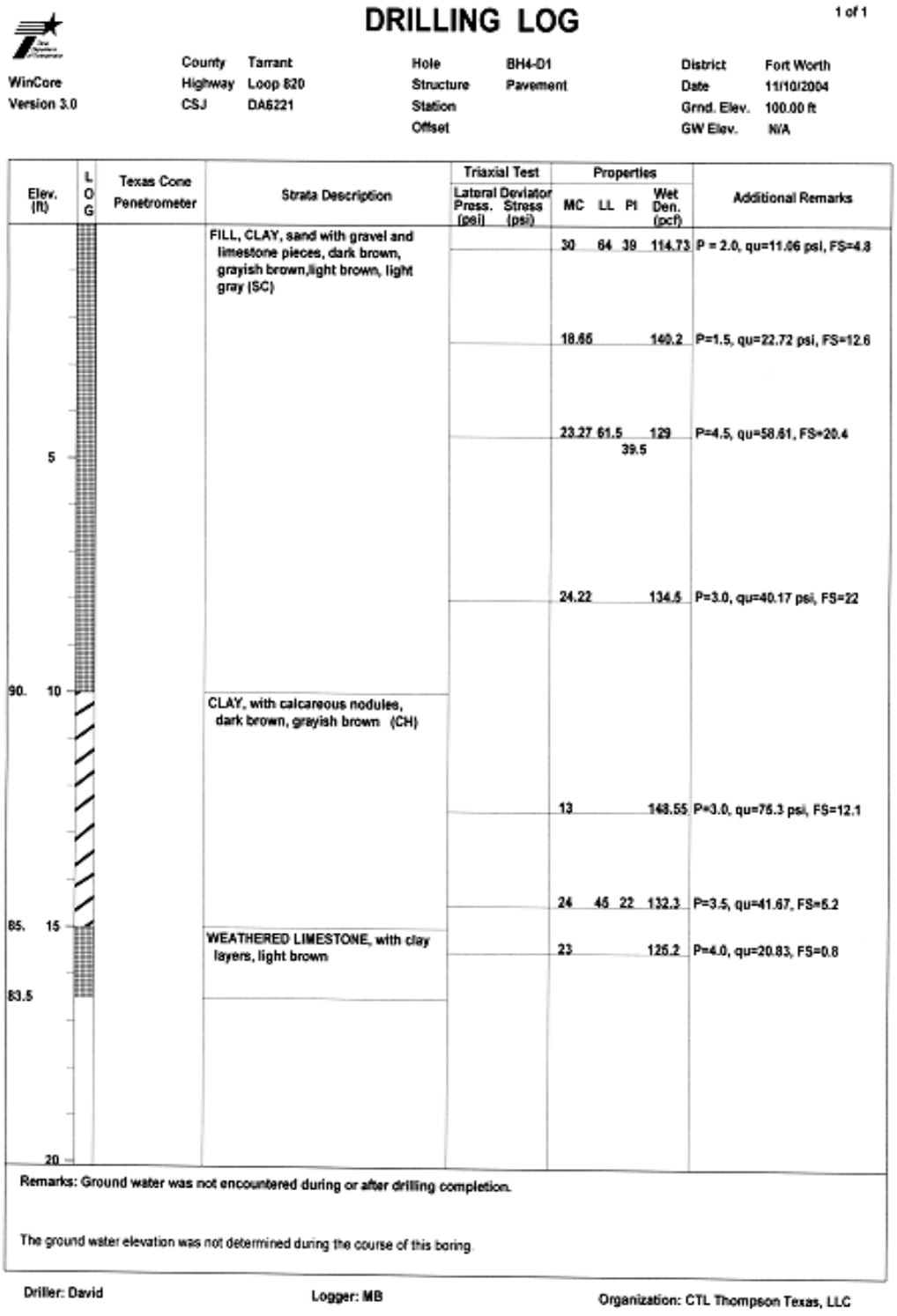

DRILLING LOG

1 of 1

WinCore
Version 3.0

County Tarrant
Highway Loop 820
CSJ DA6221

Hole BH4-D1
Structure Pavement
Station
Offset

District Fort Worth
Date 11/10/2004
Grnd. Elev. 100.00 ft
GW Elev. N/A

Elev. (ft)	LOG	Texas Cone Penetrometer	Strata Description	Triaxial Test: Lateral Press. (psi)	Triaxial Test: Deviator Stress (psi)	Properties: MC	LL	PI	Wet Den. (pcf)	Additional Remarks
			FILL, CLAY, sand with gravel and limestone pieces, dark brown, grayish brown,light brown, light gray (SC)			30	64	39	114.73	P = 2.0, qu=11.06 psi, FS=4.8
						18.66			140.2	P=1.5, qu=22.72 psi, FS=12.6
						23.27	61.5	39.5	129	P=4.5, qu=58.61, FS=20.4
5										
						24.22			134.5	P=3.0, qu=40.17 psi, FS=22
90. 10			CLAY, with calcareous nodules, dark brown, grayish brown (CH)							
						13			148.55	P=3.0, qu=75.3 psi, FS=12.1
						24	45	22	132.3	P=3.5, qu=41.67, FS=5.2
85. 15			WEATHERED LIMESTONE, with clay layers, light brown			23			125.2	P=4.0, qu=20.83, FS=0.8
83.5										
20										

Remarks: Ground water was not encountered during or after drilling completion.

The ground water elevation was not determined during the course of this boring.

Driller: David Logger: MB Organization: CTL Thompson Texas, LLC

Figure 4.1 Bore log data and engineering properties of Test Site 1 (Low PI site).

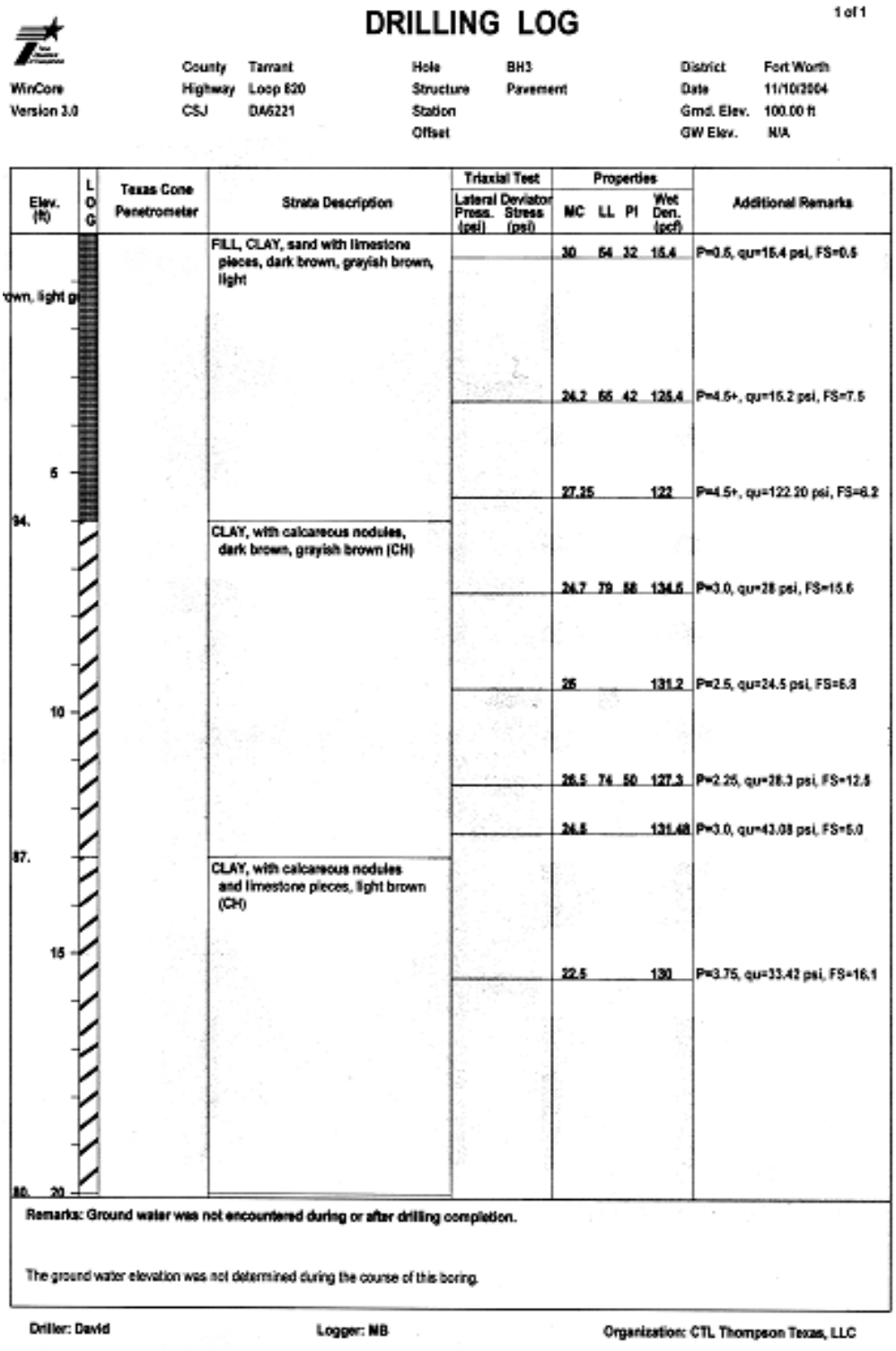

DRILLING LOG

1 of 1

WinCore Version 3.0	County	Tarrant	Hole	BH3	District	Fort Worth
	Highway	Loop 820	Structure	Pavement	Date	11/10/2004
	CSJ	DA6221	Station		Grnd. Elev.	100.00 ft
			Offset		GW Elev.	N/A

Elev. (ft)	LOG	Texas Cone Penetrometer	Strata Description	Triaxial Test: Lateral Press. (psi)	Triaxial Test: Deviator Stress (psi)	Properties: MC	LL	PI	Wet Den. (pcf)	Additional Remarks
			FILL, CLAY, sand with limestone pieces, dark brown, grayish brown, light			30	64	32	15.4	P=0.5, qu=15.4 psi, FS=0.5
own, light g						24.2	65	42	125.4	P=4.5+, qu=15.2 psi, FS=7.5
5						27.25			122	P=4.5+, qu=122.20 psi, FS=8.2
94.			CLAY, with calcareous nodules, dark brown, grayish brown (CH)			24.7	79	58	134.5	P=3.0, qu=28 psi, FS=15.6
						25			131.2	P=2.5, qu=24.5 psi, FS=6.8
10						26.5	74	50	127.3	P=2.25, qu=28.3 psi, FS=12.5
						24.5			131.48	P=3.0, qu=43.08 psi, FS=5.0
87.			CLAY, with calcareous nodules and limestone pieces, light brown (CH)							
15						22.5			130	P=3.75, qu=33.42 psi, FS=16.1
80. 20										

Remarks: Ground water was not encountered during or after drilling completion.

The ground water elevation was not determined during the course of this boring.

Driller: David Logger: MB Organization: CTL Thompson Texas, LLC

Figure 4.2 Bore log data and engineering properties of Test Site 2 (High PI).

As explained in Chapter 3, based on visual classification and bore log data, identical soil layers are classified into similar soil zones throughout the depth of the borehole. Representative soil specimens from each zone were sampled and subjected to laboratory tests to determine physical and engineering properties. Results from these tests are explained in the subsequent subsections.

4.2.2 Physical Properties of Control Soils

Atterberg limit tests were conducted on representative soil samples collected from each group along the depth explored for both test sections. Representative sample indicates that it represents the properties of soil over the depth of the respective zone. These samples were prepared by collecting equal amounts of bulk soil sample from all the soil cores obtained over that zone. The soil consistency limits, including liquid limit (LL), plastic limit (PL) and plasticity index (PI), determined from these tests are depicted in Figures 4.1 and 4.2. It can be noticed that the PI of soils from Site 1 and Site 2 ranged from 22 to 39% and 32 to 58% with depth, respectively; thus, indicating that the expansive soils represent medium to high swell potential based on the characterization by Chen (1988). The subsequent grain size analysis classified soils from both sites as highly compressible clays (CH) under the USCS (Unified Soil Classification System) classification system (Table 4.1).

Table 4.1 Physical properties of control soils from Sites 1 and 2.

Property	Test Designation		Site 1	Site 2
	TxDOT	ASTM		
Specific gravity	Tex-108-E	ASTM D854	2.70	2.72
Gravel (%)	Tex-110-E	ASTM D422	0	0
Sand (%)	Tex-110-E	ASTM D422	3	2
Silt (%)	Tex-110-E	ASTM D422	32	24
Clay (%)	Tex-111-E	ASTM D422	59	50
Organic content (%)	Tex-408-A	ASTM D2974	5.24	2.96
Soluble sulfates (ppm)	Tex-145-E	UTA Method	922.6 / 2156	94.66 / 0.00
pH	Tex-121-E	ASTM D4972	7.95	7.88
Linear bar shrinkage (%)	Tex-107-E		22.42	18.32
USCS classification	Tex-142-E	ASTM D2487-00	CH	CH

The results obtained from the organic content, soluble sulfate and pH tests are also tabulated in Table 4.1. The organic content and pH of both soils (Sites 1 and 2) are less than 6 and close to 8, respectively. These results indicate that the soil is not acidic and is inorganic in nature. It is also important to measure the sulfate levels in soils subjected to chemical treatment to make sure that it will not lead to sulfate related heaving. In the process, the soluble sulfate tests performed following UTA method yielded sulfate levels less than 1000 ppm (Table 4.1). Based on current TxDOT soluble sulfate levels, these levels are considered not harmful for treatment using lime and Type 1 cement. Currently, ‘‘low to moderate’’ and ‘‘high’’ sulfate soils are those with soluble sulfates less than 2000 ppm and more than 2000 ppm, respectively (Puppala et al. 2002).

The in situ natural moisture content (w_n) and bulk unit weight (γ_b) along the depth explored were determined during strength and stiffness measurements on undisturbed cores. The

variations of w_n and γ_b with depth are depicted in both bore log sheet (Figs. 4.1 and 4.2) and Fig. 4.3. The moisture content at Site 2 shows a fairly constant trend with depth up to 16 ft and varies from 30% at the surface to 22% at 16 ft. In the case of Site 1, the moisture content decreased with depth from 30% at the surface to 13% at 12.5 ft and then increased to 24% at 16 ft. The bulk unit weights of the undisturbed cores represent in situ density and varied in the ranges of 114 to 148 pcf and 120 to 134 pcf, respectively, for Sites 1 and 2.

4.2.3 Engineering Properties of Control Soils

4.2.3.1 Shrink and Swell Properties

The free swell (F_s) strains of the control soils from Sites 1 and 2 ranged from 5 to 22% and 1 to 16%, respectively. The variations of F_s with depth are depicted in Fig. 4.3. It can be noticed that the highest free swell is recorded at a depth of approximately 4 to 9 ft and 7 to 16 ft, respectively, for Sites 1 and 2. The percent of free swell with time is reported in Fig. 4.4 and these results indicate that the maximum swell was recorded in about 480 min under saturated conditions. Contrary to the conventional hypothesis, the maximum swell strains are recorded for Site 1 with medium PI when compared to Site 2 with high PI. Though swell properties do not correlate well with PIs of soils, the swell behavior of the control soil can be better explained by studying their mineralogical composition. Mineralogical studies on control, laboratory treated and wet grab samples are presented in Chapter 6. The active depths of expansive soils in the DFW (Dallas Fort Worth) area are reported to vary between 10 and 20 ft. Hence, the deep soil mixing treatment was recommended to stabilize the expansive soil strata up to a depth of 15 to 20 ft. The shrinkage strains from the linear shrinkage bar tests (Tex-107-E) performed on representative control soil samples from Sites 1 and 2 yielded shrinkage values of 22.42 and 18.32 % respectively (Table 4.1).

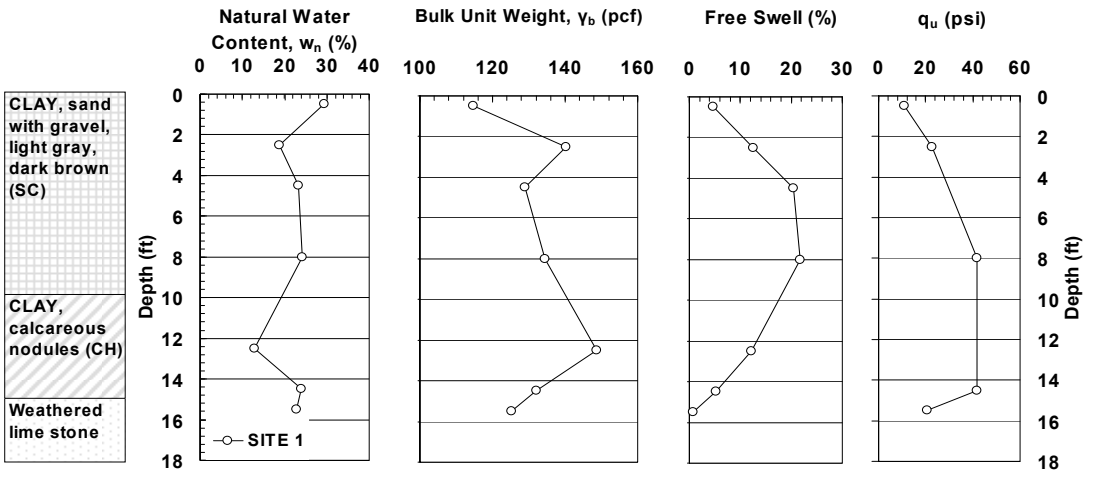

(a) Site 1

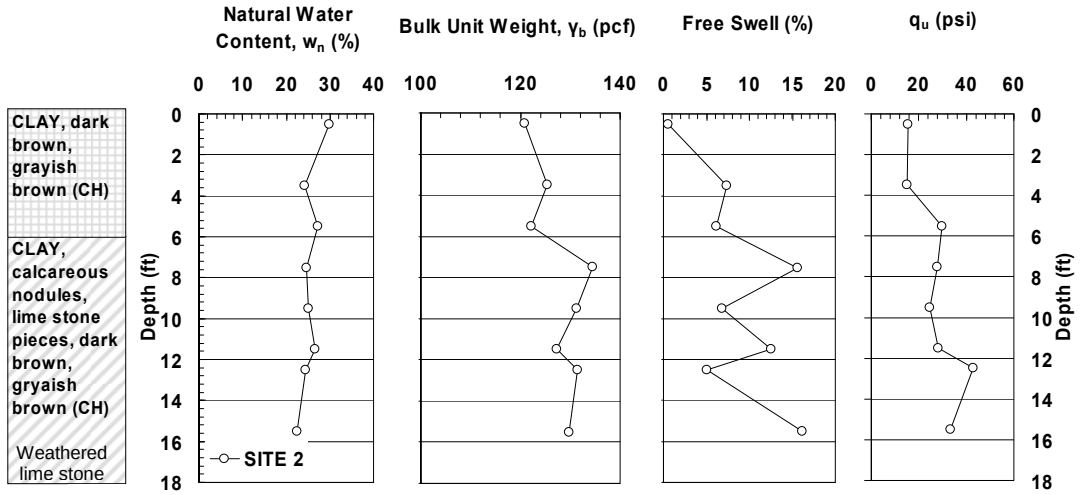

(b) Site 2

Figure 4.3 Classification of physical and engineering properties of untreated soils for Sites 1 and 2.

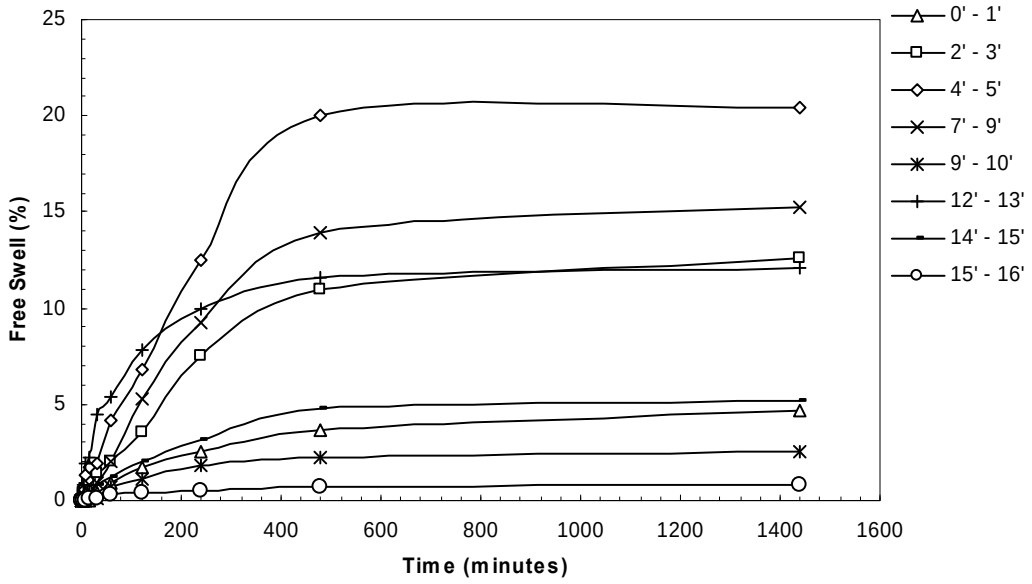

(a) Site 1

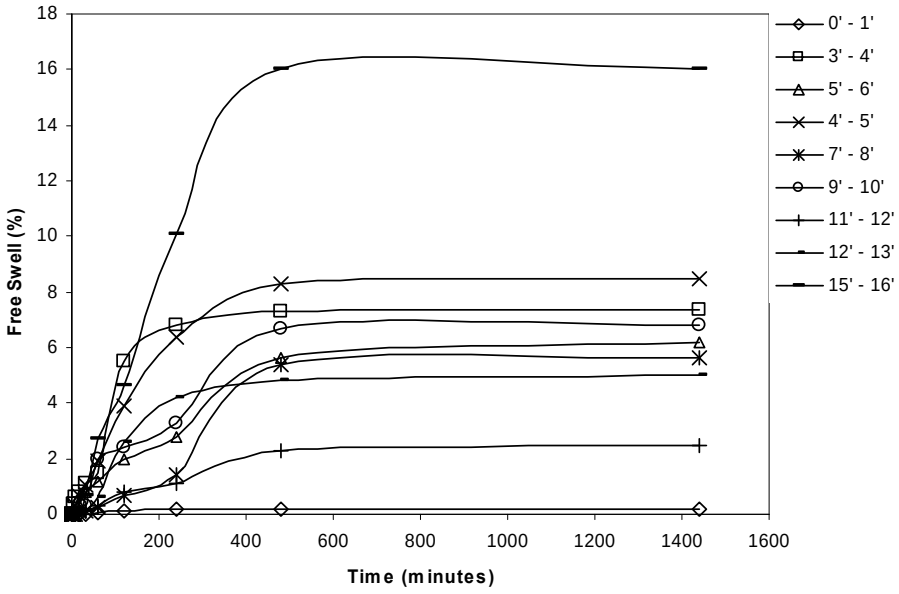

(b) Site 2

Figure 4.4 Free swell test results with depth on control soils.

The results from the constant volume swell pressure tests are also reported here in Table 4.2 and a typical plot from the test is depicted in Fig. 4.5.

Table 4.2 Corrected swell pressures (psi) with depth of untreated soils from constant volume swell test.

Depth (ft)	Site 1	Site 2
0-1	12	28
4.5	28	26
9-10	11	16

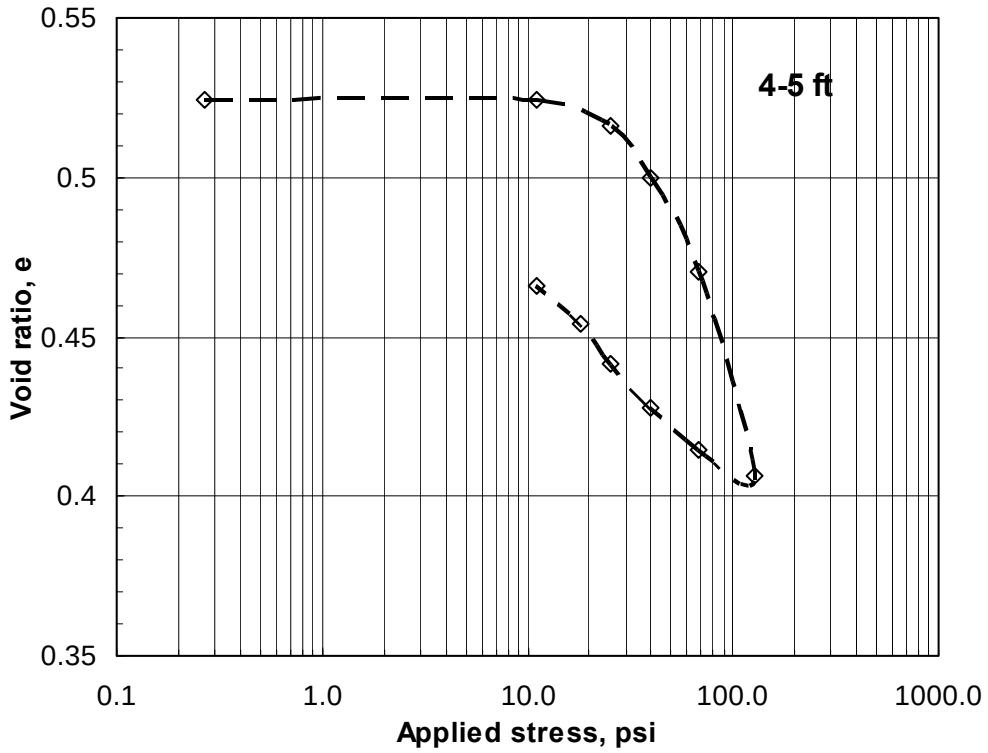

Figure 4.5 Typical plot of applied stress (σ') versus void ratio (e) from constant volume swell test.

4.2.3.2 Strength and Stiffness Properties

The strength and stiffness properties of the soils at both test sections were evaluated through unconfined compression (UC) and bender element (BE) tests, respectively. The undisturbed specimens are first subjected to the BE test, being a non-destructive test, and

subsequently to the UCS test. These tests are performed in accordance with procedures explained in Sections 3.3.6 and 3.3.7. The small strain shear modulus (G_{max}), unconfined compressive strength (q_u) and initial tangent modulus (E_i) are estimated from Equations (3.2), (3.5) and stress-curve, respectively. The variations of q_u with depth for both sites are depicted in Fig. 4.3. The UCS values for Site 1 ranged from 10 to 40 psi (70 to 275 kPa) and for Site 2 from 16 to 46 psi (100 to 300 kPa). Based on the average UCS values with depth, the control soil from both sites can be classified as medium to stiff expansive clays (Lambe and Whitman 2000).

The initial tangent modulus, E_i was determined from the stress-strain response obtained from the UCS test and the procedure is shown in Fig. 4.6. The slope of initial linear portion of the stress-strain curve is known as the initial tangent modulus. The values of G_{max} and E_i with depth for both test sections are tabulated in Table 4.3. The G_{max} of soils is higher at depths greater than 0.6 m when compared to those at the surface, revealing the effect of confinements on stiffness properties and lack of desiccation at the site. It should be noted here that the sites were covered with lime treated base from adjacent pavement sections, which controlled desiccation cracking at the project sites.

These results are useful for quality assessment studies and for estimation of degree of improvement of the DSM technology in the field. On the other hand, these strength and stiffness measurements can also be used in design and numerical analysis of DSM column treated ground. It can be observed from Fig. 4.3 and Table 4.3 that the stiffness behavior of soils at both sites is in accordance with the variation of bulk unit weight with depth.

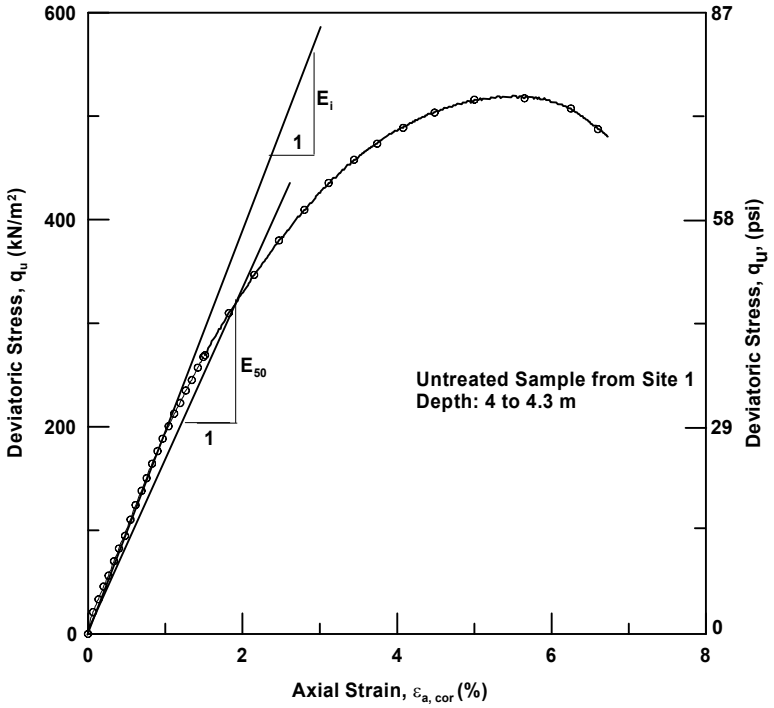

Figure 4.6 Demonstration of initial tangent modulus (E_i) estimation from stress-strain curve.

Table 4.3 Shear moduli, G_{max} and initial tangent moduli, E_i of control soil from Sites 1 and 2 with depth.

Depth (m)	Shear Modulus G_{max} in ksi (MPa)		Initial Tangent Modulus, E_i in ksi (MPa)	
	Site 1	Site 2	Site 1	Site 2
0-0.6	5.9 (40.5)	5.1 (35.0)	1 (6.6)	4.8 (33)
1.5-2.1	9.6 (66.4)	8.9 (61.1)	5.6 (39)	7.8 (53.5)
2.1-3.0	NR[1]	8.6 (59.6)	NR[1]	9.1 (62.5)
4.0-4.6	9.2 (63.6)	7.6 (52.4)	2.3 (16)	6.5 (44.5)

Note: [1]NR – Not reported

4.3 Effects of Research Variables on Treated Expansive Soil Behavior

The following sections analyze and explain in detail the effects of the research variables – binder type (lime and cement), binder dosage (α), binder proportions (L:C), water-binder (w/b) ratio and curing time, considered in the present study on treated expansive soil behavior. The testing program included the determination of linear shrinkage strains, free swell strains, and strength and stiffness enhancements of the treated soils. Duplicate specimens for each variable combination were prepared and tested to ensure the repeatability of the test results. The current discussion also focuses on the homogeneity of the specimens, prepared following the laboratory DSM protocol developed in Chapter 3, through unit weight distribution in each of the tests performed in this research. Typical results of unit weight distribution for a water-binder ratio of 1.0 are presented here to explain the specimen homogeneity.

4.3.1 Linear Shrinkage Strains

The linear bar shrinkage tests were conducted on the treated soils at both molding water content (total clay water content) and liquid limit of the soil-binder mixture. Liquid limit is determined prior to casting the specimen by adding a sufficient amount of water that would close the grove in the Cassagrande device at approximately 25 blows (ASTM D 4318-00).

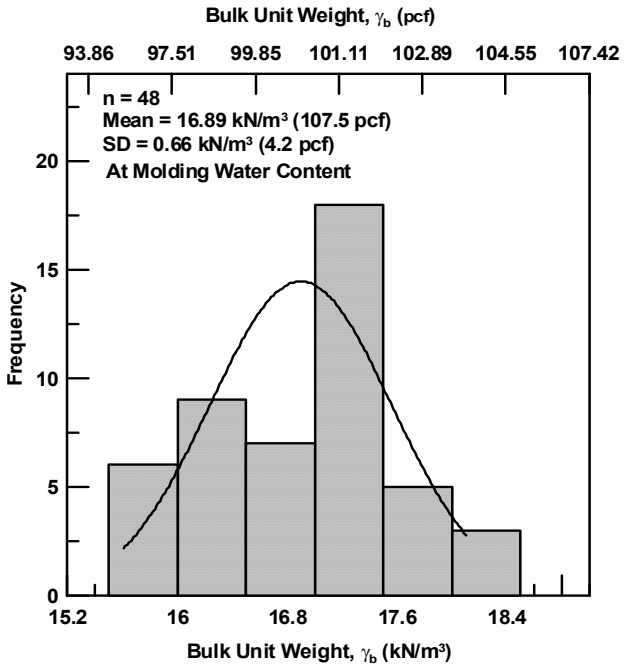

(a)

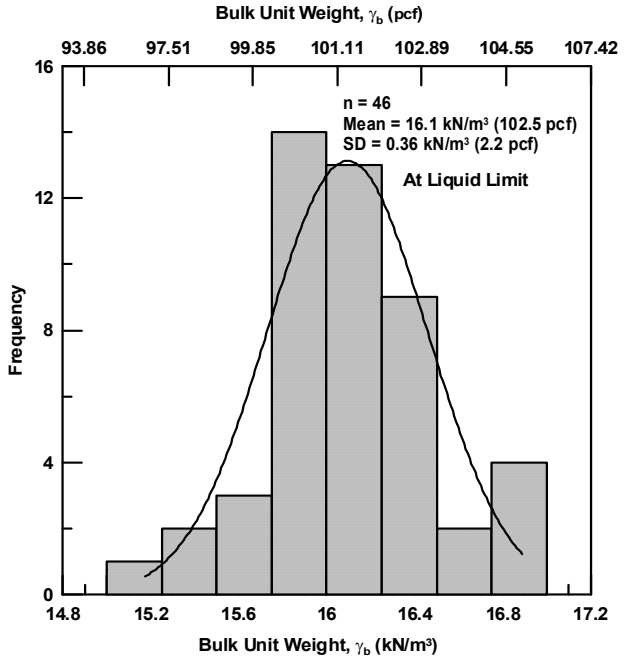

(b)

Figure 4.7 Distribution of unit weights of shrinkage specimens from Sites 1 and 2 at (a) molding water content and (b) liquid limit.

4.3.1.1 Specimen Homogeneity

Figures 4.7(a) and (b) show the summary of distribution of unit weight data of the treated specimens of both sites prepared at the molding water content and liquid limit, respectively. The standard deviation ($\overline{\sigma}$) of the unit weight data at the molding water content was 4.2 pcf (0.66 kN/m^3) and at liquid limit was 2.2 pcf (0.36 kN/m^3); these low values in $\overline{\sigma}$ indicate the consistency in specimen preparation. The difference in standard deviation explains a better unit weight distribution for specimens compacted at water contents close to the liquid limit. This may be due to better workability at higher water contents. The difference in plasticity indices and clay contents of the samples from Sites 1 and 2 did not show significant effect on the unit weight distribution in the linear shrinkage tests.

The shrinkage specimens were tested at different binder dosages, lime and cement proportions, curing time and water binder ratio. The shrinkage strains of all treated specimens improved considerably relative to the control soil and yielded values corresponding to those that are characterized as low severity levels. The mechanisms involved in the linear shrinkage can broadly be characterized as a result of tensile failure, loss of contact points due to propagation of cracks from the surface of the soil and the effect of thermal conductivity on the magnitude of shrinkage. Though the latter is outside the scope of the current discussion, crack formation due to tensile stresses developed within the soil mass plays a vital role in shrinkage strains. Conventionally, shrinkage in expansive soil can be directly related to the change in moisture content in the soil structure, which results in the formation of discontinuities in the soil medium due to crack propagation.

Even though the magnitude of shrinkage strains for all combinations of variables are low and show negligible difference, small hairline like cracks were observed on the surface of the treated soils (Fig. 4.10). Therefore, in order to understand the possible reasons responsible for

this behavior, the results are plotted on enlarged scales to study the variations in shrinkage strains with respect to the research variables.

4.3.1.2 Effect of Binder Dosage and Proportions

The following observations made in the present study are similar for soils from both test sections. Figures 4.8 and 4.9 depict the effects of binder dosage (α) and proportion (L:C) on linear shrinkage strains of treated soil specimens for both Sites 1 and 2 at a 7-day curing period. For a given binder proportion (L:C), linear shrinkage strains decreased with an increase in binder dosage, possibly due to an increased amount of cementitious products formed in the stabilized soil. In contrast, for a constant binder dosage, it is observed that shrinkage strains increased with an increase in the cement binder proportion. This is attributed to the production of greater heat of hydration with increased cement content. Overall, higher shrinkage values are noticed for a binder dosage of 100 kg/m^3 and 100% cement content, whereas lower values are observed for 200 kg/m^3 and 100% lime content (Tables 4.4 and 4.5).

The treatment was effective for all combinations of research variables, as there were no patterns of warping or curling of the treated specimens from linear shrinkage tests as was in the case of the control soil (Fig. 4.10). However, it was noticed that hairline cracks formed on the surface of specimens gradually developed along the depth of the mold under constrained boundary conditions. The localization of shrinkage cracks is attributed to the zones of moisture concentration within the specimen and may be prevented by thorough mixing of soil and binder for uniform distribution of moisture.

As expected, the increase in moisture content from molding water to the liquid limit (LL) of the soil-binder mixture resulted in increased shrinkage strains (Fig. 4.8). This behavior can be attributed to the availability of more moisture in the case of specimens prepared at LL; i.e., close to saturation moisture content. The majority of voids in the three phase system of the stabilized

soil are occupied by water which predominantly governs the interparticle bonding forces. The resultant void spaces created during drying due to hydration or mobilization of excess water along the length of the specimen might result in gradient of moisture concentrations and subsequently the generation of tensile stresses. The disruption or disturbance in the soil structure due to the domination of tensile stresses leads to the propagation of the initial cracks on the surface along the depth of the specimen. This results in an open fabric, which yields space for rearrangement of soil particles in the voids. The collapse of the soil structure could be both in the transverse and longitudinal directions.

Visual observation of all the treated specimens, after drying, confirms this behavior in shrinkage patterns. Also, there is a decrease in unit weight of specimens prepared at the liquid limit and hence, more water and relatively less number of solid particles exist per unit volume. As mentioned before, it should be noted here again that the difference in shrinkage strains at both molding water content and liquid limit is very small.

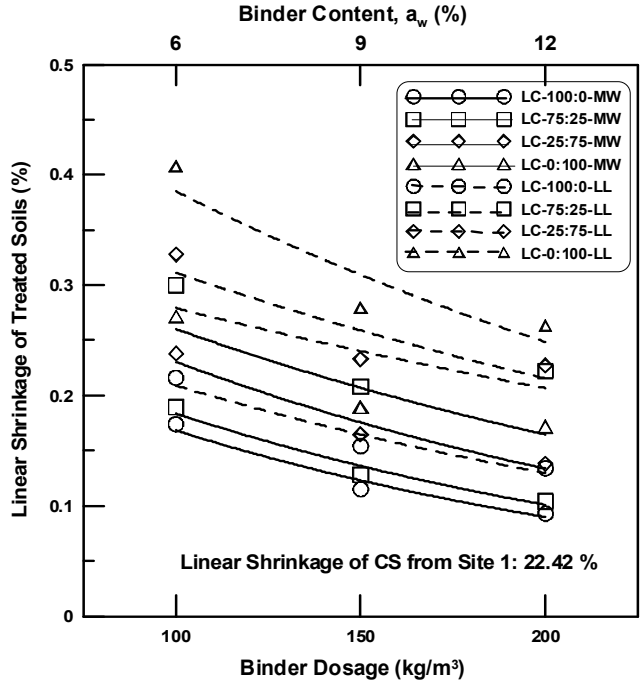

(a)

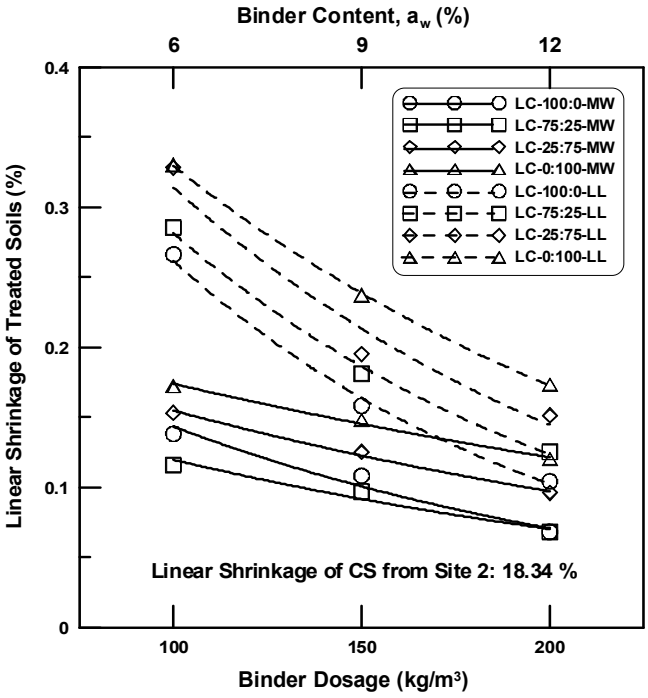

(b)

Figure 4.8 Effect of binder content, a_w (%) on linear shrinkage strains of treated soil samples at 7-day curing from Sites 1 and 2.

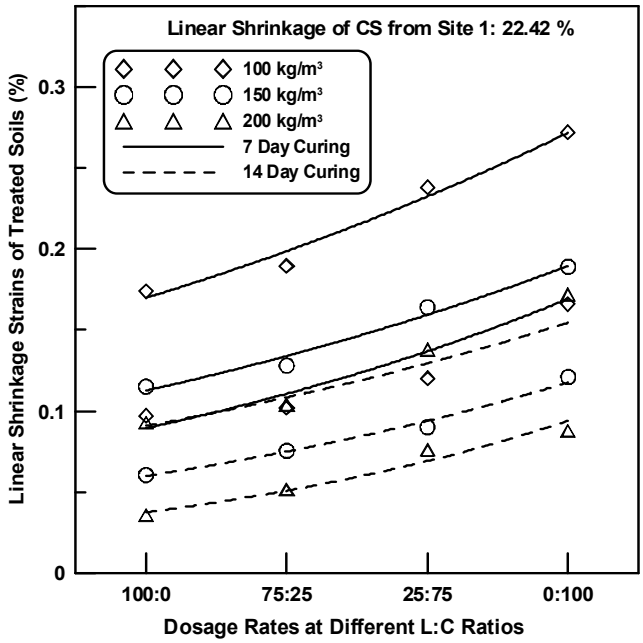

(a)

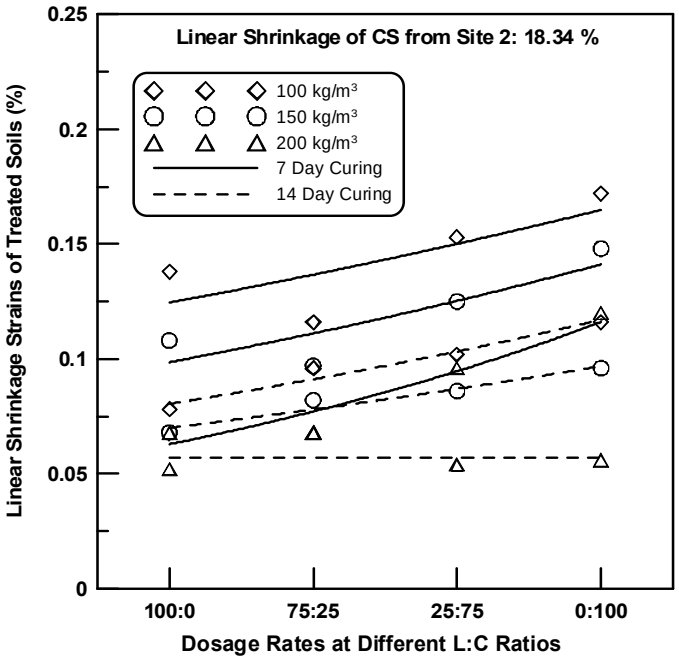

(b)

Figure 4.9 Effect of binder proportions and curing period on linear shrinkage strains of treated specimens at molding water content.

4.3.1.3 Effect of Curing Period

Figure 4.9 also depicts the effect of curing period on shrinkage strains of the treated soils, for both test sections, at molding water content and for w/b = 1.0. A decrease in shrinkage potentials for all binder dosages and proportions is noticed with a longer curing period. This can be attributed to the formation of more cementitious products (CSH and CAH) through pozzolanic reactions and, thereby, results in strength development and subsequent hardening with time. A maximum shrinkage strain of approximately 0.3% is noted for Site 1 at 100% cement treatment for α = 100 kg/m^3, w/b = 1.3 and 7-day curing at molding water content.

Molding water content (MW) is the total water in the clay at which field construction of the DSM columns will be carried out. In Site 2, treated specimens yielded slightly lower values compared to those of Site 1. A 100% cement treated specimen of Site 2 for the above combination of other parameters produced a maximum shrinkage strain of 0.17%. This variation in shrinkage strains can be attributed to the presence of high percent of fines in the Site 2 soil. Also, from the slopes of typical curves in Fig. 4.9, the rate of increase in shrinkage strains of specimens of Site 1 is same irrespective of curing time. Whereas, in case of Site 2, the rate of increase in shrinkage strain decreased with curing time and is zero for 200 kg/m^3 dosage rate (Fig. 4.9[b]). Otherwise, for Site 2 treated specimens after a curing period of 14 days, an increase in cement content at 200 kg/m^3 dosage did not show any influence on shrinkage strains when compared to those from Site 1 (Fig. 4.9[a]).

The specimens prepared at the liquid limit yielded a similar response to increasing dosage rates and lime-cement proportions at both 7 and 14 days curing. Figure 4.10(a) shows the patterns of shrinkage in the control soil along the transverse and longitudinal directions, which were minimized considerably after treatment (Figure 4.10[b]). The untreated specimens were brittle and warped considerably in the vertical direction. But all of the treated specimens

exhibited hairline cracks on the surface in the transverse direction with no warping or curling observed.

(a)

(b)

(c)

(d)

Figure 4.10 Typical shrinkage patterns of untreated and treated specimens of Site 1 for α = 200 kg/m^3; L:C = 25:75; curing time = 7 days and at w/b of (a) 0 (b) 0.8 (c) 1.0 and (d) 1.3.

Table 4.4 Linear shrinkage strains in (%) for Site 1 after 7-day curing period with varying dosage rates for different w/c ratios at (a) LL and (b) MW.

(a)

Binder Dosage (kg/m^3)	w/c	100-0	75-25	25-75	0-100
	0.8	0.132	0.145	0.203	0.207
100	**1**	0.174	0.1894	0.238	0.272
	1.3	0.193	0.212	0.257	0.298
	0.8	0.091	0.104	0.135	0.17
150	**1**	0.115	0.128	0.164	0.189
	1.3	0.152	0.167	0.196	0.237
	0.8	0.052	0.088	0.101	0.149
200	**1**	0.093	0.104	0.138	0.172
	1.3	0.127	0.131	0.149	0.193

(b)

Binder Dosage (kg/m^3)	w/c	100-0	75-25	25-75	0-100
	0.8	0.194	0.247	0.271	0.322
100	**1**	0.216	0.3	0.328	0.406
	1.3	0.257	0.344	0.369	0.490
	0.8	0.109	0.165	0.209	0.214
150	**1**	0.154	0.208	0.233	0.278
	1.3	0.178	0.241	0.278	0.307
	0.8	0.102	0.177	0.191	0.219
200	**1**	0.134	0.222	0.227	0.262
	1.3	0.159	0.261	0.273	0.319

Table 4.5 Linear shrinkage strains in (%) for Site 2 after 7-day curing period with varying dosage rates for different w/c ratios at (a) LL and (b) MW.

(a)

Binder Dosage (kg/m^3)	w/c	100-0	75-25	25-75	0-100
	0.8	0.102	0.134	0.141	0.153
100	**1**	0.138	0.116	0.153	0.172
	1.3	0.175	0.188	0.17	0.194
	0.8	0.076	0.098	0.111	0.129
150	**1**	0.108	0.097	0.125	0.148
	1.3	0.133	0.124	0.149	0.177
	0.8	0.051	0.082	0.088	0.102
200	**1**	0.068	0.068	0.096	0.12
	1.3	0.090	0.096	0.124	0.155

(b)

Binder Dosage (kg/m^3)	w/c	100-0	75-25	25-75	0-100
	0.8	0.133	0.173	0.239	0.277
100	**1**	0.266	0.285	0.328	0.33
	1.3	0.304	0.341	0.366	0.39
	0.8	0.119	0.144	0.149	0.185
150	**1**	0.158	0.181	0.195	0.237
	1.3	0.301	0.292	0.298	0.367
	0.8	0.064	0.099	0.139	0.155
200	**1**	0.104	0.125	0.151	0.173
	1.3	0.135	0.169	0.244	0.249

4. 3.1.4 Effect of Water-Binder Ratio

The effect of variation in moisture quantity within the soil mass is also analyzed here and depicted in Figures 4.10 and 4.11. In earlier subsections, the effect of dosage rate (α) and binder proportion (L:C) are discussed for a given w/b ratio of 1.0. Similar observations are also noted for w/b ratios of 0.8 and 1.3. However, as expected, the increase in w/b ratio increased the linear shrinkage strains. But, the interesting observation is that with an increase in the w/b ratio, the difference in shrinkage strains with regard to L:C proportion decreased for the Site 2 soils. For Site 1 soils, the difference in shrinkage strains with regard to L:C remained almost the same for all the w/b ratios. It can also be visually noticed from Figure 4.10 that the width of hairline cracks is larger as the moisture quantity in the treated soil specimens increased.

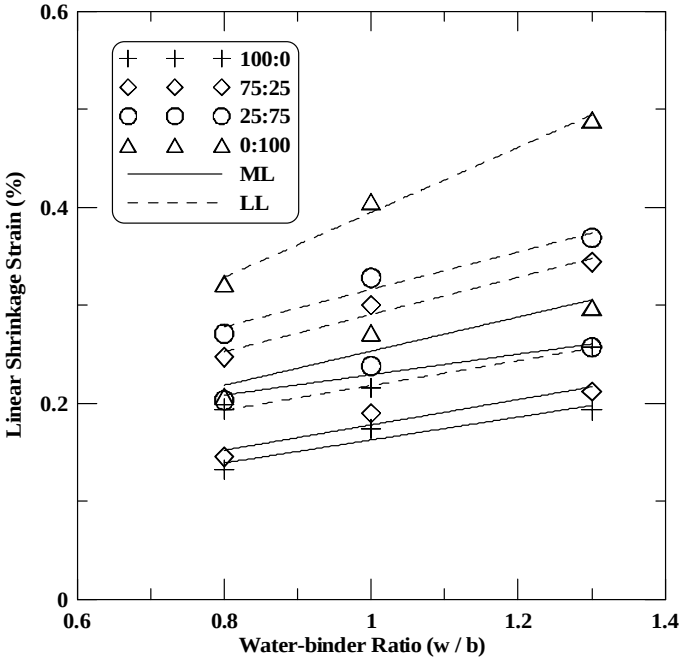

(a)

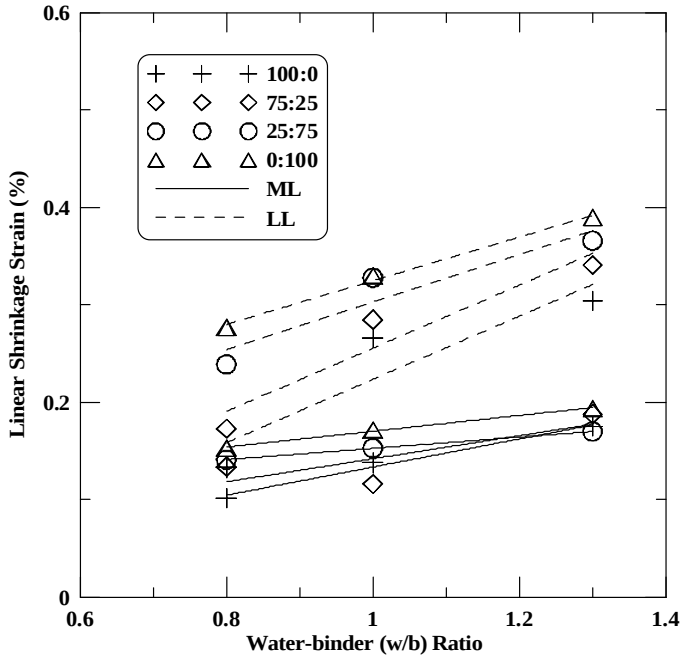

(b)

Figure 4.11 Effect of variation in w/b ratio (i.e., moisture quantity) on linear shrinkage strains at α=100 kg/m^3 (a) Site 1 and (b) Site 2.

4.3.2 Free Swell Strains

An acrylic mold, 2.75 in. (70 mm) in diameter and 1 in. (25 mm) in height, was used for the preparation of the treated soil specimens for free swell testing. No free swell data were recorded in the treated specimens, for all binder proportions, dosage rates and w/b ratios at both curing periods, as the magnitudes of potential free swells of these specimens are close to zero. This may be attributed to the physico-chemical changes that take place at the particle level upon lime, cement or lime-cement treatment reducing the affinity of expansive soils for water. The formation of cementitious products with time also help in reducing expansiveness of the soil through an increase in particle size (flocculation and agglomeration) to almost silt-like material and thereby decreasing its plasticity. Fig. 4.12 depicts the pictures of both untreated and treated specimens of Test Sections 1 and 2 at the end of the free swell testing with respect to the mold used for the specimen preparation. It can be noticed that the size of treated specimens is almost the same before and after the swell test.

Fig. 4.13 presents the distribution of unit weight data from the specimen preparation for the free swell tests. The range of unit weights for Site 1 and Site 2 are 18.2 to 20.2 kN/m^3 (116 to 128.7 pcf) and 18.3 to 20.0 kN/m^3 (116.4 to 127.3 pcf), respectively. Since no significant difference is observed in the range and distribution of the unit weight data of both sites, the data were combined for the normal distribution plot presented in Figure 4.13. The average unit weight and $\overline{\sigma}$ of the unit weight data are 19 kN/m^3 and 0.48 kN/m^3, respectively. A low value of $\overline{\sigma}$ indicates that the specimen preparation is consistent.

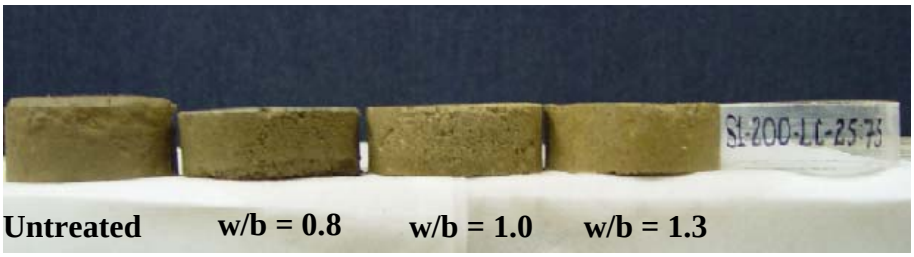

(a)

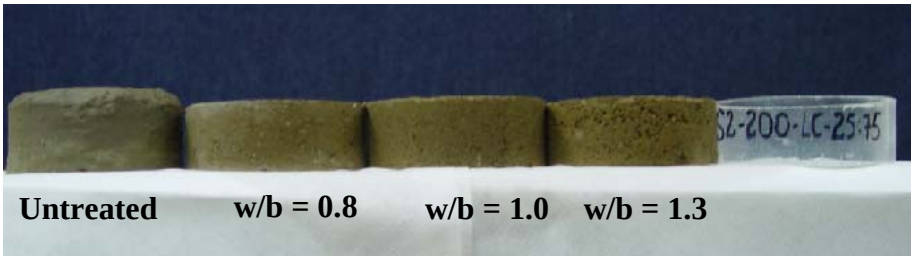

(b)

Figure 4.12 Pictures of untreated and treated specimens after free swell test at Sites 1 and 2.

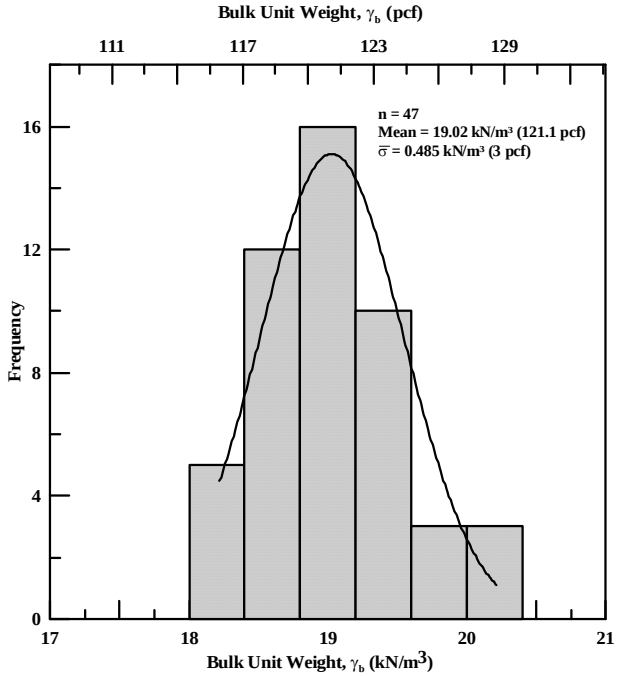

Figure 4.13 Distribution of bulk unit weight data of free swell specimens from both site soils.

4.3.3 Unconfined Compressive Strength

4.3.3.1 Specimen Homogeneity

Unconfined compressive strength (UCS) tests were performed at all dosage levels, binder proportions and curing periods to evaluate the best performing binder combination to optimize the strength and shrink-swell behavior of DSM and, thereby, the performance of the composite ground. As mentioned earlier in the specimen preparation procedure, a split type acrylic mold was used for the UCS specimen preparation. The specimens were prepared following the step-by-step procedure explained in the laboratory DSM protocol section in Chapter 2. Fig. 4.14 shows the typical normal distribution of bulk unit weight data of the UCS specimens from both sites for a water-binder ratio of 1.0 with standard deviation, $\overline{\sigma}$ of 0.69 kN/m^3 indicating that the bulk density of the treated specimens is fairly constant and, therefore, the variation in strength can be attributed to the variation in binder content and proportions at the respective curing periods and water-binder ratios. The results indicated a consistent preparation of the UCS specimens following the suggested specimen preparation procedure.

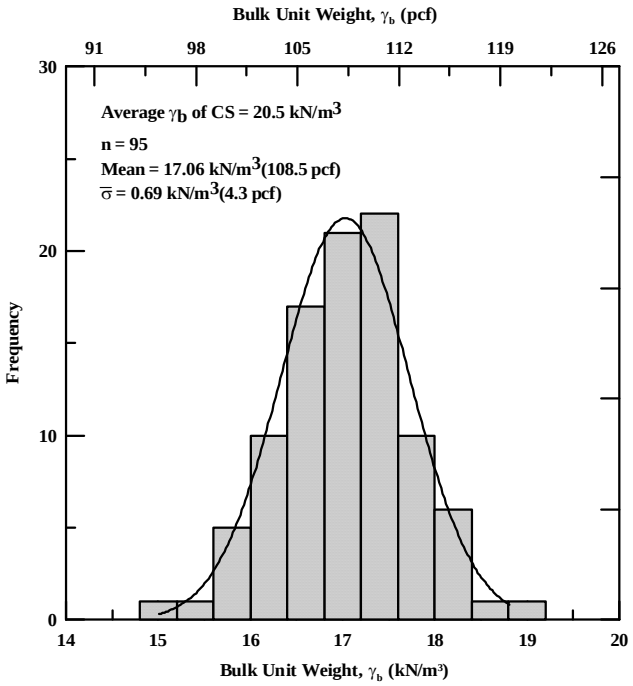

Figure 4.14 Normal distribution unit weight data of treated UCS specimens of both sites.

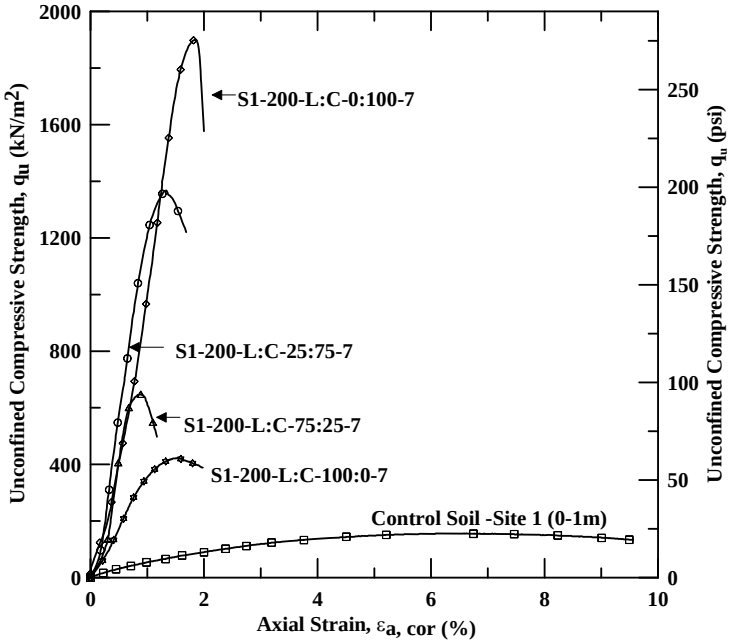

Figure 4.15 Stress strain response, post peak strength and failure axial strain profiles for various binder proportions (S1-200-L:C-X-7-1.0).

4.3.3.2 Stress-Strain Behavior of the Treated Soils

Typical stress-strain of plots of the treated specimens of the Site 1 soils for different binder proportions and water-binder ratio are depicted in Figures 4.15 and 4.16. All treated specimens exhibited brittle failure contrary to the undisturbed untreated specimens, which exhibited ductile failure. The failure strains of all the treated specimens from both of the test sections are in the range of 1 to 2%. A sudden drop in post peak strength was noticed in the stress-strain response of the treated specimens and this behavior is predominant with an increase in cement content (Fig. 4.15). It is clear from Fig. 4.16 that increases in the w/b ratio resulted in a decrease of peak strength, but no particular trend is noticed in the failure strains. These results suggest that with an increase in total moisture, the peak strength was reduced indicating more moisture in the soil that did not result in more enhancements from the pozzolanic reactions.

Due to the number of parameters studied in the current research, the effect of binder dosage and proportions, curing time and water-binder ratio on strength and stiffness are analyzed and discussed individually in the following sections.

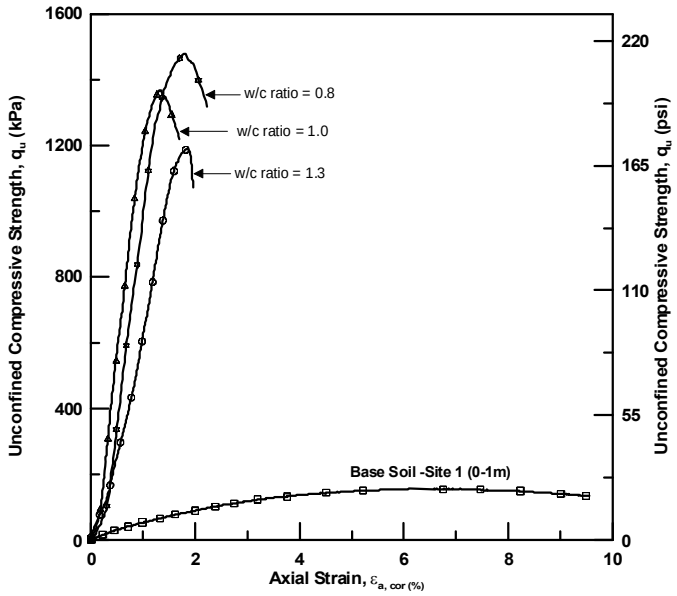

Figure 4.16 Stress strain response, post peak strength and failure axial strain profiles at different w/c ratios - Site 1, 25:75 (L:C) proportion, 200 kg/m^3 and 7-day curing.

4.3.3.3 Effect of Binder Dosage and Proportions

Fig. 4.17 depicts the effects of binder dosage and proportions for both curing periods (7 and 14 days) on the unconfined compressive strength (UCS) of the treated soils from both sites at a typical water-binder ratio of 1.0. For all water-binder ratios (0.8 to 1.3), the rate of strength enhancement; i.e., slope of trend lines, is significant with an increase in the binder dosage with 75 and 100% cement proportions as compared with the 75 and 100% lime proportions. The low to negligible strength enhancements with binder dosage when the lime proportion is more than 25% could possibly be due to the lack of enough time for the formation of pozzolanic compounds. From previous studies presented in Chapter 2, it is clear that lime treatment improves physico-chemical properties in a short time, but yields significant strength enhancements or even more than that of cement treatment in the long term only. Therefore, in the

present study a curing period of 14 days is considered to be short for binder dosages with lime proportions more than 25% to show any considerable strength enhancements. The UCS obtained for each combination of binder dosage (α), binder composition or proportion (L:C) and water-binder ratio for both curing times are presented in Tables 4.6(a) and (b).

Table 4.7 shows the increase in strength for all binder dosages and proportions for a typical water-binder ratio of 1.0 with respect to the untreated soil strength. The percent increase in strength with binder dosage, of 100% lime and 100% cement, of treated soil from Site 1 is in the ranges of 45 to 65% and 80 to 90%, respectively, irrespective of curing time.

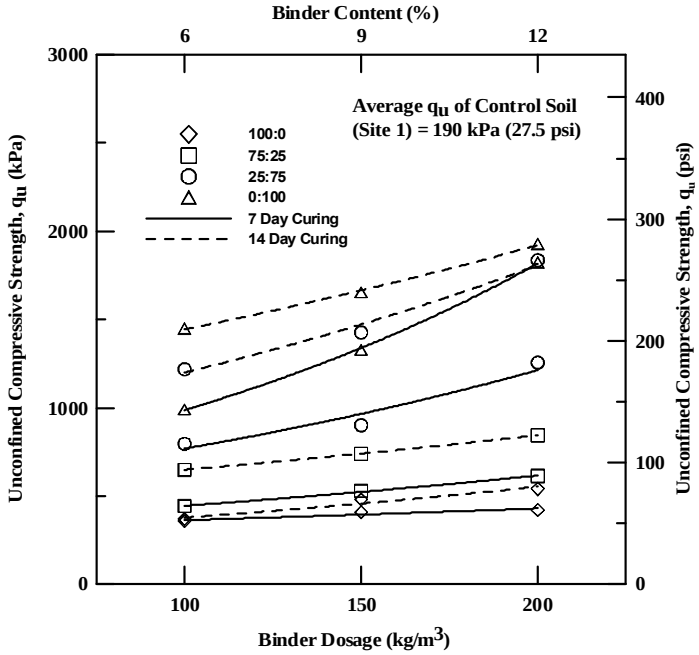

(a)

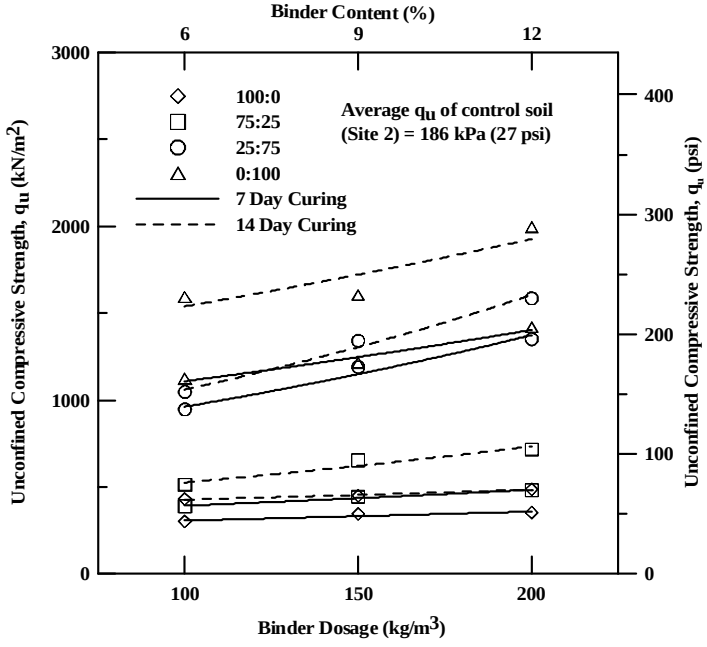

(b)

Figure 4.17 Effect of binder dosage and proportions on UCS of treated specimens from both test sections at w/b = 1.0 at Sites 1 and 2.

Table 4.6 UCS in kPa (1 kPa = 0.145 psi) of treated soils.

(a) Site 1

Binder Dosage (kg/m^3)	w/b	Curing Time (days)	Binder Proportion (L:C) S1			
			100:0	75:25	25:75	0:100
100	0.8	7	370	480	1175	1025.8
		14	403	714	1700	1672
	1	7	357	443	795.8	990.5
		14	369	649	1218.4	1448.8
	1.3	7	310	412.7	727	911.23
		14	340	617.9	1019.2	1211.1
150	0.8	7	428.5	540	1295.6	1420.6
		14	511.3	775.4	1562	1744.1
	1	7	409	528.7	901.13	1330
		14	480	740	1426.6	1654
	1.3	7	386.2	413.9	874.8	1297
		14	402.2	594	1390	1547
200	0.8	7	460	642.3	1308	1910.2
		14	560.2	994	1911.5	1980
	1	7	422.7	613.5	1256.4	1824
		14	540	845	1836	1928.2
	1.3	7	394.1	598	1120	1719
		14	532	813.3	1782	1790

(b) Site 2

Binder Dosage (kg/m^3)	w/b	Curing Time (days)	Binder Proportion (L:C)			
			100:0	75:25	25:75	0:100
100	0.8	7	344	600	1186	1386
		14	453	740	1214	1667
	1	7	302	390	946	1123.5
		14	430	513.8	1047	1595
	1.3	7	280	310	880	949.9
		14	419.7	507	934	1294
150	0.8	7	357	765	1287	1395
		14	475	865	1528	1742
	1	7	344.7	442.5	1190	1216
		14	450	653.5	1341	1605
	1.3	7	307.1	419	908.3	940.5
		14	422.6	611.8	940	1493
200	0.8	7	370.3	790.7	1391.2	1559
		14	505	870.6	1711.3	2221
	1	7	353	481	1351	1422
		14	487	716.7	1585	1996
	1.3	7	351	457.5	893	1363.3
		14	413	690	947	1841

Site 2 soils, with high PI, also exhibited similar increase in strength approximately in the same ranges indicating that the difference in PI of both soils did not show any effect on strength gain. The maximum strength increase is noticed in the specimens treated with a w/b ratio of 0.8.

Table 4.7 Percentage increase in strength of treated soils of both sites for w/b = 1.0 (Sites 1 and 2).

(a) Site 1

Curing Period	**Dosage**	**100:0 (%)**	**75:25 (%)**	**25:75 (%)**	**0:100 (%)**
7- Day	100 kg/m^3	46.78	57.11	76.12	80.82
	150 kg/m^3	53.55	64.06	78.9 2	85.71
	200 kg/m^3	55.05	69.03	84.88	89.58
14 – Day	100 kg/m^3	48.51	70.72	84.41	86.89
	150 kg/m^3	60.42	74.32	86.68	88.51
	200 kg/m^3	64.81	77.51	89.65	90.15

(b) Site 2 (check appropriateness of this table % increase = [qu(t)-qu(ut)]/qu(t)?)

	Dosage	**100:0 (%)**	**75:25 (%)**	**25:75 (%)**	**0:100 (%)**
7-day Curing	100 kg/m^3	38.41	52.31	80.34	83.44
	150 kg/m^3	46.04	57.97	84.37	84.70
	200 kg/m^3	47.31	61.33	86.23	86.92
14-day Curing	100 kg/m^3	56.74	63.80	82.23	88.34
	150 kg/m^3	58.67	71.54	86.13	88.41
	200 kg/m^3	61.81	74.05	88.26	90.68

Fig. 4.17 and Table 4.6 also demonstrate the effect of the binder proportion (L:C) on the unconfined compressive strength (q_u). But for better understanding of the results, Fig. 4.17 is reproduced with q_u as a function of L:C (Fig. 4.17). For Site 1, at a given binder dosage, the variation in the binder proportion, L:C, from 100:0 to 0:100 resulted in a strength gain from 46 to 80% at 100 kg/m^3 and 55 to 90% at 200 kg/m^3 at 7-day curing and w/b = 1.0 (Table 4.7). The ranges are about the same for soils from Site 2 for the above combination of other variables; however, the highest percentage increase in strength gain with L:C for both soils is recorded for a dosage rate of 200kg/m^3, 14-day curing and w/b = 0.8. The lower bound values are observed for a w/b ratio of 1.3.

From Fig. 4.18, the slope of trend lines; i.e., the rate of strength with cement content, increased with binder dosage and curing time. These figures clearly show the effect of lime content in the binder on the strength gain, irrespective of curing time and dosage rate. The unconfined compressive strength of the 100% lime treated soil specimens is approximately 23 to 36% of the strength of the 100% cement treated soil specimens. For example, for a dosage rate 200 kg/m^3, lime treatment of the Site 1 soils resulted in strengths between 420 to 540 kPa, whereas cement treatment resulted in 1820 to 1930 kPa, as shown in Fig. 4.18(a). Hence, it is important to understand the effects of adding lime when the binder used for stabilization of soils is a combination of one or more stabilizer types including lime. Also the selections of binder dosage and binder type are primarily governed by the project requirement. In cases, where high strengths of foundation subgrades are of importance (such as embankment on soft soils) then high percentages of cement are preferred.

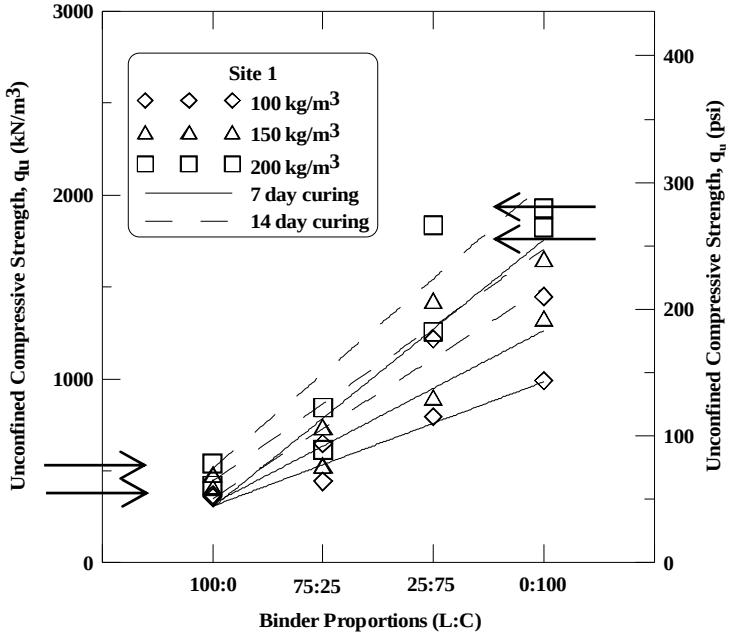

(a)

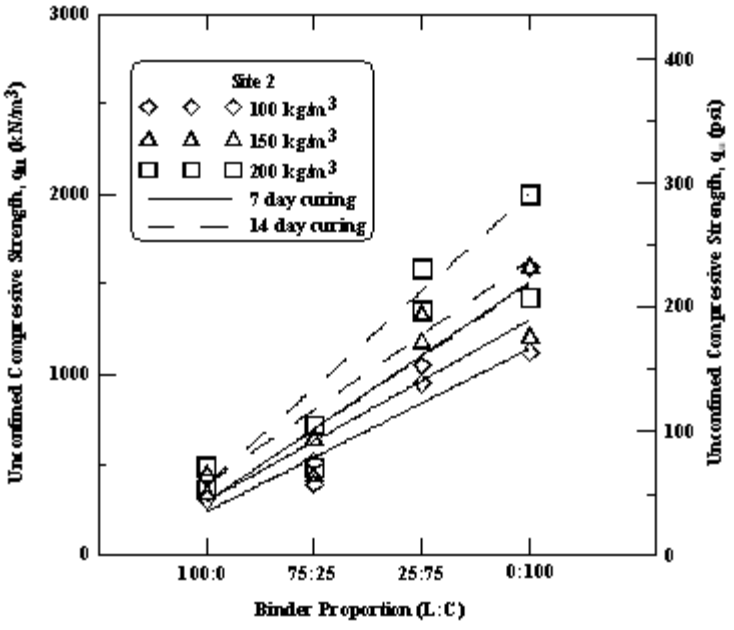

(b)

Figure 4.18 Effect of binder proportion on unconfined compressive strength for a typical w/b ratio of 1.0.

In cases where reductions in volumetric changes in expansive soils are of importance, then moderate to high amounts of lime are preferred along with cement additives.

4.3.3.4 Effect of Curing Period

The effect of curing period on strength gain is studied at 7 and 14 days. The specimens were sealed and stored in a 100% relative humidity room maintained at 20±3ºC. The unconfined compressive strengths after 7 and 14 days of curing are depicted in Fig. 4.19 irrespective of binder type, dosage rate and soil type for all water-binder ratios. The results yielded a 25 to 29% increase in UCS after 14-day curing as compared to those after 7-day curing period. The difference in water-binder ratio did not show any effect on the percent of strength enhancement with curing time.

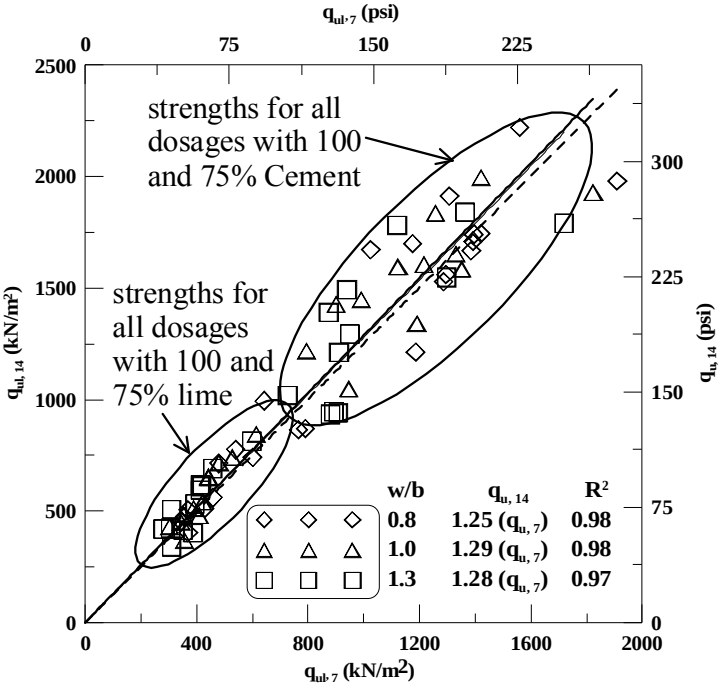

Figure 4.19 Effect of curing time on UCS of treated soils for all binder dosages and proportions from Sites 1 and 2.

In all the cases (i.e., w/b 0.8 to 1.3), scatter in the UCS data is noticed for binder dosages with high cement proportions (75 and 100%). The scatter in data at high cement contents can be attributed to variabilities in cemented specimens and different operators working with different

binder ratios. Nevertheless, the variations at such high strengths are small and practically insignificant.

The initial elastic modulus (E_i) and secant modulus at 50% failure stresses (E_{50}) are estimated from the stress-strain responses of the treated soils. The parameters E_i and E_{50} are measured as the slopes of the initial tangent and secant at 50% of the failure stress, respectively, as demonstrated in Fig. 4.20.

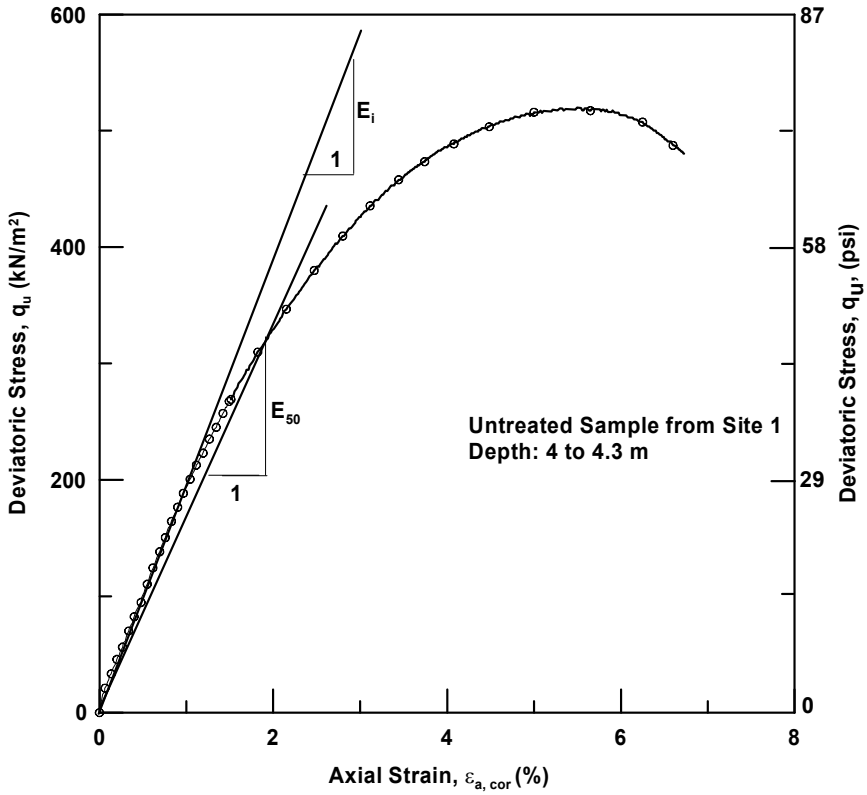

Figure 4.20 Schematic of stress-strain response demonstrating estimation of E_i and E_{50} from initial tangent and secant at 50% failure stress.

The effect of curing time on these parameters is studied and presented in the following sections for a typical water-binder ratio of 1.0. The relationship between the unconfined compressive strength (q_u) and the secant modulus (E_{50}) of the treated specimens from both site soils for all binder dosages and proportions is depicted in Fig. 4.21. The secant modulus of specimens treated with binder containing more than 75% cement and 75% lime are in the ranges

of 14.5 (100 MPa) to 34.8 ksi (240 MPa) and 5.8 (40 MPa) to 18.13 ksi (125 MPa), respectively, for both curing periods. Therefore, it can be concluded that binders with high percentages of lime content result in low strength and stiffness properties early on and may not be suitable for projects such as pavements with short restoration time.

From Table 4.8, it is noticed that the ratio E_{50}/q_u is about 150 to 160 and 116 to 124 for treatment with binders possessing more than 75% lime and cement, respectively. The average of the ratio, E_{50}/q_u, irrespective of binder composition is about 120 to 127. The ratio of stiffness to strength decreased slightly with curing time. The relationships derived above from the experimental data are observed to be in good agreement with those reported in the literature. The variation in strength and stiffness properties based on binder composition is considerable and, therefore, it is recommended to use the respective values from the laboratory studies in the design and analytical and/or numerical studies instead of average values.

Table 4.8 Stiffness properties of treated specimens.

Stiffness	Binder Composition	Curing Period (Days)	
		7	14
E_{50} (MPa)	Lime > 75%	100 to 200	120 to 240
	Cement > 75%	40 to 110	60 to 125
E_{50}/q_u	Lime >75%	124	116
	Cement >75%	160	150
	Irrespective of composition	127	120

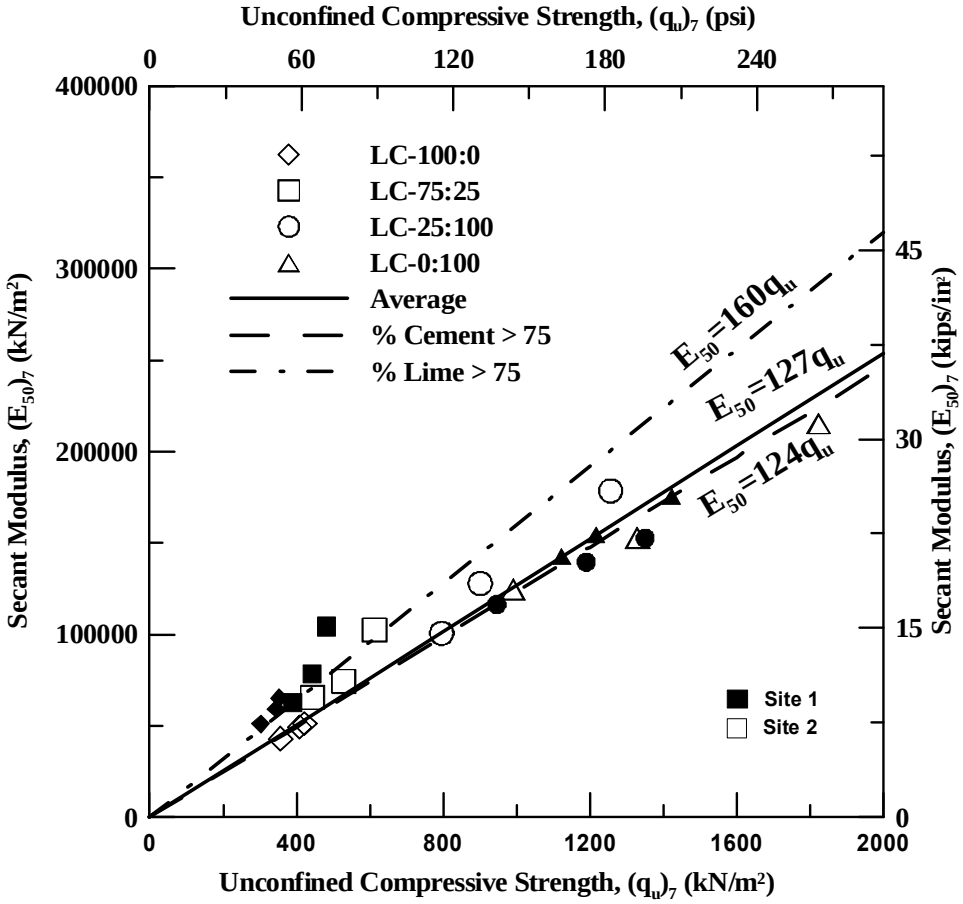

(a) 7-day curing period

Figure 4.21 Relationship between stiffness and UCS values for all dosages and proportions at 7- and 14-day curing periods.

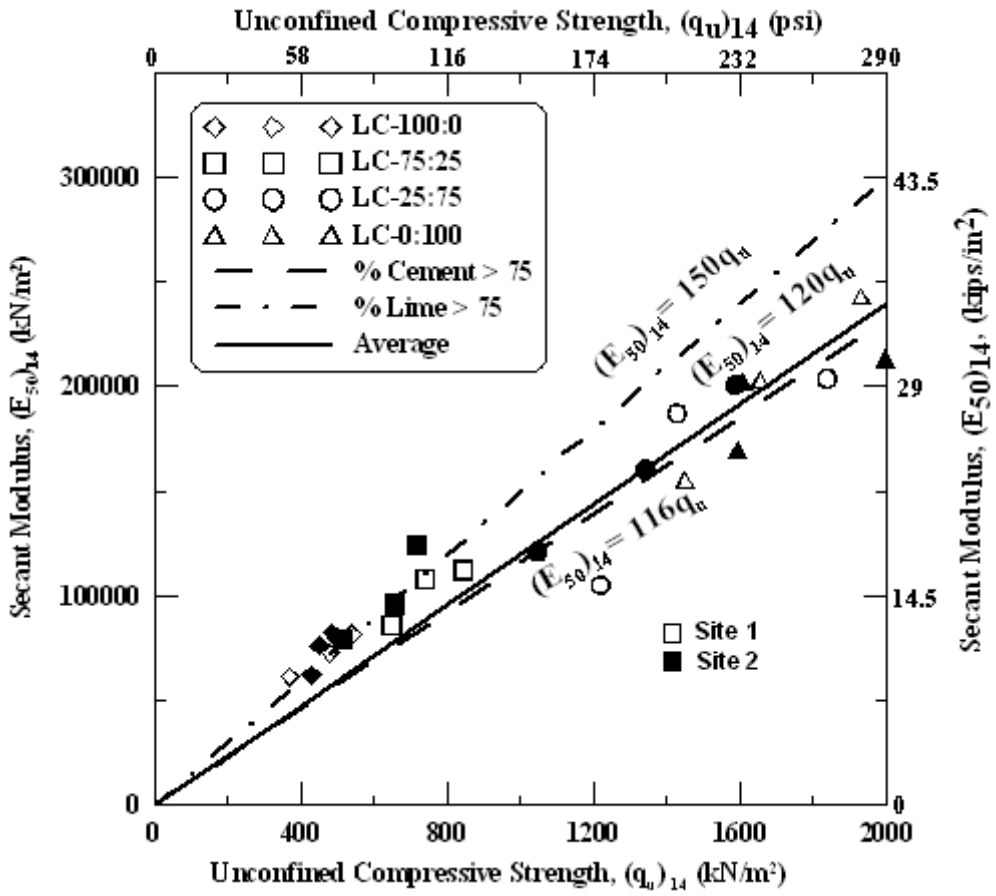

(b) 14-day curing period

Figure 4.21 Relationship between stiffness and UCS values for all dosages and proportions at 7- and 14-day curing periods (continued).

The initial tangent modulus (E_i) computed from the stress-strain response, as demonstrated in Figure 4.20, is presented here as a function of the secant modulus (Fig. 4.22). Irrespective of soil type, binder type, dosage and proportions and curing time, E_i can be estimated as 1.2 times E_{50} for a typical w/b ratio of 1.0.

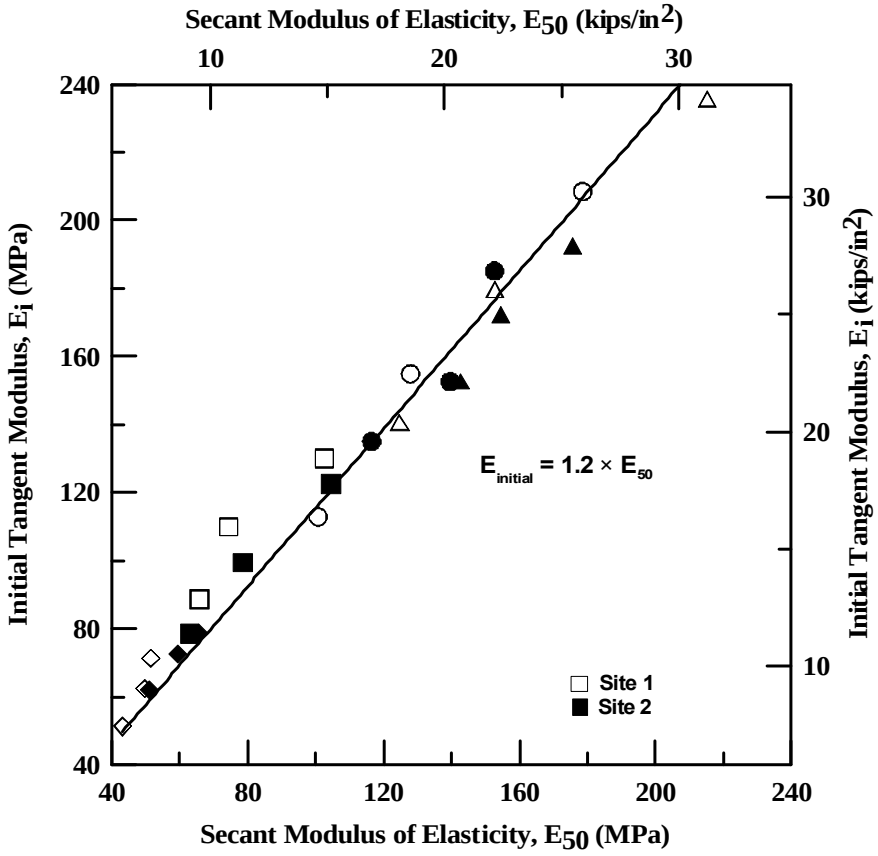

Figure 4.22 Relation between initial and secant modulus of elasticity.

4.3.3.5 Effect of Water-Binder (w/b) Ratio

From the literature review, it was noticed that the general range of water-binder ratio used in practice is 0.6 to 1.3 (Okumara 1997). High values are used when in situ moisture contents are low, whereas low values are used if the in situ moisture contents are high as in soft marine clays. In order to study the effects of w/b ratios on the behavior of treated soils, the present study considered three w/b ratios of 0.8, 1.0 and 1.3. Figures 4.23(a) and (b) depict the typical variation of strength of the treated specimens with respect to w/b ratio for both soils, all binder dosages and curing periods for a L:C proportion of 25:75. It can be noticed that the strength decreased nonlinearly with the w/b ratio and high strengths are recorded at low w/b ratio, high dosage rate and 14-day curing time. In the case of the Site 2 soils, the range of

strength at a w/b ratio of 1.3 is 880 to 950 kPa, indicating that the strength enhancement at high w/b ratios is almost negligible. Contrary to Site 2 data, the Site 1 soils showed considerable enhancements in strengths at all w/b ratios. The strengths of the Site 1 soils are in the ranges of 1300 to 1900 kPa and 720 to 1780 kPa at low (0.8) and high (1.3) w/b ratios, respectively. Similar trends are noticed for other proportions studied here. Typical shear failures of the UCS specimens at low and high water-binder ratios at a binder dosage of 200 kg/m^3 and for L:C proportion of 25:75 are depicted in Figure 4.24.

Horpibulsuk et al. (2001) and Miura et al. (2001) proposed a new parameter known as total clay water content-binder ratio (w_c/b) to accommodate the variations in water content during DSM by the wet method. The parameter (w_c/b) resulted in a unique relationship with strength (q_u) for a particular curing time, soil type, binder type etc. (Miura et al. 2001; Horpibulsuk et al. 2003 and Lorenzo and Bergado 2004). The empirical expression for strength development as a function of w_c/b ratio is an exponential variation, as follows:

$$q_{u,t} = A/B^{wc/b} \quad (4.1)$$

where A and B are empirical constants depending on soil type, binder type, and curing time. The ratio of total clay water to binder (w_c/b) is defined as the weight of all forms of water present in the clay-water-cement paste to the weight of binder; i.e., total clay water content to binder content, both in percentage. The equation for total clay water content (w_c) as given by Lorenzo et al. (2006) is

$$w_c = w + (w/b) \times a_w \quad (4.2)$$

where, w is the in situ moisture content; w/b is the water-binder ratio and a_w is the binder content

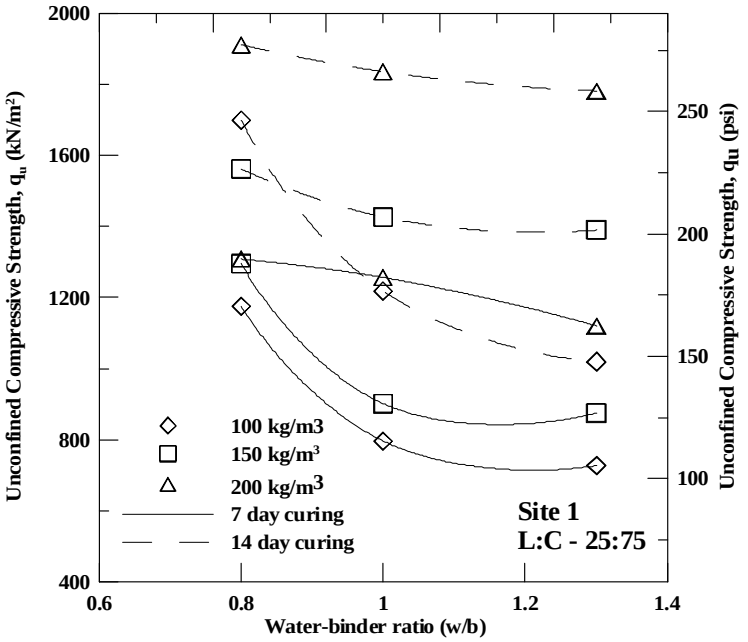

(a)

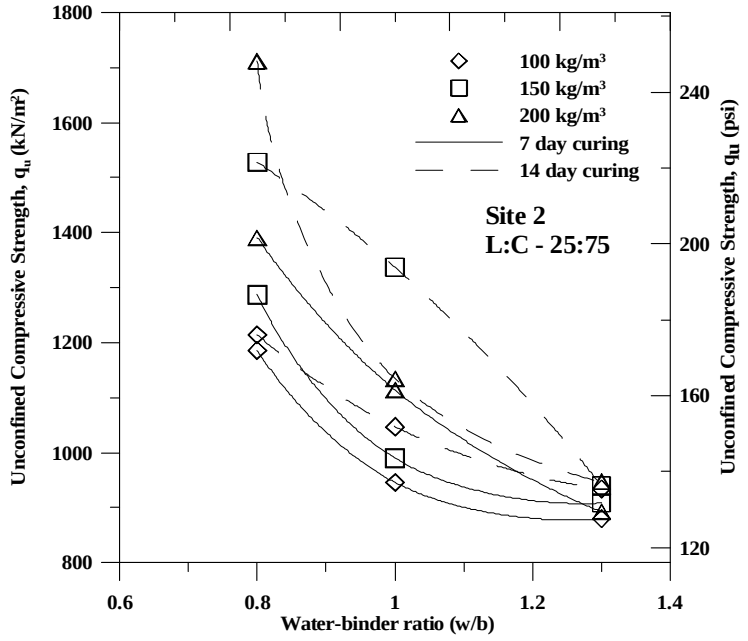

(b)

Figure 4.23 Effect of water-binder ratio on unconfined compressive strength at a lime-cement binder composition of 25:75 for Sites 1 and 2.

(a)

(b)

Figure 4.24 Typical failures of UCS specimens at 25:75 (L:C) binder proportion and 200 kg/m^3 binder dosage after 14-day curing period; (a) w/b = 0.8 and (b) w/b = 1.3.

in percent. In the present study, the parameters A and B are estimated for all the binder proportions; i.e., all binder types (lime, cement, 75% lime + 25% cement and 25% lime + 75% cement) at both curing periods and for soils at both sites. The parameter w_c/b for water-binder ratios of 0.8, 1.0 and 1.3 for Sites 1 and 2 is calculated using equation (4.2). The variations of strength with w_c/b for 100% lime and 100% cement treatments for both soils are depicted in Fig. 4.25. Compared to the water-binder (w/b) ratio the parameter w_c/b yielded a unique relationship with strength by normalizing the effect of the binder dosage or content. The parameters A and B are determined by fitting an exponential function to the experimental data for each soil type and binder type. The results from present and previous studies are tabulated in Table 4.9.

The experimental data from previous studies (Horpibulsuk et al. 2003) on cement treated soft Ariake and Bangkok clays were also included in Fig. 4.25(b) along with the present results of cement treated expansive clays. The trends noticed for expansive soils in this research are similar to those reported in the literature. However, the range of w_c/b covered in the present study is narrow when compared to those reported by Miura et al. (2001), Horpibulsuk et al. (2003), and Lorenzo and Bergado (2004) for soft soils. The empirical constant A is varied significantly for a given soil type depending on both binder type and curing, whereas the constant B is in the ranges of 1.14 to 1.37 and 1.06 to 1.29 for Sites 1 and 2 soils, respectively, which are close to those obtained for soft soils. This indicates that B is independent of soil type, binder type and curing time. The empirical relationship of Eq. (4.1) along with the Table 4.9 data can be used to predict strengths at different w_c/b ratios at a particular curing time period for a given soil type. Eq. (4.2) is useful in estimating the w/b (water-binder) ratio to be used in field construction when the in situ moisture content varies from the time of sampling conducted for laboratory studies and/or to accommodate the increase in water content during the wet mixing method.

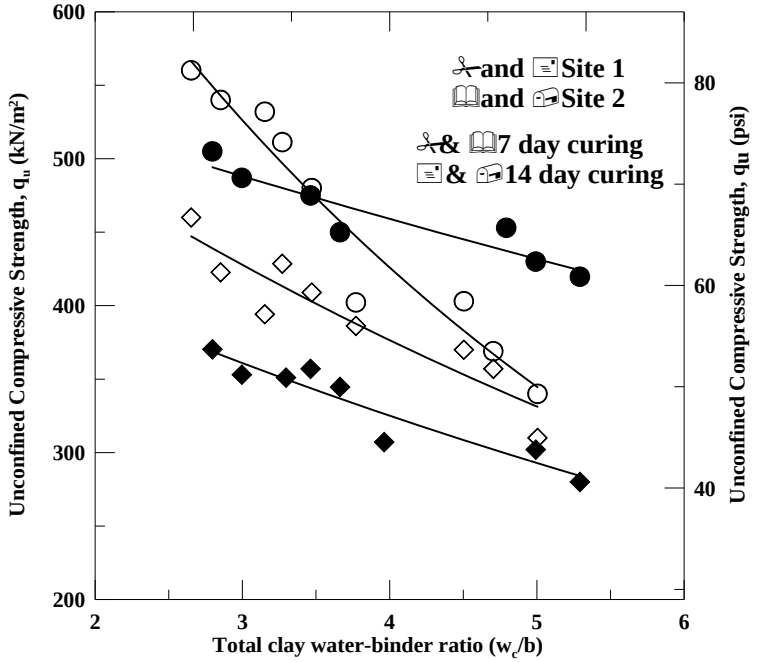

(a) 100% Lime treatment

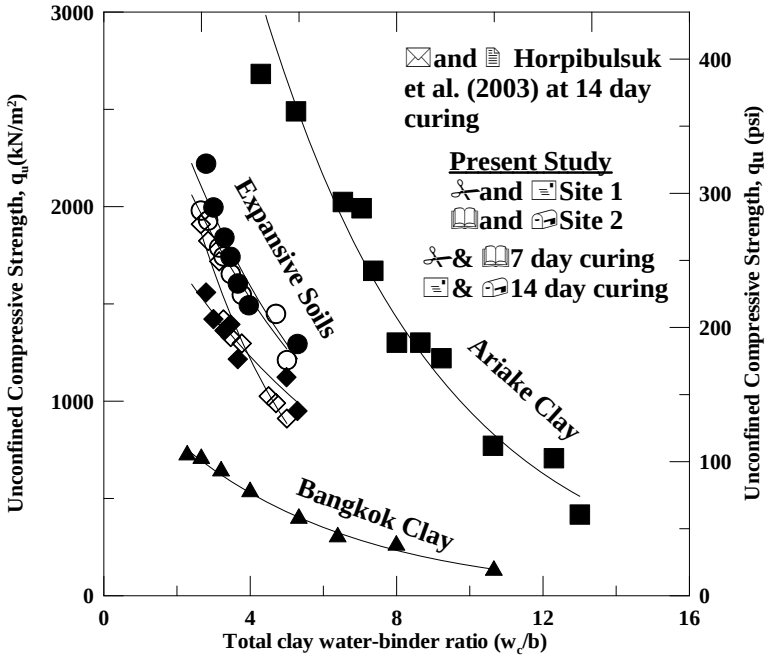

(b) 100% Cement treatment

Figure 4.25 Variation of strength with total clay water-binder ratio for different soil types and curing time for (a) 100% lime treatment and (b) 100% cement treatment.

Table 4.9 Empirical constants A and B from present and previous studies.

Author	Soil Type	Binder Type	Curing Time (Days)	Empirical Constants	
				A	B
Present Study	Site 1: Medium PI Expansive Clay	L	7	627.47	1.136
			14	991.94	1.235
		C	7	4344	1.37
			14	3224.1	1.205
		75%L +25%C	7	996.97	1.188
			14	1350.3	1.168
		25%L +75%C	7	1112	1.229
			14	1274.5	1.177
	Site 2: High PI Expansive Clay	L	7	493.56	1.11
			14	586.4	1.063
		C	7	2379	1.18
			14	3659.5	1.231
		75%L +25%C	7	2529	1.289
			14	3666	1.284
		75%L +25%C	7	1795	1.134
			14	2397	1.189
Miura et al. (2001)	Soft Hong Kong Clay	Cement	28	2461	1.22
Horpibulsuk et al. (2003)	Soft Ariake Clay	Cement	7	4661	1.21
			14	7504	1.23
			28	7949	1.23
	Soft Bangkok Clay	Cement	7	969	1.24
			14	1130	1.24
			28	1739	1.24

4.3.4 Strength Improvement Ratio (S_{IR})

A factor, $S_{IR,}$ termed as strength improvement ratio was proposed here and estimated for a better understanding of improvement effects and for the appropriate selection of binder dosage and proportion based on target strength and untreated soil properties. The factor S_{IR} is defined as the ratio of unconfined compressive strength of the treated soil at a curing time, t, to the untreated soil. The expression for S_{IR} is as follows:

$$S_{IR} = \frac{q_{u,t}}{q_{u,0}} \tag{4.2}$$

where $q_{u,\,t}$ corresponds to the ultimate strength of the treated soil at the end of the curing period, t, viz. 7, 14, 28 or 56 days. In the present study, only two curing times of 7 and 14 days are considered. The typical variation of S_{IR} with binder dosage is depicted in Fig. 4.25 for soils from both sites at a water-binder ratio (w/b) of 1.0 and 7-day curing period. The ratios, S_{IR}, for other combinations of the research variables for both site soils are tabulated in Tables 4.10 and 4.11, respectively.

As expected, the trends of S_{IR} versus α are similar to those for q_u versus α. From Tables 4.10 and 4.11, the 100% lime treatment of soils from both sites resulted in strength improvement equal to 2 to 3 times the untreated soil strength. In this case, an increase in binder dosage and curing time didn't show any significant influence on strength improvement (S_{IR}). One hundred percent cement treatment of soils from both sites showed variation in the strength improvement ratio with dosage rate, water-binder ratio and curing time. However, the increase in curing time did not show considerable variation on the strength improvement (S_{IR}) of cement treated soils from Site 1 as compared to that from Site 2 soils. The strength improvement for cement treated soils of Site 1 is 5 to 10.4 times that of the UCS of the untreated soil for both

curing periods, whereas for Site 2 soils the strength improvement is equal to 5 to 8.4 times and 7 to 12 times that of the untreated soil strength at 7- and 14-day curing periods, respectively.

A brief example of the application of variations of S_{IR} with α in determining the dosage rate and binder proportion based on the target strength properties is cited below. For a case of a required strength improvement ratio of $S_{IR} = 5$, determined from the target strength as per project requirement and the untreated soil strength, say of Site 1, from the depths to be treated. Several viable combinations of binder dosage, binder proportion, and w/b ratio can be obtained referring to figures similar to Fig. 4.26 for other w/b ratios. Following are the few combinations of these variables to achieve the target strength:

- 50:50 at a dosage rate of 200 kg/m^3 at w/b = 0.8
- 25:75 at a dosage rate of 200 kg/m^3 at w/b = 1.0
- 50:50 at a dosage rate of 150 kg/m^3 at w/b = 1.0
- 50:50 at a dosage rate of 200 kg/m^3 at w/b = 1.3
- 25:75 at a dosage rate of 150 kg/m^3 at w/b = 1.3

Selection of an appropriate combination of variables from the above possible ones further depends on the mixing parameters and w/b ratio that yields a workable state or condition.

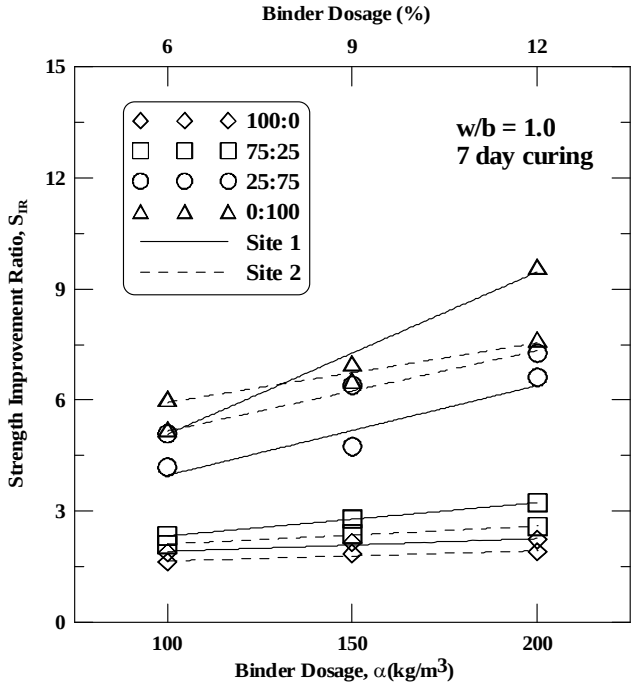

(a)

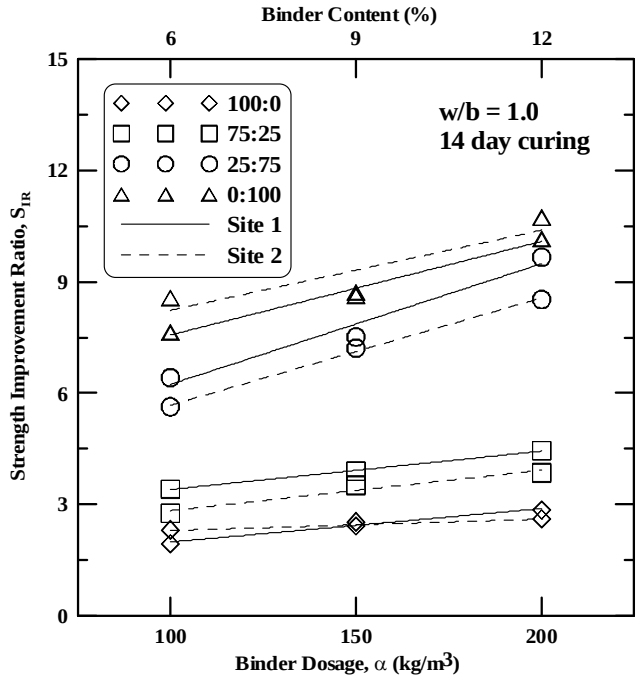

(b)

Figure 4.26 Variation of strength improvement ratio (S_{IR}) for typical w/b of 1.0 at (a) 7-day curing and (b) 14-day curing.

Table 4.10 Strength improvement ratio (S_{IR}) for Site 1 soils for 7- and 14-day curing periods.

(a) 7-day curing

Binder Dosage	w/b ratio	Binder Proportion (L:C)			
		100:0	75:25	25:75	0:100
100	0.8	1.9	2.5	6.2	5.4
	1	1.9	2.3	4.2	5.2
	1.3	1.6	2.2	3.8	4.8
150	0.8	2.3	2.8	6.8	7.5
	1	2.2	2.8	4.7	7.0
	1.3	2.0	2.2	4.6	6.8
200	0.8	2.4	3.4	6.9	10.1
	1	2.2	3.2	6.6	9.6
	1.3	2.1	3.1	5.9	9.0
Range		**1.9 to 2.4**	**2.2 to 3.4**	**3.8 to 6.9**	**4.8 to 10.1**

(b) 14-day curing

Binder Dosage	w/b ratio	Binder Proportion (L:C)			
		100:0	75:25	25:75	0:100
100	0.8	2.1	3.8	8.9	8.8
	1	1.9	3.4	6.4	7.6
	1.3	1.8	3.3	5.4	6.4
150	0.8	2.7	4.1	8.2	9.2
	1	2.5	3.9	7.5	8.7
	1.3	2.1	3.1	7.3	8.1
200	0.8	2.9	5.2	10.1	10.4
	1	2.8	4.4	9.7	10.1
	1.3	2.8	4.3	9.4	9.4
Range		**1.8 to 2.9**	**3.3 to 5.2**	**5.4 to 10.1**	**6.4 to 10.4**

Table 4.11 Strength improvement ratio (S_{IR}) for Site 2 soils for 7- and 14-day curing periods.

(a) 7-day curing

Binder Dosage	w/b ratio	Binder Proportion (L:C)			
		100:0	75:25	25:75	0:100
100	0.8	1.8	3.2	6.4	7.5
	1	1.6	2.1	5.1	6.0
	1.3	1.5	1.7	4.1	5.1
150	0.8	1.9	4.1	6.9	7.5
	1	1.8	2.4	6.4	6.5
	1.3	1.6	2.3	4.9	5.1
200	0.8	2.0	4.3	7.5	8.4
	1	1.9	2.6	7.3	7.6
	1.3	1.9	2.5	4.8	7.3
Range		**1.5 to 2.0**	**2.1 to 4.3**	**4.1 to 7.5**	**5.1 to 8.4**

(b) 14-day curing

Binder Dosage	w/b ratio	Binder Proportion (L:C)			
		100:0	75:25	25:75	0:100
100	0.8	2.4	4.0	6.5	9.0
	1	2.3	2.8	5.6	8.6
	1.3	2.3	2.7	5.0	7.0
150	0.8	2.6	4.7	8.2	9.4
	1	2.4	3.5	7.2	8.6
	1.3	2.3	3.3	5.1	8.0
200	0.8	2.7	4.7	9.2	12.0
	1	2.6	3.9	8.5	10.7
	1.3	2.2	3.7	5.1	9.9
Range		**2.2 to 2.6**	**2.7 to 4.7**	**5.1 to 9.2**	**7 to 12**

4.3.5 Shear Moduli from Bender Element (BE) Tests

The small strain shear moduli, G_{max}, of the undisturbed cores collected from the various depths at Sites 1 and 2 are presented in Table 4.2 and are discussed in section 4.2.3.2. The shear wave velocities obtained from the bender element tests performed on treated soils of both sites are tabulated in Tables 4.12 and 4.13. The shear wave velocities increase slightly for all dosage rates, proportions and w/b ratio when the curing period is increased from 7 to 14 days for soils from both sites. This is due to increase in stiffness with time, thereby resulting in the decreased time of flight; i.e., travel time of shear wave from transmitter bender element to receiver bender element.

For a given curing time and w/b ratio, the increase in the cement content resulted in higher shear wave velocities and shear moduli properties of the soils from Sites 1 and 2. The range of shear wave velocity for medium (Site 1) and high (Site 2) PI treated soils at both curing periods are 161 to 314 m/s and 161 to 392 m/s, respectively. The corresponding shear moduli are in the ranges of 9 ksi (62 MPa) to 29 ksi (200 MPa) and to 9.28 (64 MPa) to 33.36 ksi (230 MPa) for Sites 1 and 2, respectively. The improvements in the treated soils, when compared to the average stiffness of the control soils, are approximately 1.1 to 3.6 times for Site 1 and 1.2 to 4.4 times for Site 2. Low stiffness enhancements are obtained for soils treated with lime and also the results indicate that the stiffness enhancements are slightly larger for high PI clays.

The typical variations of small strain shear moduli (G_{max}) with binder proportions (Lime:Cement) and dosages at w/b = 1.0 and both curing periods for soils from Site 1 are depicted in Fig. 4.27. Similar variations are also noticed for the Site 2 soils. The increase in the shear modulus with curing time from 7 to 14 days is not significant. This may be because the curing periods considered here are short and the strengths are expected to increase significantly over a long time. The enhancements in the shear moduli with the binder dosage and proportions

for a given w/b ratio are significant for both site soils. High enhancements in G_{max} are recorded for lime to cement binder proportions of 25:75 and 0:100, indicating higher enhancements are possible when cement is the dominant component in the binder composition. This is also evident from the slopes of the best-fit lines passing through the individual measurements at various dosages.

This reconfirms that the cement stabilizer is the most effective additive in enhancing stiffness properties of soils in the short term. Overall, the percent increase in G_{max}, when 100% lime was replaced with 100% cement, for a typical water-binder ratio (w/b) of 1.0, at dosage rates of 100, 150 and 200 kg/m^3 are 62%, 60% and 80% for Site 1 and 84%, 135% and 129% for Site 2, respectively. Stabilizer enhancements are noticed to be highest for soils from Site 2 (high PI clays).

Table 4.12 Shear wave velocities in m/s (**1 m/s = 3.28 ft/s**) from bender element tests on soils from Site 1 (a) 7-day curing and (b) 14-day curing.

(a)

Binder Dosage (kg/m^3)	**w/b**	**Binder Proportion (L:C)**			
		100:0	**75:25**	**25:75**	**0:100**
	0.8	181.18	194.3	211.9	222.2
100	1	170.5	187.76	199.45	210.05
	1.3	161.24	188.28	187.06	198.14
	0.8	204.73	226.4	254.1	264.81
150	1	208.95	218.63	256.68	256.77
	1.3	180.9	194.11	220.5	240.8
	0.8	229.31	240.4	277.18	279.08
200	1	213.08	226.46	264.09	282.4
	1.3	203.6	209.9	215.6	230.3

(b)

Binder Dosage (kg/m^3)	**w/b**	**Binder Proportion (L:C)**			
		100:0	**75:25**	**25:75**	**0:100**
	0.8	186.08	187.6	231.24	249.33
100	1	173.36	189.63	224.02	237.05
	1.3	165.4	180.1	196.07	204.11
	0.8	229.06	249.93	270.07	280.19
150	1	212.56	217.27	257.82	274.3
	1.3	211.14	221.01	238.44	255.5
	0.8	236.13	250.04	289.18	314.41
200	1	230.96	237.48	278.77	301.03
	1.3	214.7	220.6	233.3	276.19

Table 4.13 Shear wave velocities in m/s (**1 m/s = 3.28 ft/s**) from bender element tests on soils Site 2 at (a) 7-day curing and (b) 14-day curing.

(a)

Binder Dosage (kg/m^3)	**w/b**	**Binder Proportion (L:C)**			
		100:0	**75:25**	**25:75**	**0:100**
	0.8	170.11	183.21	219.79	232.16
100	1	176.2	180.9	224.28	225.83
	1.3	178.07	161.14	199.96	208.64
	0.8	214.0	229.12	260.06	358.5
150	1	198.62	203.7	262.3	292.45
	1.3	173.37	188.6	214.45	247.16
	0.8	240.13	227.74	279.0	372.47
200	1	213.5	212.41	277.28	316.38
	1.3	200.08	207.23	241.32	294.14

(b)

Binder Dosage (kg/m^3)	**w/b**	**Binder Proportion (L:C)**			
		100:0	**75:25**	**25:75**	**0:100**
	0.8	220.6	242.08	266.73	315.5
100	1	220.01	237.5	261.66	284.56
	1.3	188.33	197.0	241.92	257.48
	0.8	227.05	249.5	290.61	370.0
150	1	239.72	251.54	283.05	305.01
	1.3	206.11	227.72	240.87	270.96
	0.8	235.14	256.9	325.11	391.91
200	1	219.10	223.27	292.13	322.55
	1.3	208.14	231.44	260.5	301.5

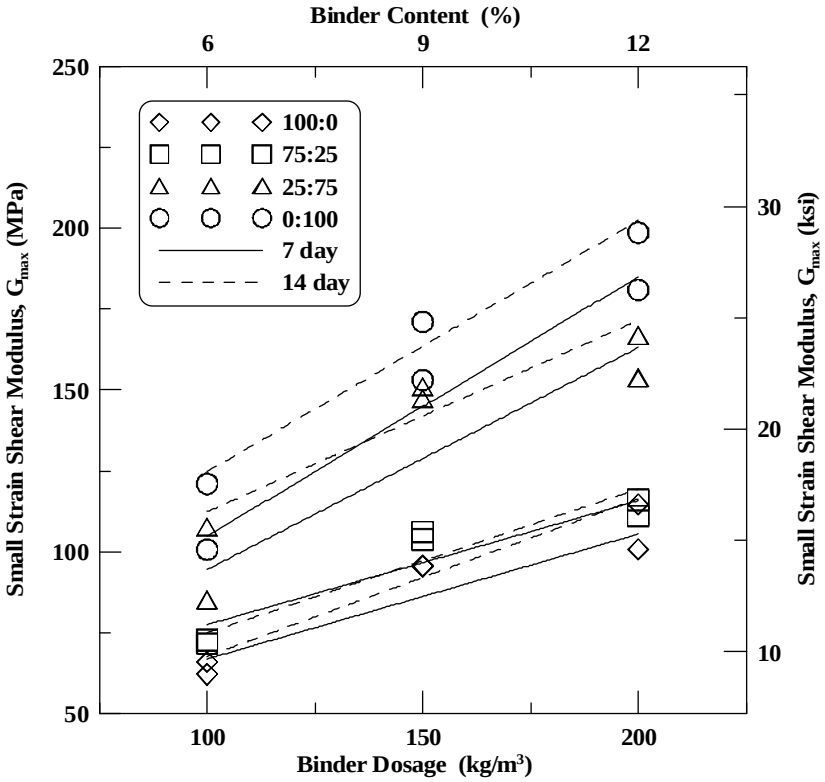

Figure 4.27 Typical variations of small strain shear moduli of treated soils with dosage rate at w/b = 1.0 for Site 1 soils.

4.4 Selection of Mixing Parameters for Field Implementation

A simplified ranking analysis was used to evaluate the best performing binder combination among the ones studied in this research. The analysis was performed by assigning equal weightage factors and ranking the treated soil properties (free swell, linear shrinkage and strength). The ranking scale was designed to accommodate a range of soil properties varying from problematic to non problematic severity levels. On a scale of 1 to 5, the least performance or lowest property enhancement is assigned a rank of 1 where as the best performance or the highest property enhancement is assigned a value of 5. Typical ranking scales for free swell, linear shrinkage and strength based on the distribution of these properties are shown in Tables 4.14, 4.15 and 4.16, respectively. Analysis was also performed considering a different set of weightage factors based on an emphasis on the project requirements. Finally, cumulative rank

(CR), which is the summation of the product of weightage factor and rank for each binder at each proportion, was estimated.

Table 4.14 Stabilizer performance classification based on vertical free swell strain (Chen 1988, Puppala et al. 2004).

Vertical Free Swell (%)	Description of severity	Rank
0-0.5	Non-Critical	5
0.5-1.5	Marginal	4
1.5-4.0	Critical	3
> 4.0	Highly Critical	2
> 8.0	Severe	1

Table 4.15 Stabilizer performance based on linear shrinkage strain (Nelson and Miller 1992).

Linear Shrinkage Strain (%)	Description of severity	Rank
< 5.0	Non-critical	5
5.0-8.0	Marginal	4
8.0-12.0	Critical	3
12.0-15.0	Highly critical	2
> 15.0	Severe	1

Table 4.16 Stabilizer performance classification based on UC strength in kPa (psi).

Unconfined Compressive	Rank
< 2000 (290)	5
174 (1200) – 232 (1600)	4
116 (800) – 174 (1200)	3
58 (400) – 116 (800)	2
> 58 (400)	1

The stabilization of the control soils in the laboratory environment was found effective with reference to shrinkage and swell behavior at all binder dosages (α), proportions (L:C) and water-binder (w/b) ratios. Hence, the characterization of the binder performance is based solely on the strength aspect of the treatment. The ranks are assigned for each combination of α, L:C and w/b ratio based on the strengths reported in Tables 4.6(a) and (b) from the laboratory studies. The ranking analysis yielded the highest CR of 5 for the following combination of mixing parameters for Sites 1 and 2, as highlighted in Tables 4.17 and 4.18, concurrently satisfying the project requirements.

Site 1:

- For α = 200 kg/m^3 and L:C of 25:75 and 0:100 at all w/b ratios (0.8 to 1.3).
- For α = 150 kg/m^3 and L:C of 0:100 at w/b ratios of 0.8 and 1.0.
- For α = 100 kg/m^3 and L:C of 0:100 at a w/b of 0.8.

Site 2:

- For α = 200 kg/m^3 and L:C of 0:100 and 25:75 at w/b ratios of 0.8 to 1.0 and 0.8, respectively.
- For α = 150 kg/m^3 and L:C of 0:100 at a w/b = 0.8.
- For α = 100 kg/m^3 and L:C of 0:100 at a w/b = 0.8.

The above combinations of α and L:C with a w/b of 0.8 and 1.3 are not considered for field implementation as the ratios represent lower and higher bounds of the range of w/b ratio corresponding to difficult working conditions and possible bleeding conditions, respectively.

Based on the previous studies, a w/b ratio of 1.0 is generally used in practice for DSM column construction (Okumara 1996; Babasaki et al. 1996; Matsuo et al. 1996; JGS 2000; Esrig et al. 2003). Considering the fact that the compressive strength achieved in the field will be

approximately in the range of 1/3rd to 1/5th of the strengths obtained in the laboratory under ideal conditions, a binder dosage of 200 kg/m^3 at a lime-cement proportion of 25:75 and a w/b ratio of 1.0 are proposed for subsequent field implementation.

The reason for choosing a binder composed of both lime and cement with lime in lower proportions is twofold. First, to avoid more viscous slurry at a w/b ratio of 1.0 as this would not yield uniform mixing due to the stiff nature of expansive soils at both sites. Second, to achieve enhanced pozzolanic reactions and high strengths in the long term, which would benefit in resisting the swell and shrink pressures generated due to expansion and compression of soils during the wet and dry seasons, respectively, and also in restraining overburden pavement loads.

Table 4.17 Cumulative ranking of various combinations of binder dosage, binder proportion and w/b ratio for Site 1 soils.

Binder Dosage (kg/m^3)	w/b	Binder Proportion (L:C)																			
		100-0					75-25					25-75					0-100				
		UCS	LS	FS	CR^1	CR^2	UCS	LS	FS	CR^1	CR^2	UCS	LS	FS	CR^1	CR^2	UCS	LS	FS	CR^1	CR^2
100	0.8	1	5	5	3.7	3	2	5	5	4	3.5	5	5	5	5	5	5	5	5	5	5
	1	1	5	5	3.7	3	2	5	5	4	3.5	4	5	5	4.7	4.5	4	5	5	4.7	4.5
	1.3	1	5	5	3.7	3	2	5	5	4	3.5	3	5	5	4.3	4	4	5	5	4.7	4.5
150	0.8	2	5	5	4	3.5	2	5	5	4	3.5	4	5	5	4.7	4.5	5	5	5	5	5
	1	2	5	5	4	3.5	2	5	5	4	3.5	4	5	5	4.7	4.5	5	5	5	5	5
	1.3	1	5	5	3.7	3	2	5	5	4	3.5	3	5	5	4.3	4	4	5	5	4.7	4.5
200	0.8	2	5	5	4	3.5	3	5	5	4.3	4	5	5	5	5	5	5	5	5	5	5
	1	2	5	5	4	3.5	3	5	5	4.3	4	5	5	5	5	5	5	5	5	5	5
	1.3	2	5	5	4	3.5	2	5	5	4	3.5	5	5	5	5	5	5	5	5	5	5

Table 4.18 Cumulative ranking of various combinations of binder dosage, binder proportion and w/b ratio for Site 2 soils.

Binder Dosage (kg/m^3)	w/b	Binder Proportion (L:C)																			
		100-0					75-25					25-75					0-100				
		UCS	LS	FS	CR^1	CR^2	UCS	LS	FS	CR^1	CR^2	UCS	LS	FS	CR^1	CR^2	UCS	LS	FS	CR^1	CR^2
100	0.8	2	5	5	4.0	3.5	2	5	5	4	3.5	4	5	5	4.7	4.5	5	5	5	5	5
	1	2	5	5	4.0	3.5	2	5	5	4	3.5	3	5	5	4.3	4	4	5	5	4.7	4.5
	1.3	2	5	5	4.0	3.5	2	5	5	4	3.5	3	5	5	4.3	4	4	5	5	4.7	4.5
150	0.8	2	5	5	4	3.5	3	5	5	4.3	4	4	5	5	4.7	4.5	5	5	5	5	5
	1	2	5	5	4	3.5	2	5	5	4	3.5	4	5	5	4.7	4.5	4	5	5	4.7	4.5
	1.3	2	5	5	4.0	3.5	2	5	5	4	3.5	3	5	5	4.3	4	4	5	5	4.7	4.5
200	0.8	2	5	5	4	3.5	3	5	5	4.3	4	5	5	5	5	5	5	5	5	5	5
	1	2	5	5	4	3.5	2	5	5	4.0	3.5	4	5	5	4.7	4.5	5	5	5	5	5
	1.3	2	5	5	4	3.5	2	5	5	4	3.5	3	5	5	4.3	4	5	5	5	5	5

Note: CR^1 - Cumulative Ranking Based on Equal Weight Factor, 0.33; CR^2 - 0.25 (FS) + 0.25 (LS) + 0.5 (qu)

4.5 Summary

This chapter analyzed and discussed in detail the results obtained from the laboratory soil-binder mixing studies representing closely the in situ deep DSM. A range of variables related to soil type, binder type, binder quantity and proportion, water-binder (w/b) ratio and curing time were studied here. Subsequently, the effects of these variables on the shrink-swell and stress-strain behaviors of the expansive soils are presented. It is noticed that all possible combinations of these variables resulted in shrink and swell potentials less than 0.1%. However, as the w/b binder ratio increased the specimens showed a few hairline cracks on the surface due to an increase in the amount of water in the soil-binder matrix.

Results from this study showed that binders composed of > 75% of lime yielded strengths of about 1.8 to 5.2 times the strength of the untreated soils. The binders with dominant amounts of cement produced strengths of about 5 to 12 times the strength of the untreated soils. The subsequent ranking analysis of these results also showed a binder dosage of 200 kg/m^3 yielded the best performance for binder compositions of 100% cement and 25 and 75% of lime and cement, respectively, at all water-binder ratios. This is followed by dosage rates of 100 and 150 kg/m^3 at 100% cement and a low water-binder ratio.

Finally, based on previous research and experience from current laboratory mixing studies a binder dosage of 200 kg/m^3 for a lime-cement proportion of 25 and 75%, respectively, at a w/b ratio of 1.0 was recommended for the pilot studies. These pilot studies included construction of DSM columns in two expansive soils test sections and evaluation of their performance in mitigating shrink-swell behavior through field instrumentation. Results from these field studies are presented in the following chapters.

CHAPTER 5

DESIGN, CONSTRUCTION AND INSTRUMENTATION OF DEEP SOIL MIXING (DSM) TREATED EXPANSIVE SOIL TEST SECTIONS

5.1 General

As discussed in Chapter 3, the current research selected deep soil mixing as a viable technique for improvement of deep seated expansive soils beneath pavements. To evaluate the application of this technique in real field conditions, a prototype study of DSM treated test sections was performed. Two test sites with medium and high PI soils were selected in the median of North Loop IH 820, near the Beach Street exit, Haltom City, and east of IH 35 W, Fort Worth. The two test sites are approximately one mile apart and at each site DSM columns were installed over an area 40 ft (12 m) in length and 15 ft (4.5 m) in width. Construction of the DSM sections was followed by instrumentation placement.

In addition to the DSM treated test sections, two adjacent control sections were also constructed on soils without the DSM treatments. Each test site has one treated and one control section, totaling two treated test sections and two control sections for performance evaluation of the DSM treatment in the present research. The subsequent sections describe the procedure(s) developed for the design of the DSM columns in the expansive soils, construction and instrumentation procedures of the DSM test sections.

5.2 Procedure for Design of DSM Columns

5.2.1 Theoretical Formulation

The present design of DSM columns in expansive soils is based on the heave prediction model originally proposed by Rao et al. (1988) and later revised by Fredlund and Rahardjo (1993). This model was evaluated as a part of this project. The model for predicting the heave of

the expansive soil was based on the variation of swell pressures with depth and is presented in the following equation (Fredlund and Rahardjo 1993):

$$\Delta h = \sum_{i=1}^{n} \frac{C_{s,i} h_i}{1 + e_{o,i}} log \frac{p'_{f,i}}{p'_{s,i}} \qquad (5.1)$$

where $C_{s,i}$, $e_{o,i}$, $p'_{f,i}$, $p'_{s,i}$ and h_i are the swell index, initial void ratio, final stress (overburden ± any changes in total stress), initial stress (swell pressure), and thickness of each layer 'I,' respectively (Fig. 5.1).

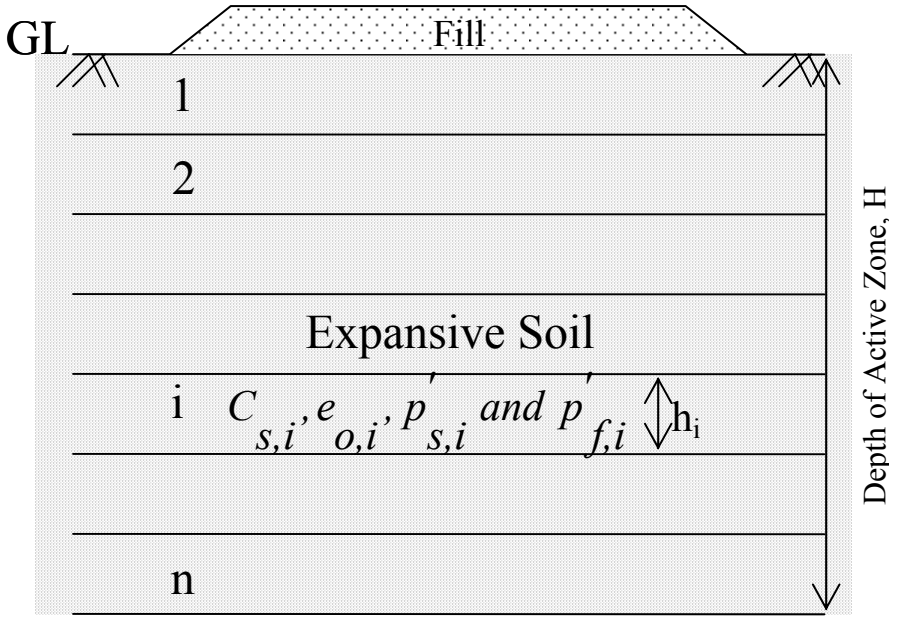

Figure 5.1 Schematic of untreated ground depicting layers for heave prediction.

According to Rao et al. (1988), in an unsaturated expansive soil, the initial stress state is measured as the corrected swell pressure, $p'_{s,i}$, from the 'constant volume' type oedometer test. The final stress state, $p'_{f,i}$, accounts for the overburden stress as well as any net changes in total stresses from either excavation or surcharge type loading. It is assumed that the final water content profile of the soil strata is near saturation at the time of full heaving.

Equation 5.1 is extended to predict the heave of the DSM treated composite test sections, in the following equation.

$$\Delta h = \sum_{i=1}^{n} \frac{C_{comp,i} h_i}{1 + e_{o,i}^{comp}} log \frac{p'_{f,comp}}{p'_{s,comp}} \tag{5.2}$$

where the parameters $C_{comp,i}$, $e_{o,i}^{comp}$, $p'_{f,comp}$ and $p'_{s,comp}$ are the composite properties of layer 'i' in the treated ground (Fig. 5.2). These parameters are estimated as shown below, based on the treated and untreated soil properties determined from the laboratory studies.

$$C_{s,comp} = C_{s,col} \times a_r + C_{s,soil} \times (1 - a_r) \tag{5.3}$$

$$p'_{s,comp} = p'_{s,col} \times a_r + p'_{s,soil} \times (1 - a_r) \tag{5.4}$$

The symbols with 'soil' in the subscript indicate untreated soil properties and those with 'col' represent lime-cement column properties. The effect of the DSM treatment is incorporated into the model by estimating the weighted average of the treated and untreated soil properties. Parameter α_r (area ratio), which is defined as the ratio of the area of treated columns to the total area, is the weighting factor.

Equation 5.2 is further simplified assuming that: (1) the initial void ratio ($e_{o,i}$) and bulk unit weight for both the untreated and treated sections are the same and constant with the depth and (2) the composite properties, $C_{comp,i}$ and $p'_{s,comp}$ are constant with depth. The simplified equation is in the form of

$$\Delta h = \frac{C_{s,comp} h}{1 + e_o} \sum_{i=1}^{n} log \frac{p'_f}{p'_{s,comp}} \tag{5.5}$$

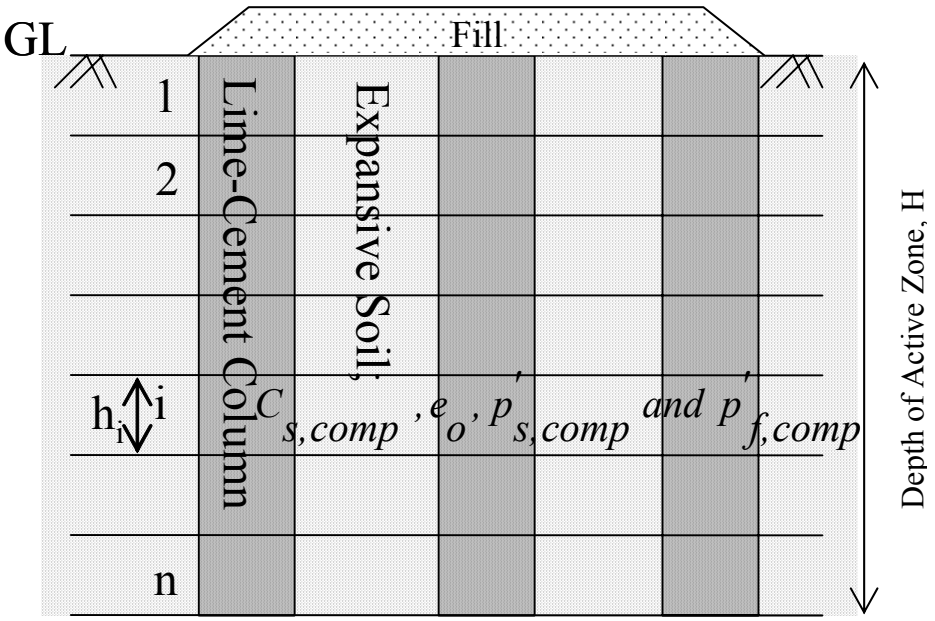

Figure 5.2 Schematic of composite ground depicting layers for heave prediction.

5.2.2 Design Steps

Based on the heave prediction models in Equations 5.1 through 5.5, the design steps shown in the flow chart (Fig. 5.3) are recommended for determining the diameter, length and spacing of the DSM columns for mitigating the heave distress emanating from deep expansive subgrades: The design steps involved are as follows:

1. Determine the representative swell index, swell pressure, initial void ratio and total unit weight of the untreated soil retrieved from the site. Consolidation tests are conducted as per the ASTM D2435-04 method to estimate the swell indices of the soils. The constant volume type oedometer test (ASTM D4546-03) is used to estimate the swell pressures expected from the soils as done for pavement design. If the native soil contains several strata, tests should be carried out on each individual layer. The representative swell index, swell pressure, initial void ratio and bulk unit weight are determined as the weighted

average of the individual properties of the soil layers from the surface to the maximum active depth.

2. Estimate the amount of heave, Δh_{unt}, of the untreated ground by using Equation 5.1. Alternatively, the method for estimating the potential vertical rise (PVR, Tex-124-E) can be used. The two methods may not yield the same results as they are developed from different theoretical and empirical formulations.

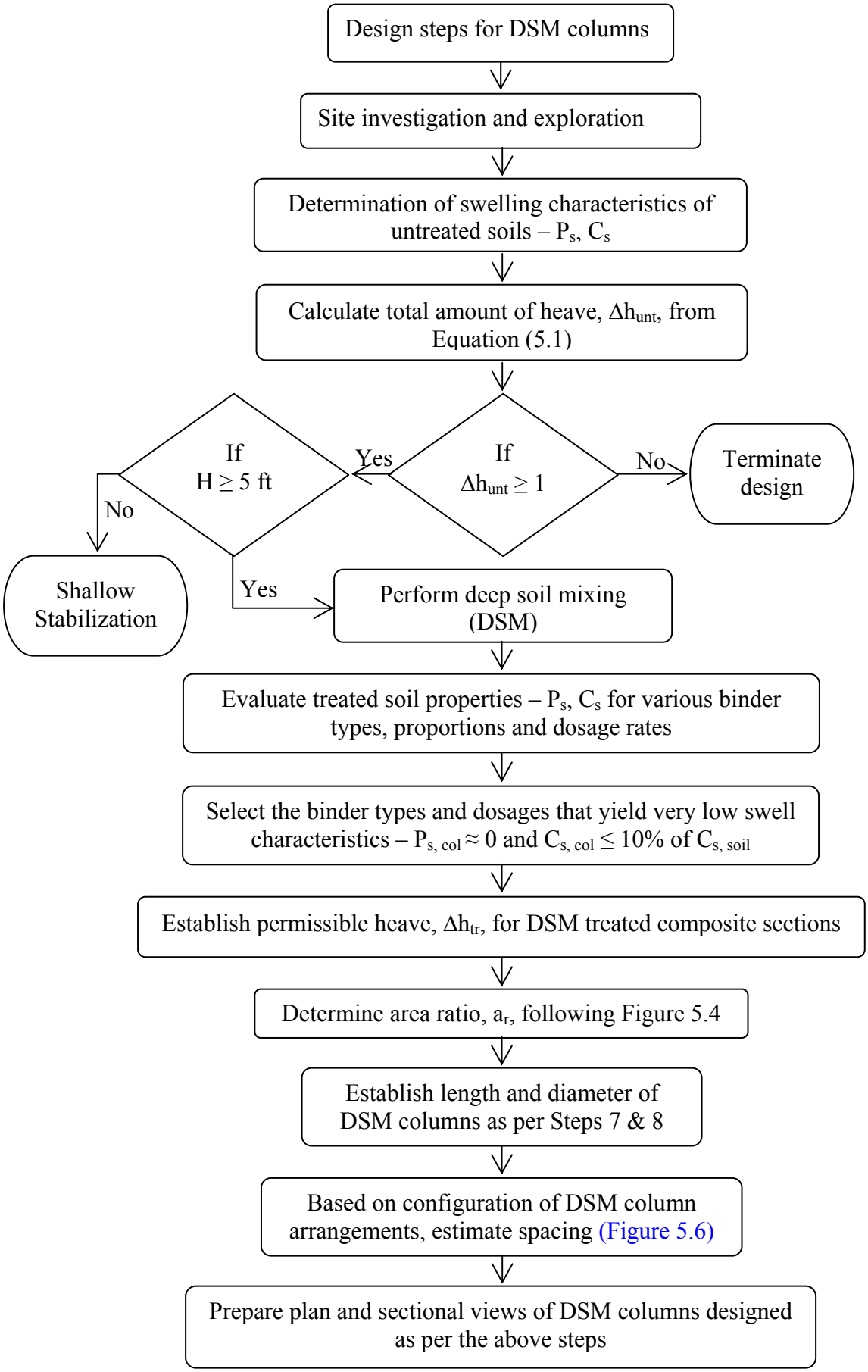

Figure 5.3 Design flow chart for DSM treatment.

3. Establish the permissible heave, Δh_{tr}, for a given project. For flexible and rigid pavement structures, a permissible heave of 0.5 in. and 0.7 in., respectively, are recommended. These values are arbitrarily established, as heaves around 1 in. are known to induce excessive pavement roughness. If the estimated heave for the soil before treatment (estimated in Step 2) is less than the permissible level, soil treatment will not be necessary. Otherwise, the next few steps should be followed to design and establish the DSM treatments for the project site. The costs involved with the field treatments are inversely proportional to the magnitudes of the established permissible heave used in this step. The lower the permissible heaving is, the higher the costs involved with the ground treatment will be, as more DSM columns will be needed. Δh_{tr} of less than 1 in. is needed in order to mitigate the pavement roughness.
4. Estimate the appropriate amount of additives for soil columns by repeating the tests included in Step 1 on soil specimens stabilized with different concentrations of additives. The main goal is to minimize the representative swell index value of the soil-additive mixtures. It is desirable to add an adequate amount of additives to reduce the swell index value of the treated soil close to 10% of the untreated soil without using more than 8% of the additives in the soil.
5. Estimate the treated area ratio required for the project for reducing the overall heaving of the treated ground to a permissible heave value prescribed in Step 3. Based on the swell index of the untreated soil measured in Step 1 and the permissible heave in Step 3, the following appropriate Fig 5.4(a), or (b) or (c) is used to estimate the area treatment ratio. This area treatment ratio is used in the following equations to estimate the column spacing. Each figure presents various predicted heave (which is equivalent to permissible heave for the design exercise) versus area ratio plots for different untreated swell

pressures and for a given swell index value. Equation 5.5 is used in the preparation of these figures. Please note that this equation for area ratio already accounts for composite swell properties of the treated and untreated ground. Binders and dosage rates that yield very low swell characteristics (Step 3) are only recommended for field implementation.

6. If the swell index of the untreated soil lies in between those that were used in the development of the design charts, then a linear interpolation method should be followed by using two charts, one lower than the swell index value under consideration and the other above the swell index value.
7. The diameter of the DSM column is either already known or pre-established based on the DSM rigs used by the hired DSM contractor in the field. If the diameter information is not known at the time of design, then the DSM columns can be designed for various diameter sizes. A DSM column size can then be selected based on the overall costs of the DSM work for the project site. For example, a DSM contractor with a rig capable of making smaller diameter columns may charge a lesser amount for mobilization costs than a DSM provider with larger diameter rigs. Hence, the DSM column diameter is based on either locally available DSM rigs or on cost considerations.

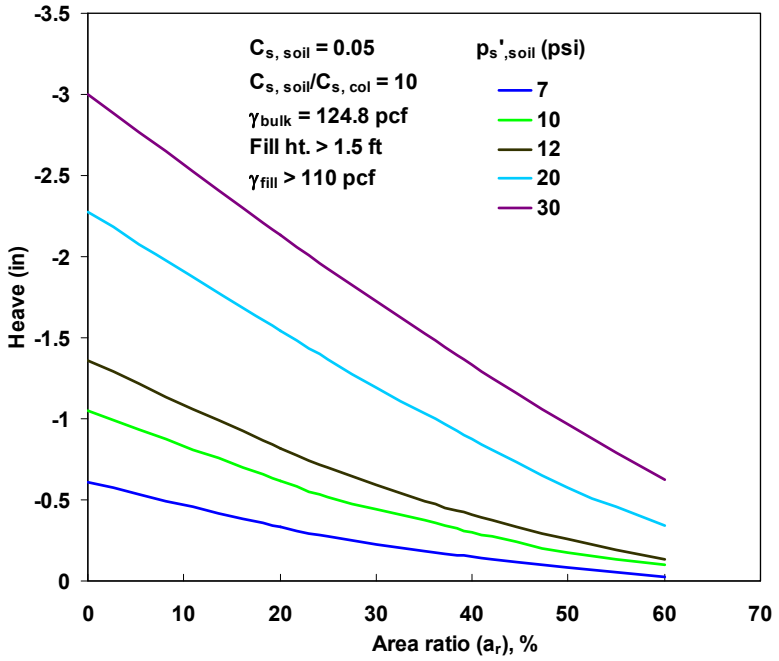

(a)

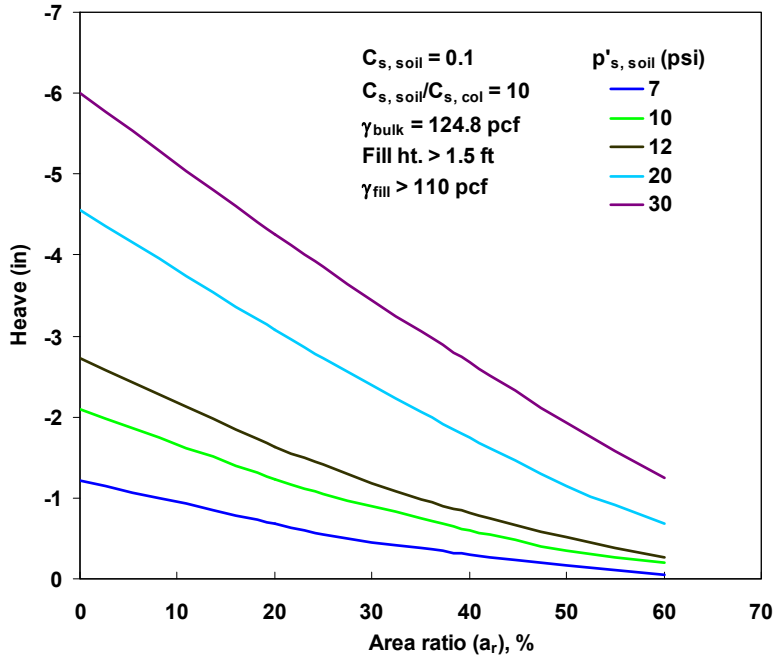

(b)

Figure 5.4 Design charts for estimating DSM area ratios for swell index, C_s values of (a) 0.05, (b) 0.1 and (c) 0.2.

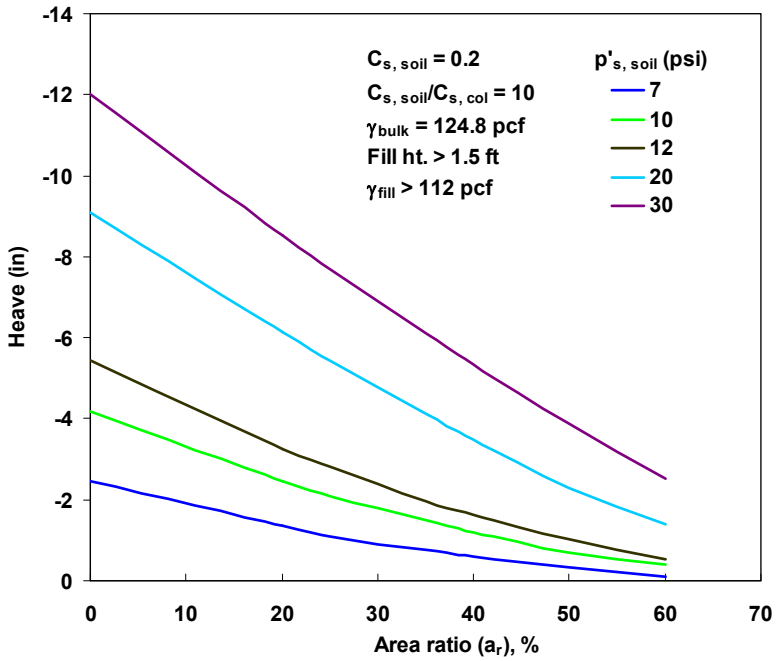

(c)

Figure 5.4 Design charts for estimating DSM area ratios for swell index, C_s values of (a) 0.05, (b) 0.1 and (c) 0.2 (continued).

8. The length of the DSM column is generally established by considering the depth of the column beyond the active zone of the expansive soil. It is recommended that the length of DSM columns be close to or below an active depth of hard non-expansive stratum. The active depths at a site can be determined by studying moisture fluctuations in the soils or based on PVR calculations of layers that contribute to overall heaving or from construction records of other projects near the project site under consideration. Typically, the active depths can vary between 5 ft (1.5 m) and 30 ft (9 m) for different regions of Texas (Table 5.1). In the present research, the DSM columns of diameter 2 ft (0.6 m) and length of 10 ft (3 m) were installed in both test Sites 1 and 2.

Table 5.1 Range of active depths in Texas (O'Neill and Poormoayed 1980).

City	Active Depth (ft)
Dallas/Fort Worth	7 to 15
Houston	5 to 10
San Antonio	10 to 30

9. In this step, the configuration of the DSM columns in the field needs to be established. Two configuration types are generally used in practice and these are the 'square' and 'triangular' type. Fig. 5.5 provides schematics of these configurations. Based on the area ratio, a_r derived in Step 5, and the diameter as well as the length of the DSM columns, the optimum spacing of DSM columns is determined by using Fig. 5.6.
10. In the case of multi-axial rigs, treated area under multiple shafts can be idealized as an equivalent circle and then the same spacing calculation can be followed as per the above step.

11. Since the aim of the construction project is to control the heaving of expansive soils, two other elements are needed. These are the use of geogrid to be placed over the columns and a placement of an anchor rod that connects the geogrid to each DSM column.
12. The final plans and section details shall be prepared using the above designed or established DSM column diameter, length and spacing information. The spacing should be rounded to a lower bound value since this ensures that the overall design is more conservative as lower bound rounding of the spacing results in higher area ratios than determined from the design chart.

The plan and sectional views developed following the above design procedure for construction of prototype test sections, along with the details of the geogrid and anchor rod used in construction are presented in the following section.

SQUARE ARRANGEMENT:

$$a_r = \frac{a_{col}}{a_{soil} + a_{col}}$$

$$= \frac{\text{area of column}}{\text{area of square}} = \frac{\left(\pi d_{col}^2 / 4\right)}{s \times s}$$

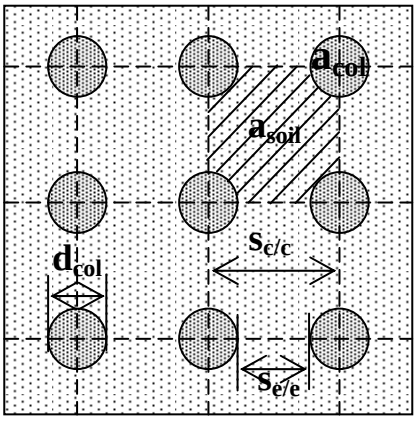

$$\boldsymbol{s = \sqrt{\frac{\pi}{4a_r}}\, d_{col}} \qquad (5.6)$$

TRIANGULAR ARRANGEMENT:

$$a_r = \frac{\frac{1}{2} a_{col}}{a_{soil} + \frac{1}{2} a_{col}}$$

$$= \frac{\frac{1}{2}\text{area of column}}{\text{area of equilateral } \Delta\text{le}} = \frac{\frac{1}{2}\left(\frac{\pi d_{col}^2}{4}\right)}{\frac{1}{2} \times s \times \frac{\sqrt{3}}{2} \times s}$$

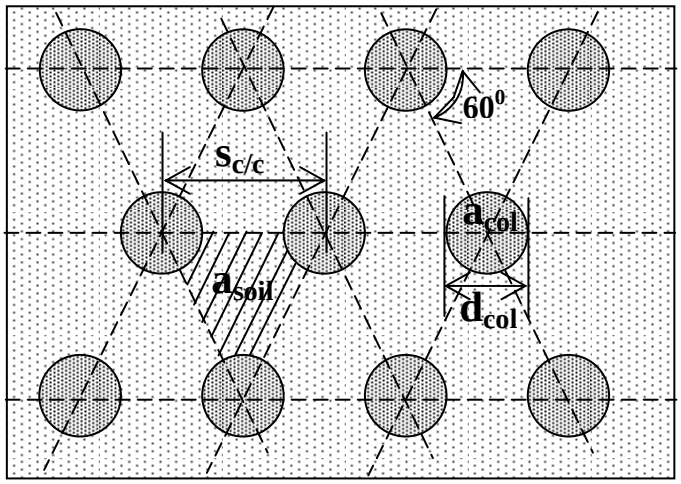

$$s = \sqrt{\frac{\pi}{3.464 a_r}}\, d_{col} \qquad (5.7)$$

Figure 5.5 Configurations of DSM columns and corresponding equations for column spacing.

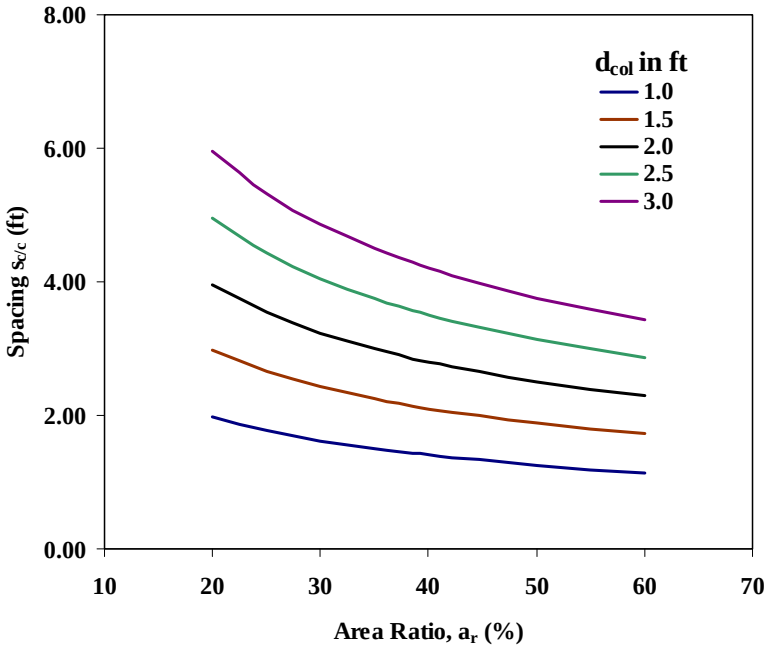

(a) Square Pattern

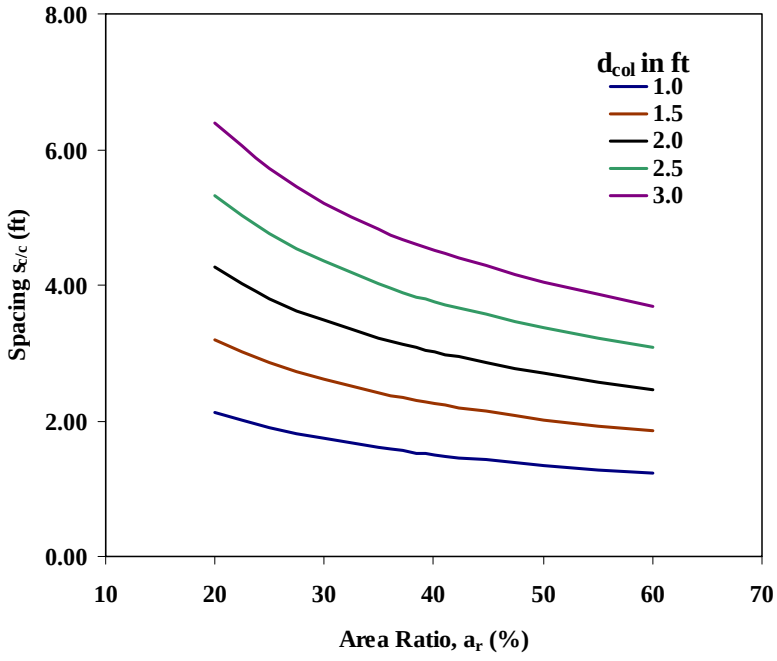

(b) Triangular Pattern

Figure 5.6 DSM column spacing details for (a) Square pattern and (b) Triangular pattern.

5.3 Design Specifications of Materials and Geometry Details for DSM Treated Test Sections

The following provides the specifications of materials used in construction of the DSM columns. The plan and sectional views showing geometrical specifications are also presented below.

5.3.1 Specifications of Binder Materials

Below are the specifications of materials, including binders and water, arrived at following the laboratory studies for construction of the DSM columns.

1. Binder composed of 25% lime and 75% cement is recommended.
2. A dosage rate of 200 kg/m^3 of combined binder mixture is recommended.
3. A water-binder ratio of 1.0 is recommended for grout preparation in field.

Based on these specifications, the total required quantities of binders and water for both test sections are estimated.

5.3.2 Specifications of Geogrid and Anchor Rod

The following table contains specification details of the geogrid and anchor rods used during construction of the DSM test sections.

Table 5.2 Details of anchor rod and geogrid.

ANCHOR ROD:
Anchor rod length: 3 ft.
Anchor rod diameter: ¾ in.
Material: Galvanized Iron
Ultimate Strength = 19 ksi
ANCHOR PLATE:
Size: 8×8 in.
Thickness: ½ in.
Material: Polypropylene
GEOGRID:
Type: Biaxial geogrid
Tensile Strength: 20 kN/m or 1400 lb/ft (both in machine and cross-machine directions)
Material: Polypropylene
Product used: Tensar BX1200 (Biaxial Geogrid)

5.3.3 Specifications of DSM Column Geometry and Arrangement

As shown in the plan views (Figs. 5.7 and 5.8) a square arrangement of the DSM columns is considered and thus, following Equation (5.6) center-to-center column spacing of 3.54 ft (1.06 m) and 3.0 ft (0.9 m) for Sites 1 and 2, respectively, is derived. The column dimensions, as mentioned in Step 9 of Section 5.2.2, are 2 ft (0.6 m) in diameter and 10 ft (3 m) in length. Then the number of columns required to achieve the design area ratio, a_r, are estimated as below from Equations (5.8) and (5.9).

$$\text{No. of columns along the length of the test section } (N_l) = \frac{L + S_{e/e}}{S_{c/c}} \qquad (5.8)$$

$$\text{No. of columns along the width of the test section } (N_w) = \frac{B + S_{e/e}}{S_{c/c}} \qquad (5.9)$$

where L and B are the length and width of the test sections; $S_{c/c}$ and $S_{e/e}$ are the design spacing from center-to-center and edge-to-edge of the columns, respectively. It is recommended to round the values, N_l and N_w, to the higher value in practice; however, in the present study the lower end values were adopted. The corresponding area ratios were 23 and 34% for the medium (Site 1) and the high (Site 2) swelling soil potential sites, respectively. Following Equations (5.6) and (5.7), the number of columns for Site 1 with a_r = 23% is 44 and for Site 2 with a_r = 34% is 65. The plan and sectional views of both the DSM treated sections are depicted in Figs 5.7 to 5.11.

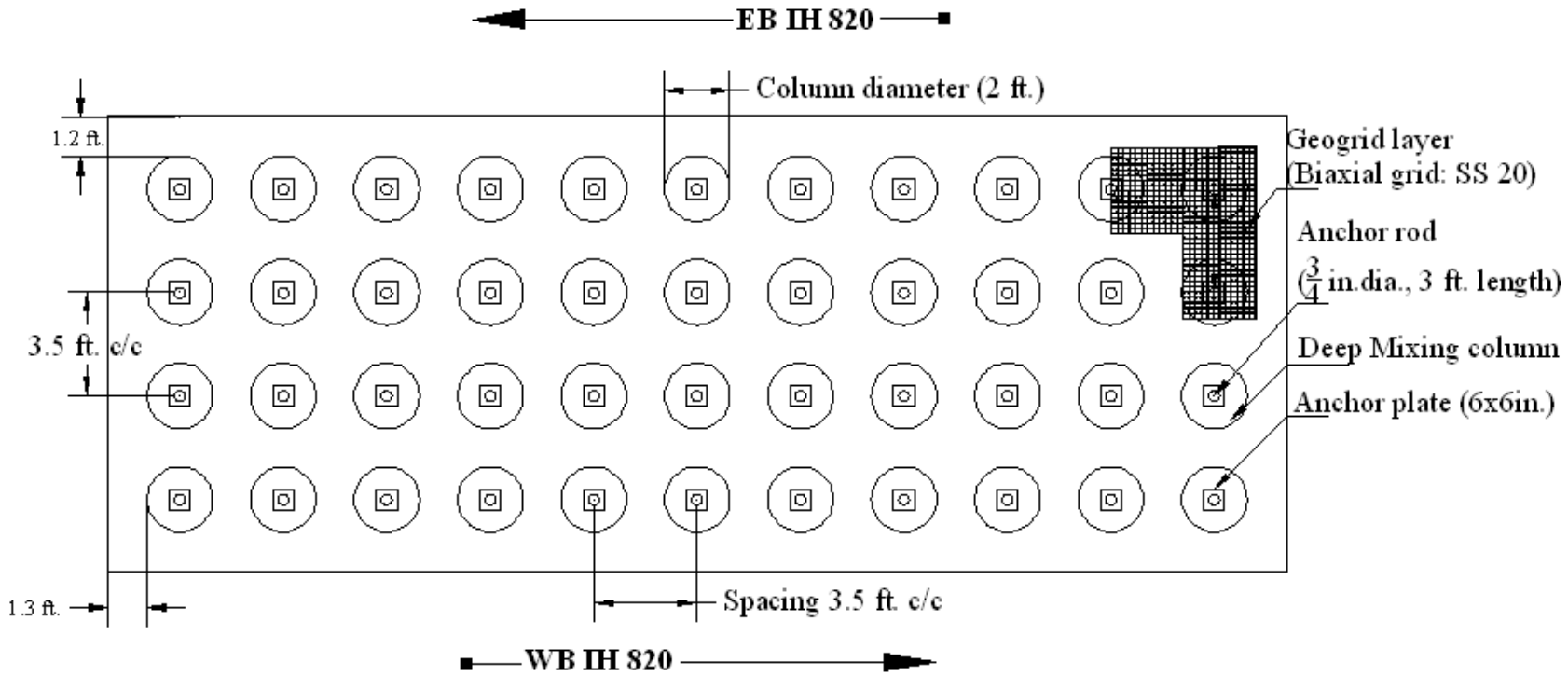

Figure 5.7 Plan view of DSM column layout of test Site 1 (15 ft × 40 ft).

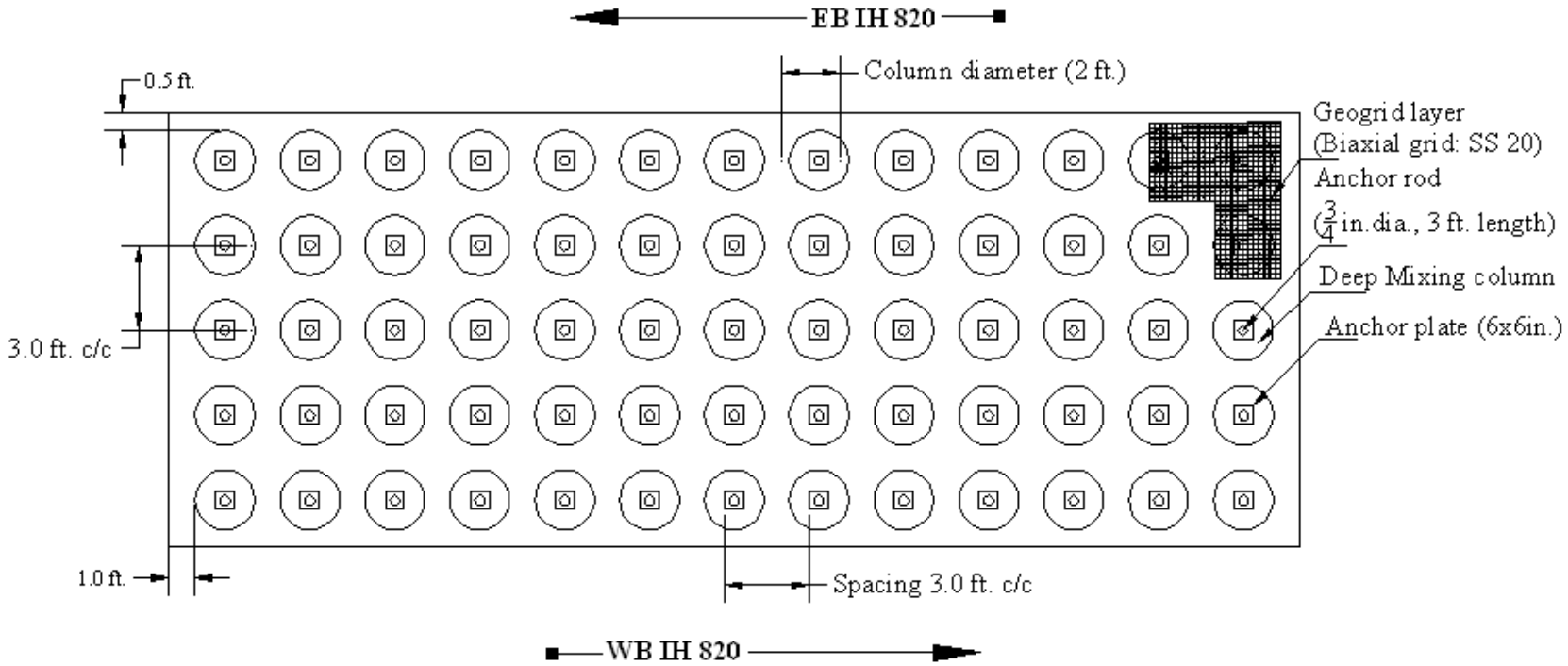

Figure 5.8 Plan view of DSM column layout of test Site 2 (15 ft × 40 ft).

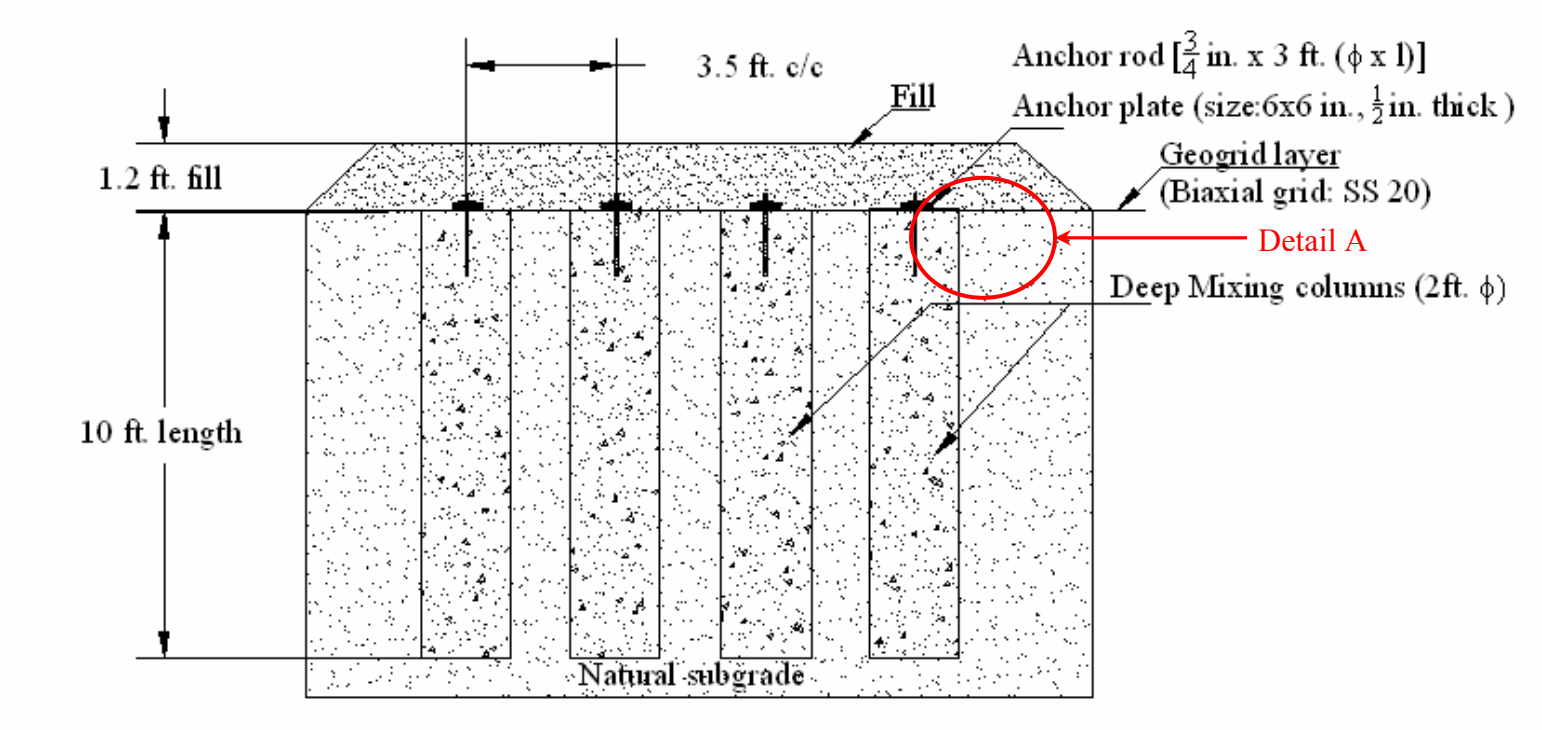

Figure 5.9 Sectional details of DSM columns at Site 1.

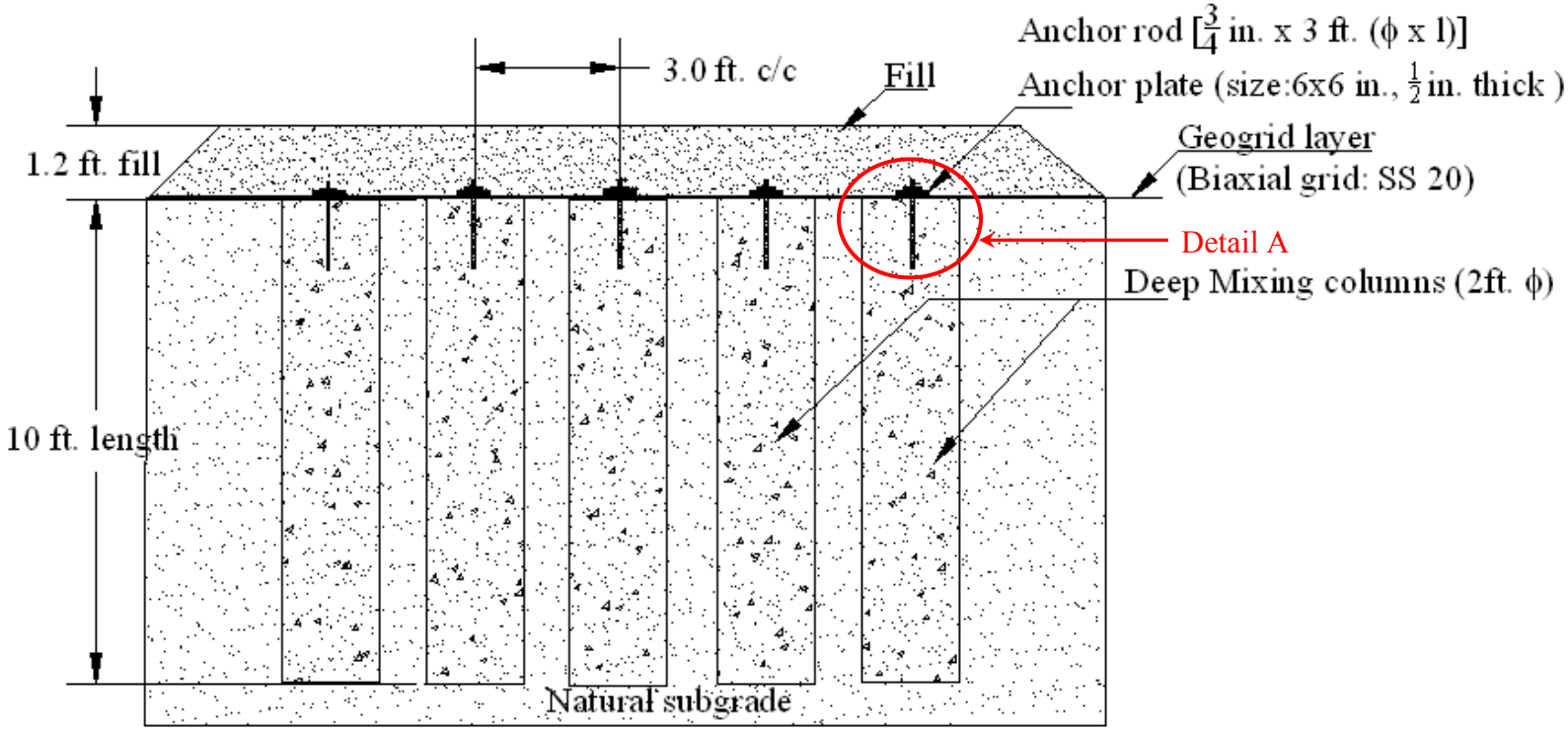

Figure 5.10 Sectional details of DSM columns at Site 2.

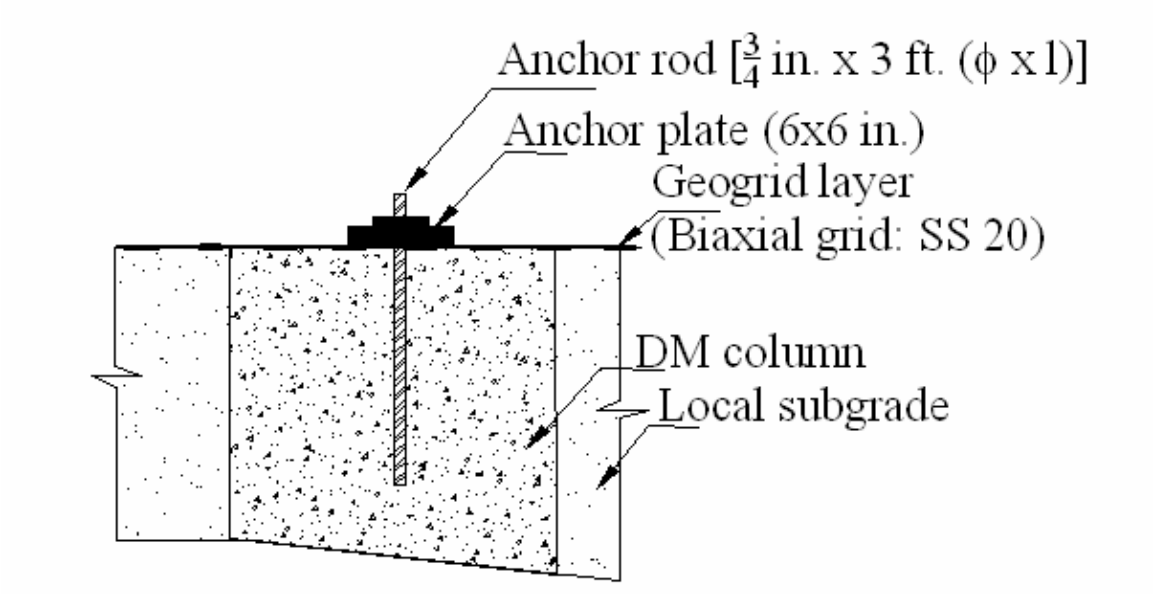

Figure 5.11 Details of anchor rod, plate and geogrid connection to the DSM column (Detail A).

5.4 Construction of DSM Columns in Medium Stiff Expansive Soils

The researchers at UTA and TxDOT have collaborated in evaluating the application of the Deep Soil Mixing (DSM) technique for stabilizing expansive soils of considerable depths beneath the pavements. In the process, the researchers proposed the construction and monitoring of two prototype DSM treated pilot scale test sections along the inside of North Loop IH 820 W, near the Beach Street exit, Haltom City, and east of IH 35 W, Fort Worth. The interstate is underlain by expansive soils and is under consideration for reconstruction and expanding the current four lane highway to 10+ lanes. The details of site locations, selection and characterization of the same are presented in earlier chapters (Chapters 3 and 4).

The dimensions of the test sections along the median are 40 ft (12 m) in length and 15 ft (4.5 m) in width. The construction of the DSM treated prototype test sections took place in May 2005 and installation of the DSM columns in each section was completed in 1½ to 2 days. The typical perspective view of the DSM treated test section is shown in Fig. 5.12. The

construction of the DSM treated test sections was followed by instrumentation placement to evaluate the performance of these sections based on the data obtained from monitoring for a period of two years (Aug 2005 to Aug 2007). The construction procedure of the DSM column installation according to the proposed material and geometrical design specifications at both test sections is presented in the following steps.

1. Before starting the construction of the DSM columns, the test sites were cut to a depth of 1 to 2 ft, as shown in Fig. 5.13.
2. Following the plan views of both test sections, the sites were marked accordingly, as shown in Fig. 5.13, to serve as a reference for the mixing rig during soil-binder column installation.
3. The binder slurry composed of lime and cement was prepared in a large mixing tank at the project site. The lime slurry was prepared first and then mixed with cement resulting in a lime-cement slurry (Fig. 5.14).
4. During the trial mixing of soil at Site 1, the researchers experienced difficulty in achieving uniform mixing because of the medium stiff to stiff nature of the soils. As a result, researchers attempted loosening the stiff soil prior to the formation of the soil-binder columns by using a different rig. Loosening of the soil was performed up to the designed column depth.
5. After loosening of the soil in each borehole, the loose soil was thoroughly mixed with the binder slurry, which can be seen in Fig. 5.15. During the mixing process, the slurry was pumped from the bottom of the rig at a rate of 2.75 cf/min. This pumping rate was performed during penetration and withdrawal of the mixing tool.

6. The mixing parameters including penetration rate, withdrawal rate and rotational speed of the mixing rig were 2.5 ft/min, 10 ft/min and 40 rpm, respectively. Fig. 5.16 depicts the soil-binder columns formed at the end of soil-binder mixing.
7. For QA/QC studies, a wet grab sampling method was used to collect soil-binder mix samples from the select DSM columns (Fig. 5.17). The soil-binder mixture was collected from different depths of the column using an air compressor unit connected to a wet grab sampler. At Site 1, only a few wet grab samples were collected due to difficulties with the sampler in applying suction while retrieving the specimens. Hence, a few samples were prepared by compacting soil-binder spoil mixture collected at the surface during column construction, in the field in 5 layers. At Site 2, wet grab specimens were successfully collected. Specimens of 3 in. diameter and 6 in. height were prepared and placed in the plastic molds, which were immediately transported to the laboratory humidity room for curing.
8. After completing the construction of the DSM columns, the spoil collected at the surface during construction was removed, as shown in Fig. 5.18.
9. The removal of the spoil from the surface was followed by the installation of anchor rods into the columns. This was carried out at the end of each day's construction of DSM columns over the test section by pushing the galvanized iron threaded rods (3/4 in.) into the columns. It is recommended to install the anchor rods into the DSM columns when they are fresh.
10. This completed the installation of the DSM columns with the anchor rods. At this stage the treated test sections were instrumented to monitor the performance of the DSM technique in minimizing the shrink-swell behavior of the expansive soils. The instrumentation includes monitoring of vertical movements from settlement plates and

horizontal inclinometers, lateral movements from a vertical inclinometer, swell pressures from total pressure cells and moisture variations from Gro-Point moisture probes. The treated test sections were monitored for a period of two years from August 2005 to August 2007. Details of the instrumentation and installation procedures are presented in the next section.

11. In order to transfer the stresses induced from the movements of the untreated soil between the DSM columns, a geogrid was placed at the surface and fastened to the rods installed into the DSM columns using a plate and bolt system, as shown in Fig. 5.19 and section detail in Fig. 5.11.
12. A fill height of 1.2 ft (0.36 m) was then placed on top of the geogrid and compacted manually using a vibratory tamper as shown in Fig. 5.20 in two layers.
13. The untreated (control) test sections were also constructed and instrumented at each test site away from the treated area. Therefore, a total of four test sections (two at each site) were constructed and monitored in the present study.
14. After completing the construction and instrumentation of the treated and control test sections, in situ tests including density probe, downhole testing and Spectral Analysis of Surface Waves (SASW) were conducted immediately in June 2005. The downhole testing and SASW tests were repeated in subsequent years of monitoring (August 2006 and May 2007). Schematics of downhole and SASW testing are shown in Fig. 5.21. Results from these tests were useful in evaluating construction quality and degree of improvement during the monitoring period. The details of QA/QC and in situ studies along with analysis of results obtained from these studies are presented in the next chapter.

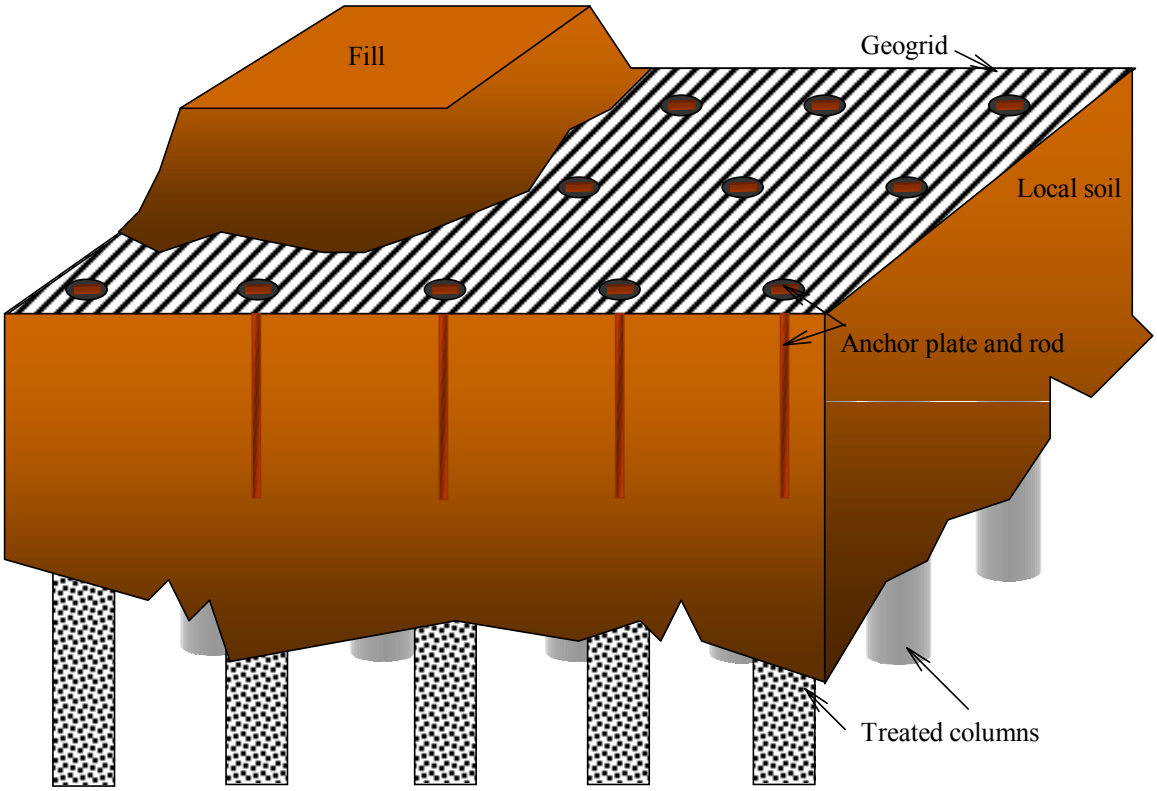

Figure 5.12 A typical perspective view of DSM treated-geogrid-reinforced test section.

Figure 5.13 Test section at Site 1 prepared for DSM column installation.

Figure 5.14 Mixing tanks used for the preparation of lime-cement slurry.

Figure 5.15 Field schematic of soil-binder mixing process and mixing auger.

Figure 5.16 Soil-binder columns formed at the end of in situ mixing.

(a) (b)

Figure 5.17 (a) Wet grab sampler (b) Extraction of wet grab sample from DSM column.

Figure 5.18 Removal of spoil from the surface at end of DSM treatment.

Figure 5.19 Test section after fastening geogrid to DSM columns using anchor rod and plate-bolt system.

Figure 5.20 Fill placement and compaction using a vibratory tamper.

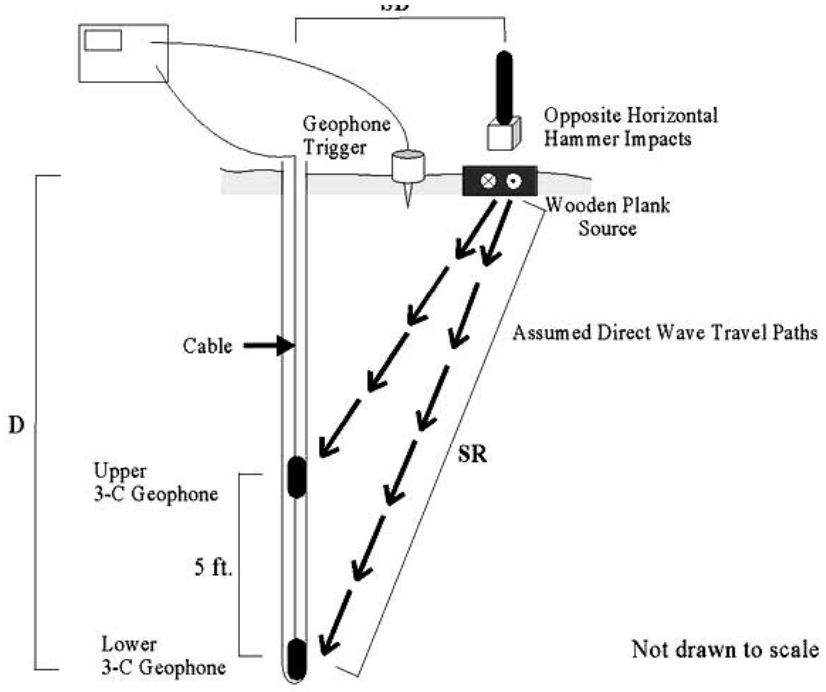

(a)

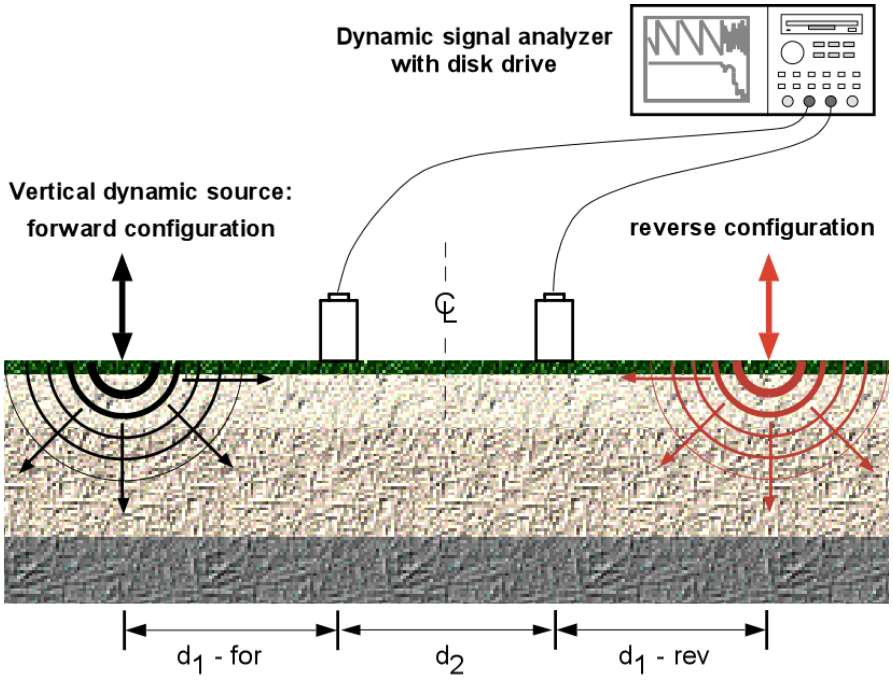

(b)

Figure 5.21 Schematics of (a) Downhole testing and (b) SASW testing.

5.5 Instrumentation

In evaluating the field performance of an engineering structure, instrumentation plays an important role in understanding the performance of the infrastructure with time. In the present study, different types of instrumentation were installed in both DSM treated composite sections at Sites 1 and 2 to observe the performance of the treated soil in providing stable non-expansive support to the overlying infrastructure.

The performance evaluation of the DSM treated sections is achieved through regular data collection and analysis related to surficial and underlying soil movements in the vertical and horizontal directions, moisture fluctuations and swell pressures with time. The instrumentation used at both sites included inclinometers, moisture probes, total pressure cells and settlement plates. This also helps in understanding the load transfer mechanisms between the DSM columns due to heaving and pressure distribution under the DSM column system. In order to facilitate the transfer of stresses produced from heaving of untreated soils between the DSM columns to the columns itself, a geogrid was laid at the interface of the treated ground and embankment fill. The following sections present the details of the instruments used and the installation procedures followed

5.5.1 Inclinometers

Inclinometers are defined as the devices for monitoring surface and subsurface deformations parallel (lateral) and normal (vertical) to the axis of a flexible plastic casing by means of a probe passing through the casing (EM 1110-2-1908 – US Army Corps). The inclinometer casing is a grooved ABS (acrylonitrile-butadiene-styrene) plastic pipe available in various diameters 1.9 in. (4.8 cm), 2.75 in. (7 cm) and 3.34 in. (8.5 cm). The small diameter casings (1.9 in.) are suitable for measuring small deformations and are not recommended for monitoring purposes in soils. Whereas, the 2.75 and 3.34 in. diameter casings are suitable for

monitoring moderate to large deformations and are suitable for application in construction projects (foundations, embankments, slopes, landslides and retaining walls). The 3.34 in. diameter casings are preferred for horizontal inclinometer probes and 2.75 in. diameter casing for vertical inclinometer probes. The casings of all diameters are available in lengths of 5 ft (1.5 m) and 10 ft (3 m), therefore for installation depths > 10 ft (3 m) the casings are assembled by pushing the female end of one casing into the male end of another, as shown in Fig. 5.22(b). Typical details of the casing are also depicted in Fig. 5.22(a). More details about repairing and assembling the casings can be found in Slope Indicator (1997). The following subsections present the principles involved, installation details and subsequent monitoring procedures of both vertical and horizontal inclinometers.

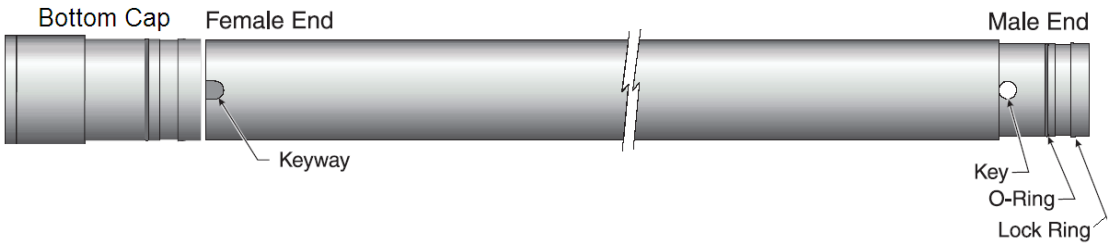

(a)

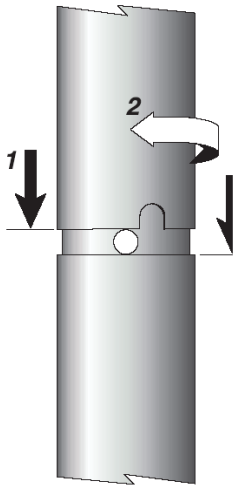

(b)

Figure 5.22 (a) Details of inclinometer casing and (b) Assembling procedure (Slope Indicator 1997).

5.5.1.1 Vertical Inclinometers

A vertical probe is used to monitor the lateral deformations of engineering structures (foundations, embankments, landslides, slopes, retaining walls etc.) by passing it through a vertical casing. The vertical inclinometer probe (Fig. 5.24[a]) consists of two force-balanced accelerometers (Fig. 5.23) to measure the inclination of the axis of the casing pipe with respect to the vertical. The details of the probe and planes of measurement are shown in Fig. 5.24. The two accelerometers help in measuring the lateral movements in both the A and B directions, as shown in Fig. 5.24(b). The plane in which the deformations are measured along the wheels is the A-axis and the one perpendicular to the wheels is the B-axis. Therefore, it is necessary to align one set of grooves along the expected direction of movement during casing installation. The components included in the inclinometer unit are a flexible plastic guide casing, a portable probe, labeled control cable, readout unit and a pulley assembly.

The principle involved in measuring the lateral deformations using a vertical probe is as follows. The probe measures the angle of inclination of the inclinometer casing axis with respect to the vertical which is then converted into lateral movement using a sine function. From Fig. 5.25, deviation, δi, at an interval 'i', is

$$\delta_i = L \times \sin \theta_i \qquad (5.10)$$

To obtain the profile of the casing the deviation at each interval is calculated by summing the values from bottom of the casing until that interval ($\Sigma \delta i$), as shown in Fig. 5.25.

In the present study, lateral movements were observed at four locations in the treated section and one location in the untreated area. The locations were selected following a series of logical steps for determining the importance/sensitivity of the locations. Considering the treatment is uniform throughout the site, the behavior of a group of four columns represents the performance of the whole site. This indicates the important locations that define the performance

of the treated area and to monitor the degree of improvement are (1) column, (2) center of four columns, and (3) center of two columns. The depth of installation, from the surface of fill, is varied from 8 to 11 ft (2.4 to 3.3 m). The schematic of the instrumentation at both sites is shown

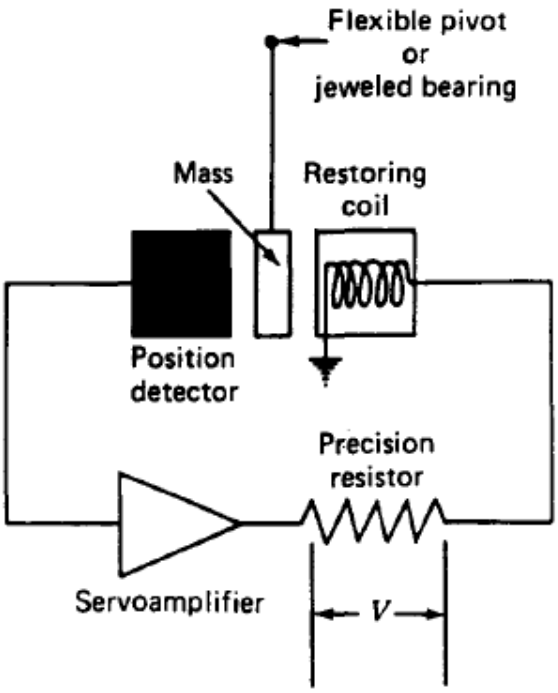

Figure 5.23 Schematic of forced-balanced accelerometer (Dunnicliff 1988).

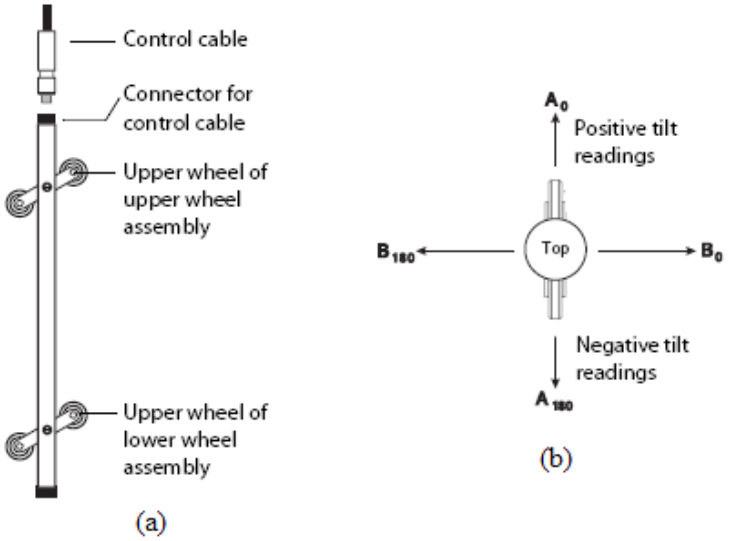

Figure 5.24 Details of inclinometer probe (Slope Indicator 2000); (a) Components and (b) Measurement planes.

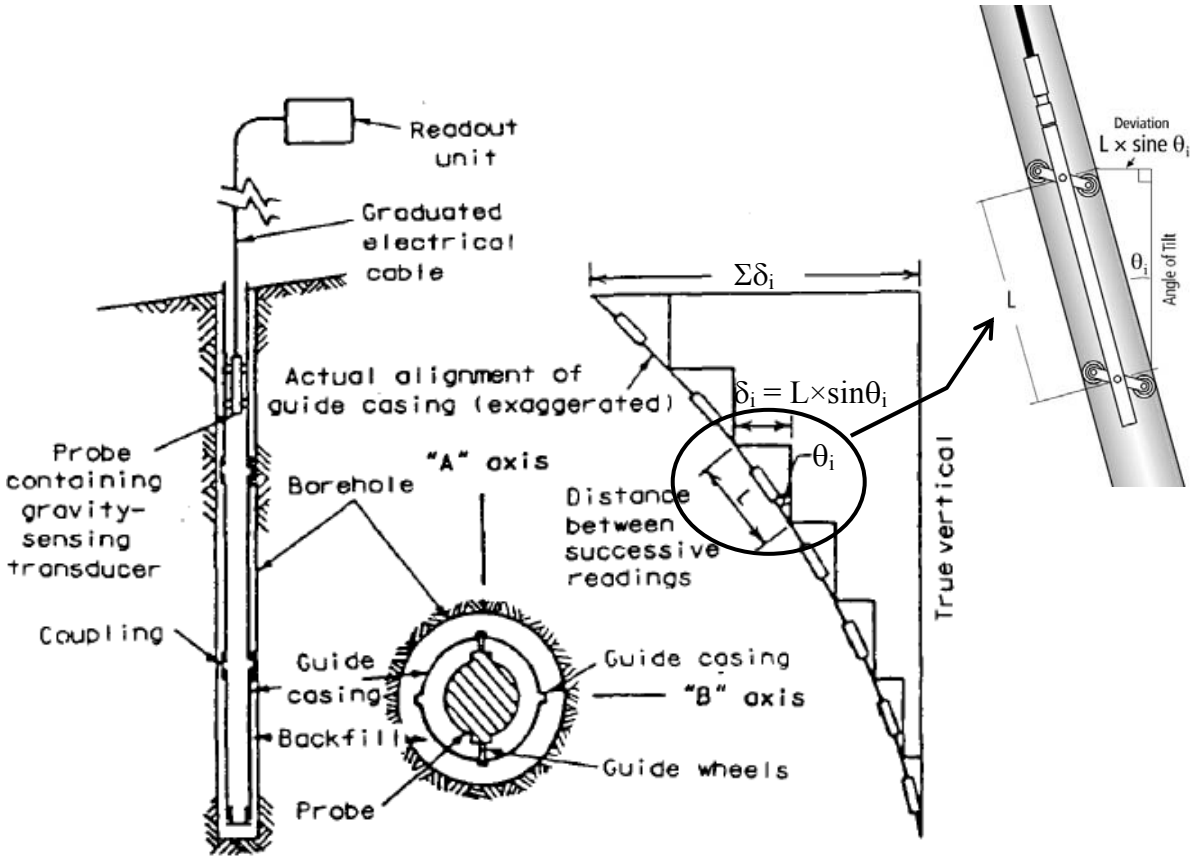

Figure 5.25 Principle used in inclinometers for measuring deformation (Dunnicliff 1988).

in Fig. 5.26. The step by step procedure followed for installation of vertical inclinometers is as follows:

1. For in-column installation, the inclinometer casings are pushed into the selected DSM column at the end of the day's construction, when the DSM column is fresh and soft (Fig. 5.26). Before inserting the first casing, the bottom of the casing is closed using a bottom cap as shown in Fig. 5.22(a).
2. When installing casing between the columns and in the untreated areas, boreholes are drilled using an auger at the selected locations after completing the construction of the DSM columns. While drilling, it is important to maintain the verticality of the borehole throughout the monitoring depth.
3. After the borehole is drilled to the required depth, the inclinometer casing is inserted into the borehole and the gap between them is filled with a bentonite-cement grout mix. The grout mix is prepared at the site in a slurry form and delivered into the gap using a grout pipe or a hose. A well prepared grout mix should be free of lumps and thin enough to pump; at the same time it should be able to set in reasonable time, but too much water will result in shrinking the grout, leaving the upper portion ungrouted (Slope Indicator 1997). Because of the low consistency of the grout mix, it is expected to maintain the continuity without any air pockets locked in between along the depth.
4. At the time of filling the gap with the grout mix, it is necessary to make sure the inclinometer casing is prevented from floating due to buoyancy forces. In the present study, this is achieved by anchoring the top of the inclinometer to the ground surface (Fig. 5.27), as the installation depths are < 15 ft (4.5 m). However, in the case of deep installation, suspension of a dead weight at the bottom of the casing is recommended rather than anchoring at the top as it might lead to distortion (bending) in the casing

profile (Slope Indicator 1997).

5. The usual practice in inclinometer casing installations is to install the bottom 3 to 5 ft (0.9 to 1.5 m) of the casing into a stable zone where no movements are expected.
6. The proportions of bentonite-cement grout mix should be adjusted such that the 28-day strength is similar to the strength of the in situ soils. The proportions of bentonite, cement and water recommended for stiff and soft in situ clayey soils can be found in Slope Indicator (1997). The proportions used in the present study are presented in Table 5.3.
7. As soon as the installation of the casings and construction of the test section is completed, the initial profile of the casing is obtained by running the inclinometer probe through the casing. Readings should be taken from bottom to top by initially lowering the probe to the bottom of the casing and then pulling it upwards to each interval. The details of monitoring and data collection procedures are presented in the following chapter.

Table 5.3 Recommended proportions for the preparation of bentonite-cement grout mix (Slope Indicator 1997).

Materials	Weight	Ratio by Weight
Bentonite	25 lb	0.3
Cement	95 lb	1.0
Water	30 gallons	2.5

Figure 5.26 Field schematic of placing inclinometer into DSM column.

Figure 5.27 Field schematic of inclinometer anchoring and grouting.

5.5.1.2 Horizontal Inclinometer

Typical applications of horizontal inclinometers include measurement of settlement and/or heave under storage tanks, embankments, dams etc. In the present study, horizontal inclinometers were used to monitor the vertical surface movements in the DSM treated composite test sections. This was achieved by passing a horizontal probe through the casing. Inclinometer casings of diameter 3.34 in. (8.5 cm) were installed at the center of the DSM column rows along the width of the sections. Two casings were placed near the edges and one at the center of the section, as shown in Fig. 5.28. Length of the casings is equal to the width of the test sections; i.e., 15 ft (4.5 m).

The components of the horizontal inclinometer include the horizontal probe, graduated control cable, pull cable, and a readout unit. The schematic of the horizontal inclinometer unit setup and details of the horizontal probe are shown in Fig. 5.29. The wheels on one side of the probe are fixed and are always kept in the bottom groove of the casing during an inclinometer survey. The principle involved in measuring vertical movements is the same as that used for the vertical inclinometer probe. Unlike the vertical probe, the horizontal probe contains one force-balanced accelerometer and measures the deviation of the casing axis along the plane of wheels from the horizontal. The profile of the casing can be obtained by plotting the measurements at each interval along the length of the casing. Any change in the profile of the casing compared to

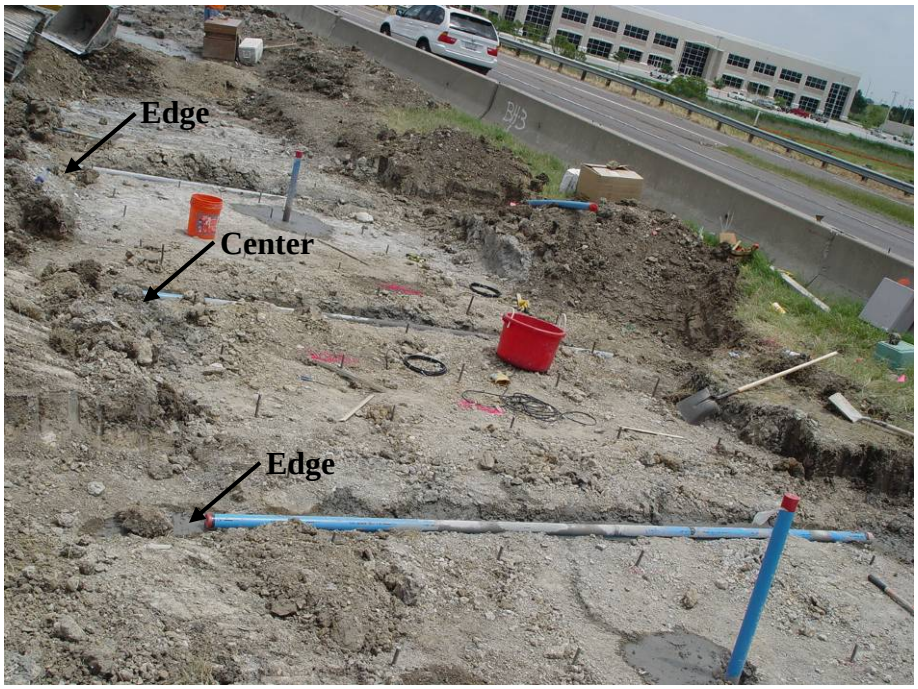

Figure 5.28 Field schematic of horizontal inclinometer casing placement.

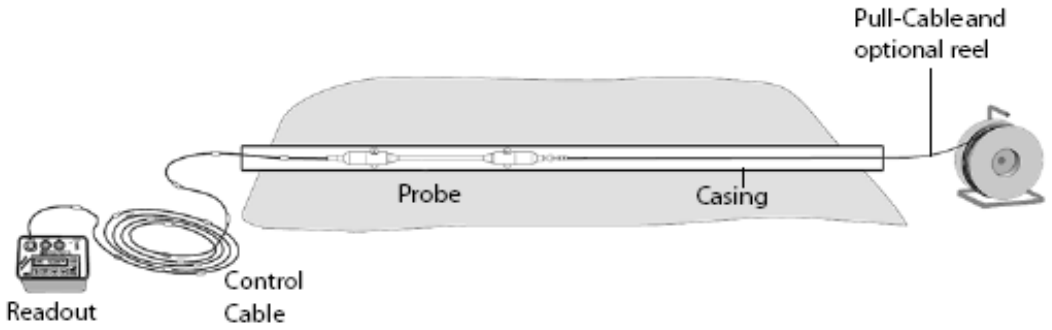

(a)

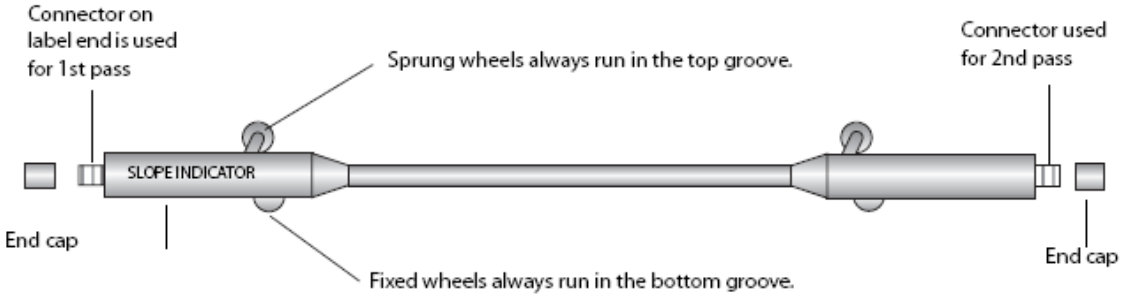

(b)

Figure 5.29 (a) Schematic of horizontal inclinometer setup and (b) Horizontal probe.

the initial profile from subsequent surveys indicates the surface movements. The following steps describe the procedure followed for installation of the horizontal inclinometers:

1. Trenches of size 1 × 1 ft (2.54 × 2.54 cm) are excavated at selected locations along the width of the test sections. As per the Slope Indicator manual (2004), a small gradient of 5% is maintained along the length of the casing for drainage purposes.
2. The trenches are then cleaned and a layer of sand is placed for proper seating of the inclinometer casing.
3. Casings are laid carefully into the trenches, while assembling from one end until the required length is reached and simultaneously a stainless steel cable is pulled through the casing. In the present study, both near and far ends of the casings are kept accessible.
4. At the time of assembling the casings, one set of grooves were aligned vertical to the ground surface to measure surface movements. The procedure for assembling the inclinometer casings are the same as that explained in the above section.
5. To check the alignment of the grooves at the junction of two casings, it is recommended to run the probe through the casing from the near end to far end and back again.
6. Care was taken to avoid any debris and dirt from entering the casing during installation.
7. Finally, the trenches were backfilled and the casing ends were closed using caps. The ends should always be kept closed, except at the time of survey, to prevent any debris from entering the casing during the monitoring period.

5.5.2 Pressure Cells

The load transfer mechanism in the DSM column reinforced expansive soils supported by the geogrid at the surface is contrary to that of the geosynthetic-reinforced and DSM column supported embankment over soft soils (Fig. 5.30). The heaving of expansive soil between the DSM columns is typically resisted by the overburden pavement and base layer weights. In case

the swell pressures related to this heaving are higher than that of the overburden pressures from the pavement system, the tension in the geogrid layer is mobilized due to heave. As the geogrid layer is anchored to the DSM columns, part of this tension force is expected to be transferred to the DSM columns in the form of lateral and uplift forces (Figure 5.30 [a]).

The heaving of expansive soil between DSM columns also exerts lateral pressures on columns due to confinement. The above hypothesis of load transfer mechanism initiates the measurement of vertical and lateral swell pressures exerted by the soil between the DSM columns. Monitoring of these pressures with time provides better understanding of the actual behavior of the system and in developing accurate predicting models in the future. In the present prototype studies, four total pressure cells of the vibrating wire (VW) type were installed at both test sections for measuring swell pressures.

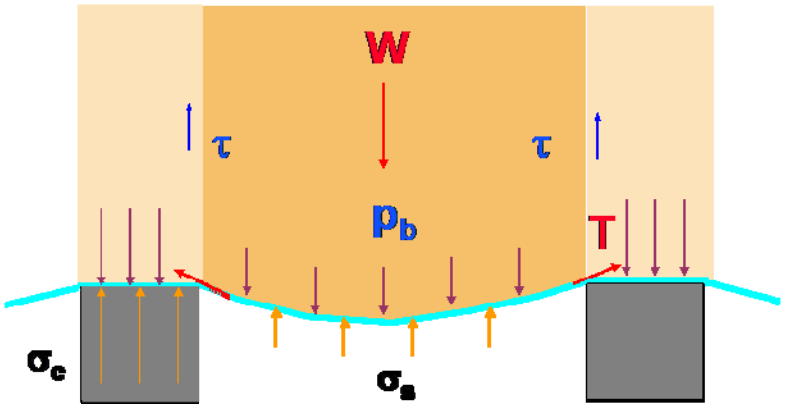

(a)

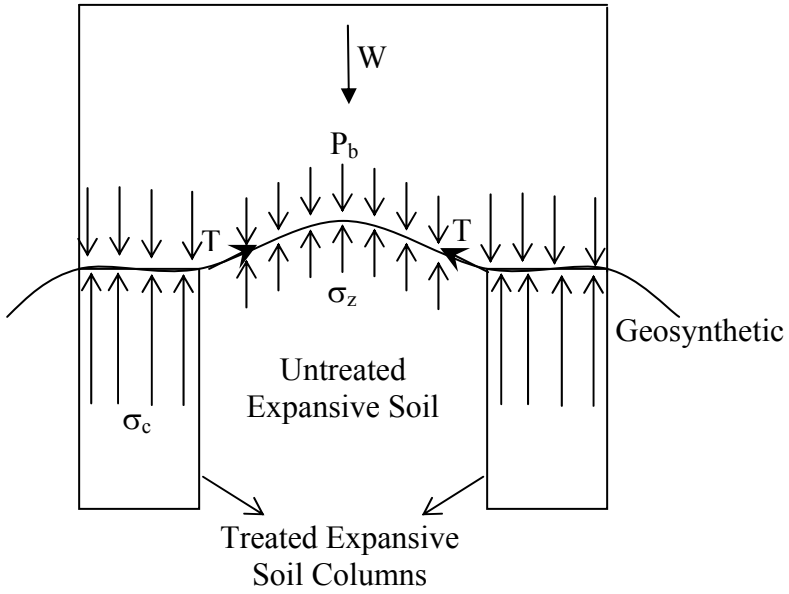

(b)

Figure 5.30 Hypothesized load transfer mechanism in DSM treated (a) Soft soils (Han 2004) and (b) Expansive soils.

The pressure cells are formed by welding two stainless steel plates together by forming a cavity inside which is filled with a non-compressible fluid and with one side being sensitive to pressure (Slope Indicator 2004). Thus, cells should be installed with the sensitive side facing downward for vertical swell pressures (Fig. 5.32[a]) and outward against a DSM column for later

swell pressures (Fig. 5.32[b]). The pressure exerted on the sensitive side is transferred to the fluid inside and then measured with a vibrating wire transducer. The schematic of the VW transducer is shown in Fig. 5.31. Details of the VW devices and the working principle of the same can be found in Dunnicliff 1988 and US Army Corps 1995.

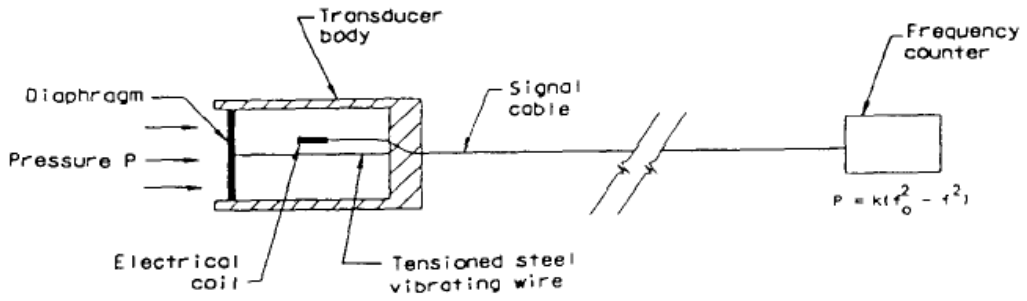

Figure 5.31 Schematic of vibrating wire (VW) transducer (Dunnicliff 1988).

As explained in Section 5.5.1 for inclinometer placement, the locations for the pressure cells were determined by considering the improvement of soil around the DSM columns. It was expected that the maximum vertical swell pressures are experienced at the center of the four and two columns; therefore, one pressure cell was placed at each location. One cell was oriented vertically against a DSM column for measuring lateral swell pressures and another one was placed in the fill. All pressure cells in the present study were placed at a depth of 1 to 2 ft (0.3 to 0.6 m) below the treated ground surface and the orientation of cells, as shown in Fig. 5.32. The installation procedure for the pressure cell includes the following steps:

1. Excavation of a trench of size equal to the size of the pressure cell and to the required depth.
2. Clear the trench from stones and level the bottom by placing a sand layer for horizontal orientation and the vertical surface for vertical orientation.
3. Place the pressure cell in the trench along the proposed orientation and then backfill the trench with the excavated soil.

4. Backfilling of the trench should be done in layers with each being compacted using hand operating equipment.

(a) (b)

Figure 5.32 Schematic of pressure cell installation (a) Horizontal orientation and (b) Vertical orientation.

5.5.3 Moisture Probes

For monitoring seasonal variations in moisture levels in both the treated and the untreated test sections, Gro-Point moisture probes were installed at depths of 3 ft (0.9 m) and 6 ft (1.8 m). A total of 3 moisture probes per site were installed. The installation procedure includes drilling a borehole to required depth and then placing the moisture probe by lowering it into the borehole as depicted in Fig. 5.33. After placing the probe at the required depth, the borehole was backfilled with excavated soil up to a depth at which another probe was intended to be placed and the same procedure mentioned before was followed.

Figure 5.33 Field schematic of Gro-Point moisture probe installation.

5.5.4 Settlement Plates

Settlement Plates (SP) shown in Fig. 5.34 were used in the present study, alongside horizontal inclinometers, to monitor vertical surface movements. These SPs were developed by researchers at UTA by attaching an acrylic plastic plate to one end of the threaded galvanized iron rod through the screw-bolt system. SPs were placed on the surface of the treated sections, at selected locations, after placing the geogrid, as shown in Fig. 5.34. Subsequently, fill was placed on the top and the movements of the SPs were observed using total station survey equipment.

Figure 5.34 Settlement plate and its placement.

5.6 Summary

Researchers developed a simplistic stepwise procedure for the design of the DSM treated sections based on the heave prediction model proposed by Rao et al. (1993) and Fredlund and Rahardjo (1993). Following this stepwise procedure, the current DSM treated sections were designed and constructed. The plan and sectional views of both treated sections were given here along with the details of the anchoring system.

A total of four test sections (two prototype deep soil mixing treated-geogrid-reinforced and two untreated test sections) were constructed and instrumented in May 2005. Field monitoring of these sections was performed for a period of two years, from August 2005 to August 2007. Because of the stiff nature of the in situ soils, researchers proposed loosening of the soil column prior to the construction of the soil-binder column. A total of 44 and 65 DSM columns were installed in the present study at Sites 1 and 2, respectively.

A step-by-step description of the construction of the DSM treated test sections is also presented here. QA/QC studies were performed subsequently by conducting laboratory tests on samples collected from the DSM columns using a wet grab sampling method and in situ tests including downhole testing and SASW tests. Details of these tests and analysis of the results obtained are presented and discussed in detail in the following chapter.

CHAPTER 6

QA/QC, MINEROLOGICAL AND FIELD MONITORING STUDIES

6.1 General

Stringent quality control procedures during construction are needed to ensure that the DSM treatment methods are constructed as per the design. Quality control essentially is comprised of evaluating the binder quality and quantity, mixing efficiency (penetration/withdrawal speeds and number of mixing blade rotations) and geometrical design specifications of the column (length, diameter and spacing of columns) throughout the construction process. Subsequent quality verification or assurance tests are also necessary to confirm the quality of the in situ stabilized DSM columns installed. Quality assurance can be ensured through laboratory tests on cores collected from the DSM columns and/or performing in situ tests on the installed columns. A typical flowchart of the QA/QC procedure for the DSM method is shown in Fig. 6.1.

In the present study, standard mixing parameters were recorded during the DSM column installation and the quality achieved during the construction process was studied through laboratory tests on wet grab samples from the field and in situ non-destructive tests conducted through installed columns. Laboratory tests included bender element and unconfined compression strength tests. In situ tests included downhole and Spectral Analysis of Surface Waves (SASW) testing on the DSM columns. Additionally, mineralogical studies were performed on the treated soil specimens in order to qualitatively understand the degree of mixing obtained in both the laboratory and field conditions. This Chapter describes all these aspects in detail and also presents the field monitoring procedures carried out in the present study to obtain data from the field instrumentation.

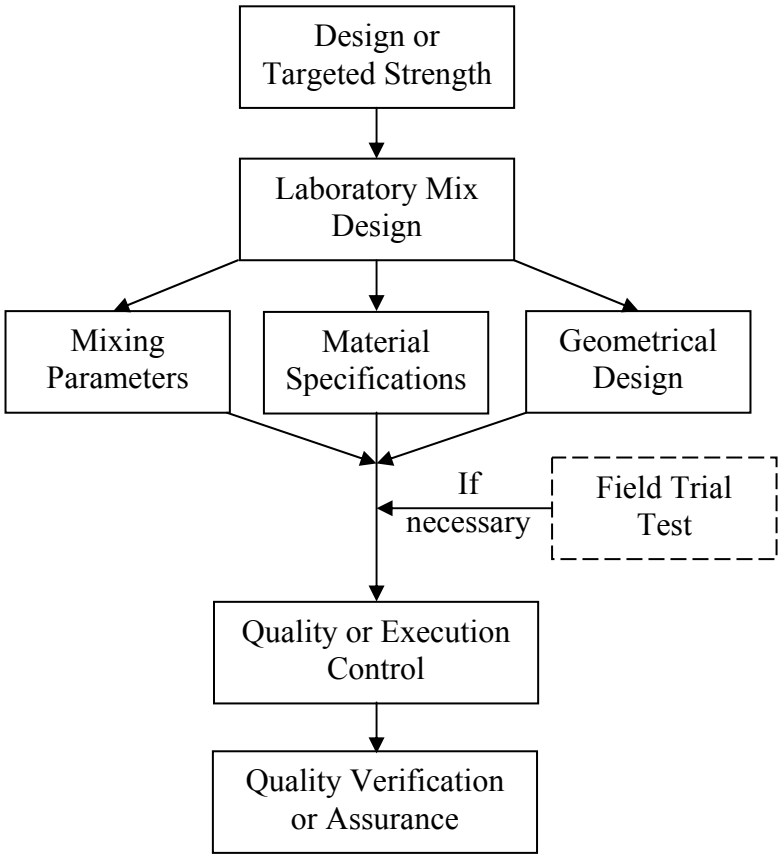

Figure 6.1 Typical QA/QC procedure for DSM method (modified after Coastal Development Institute of Technology 2002 and Usui 2005).

6.2 QA/QC Studies Based on Laboratory Tests

6.2.1 Quality / Execution Control

At the time of construction of the DSM columns in the present study, the researchers from UTA and Engineers from TxDOT were on the project site to ensure the design specifications (material and geometrical) established were followed closely by the DSM construction in the field. The laboratory mix design in the present research was limited to establishing binder type, optimum binder quantity and water-binder ratio. Standard mixing conditions including penetration/withdrawal speeds and rotation of the mixing blade that are commonly recorded in the DSM construction practice were adopted here. Table 6.1 presents the mixing conditions used for the construction of DSM columns in the present study.

Table 6.1 Specifications for mixing conditions of DSM column execution.

Mixing Conditions	Penetration	Withdrawal
Shaft Velocity	2.5 ft/min (0.76 m/min)	10 ft/min (3.05 m/min)
Mixing Blade Rotation	40 rpm	40 rpm
Binder Injection Rate	2.75 ft^3/min (0.078 m^3/min)	2.75 ft^3/min (0.078 m^3/min)

6.2.2 Quality Assurance / Verification

During the field construction of the DSM columns with the lime-cement additives, a wet grab sampling method (Fig. 5.17[a]) was used to collect the soil-binder mix from the selected DSM columns (Fig. 5.17[b]). The soil-binder mix was collected from different depths using an air compressor unit connected to a wet grab sampler and this mix was used to compact and prepare soil cylinders in the field for laboratory testing. At Site 1, difficulties were experienced

while soil sampling with the wet grab sampler. Hence, a few specimens were prepared from the spoil mix generated during construction. At Site 2, wet grab sampling was performed without any difficulty and hence all planned wet grab samples were collected.

Soil specimen fabrication was conducted in the field such that the unit weights of the resulting specimens were close to those achieved during laboratory testing. In order to accomplish this, a predetermined weight of the soil-binder mix was collected and then poured into plastic sampling molds of 3 in. (76 mm) in diameter and 6 in. (152 mm) in height, along with the collar. During the process, the mix was tapped with 0.2 in. (5 mm) rod for about 30 times for each lift. A total of 4 to 5 lifts were needed to complete each specimen preparation.

The specimens prepared from both the wet grab samples and spoils around the columns were carefully extruded from the compaction molds and then wrapped in a plastic sheet and transported to the laboratory curing room in a transportation container. This container is fitted with racks to accommodate the specimens and minimize the sample disturbances during transportation. The unit weights of the specimens were measured prior to transportation and at the laboratory and no variations in the unit weights were noticed due to the transportation and handling process.

The comparison of the total unit weights from the field specimens and laboratory mix design specimens is presented in Fig. 6.2 and the unit weights appear to be are fairly close to those achieved in the laboratory mix design. After a curing period of 14 days, the specimens were extracted from the plastic molds and were subjected to stiffness measurement tests using bender elements and subsequently to unconfined compression strength (UCS) tests. Free swell and linear shrinkage tests were also performed on the specimens collected from the field.

Both the stiffness and strength test results on the field specimens are presented in Table 6.2 and compared with the laboratory specimens prepared using a 200 kg/m^3 binder

dosage, lime-cement ratio of 25:75 and w/b ratio of 1.0. The nearly consistent results of the stiffness and strength with depth indicate a uniform mixing of the soil and stabilizer in the field conditions. The shear wave velocity for moderate (Site 1) and high PI (Site 2) treated soils at both curing periods of 7 and 14 days and for w/b of 1.0 were 24.6 (170 MPa) to 43.6 psi (301 MPa) and 25.5 (176 MPa) to 46.7 psi (322 MPa), respectively (Tables 4.12 and 4.13). The improvement in stiffness of treated soils, when compared to the control soils, was approximately 4 to 7 times for Site 1 and 5 to 9 times for Site 2. The ratios of $q_{u,field}$ and $q_{u,lab}$ for Site 1 and Site 2 varied from 0.67 to 0.7 and 0.83 to 0.86, respectively (Table 6.3). Both stiffness and strength ratios indicate that the field stiffness and strength values are 40 % and 20 to 30 % lower, respectively, when compared to the laboratory treatments.

These treatment variations are in agreement with those reported in the literature review (Kamon 1997, Hayashi and Nishimoto 2005). Variations in G_{max} and strength properties are attributed to the mixing methods and energies used in the field and laboratory treatments. It can be noted from the above discussion that increase in strength and stiffness properties of treated soils was more for high PI soil compared to medium PI soil. This is attributed to the presence of relatively high amounts of fines in the high PI clayey soil. Quality assessments (QA) based on the laboratory tests also showed that the field treatments, due to large areas of treatment, often tend to provide lower enhancements when compared to deep soil mixing studies in a controlled laboratory environment.

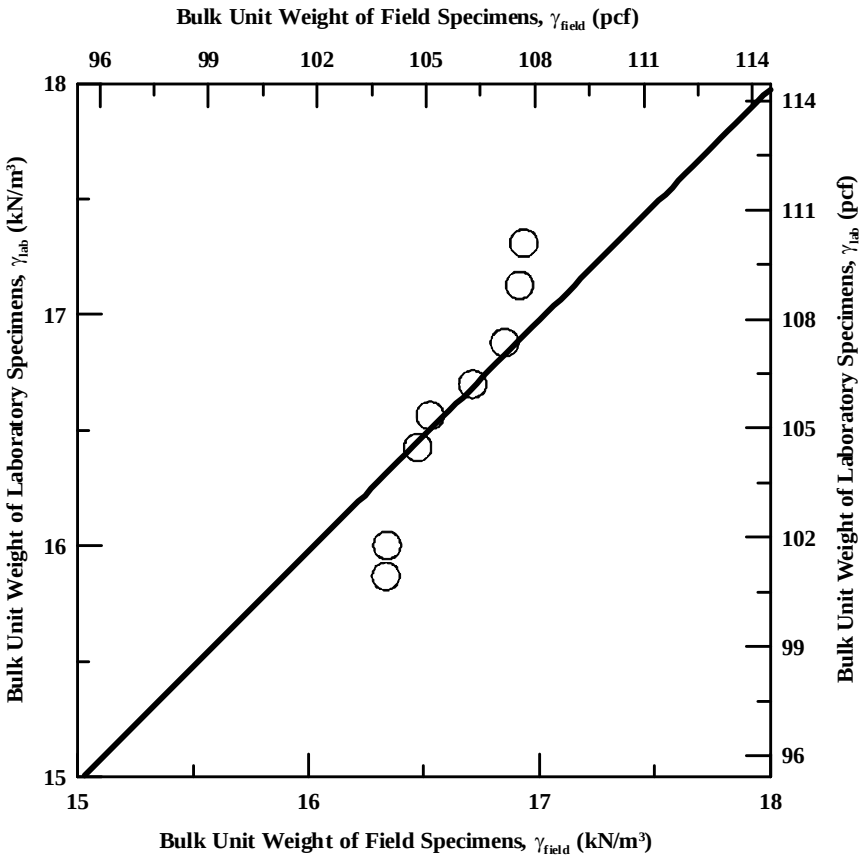

Figure 6.2 Comparisons of bulk unit weight data from field and laboratory specimens.

Table 6.2 Comparison of G_{max} and q_u determined on laboratory and field wet grab specimens (2.8 in. diameter).

Site	**Laboratory Samples**		**Field Wet Grab Samples (after 14-day curing period)**	
	G_{max} in MPa (Curing Period)	**q_{ucs} in kPa (Curing Period)**	**G_{max} in MPa (depth in ft)**	**q_u in kPa (depth in ft)**
1 (Medium PI)	153.7 (7) 166.9 (14)	1321.1 (7) 1641.6 (14)	119.7 (5) 71.9 (Mix) 99.8 (Mix) 112.5 (Mix)	1108.2 (5) 1154.5 (Mix) 1140.3 (Mix) 1099.1 (Mix)
2 (High PI)	171.2 (7) 192.5 (14)	1114.6 (7) 1360.0 (14)	108.4 (2) 112.1 (4) 125.0 (6) 113.8 (8)	1140.0 (2) 1142.3 (4) 1154.1 (6) 1176.0 (8)

Note: Mix – Field Soil-Binder Mix Collected from the Borehole and **1 kPa = 0.145 psi**

Table 6.3 Strength and stiffness ratios of laboratory and field treatments.

Site	$G_{max, field}/G_{max, lab}$	$q_{u, field}/q_{u, lab}$
1	0.43-0.67	0.67-0.70
2	0.56-0.65	0.83-0.86

6.2.3 Correlation between q_u and V_s for Quality Assessment Studies

In this section, empirical correlations between the unconfined compressive strength (q_u) and shear wave velocity (V_s) are developed based on the laboratory test results from lime-cement treated expansive clay specimens. The dependent and independent correlation attributes are considered since they account for the amount of lime and cement in the given binder dosage, w/b ratio and curing time used prior to the laboratory measurements. Fig. 6.3 depicts the variation of q_u with V_s and it can be noticed that the UCS increase with V_s and this increase appears to be non-linear in nature The trends of these variations are consistent with those reported by Hird and Chan (2005) and Mattsson et al. (2005) on cement and lime-cement stabilized soft clays, respectively. The correlations obtained for q_u versus V_s are of the following form:

$$q_u = AV_s^B \tag{6.1}$$

The parameters A and B are constants depending on soil type and binder type and it should be noted here that q_u is in kPa and V_s in m/s. From Fig. 6.3, it can be noted that the parameters A and B varied from 0.029 to 0.614 and 1.367 to 1.957, respectively, for moderate (Site 1) to highly (Site 2) expansive soils treated with the binder (lime+cement) containing more than 75% of cement. Whereas, A and B varied from 0.0048 to 0.0086 and 2.055 to 2.146, respectively, for soils treated with the binder containing more than 75% of lime.

The empirical correlations developed here are useful in quality assessments based on the results obtained from the in situ tests such as downhole testing. This is attempted by estimating the strength of the treated soil sections using shear wave velocity (V_s) interpretations obtained from the in situ testing. The applicability of Eq (6.1) is verified by estimating the strengths of the wet grab specimens based on the V_s obtained on these specimens from the bender element tests. Wet grab specimens of 2 in. (5 cm) and 4 in. (10 cm) dia. were obtained during the construction of DSM columns and later were subjected to the bender element (BE) and the unconfined

compressive strength (UCS) tests. Strengths ($q_{u,pred}$) of these specimens predicted using Eq (6.1) are close to the measured strengths ($q_{u,field}$) from the UCS tests and the results are depicted in Figure 6.4. Results revealed that Eq (6.1) yielded fair estimates of the strength of the in situ soil-binder mix. The average strength of the 4 in. dia. specimens is approximately two times those obtained from the 2 in. dia. specimens (Fig. 6.4).

The developed correlation is useful and is currently recommended for the soil type for which it is developed. Further research on various soil types is recommended to develop a generalized equation for wider applications.

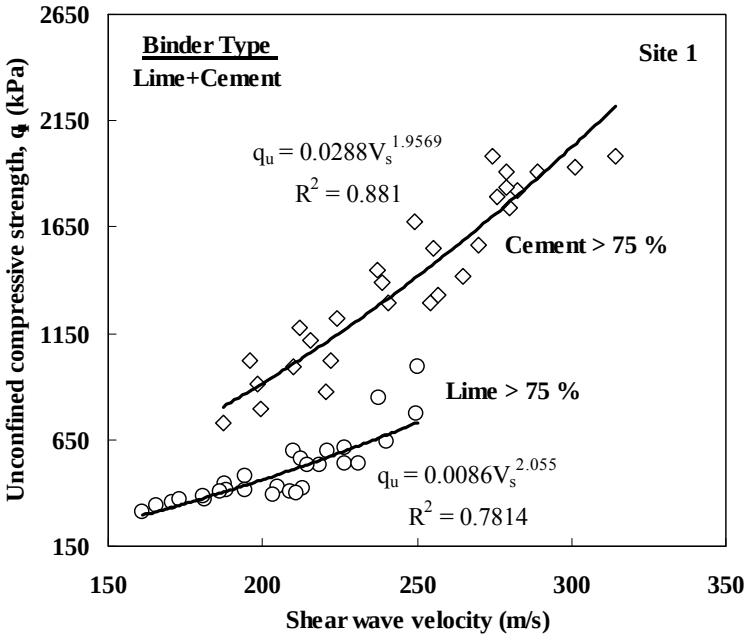

(a)

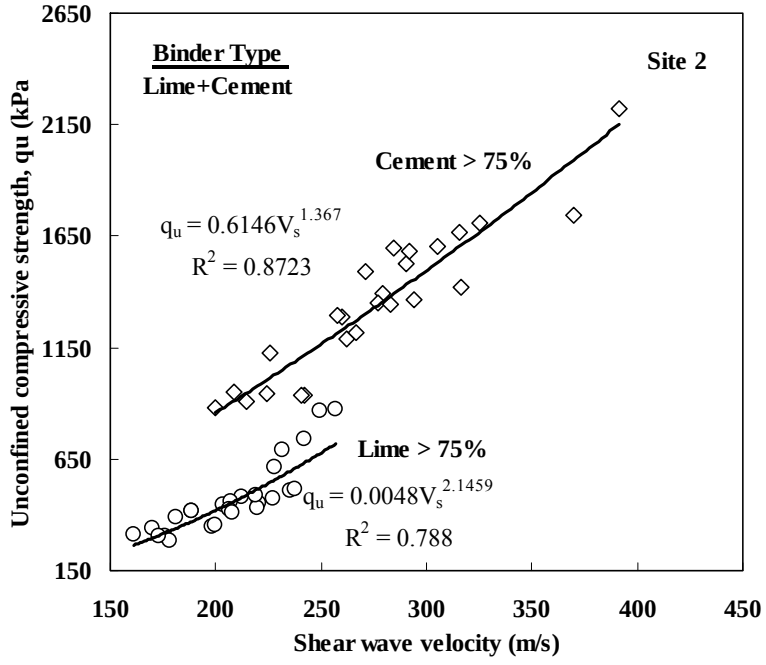

(b)

Figure 6.3 Empirical correlations between q_u and V_s for lime-cement treated expansive clays; (a) Moderate (Site 1) and (b) High (Site 2).

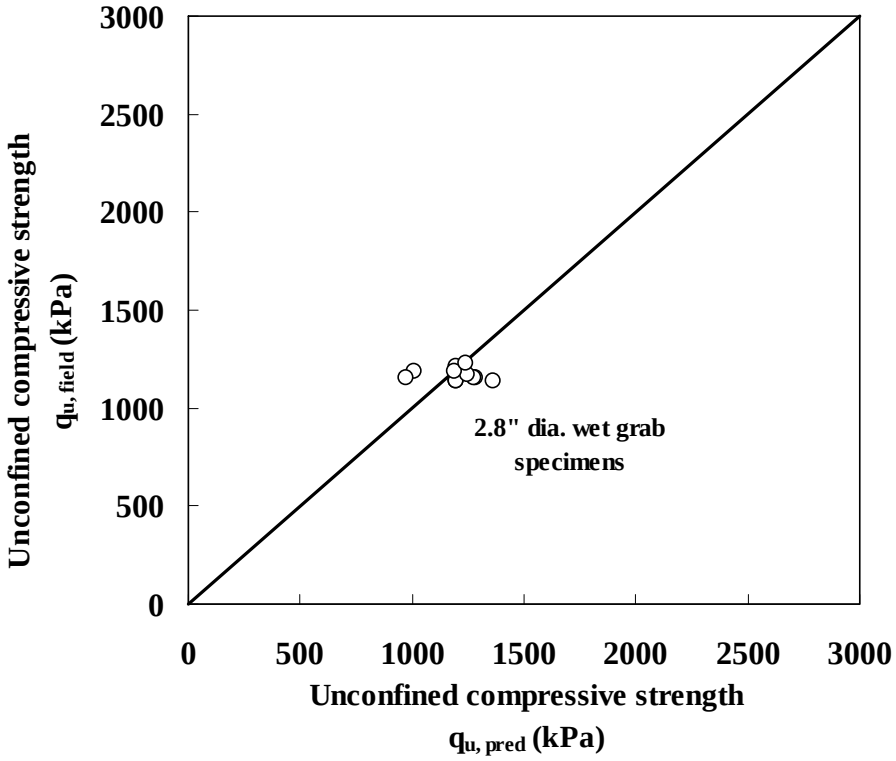

Figure 6.4 Comparison of predicted and calculated strengths for quality assessment.

Note: 1 kPa = 0.145 psi.

6.3 QA/QC Studies Based on In Situ Testing

Three non-destructive testing methods were used for the initial QA studies at the two DSM sites in June 2005. The tests performed were the natural gamma logging, the downhole P-wave velocity and the Spectral Analysis of Surface Wave (SASW).

Natural gamma-ray measurements and downhole P-wave velocity tests were performed in the cased boreholes at each site. SASW tests were performed along two parallel lines (to balance the effect of wave paths relative to the DSM columns for shallow depths) in the treated area and one line in the untreated area (outside the treated area) at each site. The tests performed and their codes are summarized in Table 6.4. Results from these tests are represented in this

chapter, along with a brief explanation of the field-testing and data-analysis procedures for each testing method.

6.3.1 Natural Gamma Logging

6.3.1.1 Background

Radioactivity is the emission of rays caused by the spontaneous change of one element into another. Although several types of rays are emitted, only gamma rays have enough penetration to be of practical use in logging the natural radioactivity of rocks or other earth materials.

Natural gamma-ray logging detects variations in the natural radioactivity originating from changes in concentrations of the trace elements uranium (U) and thorium (Th) as well as changes in concentration of the major rock forming element potassium (K). Since the concentrations of these naturally occurring radio elements vary between different rock types, natural gamma-ray logging provides a useful tool for lithologic mapping and stratigraphic correlation. In sediments or natural soils, potassium is, in general, the principal source of natural gamma radiation, primarily originating from clay minerals such as illite and montmorillonite. In general, the radioactivity of clays is significantly higher than that of sands.

Table 6.4 Tests performed and their notation.

Test	Site 1 (Moderate PI)		Site 2 (High PI)	
	Code	Location	Code	Location
Gamma-Ray and Downhole	S1-100	In a DSM column	S2-100	Untreated area
	S1-200	In a DSM column	S2-200	In a DSM column
	S1-300	Between 4 DSM columns	S2-300	Between 2 DSM columns
	S1-400	Between 2 DSM columns	S2-400	Between 4 DSM columns
	S1-500*	Untreated area	S2-500	In a DSM column
SASW	Site 1a	Treated area	Site 2a	Treated area
	Site 1b	Treated area	Site 2b	Treated area
	Site 1c	Untreated area	Site 2c	Untreated area

* No tests were performed in this borehole.

6.3.1.2 Result Representation

The representative results from natural gamma logging are depicted in Figure 6.5.

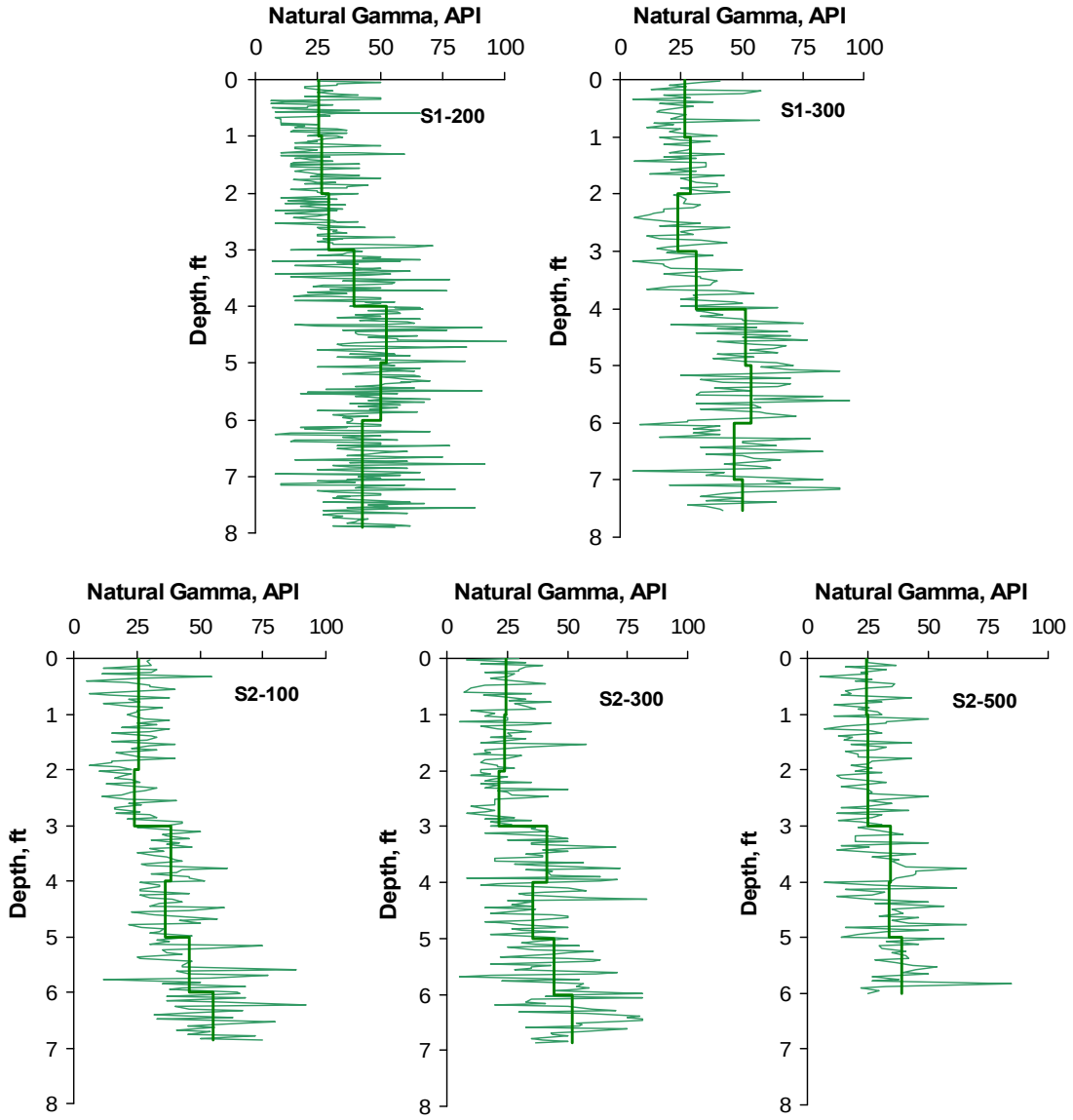

Figure 6.5 Results from natural gamma logging.

API (American Petroleum Institute) in the figure is a standard unit used in gamma-ray measurement. As shown in Fig. 6.5, the results from the gamma-ray measurements taken place in different boreholes (located in a DSM column, between DSM columns and in the untreated area)

at the two sites are very similar. The slightly higher gamma-ray values measured at depths below 3 ft (1.5 m) indicate, normally, an increase in clay component.

6.3.2 Downhole Test

6.3.2.1 Background

The downhole compression or P-wave velocity method is a fast alternative for estimating the variation of the seismic wave velocity with depth at significant savings by requiring only one borehole per test location for each test. The borehole is usually PVC-cased and grouted to ensure the hole remains open and that the casing is in firm contact with the surrounding soil or rock mass.

The test consists of lowering a geophone to a specified depth in the borehole and clamping it to the casing. An impact source is placed at the surface near the borehole. Generally, the source is a sledge hammer which is struck vertically onto a metal plate. The travel time from the moment of source initiation until reception at the geophone is recorded. The geophone is moved to a new depth and the process is repeated. Interval velocity (instantaneous velocity over a time interval) is directly determined by comparing successive readings (travel time difference).

The downhole seismic equipment used for the initial tests consists of a Geometrics Seismograph, Model SmartSeis S-24 and a Geostuff BHG-2 borehole geophone. The SmartSeis is a 24-channel digital recording seismograph system specially designed for collecting high-resolution seismic information.

6.3.2.2 Result Representation

The average P-wave velocities from downhole tests are summarized in Table 6.5. The global averages in the downhole P-wave velocity in the treated areas are 3800 ft/s (1140 m/s) and 3600 ft/s (1080 m/s) for Site 1 and Site 2, respectively. The velocity of about 2600 ft/s (780 m/s)

in the untreated area (S2-100) is significantly lower than the global average in the treated area at Site 2.

Table 6.5 Average P-wave velocities from downhole tests.

Site 1			Site 2		
Borehole	Depth Range (ft)	P-wave Velocity (ft/sec)	Borehole	Depth Range (ft)	P-wave Velocity (ft/sec)
S1-100	1 - 7	3468	S2-100	2 - 6	2564
S1-200	1 - 7	3974	S2-200	1 - 5	3670
S1-300	1 - 7	3727	S2-300	2 - 6	2920
S1-400	0 - 7	4046	S2-400	0 - 4	3774
S1-500	NA	NA	S2-500	0 - 5	4000

6.4 Field Monitoring Studies

The performance of the treated sections was studied by conducting surveying of inclinometers and settlement plates at regular intervals; i.e., for every two to three weeks. The data from the pressure cells and moisture probes were collected continuously using an automatic data acquisition system. The data acquisition system used in the present study is a CR10X type data logger (Fig. 6.6). The CR10X is a multiplexer and can accommodate 16 vibrating wire type sensors and 32 moisture probes. In the present study, only four VW channels and 2 moisture probe channels were activated as per the project requirement. The data loggers were supplied with a monitoring program created using LoggerNet software. This program helps in collecting data at regular intervals from the sensors and then transfers the data to the logger memory. Later, during field visits the data stored in the logger memory were transferred to a laptop computer via a data acquisition program.

Each site was installed with one data logger stationed in a weatherproof box, fastened to the concrete barrier on the eastbound inside shoulder, as shown in Fig. 6.7, and it ran on a rechargeable 12V lead acid battery. As mentioned in a previous chapter, the data collection was carried out from July 2005 to Aug 2007 in two phases, covering two fall, two spring and two summer seasons. The first phase of data collection was from July 2005 to Aug 2006 and the second phase was from Aug 2006 to June 2007. The rainfall data for each month throughout the monitoring period were also collected from http://www.noaa.gov/ (National Oceanographic and Atmospheric Administration, NOAA) and tabulated in Table 6.6a. Also, the cumulative precipitation recorded for each season and monitoring phase was calculated and presented in Table 6.6b. It is noticed from the rainfall data collection at NOAA that the year 2005 recorded the least precipitation (19 in.) in the last three decades and during the period of monitoring (July 2005 to August 2006), a cumulative rainfall of 22.7 in. was recorded (http://www.srh.noaa.gov/). This resulted in an overall increase in volumetric moisture levels to about 30% from an initial moisture level of 20% in both the treated and untreated sections at Sites 1 and 2. Because of the low variation in the field moisture levels during the first monitoring period, the researchers proposed manually wetting Sites 1 and 2. This was proposed to increase the in situ moisture levels to those corresponding to heavy precipitation at which full saturation of soils is expected. This would provide an opportunity to evaluate the performance of the DSM treated sections under extreme saturation conditions during wetting followed by drying due to reduction in the moisture levels. The following subsection explains in detail the simulation of the high precipitation in the present study at Sites 1 and 2.

Table 6.6a Precipitation (inches) during each month of monitoring period.

(http://www.srh.noaa.gov/)

Year	Precipitation												Total
	Jan	Feb	Mar	Apr	May	Jun	Jul	Aug	Sep	Oct	Nov	Dec	
2005							0.74	2.46	1.36	0.89	0.02	0.33	5.8
2006	2.25	3.85	4.4	1.86	1.9	0.34	1.78	0.52	2.6	4.34	2.58	3.33	29.75
2007	5.58	0.43	3.81	2.82	8.34	11.1	5.54	0.35					37.97

Table 6.6b Cumulative precipitation in inches during each season and phase.

Seasons	Total Precipitation	
	Season	Phase and Total
Fall 2005	5.8	I and 22.7
Spring & Summer 2006	16.9	
Fall 2006	12.85	II and 50.82
Spring & Summer 2007	37.97	

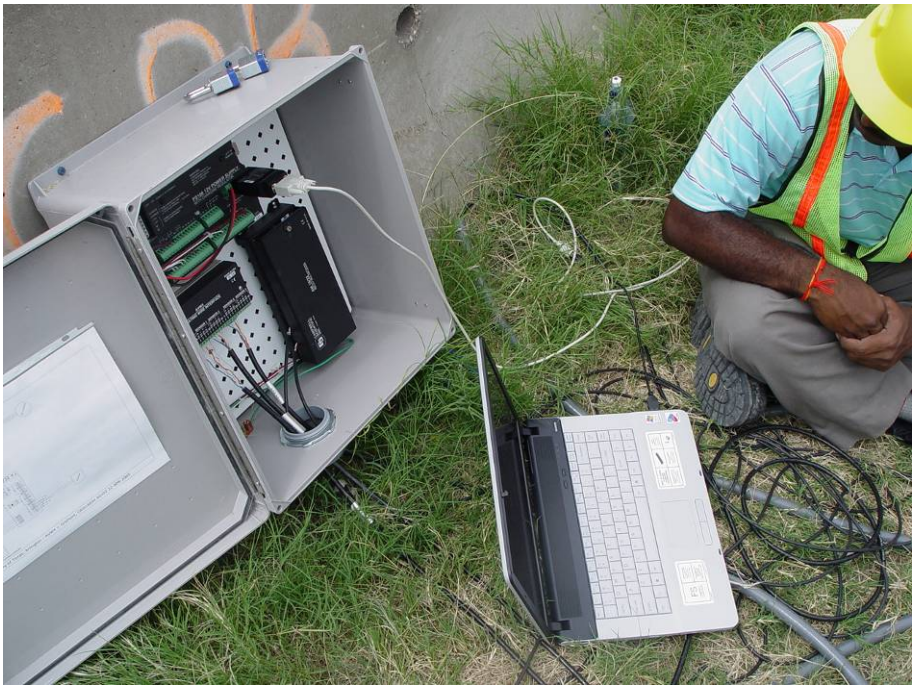

Figure 6.6 CR10X Data logger and on site data transfer to LAPTOP.

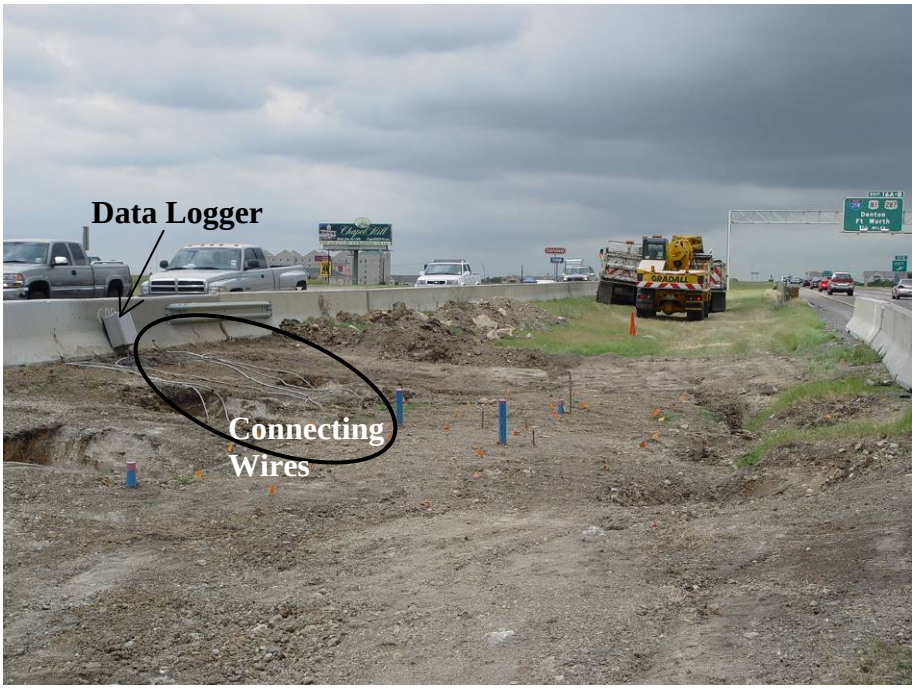

Figure 6.7 Data logger fastened to barrier on eastbound at Site 2.

6.4.1 Simulation of High Precipitation

The details of watering Sites 1 and 2 are presented in the following steps:

- Researchers estimated the tentative amount of water required for each site based on their density and in situ moisture content levels prior to saturation.
- Approximate water amount needed for saturating the site was calculated and a large water tank that stores the necessary quantity of water was placed at the site.
- After considering different sprinkler systems to simulate raining at sites, the researchers selected a drip hose system since the sprinkler system and subsequent spray due to wind may cause distractions to drivers passing by the sites.
- A schematic of the drip hose system layout and the typical setup used at Sites 1 and 2 are depicted in Figs. 6.8 and 6.9(a), respectively. After laying out the drip hose lines, the unit was connected to the water tank placed at the site.
- Sites 1 and 2 were watered for a period of 3 to 4 months. Site 1 was watered from November 2006 to February 2007 and Site 2 from March 2007 to June 2007.
- The sites were watered continuously for a period of 2 to 3 days and then both inclinometer and total station surveys were conducted for data collection. Data recorded by pressure cells and moisture probes were also downloaded from the data logger. The process of watering and subsequent data collection was performed in cycles and each cycle lasted for a week.
- It was noticed that in the first 24 hrs, the sites were wet and water was seeping to the adjacent trenches (Fig. 6.9[a] and [b]), and after 48 hrs, sites were flooded with water (Fig. 6.9[c] and [d]).
- In situ tests, including downhole logging and SASW testing, were performed after the saturation process at Site 2 in May 2007. During testing, the average moisture content

levels at Sites 1 and 2 were 45% (volumetric moisture contents) corresponding to full saturation of sites. The high moisture levels at Site 1 during this period are also attributed to heavy natural precipitation prior to testing. Site conditions at the time of testing are depicted in Figure 6.10.

- The data collected during the second period of monitoring were analyzed and discussed with that from the first period of monitoring in the following chapter.

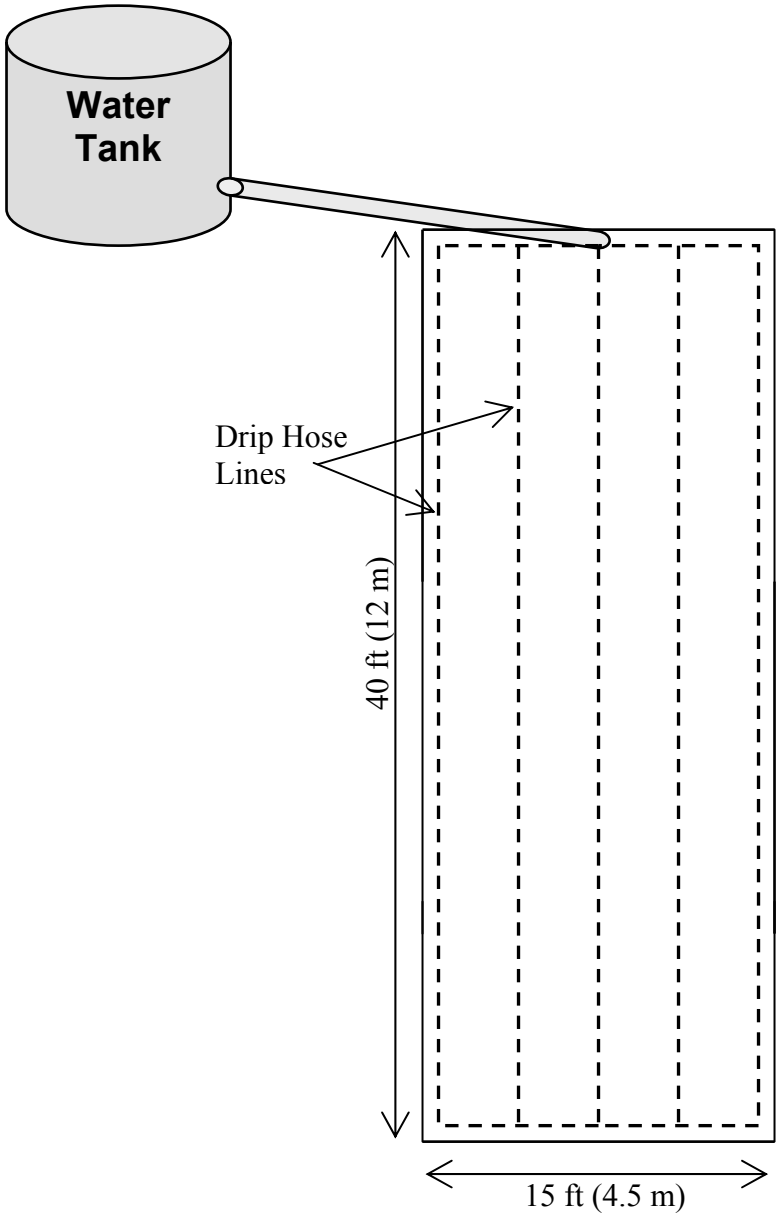

Figure 6.8 Schematic of layout of drip hose system simulating precipitation used at Sites 1 and 2.

(a)

(b)

(c)

(d)

Figure 6.9 (a) Setup and condition after 24 hrs (b) Seeping of water from sides (c) and (d) Condition after 48 hrs.

(a)

(b)

Figure 6.10 Site conditions at the time of in situ testing in May 2007 at Sites 1 and 2.

6.5 Mineralogical Studies

Mineralogical studies including Scanning Electron Microscopy (SEM) and Electron Dispersive X-ray analysis (EDAX) were performed in the present study on both laboratory and field mixed soil-binder samples. These tests were carried out in the NANOFAB facility at UTA. SEM analysis provided qualitative understanding of the degree of mixing achieved in the field as compared to that in the controlled laboratory environment. Whereas, EDS helped in determining the elements/compounds formed at the particle level and thereby the formation of cementitious and pozzolanic compounds. The equipment used to carry out these tests is depicted in Fig. 6.11. For this purpose, the treated soil sample pieces of 0.2 in. (5 mm) average size were collected from the UCS specimens after testing for SEM analysis. These samples were then thoroughly cleaned of any dust and mounted on pin type stubs with a ½ in. (1.25 cm) dia. surface using a tape (sticky on both sides), as shown in Fig. 6.12. The samples were subjected to carbon coating prior to SEM testing. The samples were ready for testing and were placed in the SEM equipment shown in Fig. 6.11. The carbon coated samples were hit with an X-ray and high resolution and magnified images were collected. Subsequently, Energy Dispersive Spectrum (EDS) analysis was also performed and the results from these tests on control, laboratory and field mixed samples are presented and discussed below.

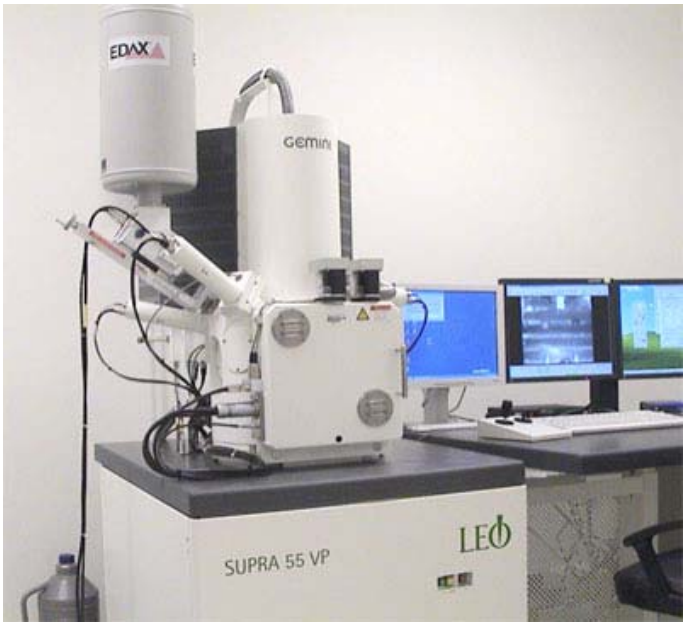

Figure 6.11 Equipment used for SEM analysis (ZEISS Supra 55 VP SEM; source: http://www.uta.edu/engineering/nano/facility.php?id=53&cat2=SEM).

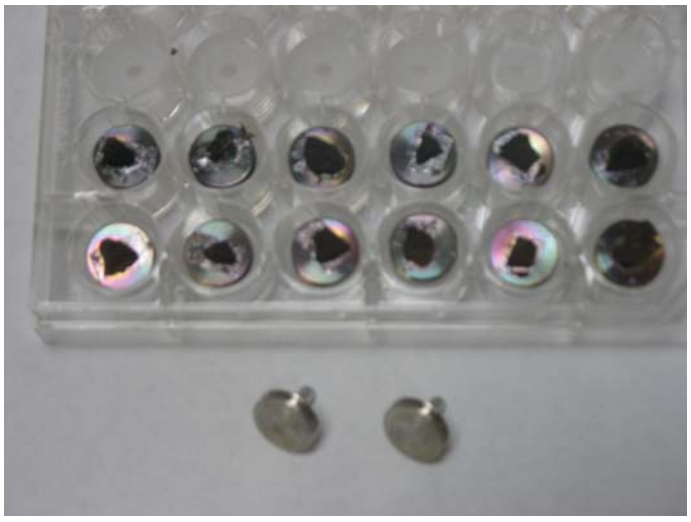

Figure 6.12 Photograph depicting SEM pin type stubs and carbon coated treated soil samples mounted and ready for SEM and EDS testing.

Fig. 6.13 shows the SEMs of the untreated soils from the test sites. It appears that both soils show mixed fabric with a certain amount of aggregation.

Fig. 6.14 presents two typical SEMs of cement-lime treated clays in the laboratory environment from both sites. From these pictures, it is observed that cementitious compounds, including platy-like calcium hydroxide and long needle-like ettringite, formed around the clay particles and it also shows that these compounds formed an interwoven structure around the clay particles (Fig. 6.14[a]). It also suggests a good mixing between soil and cement-lime additives, showing the formation of a dense treated soil mixture (Fig. 6.14[b]). Similar structures are noted in the case of the SEM images of other chemically treated specimens. Both chemical reactions around clays and intrusion of pozzolanic compounds in the treated soils appear to be influenced by the rotational type mixing process used to mix the soils and binders in the presence of high moisture content. Also, several brayed edges are found in the treated soil structure, which can be interpreted as a dissolution process that results in reactive alumina and silica to form cementitious compounds. Also, the SEMs reveal a more structured fabric of the treated soil, which is considered close to a flocculated structure. The presence of cementing compounds in the form of needle-like fibers and platy structures as well as a dense soil mixture might have contributed to increase in the soil properties.

Fig. 6.15 shows typical EDAX pictures with chemical elements identified in the scanned material. The chemical elements including calcium, silica and aluminum and their presence support the formation of cementitious compounds in the treated material. The dominating peaks in the EDAX figure shows considerable amount of calcium in the treated area, which might have come from both the cement and lime binders.

Other peaks suggest the presence of silica and aluminum in the treated areas. Calcite formation can be low in magnitudes as the carbon peaks are small in the figure. Overall, both

SEM and EDAX studies indicate that the present treatment procedures adapted in this research resulted in the better mixing of the cement-lime treated soil mixture.

Fig. 6.16 presents two SEM photographs on field treated specimens coated with carbon. Comparing the structure of the treated material at the similar magnification reveals the similar structured fabric as those of the laboratory specimens. Additionally, cementitious fibrous structures can be seen on the coated clay particles. This reconfirms that the laboratory and field mixing has resulted in similar type of chemical treatments of the soils.

6.6 Summary

Quality assessments of the DSM columns constructed in the present study are performed following the results from the laboratory tests on wet grab samples and in situ downhole and SASW testing on the treated ground. The procedures followed in carrying out these tests were discussed in this chapter. Empirical correlations relating strength with shear wave velocity were developed using the laboratory test results reported in Chapter 4. The validity of these correlations is verified by applying them to the results obtained from tests on wet grab samples and it is noticed that the proposed correlations estimated strengths fairly close to the calculated ones.

This chapter presents the QA/QC studies and monitoring procedures carried out in the present study. Finally, this chapter explains the field monitoring procedures during the first and second phases of data collection followed by the stepwise explanation of simulating high precipitation at the sites to study the behavior of the treated ground at extreme moisture conditions.

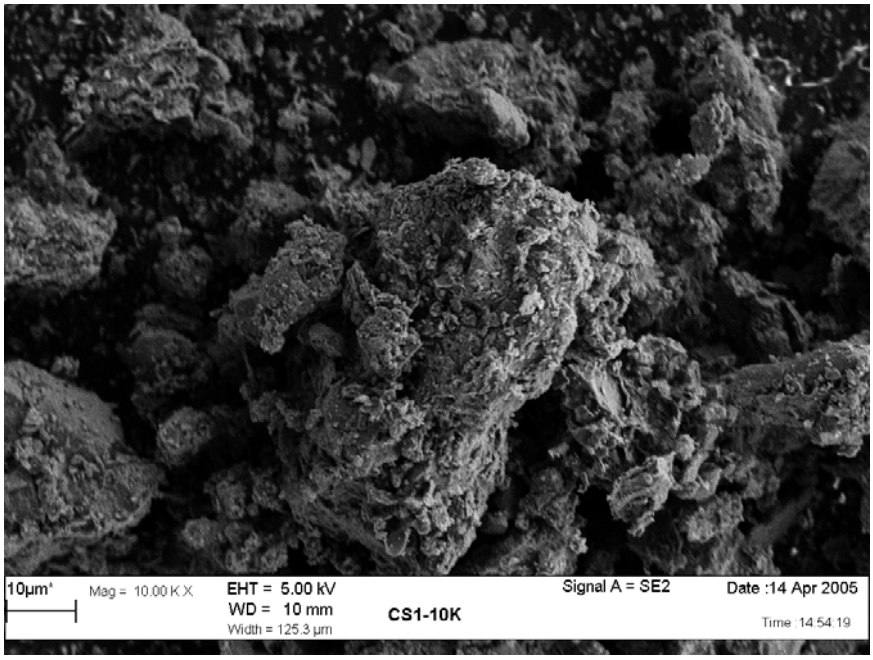

(a) Site 1

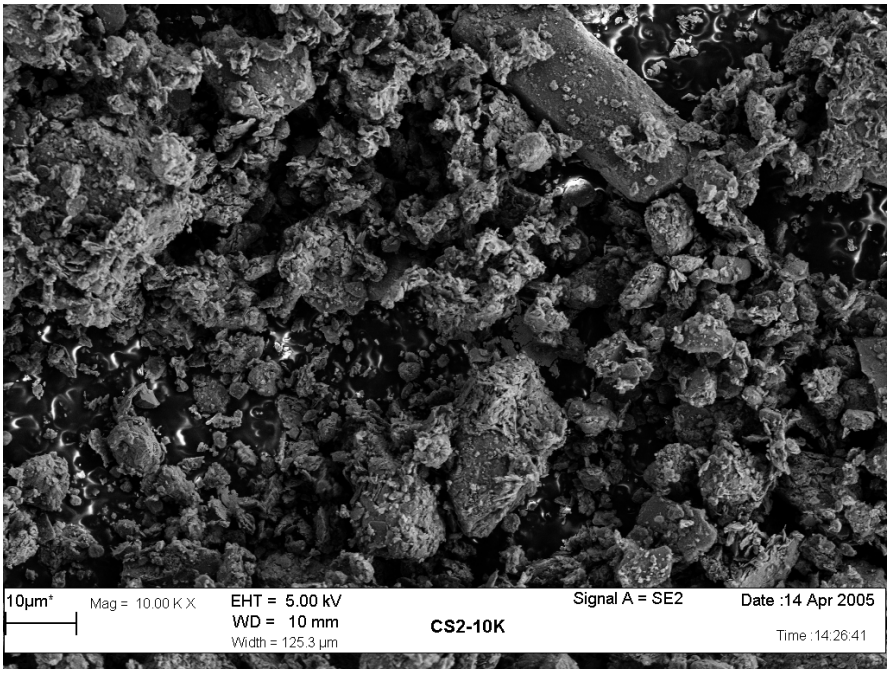

(b) Site 2

Figure 6.13 SEM analyses of control soils.

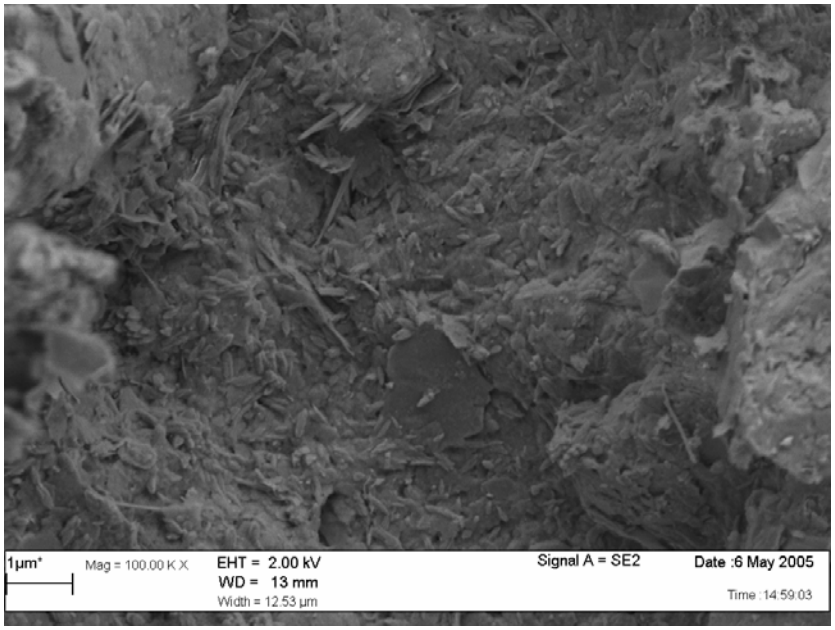

a) S1-100-L:C-25:75-1.0

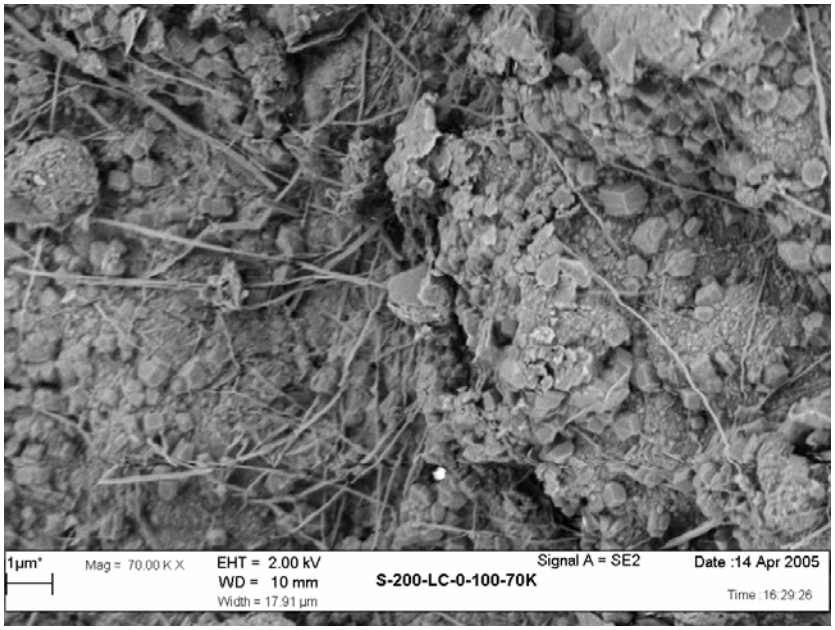

b) S2-150-L-C-25:75-1.0

Figure 6.14 Typical SEM results of cement-lime mixed expansive clays in laboratory.

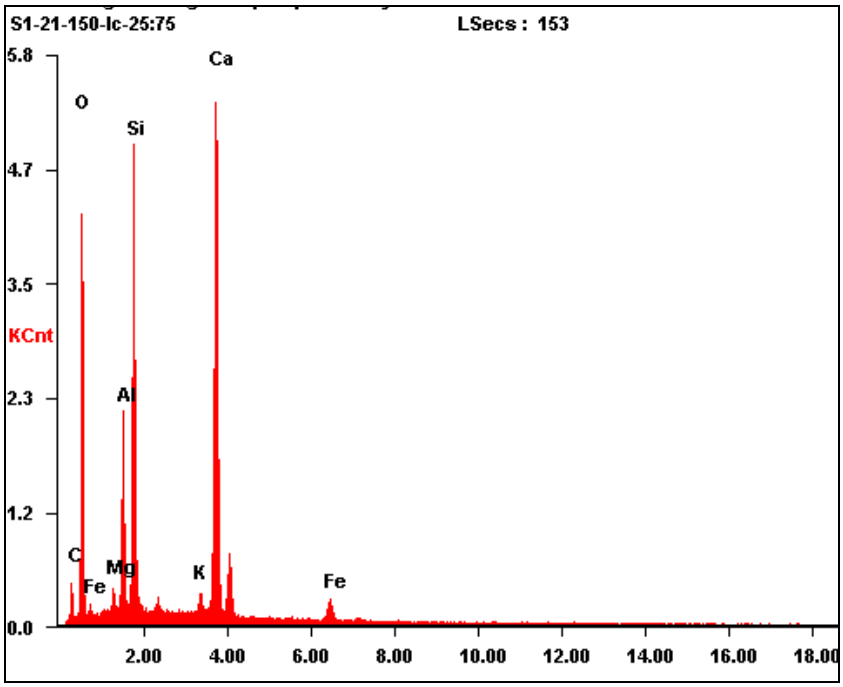

(a) Site 1

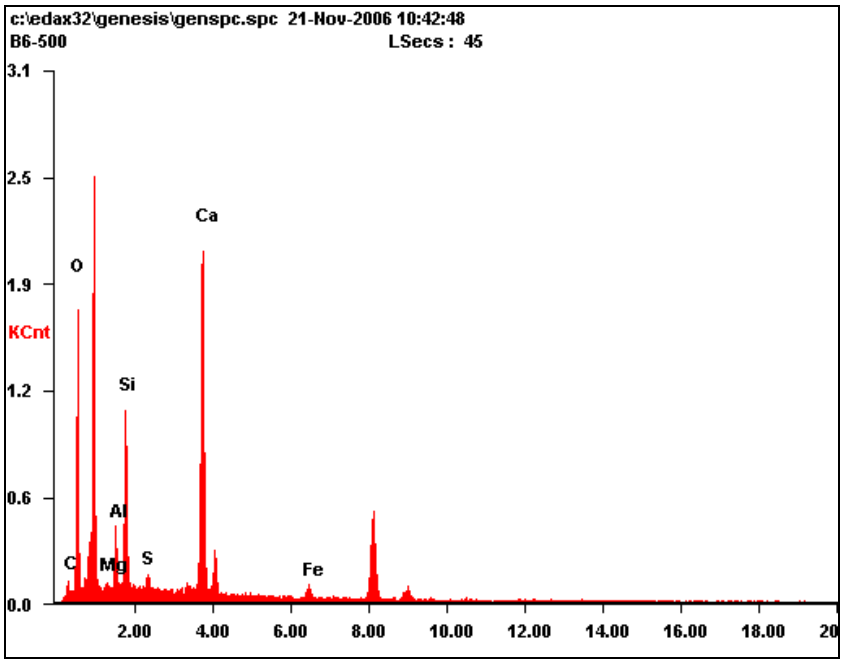

(b) Site 2

Figure 6.15 Typical EDAX analyses on the lime-cement mixed expansive clays.

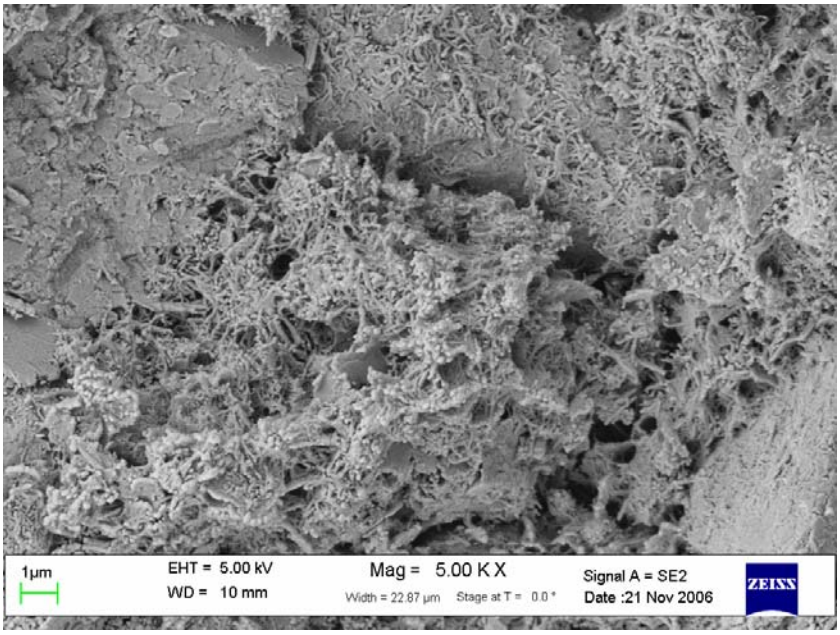

(a) Site 1

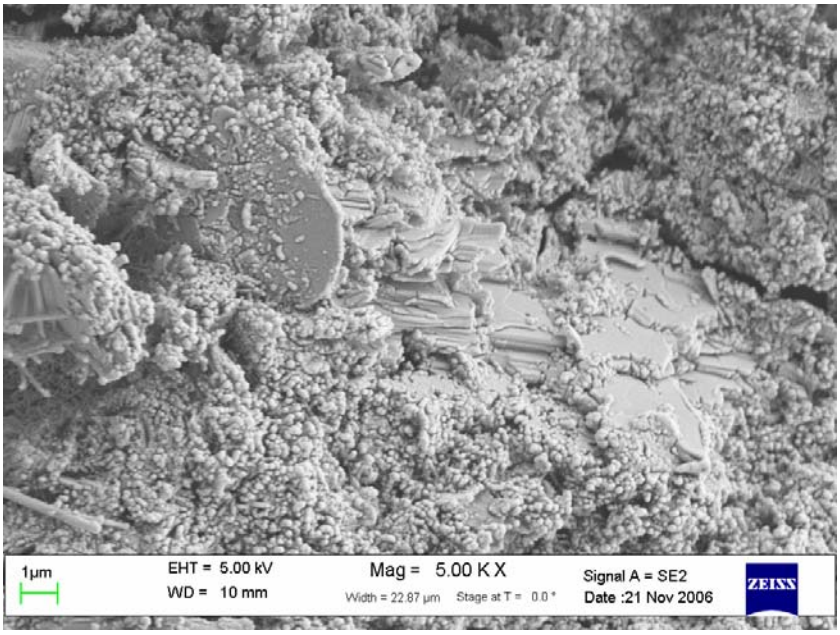

(a) Site 2

Figure 6.16 Typical SEM results of cement-lime treated expansive clays in field.

CHAPTER 7

ANALYSIS OF FIELD DATA OF DSM TREATED COMPOSITE SECTIONS

7.1 General

Treatment of expansive clays to moderate depths using the DSM technique was studied in two parts, as mentioned in Chapter 1, including laboratory and field studies. Field studies were performed to evaluate the effectiveness of the DSM technique in minimizing the shrink-swell behavior of the expansive clays with seasonal variations. This included monitoring of the DSM treated pilot test sections through data collection from instrumentation and in situ testing for a period of two years; i.e., from June 2005 to August 2007. The following sections analyze and discuss in detail the results obtained from the field instrumentation and in situ testing.

7.2 Performance Evaluation Based on Field Instrumentation

Data collected from the field instrumentation were analyzed and discussed for each season (fall and spring) during the monitoring period and compared the results to address the effect of seasonal fluctuations on the performance of the DSM treated sections.

7.2.1 Moisture Probe Data

The moisture levels of the treated and untreated sections at Sites 1 and 2 were monitored during Phases I and II in the present study. Gro-Point moisture probes shown in Fig. 5.33 were used for this purpose. As explained in an earlier section for pressure cells, the data read by the moisture probes were also collected continuously by the CR10x data logger and stored in its memory and was later transferred to a laptop computer using LoggerNet data acquisition software. The output data recorded by the moisture probe were in mA in the range of 0 to 5.0 mA, and the manufacturer reported that the output is linear proportional and equivalent to

0 to 50% (volumetric). Therefore, the data recorded in mA were converted into volumetric moisture content by multiplying the reading with a factor of 10. The results thus obtained were presented with time in Figs. 7.1 and 7.2 and analyzed subsequently in the following sections.

During Phase II of the monitoring, simulation of high rainfall was carried out at Sites 1 and 2 and the moisture levels during this period were determined by conducting soil sampling around different boreholes. Soil samples were collected along the depth at four locations per site; three borings were located within the treated section and one boring in the untreated section. The schematic showing the locations of borings for Sites 1 and 2 is presented in Fig. 7.3.

For Site 1, the data were collected during Fall 2005 but starting Spring 2006, the moistures probes failed to collect data. Following this, the researchers installed two more moisture probes during Phase II (i.e., Fall 2006) monitoring, but again the one installed in the treated section failed to collect data since January 2007. However, the overall moisture conditions at Site 1 were expected to be close to those at Site 2 as both the sites are close to each other (1 mile apart) during any precipitation and saturation process during the monitoring period. The data collected from Site 1 during Phase I and Phase II of monitoring are tabulated in Table 7.1 and depicted in Fig. 7.1, respectively. Similarly, the results obtained from moisture probes at Site 2 are depicted in Fig. 7.2, whereas, the results from field sampling at the end of Phase II (i.e., during saturation process of Site 2) are presented in Table 7.2.

The variations in moisture levels recorded by moisture probes at Sites 1 and 2 reflect the precipitation that occurred during the monitoring (Table 6.6a, Figs. 7.1 and 7.2). It can also be noticed that the moisture levels (Table 7.3) during the saturation process of the sites in Phase II of monitoring, represent extreme conditions that correspond to those during high precipitation (flooding). Performance of the treated and untreated sections under these conditions was monitored and the results were analyzed and discussed in the following sections. It is noticed that

the soil movements and swell pressures of the treated sections at Sites 1 and 2 are less than those encountered in the untreated soils. However, the soil movements and swell pressures recorded during Phase II are slightly more than those recorded during Phase I due to the increased moisture levels. Evaluations of the treated sections' behavior in terms of soil movements and swell pressures related to moisture variations indicate that the DSM technique was effective in reducing the shrink-swell behavior of the expansive soils to considerable depths. The same has been further evaluated by conducting in situ tests (downhole measurements and SASW testing). The results from these tests are presented and discussed in the subsequent sections.

Finally, the moisture probe results presented here show that the moisture content of the soils to considerable depths varied from minimum to fully saturated (Phase II) states during the monitoring period. Hence, the soil deformation, swell pressure and non-destructive testing results in the following sections correspond to the extreme moisture variations, particularly the Phase II results correspond to full saturation conditions.

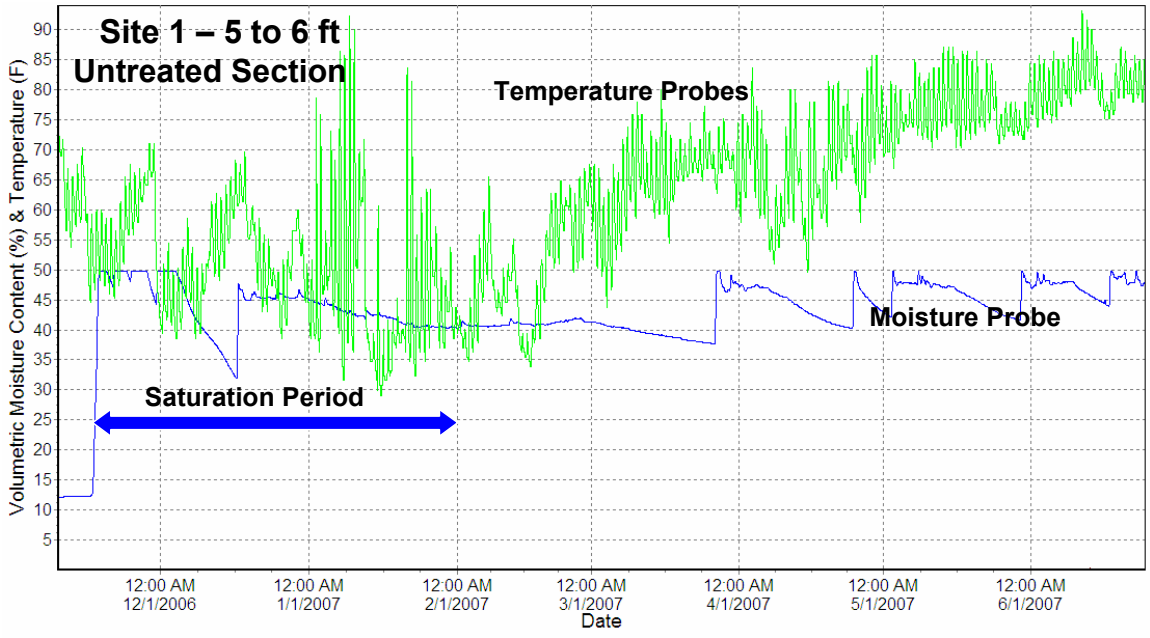

(a) Untreated (from Gro-Point Datalogger)

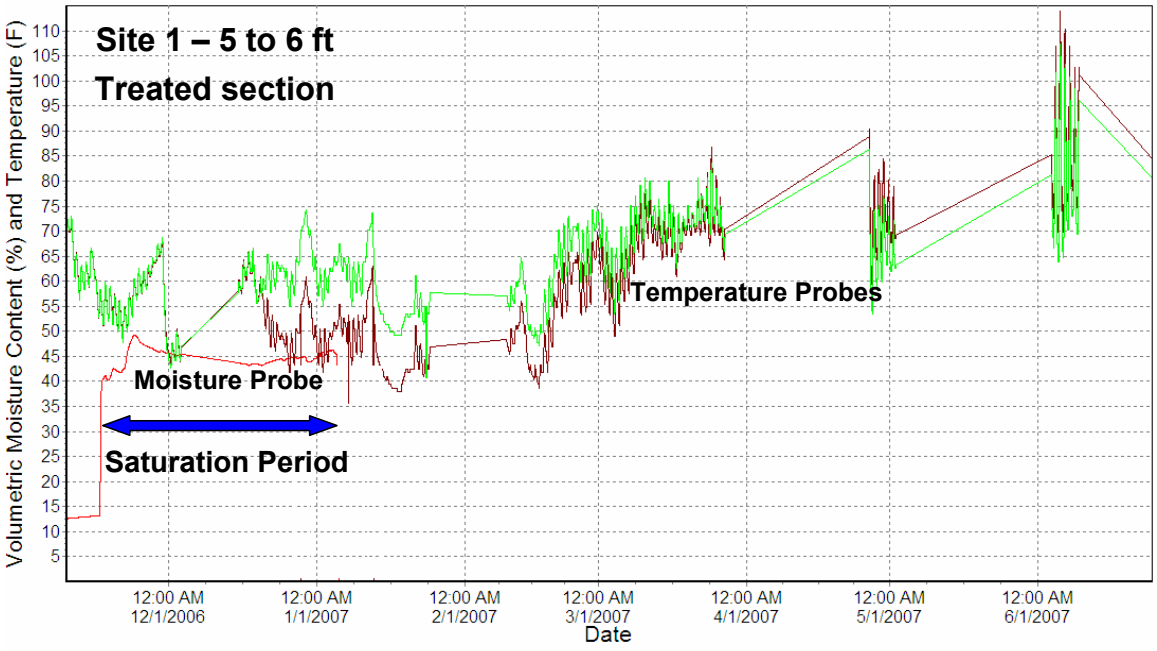

(b) Treated (from Gro-Point Datalogger)

Figure 7.1 Volumetric moisture content with time at Site 1 during Phase II of monitoring.

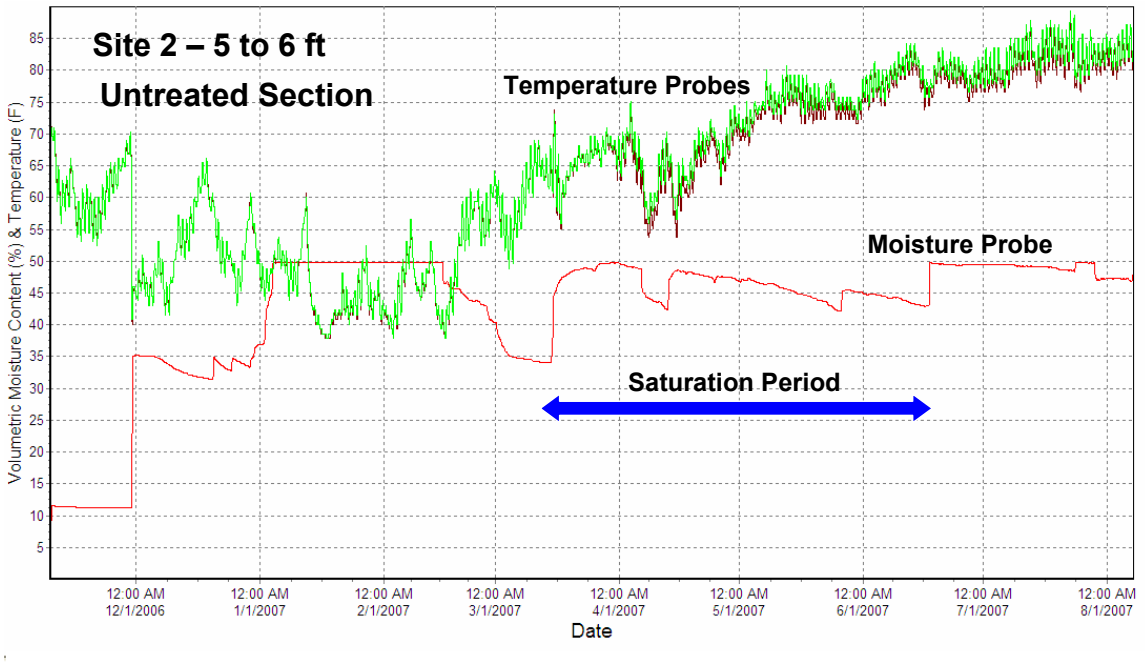

(a) Untreated section (from GroPoint Datalogger)

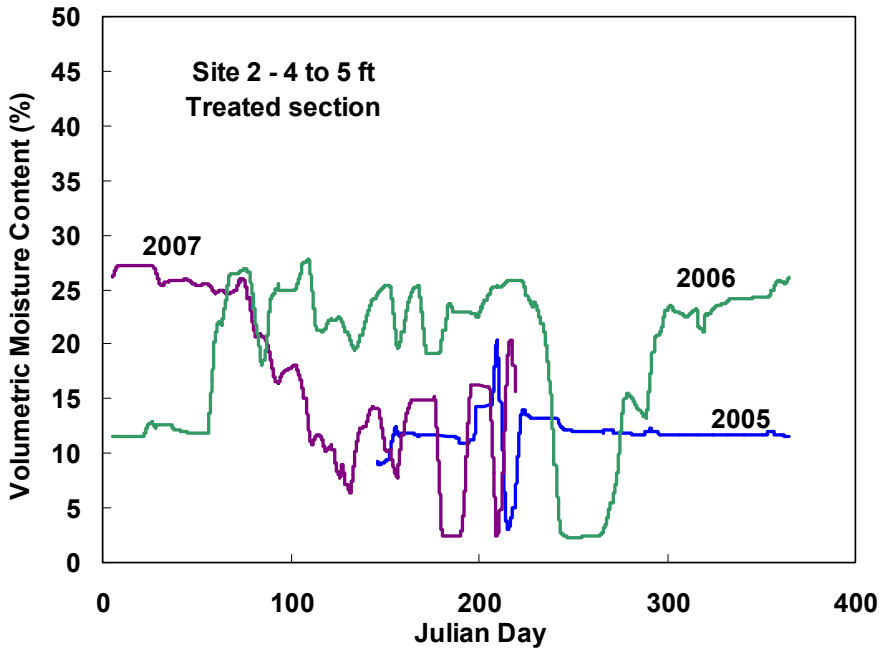

(b) Treated section (from CR10x Datalogger)

Figure 7.2 Volumetric moisture content with time at Site 2 during Phases I and II of monitoring.

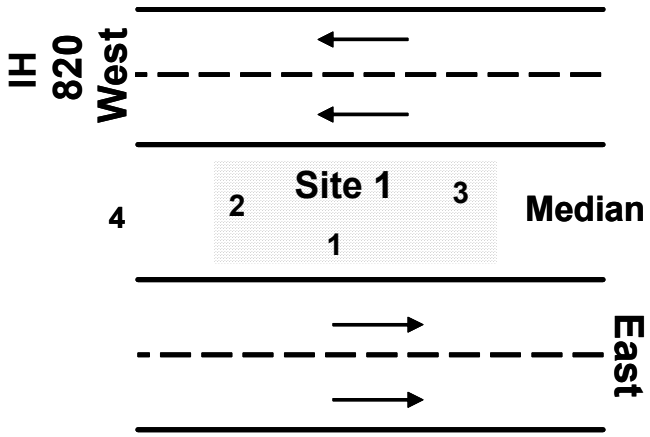

(a)

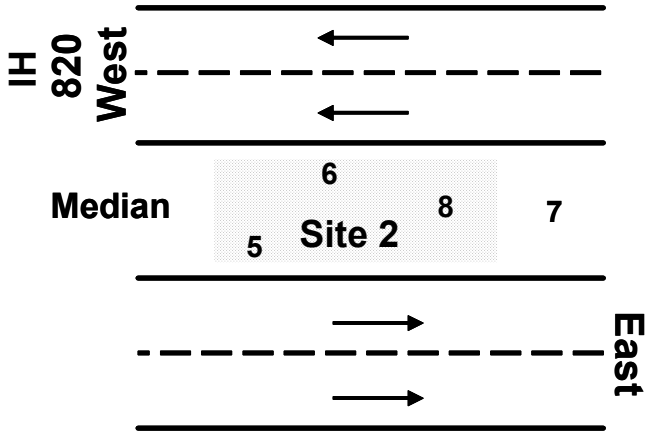

(b)

Figure 7.3 Schematic showing borings for sample collection to estimate moisture levels during saturation; (a) Site 1 and (b) Site 2.

Table 7.1 Volumetric moisture content levels at Site 1 during Phase I.

Month / Year	Volumetric moisture content (%) from moisture probe
June – July / 2005	9 to 20
Aug – Oct / 2005	15 to 35
Nov – Dec / 2005	9 to 15
Jan – Feb / 2006	10 to 30
Mar / 2006	10 to 35

Table 7.2 Moisture content results from soil borings during saturation at Sites 1 and 2.

(a) Site 1

Depth (ft)	Moisture content (%)				
	Borehole				Average Initial Values
	1	2	4	5	
0 to 3	25	32	29	20	29.4
3 to 6	19	18	23	17	23.3
6 to 9	27	23	25	22	24.2
9 to 12	26	22	22	-	-
12 to 14	26	22	22	-	13

(b) Site 2

Depth (ft)	Moisture content (%)				
	Borehole				Average Initial Values
	1	2	4	5	
0 to 3	28	36	35	25	29.9
3 to 6	21	31	44	25	27.3
6 to 9	27	29	51	32	24.7
9 to 12	29	27	53	35	26.5
12 to 14	40	27	36	47	24.4

Table 7.3 Ranges of moisture content and precipitation levels at Sites 1 and 2 .

Season		Volumetric moisture content (%)		Precipitation in inches
		Site 1	Site 2	Treated
Phase I	F 2005	9 to 35	3 to 20	5.8
	Sp 2006	NR	12 to 27	16.9
Phase II	F 2006	13 to 48	8 to 40	12.85
	Sp 2007	37 to 50	35 to 50	37.97

Note: NR – not recorded; F-Fall and Sp-Spring

7.2.2 Soil Movements

Both lateral and vertical deformations in the treated and untreated expansive soils at Sites 1 and 2 were recorded through inclinometer instrumentation. The data collected through surveying of the inclinometer casings at regular intervals were analyzed and the results presented in the following subsections.

7.2.2.1 Lateral Soil Movements

Vertical inclinometer casings of 2.75 in. (7 cm) diameter were installed in both the treated and untreated sections at Sites 1 and 2 during the construction of the pilot test sections. A total of five casings were installed in each site; four in the treated and one in the untreated section. All of them are used to monitor the soil movements at periodic intervals, usually twice a month. Fig. 7.4 depicts the plan view of Sites 1 and 2 showing the locations of the instrumentation — inclinometers casings (vertical and horizontal), pressure cells, moisture probes and settlement plates.

Inclinometer surveying was performed by sending the inclinometer probe into the casing in the A – direction (See Chapter 5) and the data at each depth interval were then collected and stored using a Digitilt DataMate connected to the inclinometer probe. The readings, thus, stored

in the DataMate were downloaded to a computer using a DataMate Manager (DMM) software. The inclinometer data were then processed for any errors such as bias, rotation, and sensitivity. Plots, as shown in Figures 7.5 and 7.6, were developed using the DigiPro software. At the same time the data were also adjusted for any depth offsets. For more details regarding the DMM and DigiPro softwares, the readers are directed to refer to the respective manuals, DMM for Windows and DigiPro for Windows.

Results from the vertical inclinometers depicting the lateral movement of soils of both the untreated and treated sections at Sites 1 and 2 are presented in Figs. 7.5a-d and 7.6a-d, respectively. It can be noticed from these figures that the overall movements in both the untreated and treated soils are small and less than an inch. These low movements in the lateral direction are attributed to high confinements. It should be noted that the inclinometers installed in the untreated soil sections and at the center of the four DSM columns showed movements that are more than those installed inside a DSM column. The swell and shrink tests conducted on the laboratory treated and wet grab specimens from the field indicated that both the swell and shrink strain potentials are close to zero. The very low overall absolute movements, 0.2 and 0.11 in. inside a DSM column (Table 7.4) at Sites 1 and 2, respectively, may be possibly due to separation between the inclinometer and the DSM column due to shrinkage of the bentonite slurry grout placed around the inclinometers.

Results tabulated in Table 7.4 also indicate that the inclinometer casing in untreated soils moved to both the north and south sides cyclically, as can be noticed from Figs. 7.5 and 7.6. This cyclic movement of the untreated soils is attributed to variations in moisture availability due to precipitation from season to season. During Phases I and II of monitoring, a total precipitation of approximately 23 and 51 in. was recorded (Table 6.6b). The soil movements in the treated soil (DSM column) and between columns within the treated area are small though similar variations

in precipitations existed for these locations. These confirm that the DSM treatment is effective in minimizing soil movements in the vicinity of the treated area.

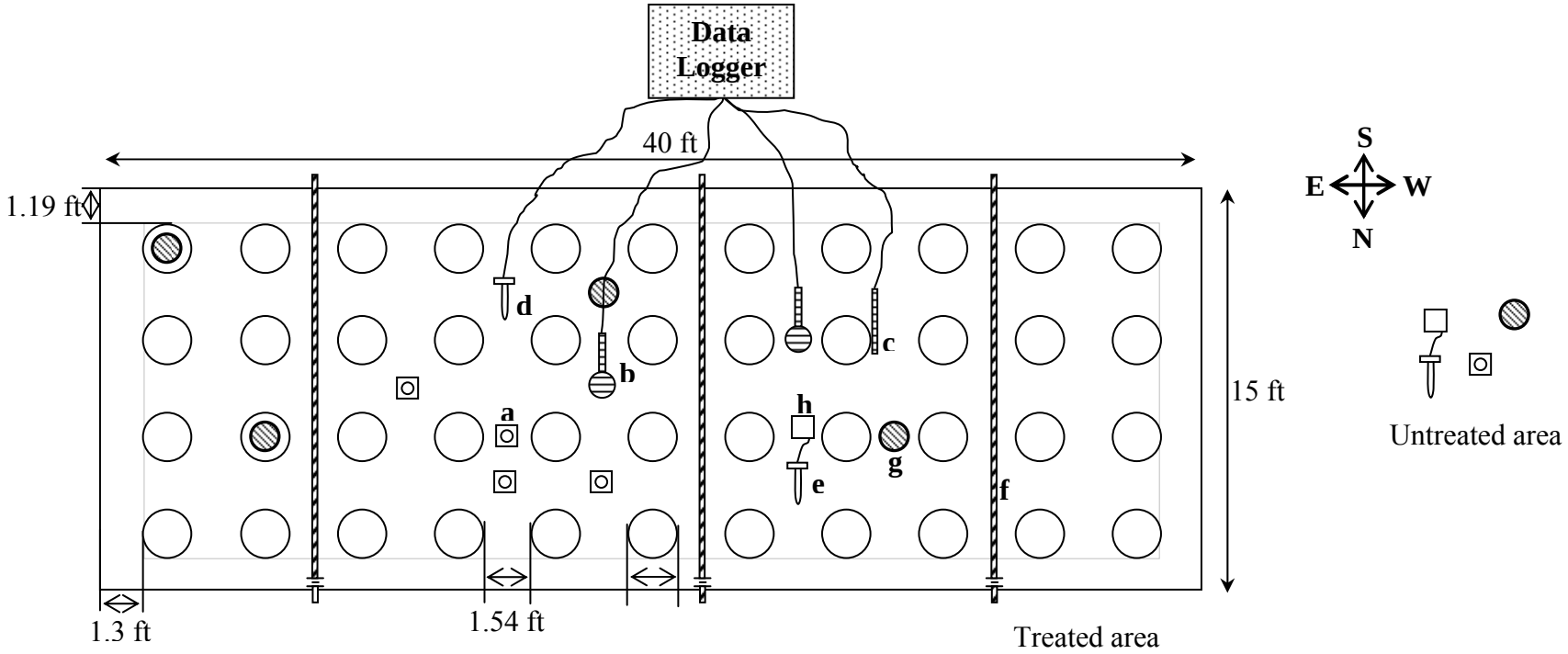

(a)

Figure 7.4a Plan view showing instrumentation at both treated and untreated areas of Site 1 (a_r = 25 %).

Total number of columns = 44 (11 × 4)

Instrumentation: a – Settlement plate; b – horizontally oriented pressure cell; c – vertically oriented pressure cell; d & e moisture; f – horizontal inclinometer; g – vertical inclinometer; and h – data logger.

Note: Drawing is not to scale.

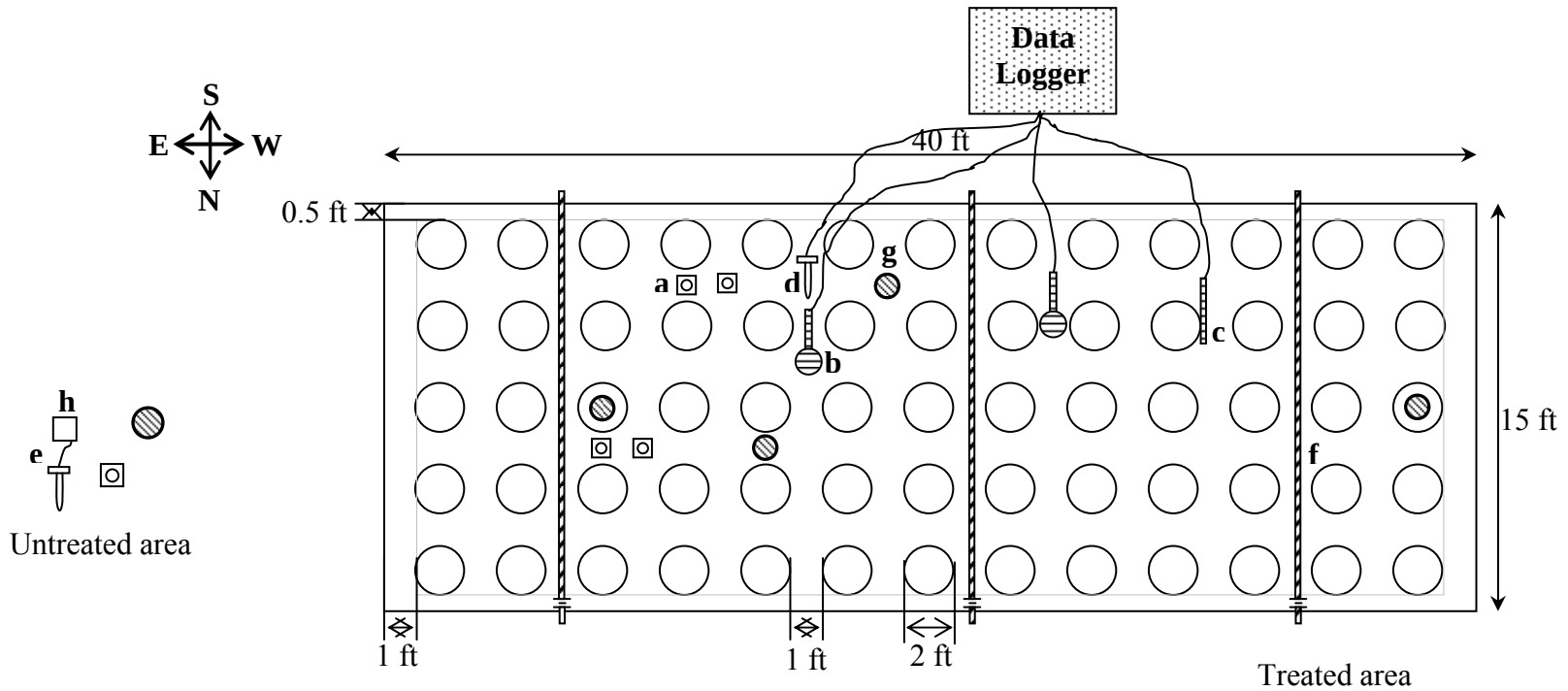

(b)

Figure 7.4b Plan view showing instrumentation at both treated and untreated areas of Site 2 (a_r = 35 %).

Total number of columns = 65 (13 × 5)

Instrumentation: a – Settlement plate; b – horizontally oriented pressure cell; c – vertically oriented pressure cell; d & e – moisture; f – horizontal inclinometer; g – vertical inclinometer; and h – Gro-Point data logger.

Note: Drawing is not to scale.

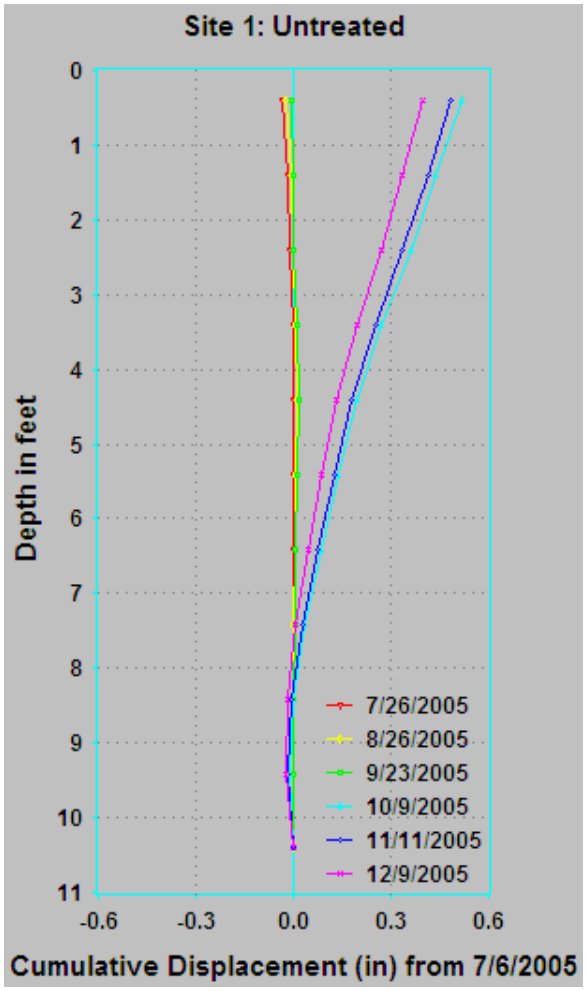

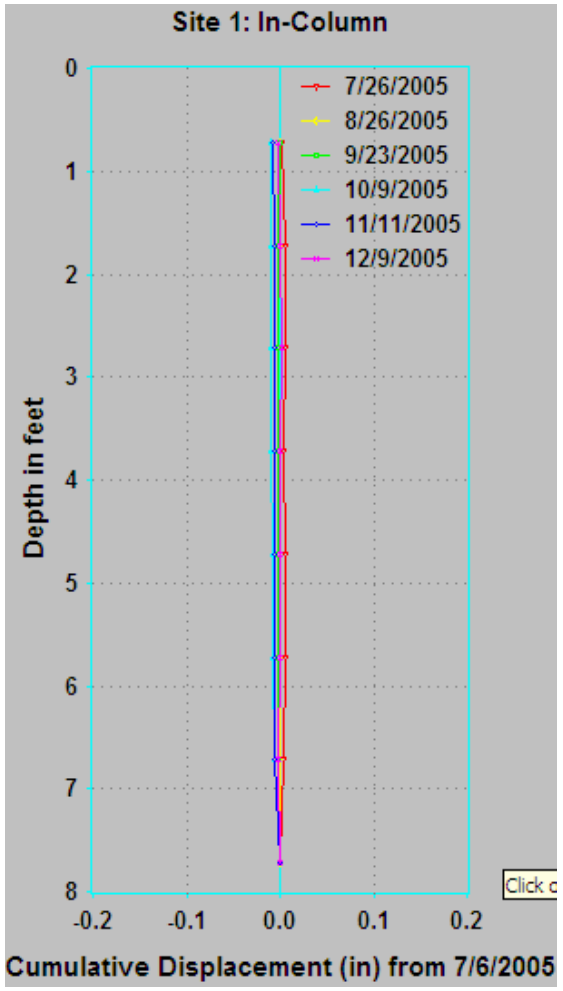

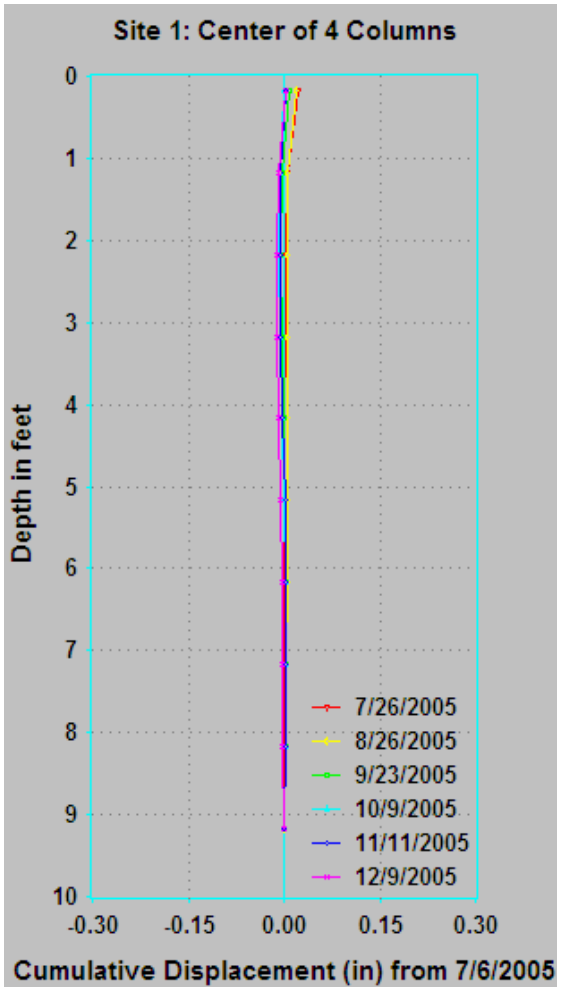

Figure 7.5a Lateral deformations at Site 1 during Fall 2005; (a) untreated, (b) in-column and (c) center of 4 columns.

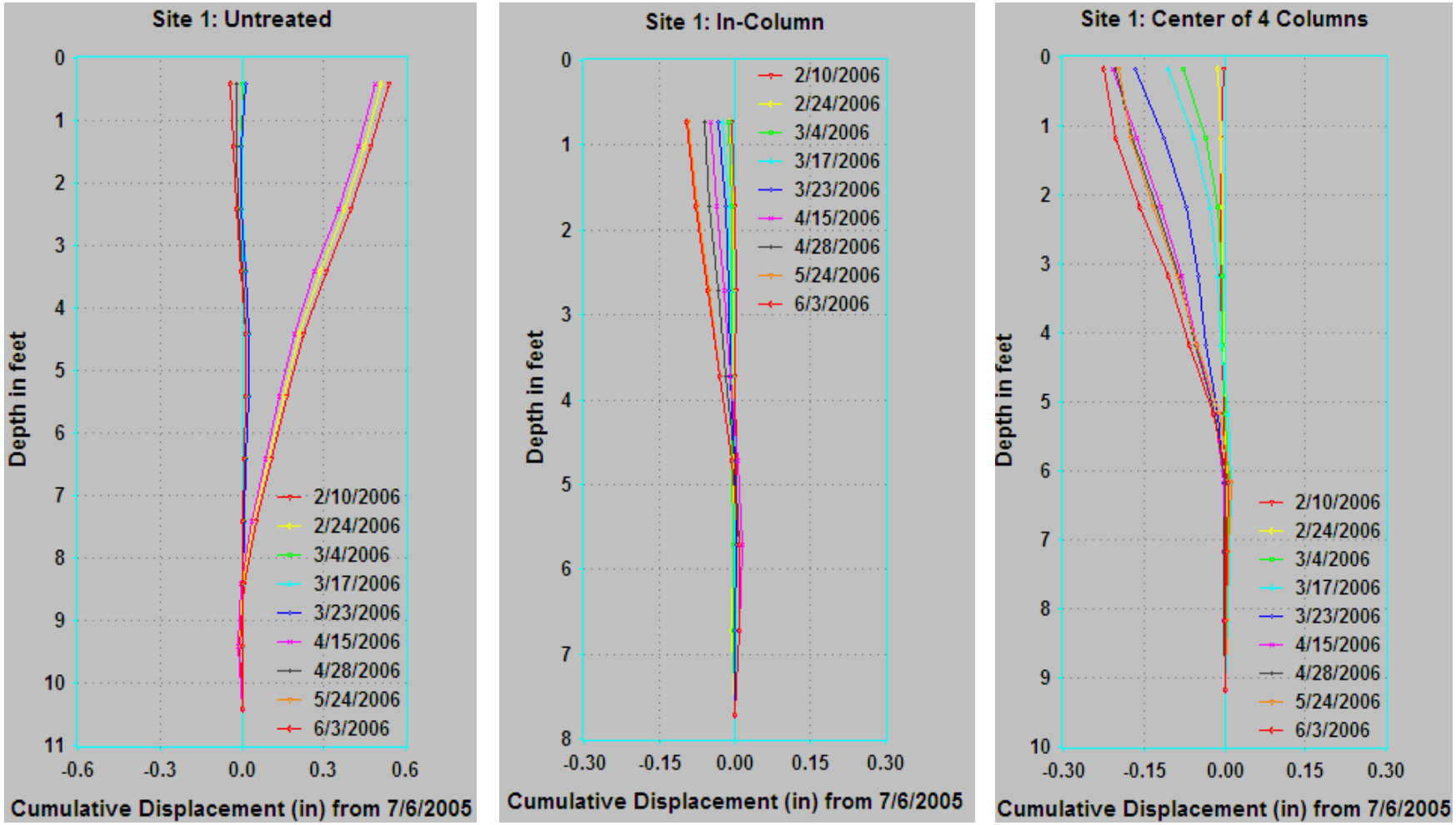

Figure 7.5b Lateral deformations at Site 1 during Spring 2006; (a) untreated, (b) in-column and (c) center of 4 columns.

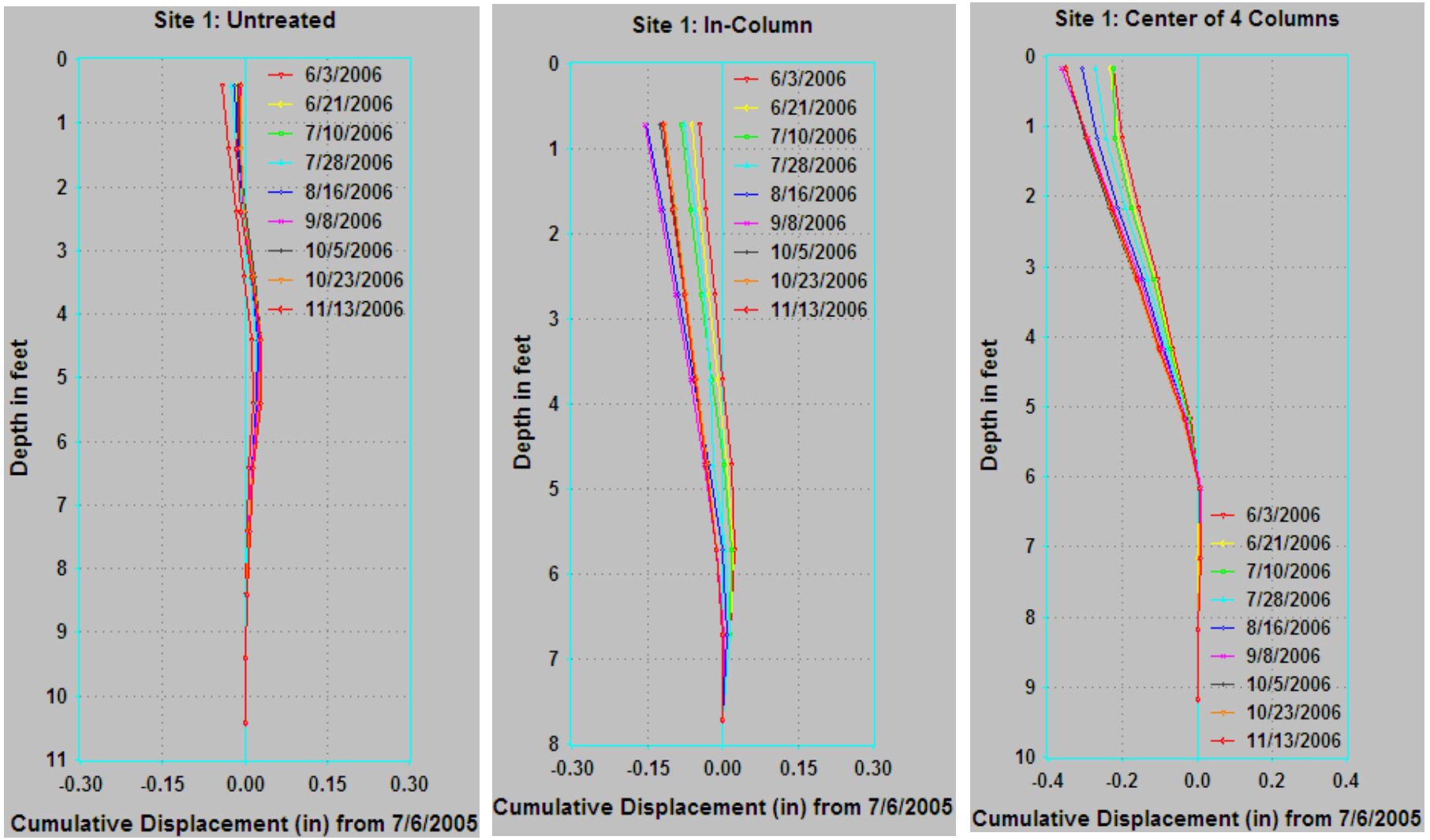

Figure 7.5c Lateral deformations at Site 1 during Fall 2006; (a) untreated, (b) in-column and (c) center of 4 columns.

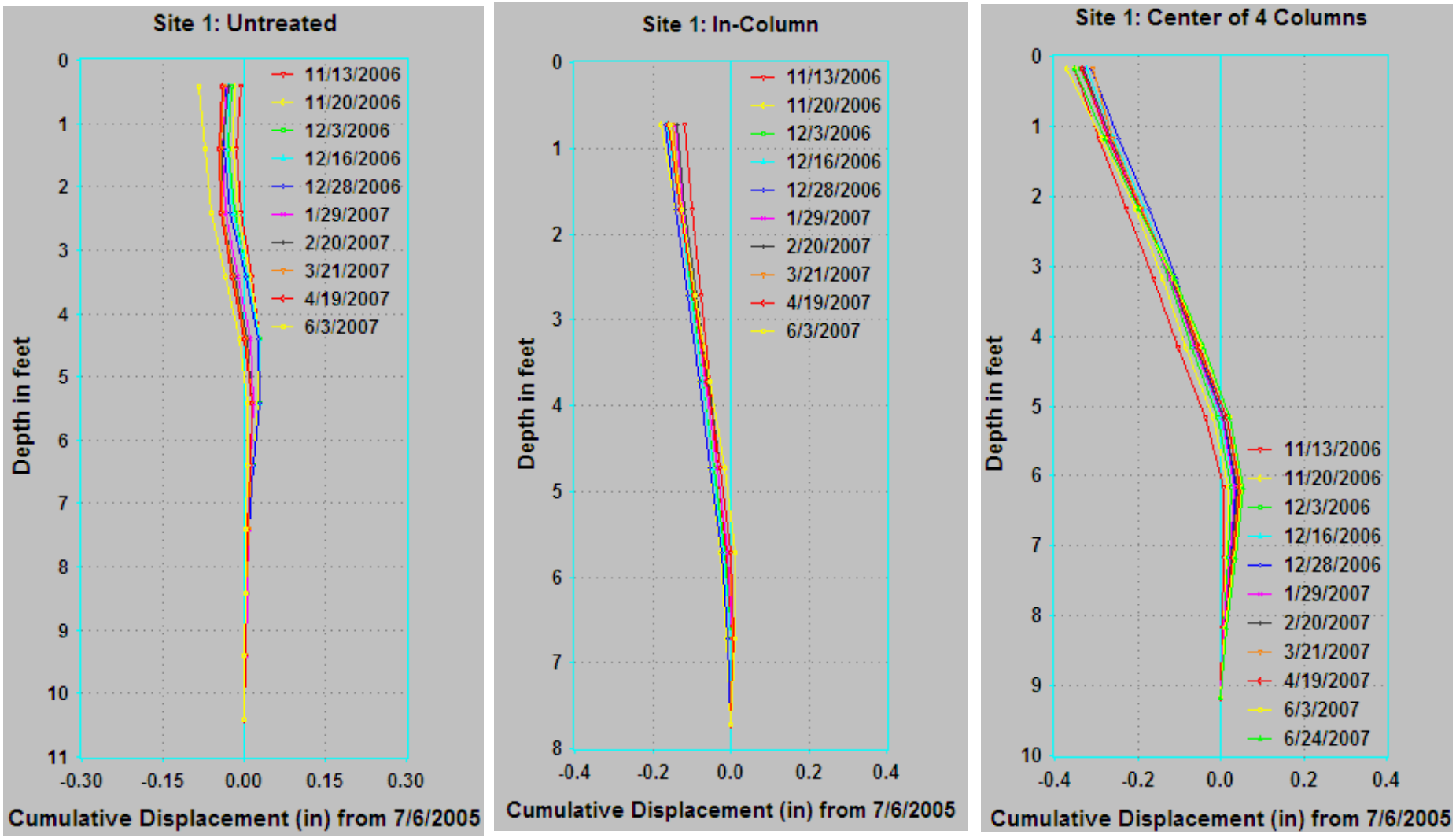

Figure 7.5d Lateral deformations at Site 1 during Spring 2007; (a) untreated, (b) in-column and (c) center of 4 columns.

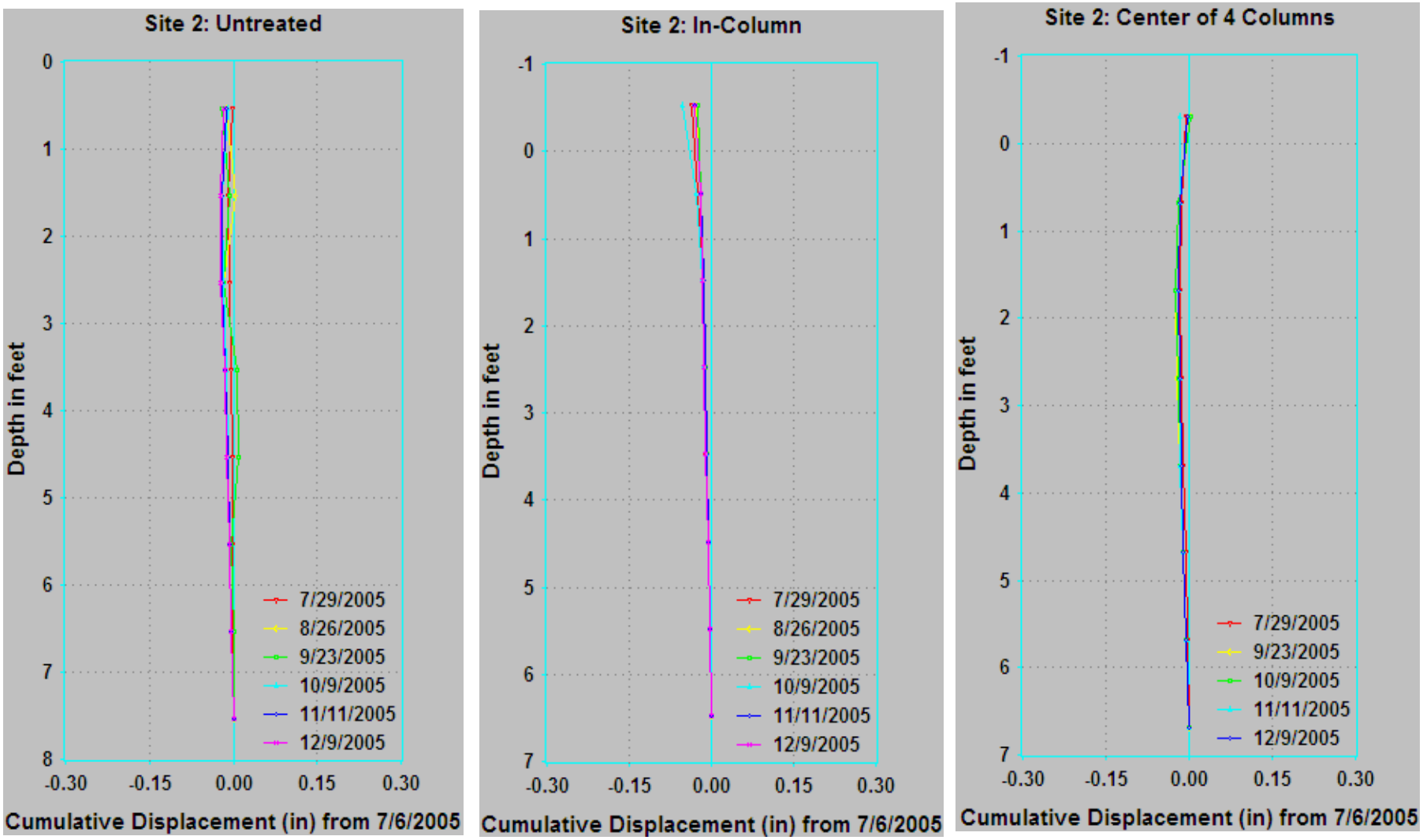

Figure 7.6a Lateral deformations at Site 2 during Fall 2005; (a) untreated, (b) in-column and (c) center of 4 columns.

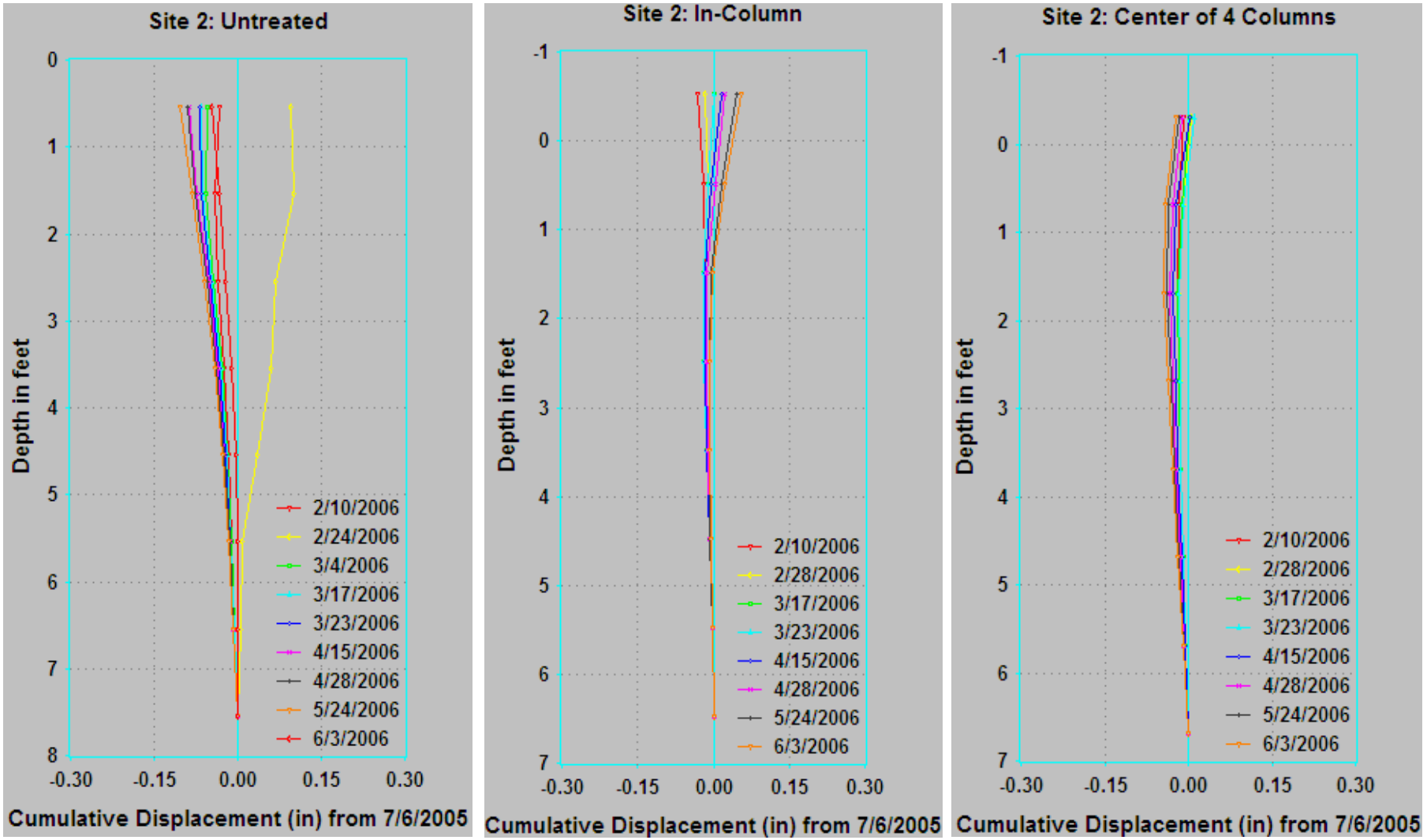

Figure 7.6b Lateral deformations at Site 2 during Spring 2006; (a) untreated, (b) in-column and (c) center of 4 columns.

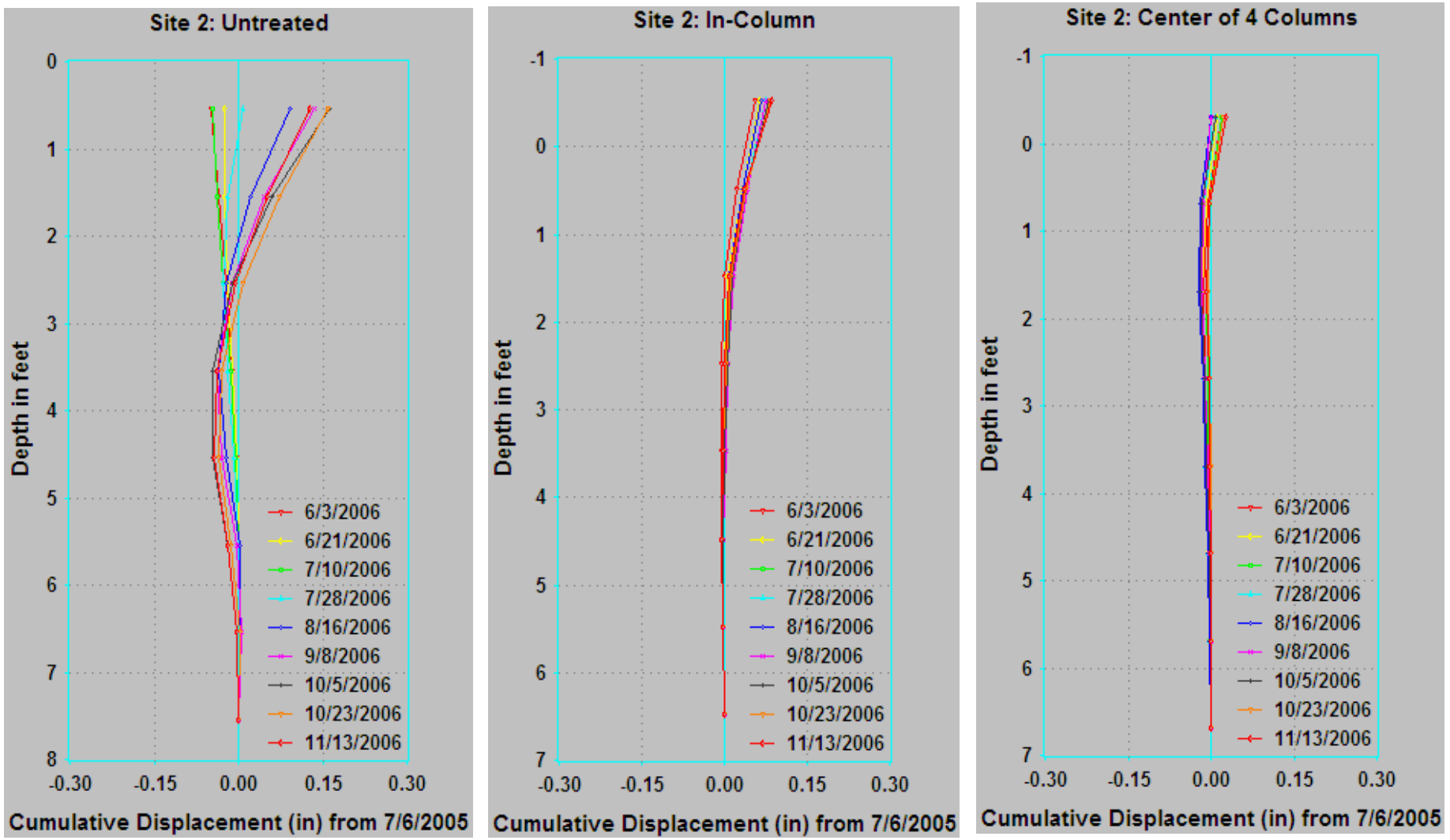

Figure 7.6c Lateral deformations at Site 2 during Fall 2006; (a) untreated, (b) in-column and (c) center of 4 columns.

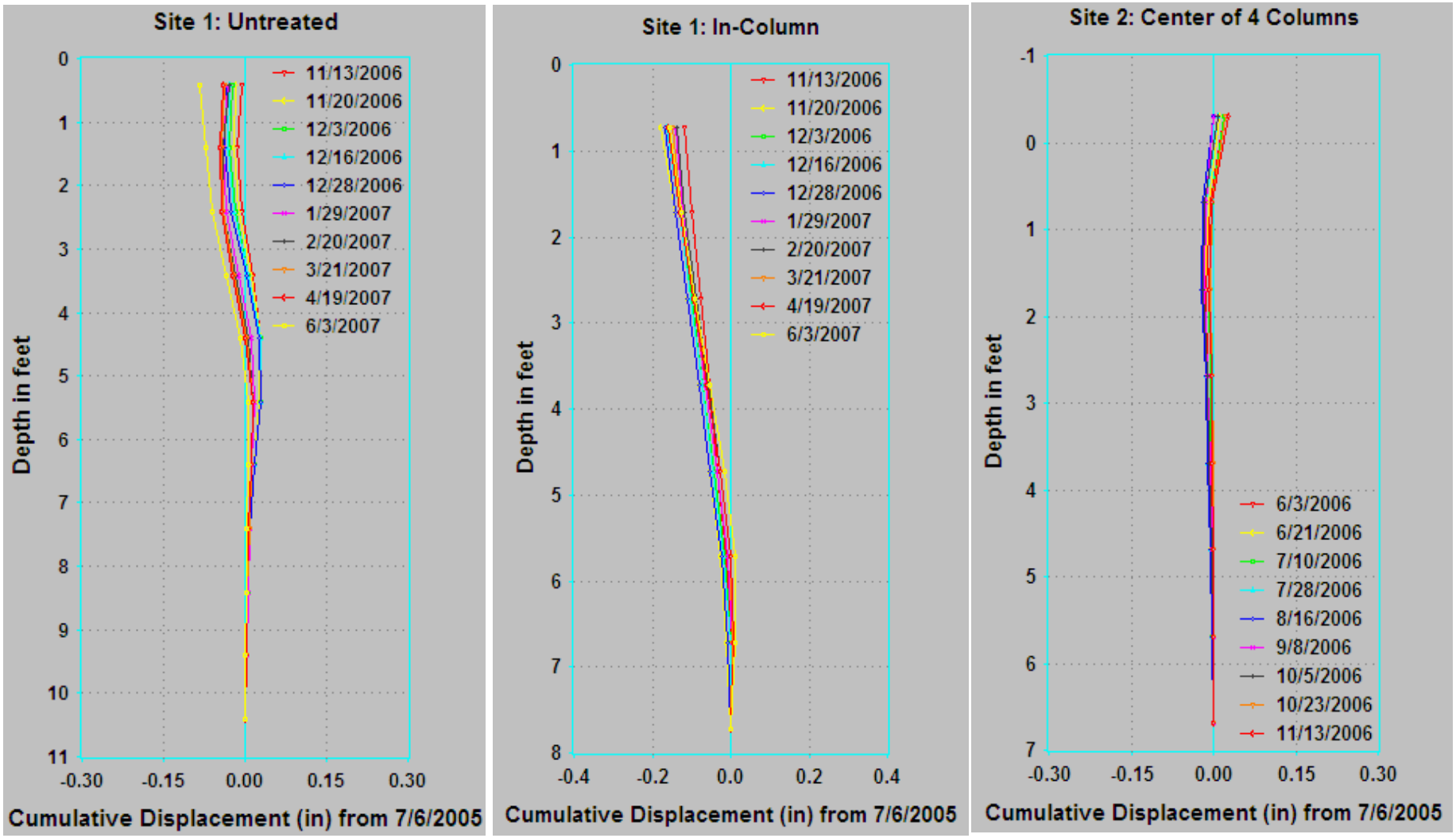

Figure 7.6d Lateral deformations at Site 2 during Spring 2007; (a) untreated, (b) in-column and (c) center of 4 columns.

Table 7.4 Lateral soil movements recorded within treated and untreated areas from inclinometer surveying.

Phases		Site 1			Site 2		
		Untrt.	In-col.	b/w col.	Untrt.	In-col	b/w col.
Phase I	Fall 2005	0.5 N	-	-	-	0.02 N	-
	Spring 2006	0.55 N	0.1 S	0.16 S	0.12 S to 0.12 N	0.03 S to 0.04 N	0.02 S
Phase II	Fall 2006	0.05 S	0.15S	0.35S	0.03 S to 0.15 N	0.07 N	-
	Spring 2006	0.12 S	0.2 S	0.38 S	0.14 N	0.075 N	0.04 S
Overall absolute soil movements		0.67	0.2	0.38	0.37	0.11	0.04

Note: N – North side; S – South side; b/w – between; Untrt – Untreated; In-Col – Inside Column

7.2.2.2 Vertical Soil Movements

Horizontal inclinometer (HI) casings of 3.34 in. (8.5 cm) dia. were installed at the surface of each of the treated sections at Sites 1 and 2. A total of three casings per site were placed along the width and between the column rows, as shown in Fig. 7.4; two of them are installed on the east and west ends and one at the center of the treated section. The details of the horizontal inclinometer probe and casing installation procedures were discussed and presented in an earlier chapter. Settlement plates (SPs) were also installed in the present study between the DSM columns in the treated and untreated areas (Fig. 7.4) to monitor vertical surface movements (from swell/shrink conditions). Each site had five SPs, four in the treated and one in the untreated area. The locations of four SPs in the treated section can be found in Fig. 7.4.

In this study, the horizontal casings were open on either side and were surveyed regularly every two to three weeks to observe the behavior of the treated sections with the environmental

changes. A standard survey of the horizontal casing included two passes of the probe through the casing with the help of the pull-cable, as shown in Fig. 7.7. In the first pass, the labeled end of the probe was connected to the control cable (Fig. 7.7[a]) and for the second pass the labeled end of the probe was connected to the pull-cable (Fig. 7.7[b]). For more information on operation details, readers are directed to the *Horizontal Digitilt Inclinometer Probe* (2004) manual. As mentioned in the previous section, the data during the survey were collected and stored using a DataMate and transferred later to a PC. The downloaded data were processed and analyzed using the DigiPro software and the results obtained are plotted, as shown in Figs. 7.8 and 7.9.

The settlement plates (SP) were also surveyed along with the inclinometer casings and the elevations of each SP at both sites were measured using a Total Station (TS) survey instrument. Typical surveying data collected from the survey at Site 2 are presented in Table 7.5. The vertical movements of the SPs were calculated by subtracting the current elevation of each SP from its initial elevation reading, which was established at the beginning of the monitoring process; i.e., immediately after the fill placement. For example, the elevation of the SP in untreated area on Aug 16, 2006, would be equal to 0.91-0.93 or -0.02 ft. This implies that the untreated surface at that location/point has undergone shrinkage by an amount of 0.04 feet. The elevation readings represent the position of the SPs with respect to a benchmark that was set up at each site at the beginning of the field construction. The results obtained from both the horizontal inclinometer surveying and the TS surveying of the SPs are analyzed here to address shrink/swell behavior of the composite treated sections and untreated sections.

Table 7.5 Typical surveying data for Fall 2006 from Test Site 2.

Date	Elevation of SPs with respect to initial reading (ft)		
	b/w 2 columns	b/w 4 columns	untreated
7/26/2005[1]	0.67[1]	0.71[1]	0.91[1]
8/16/2006	0.62	0.66	0.93
9/11/2006	0.63	0.67	0.95
10/2/2006	0.6	0.66	0.95
10/26/2006	0.64	0.68	0.97

Note: [1] Initial reading

Typical results from the horizontal inclinometers (HI) installed at Sites 1 and 2 are presented in Figs. 7.8a to c and 7.9a to c, respectively; swelling is indicated by positive displacement values and shrinking by negative displacement values. Similarly, potential surface movements with time from the SP surveying results were estimated and presented in Figs. 7.10(a) and (b).

Maximum relative swell/shrink movements of the treated and untreated sections were estimated from the HI and TS surveying data presented in the above figures for both Sites 1 and 2 during each season of Phases I and II and tabulated in Table 7.6. The results presented in Table 7.6 represent the relative shrink/swell movements of the horizontal inclinometer casings and SPs with respect to their previous position. The estimations from the HI data show that the swell/shrink movements during each season of Phases I and II are less than an inch, even when the sites were saturated during Phase II (i.e., moisture levels of Sites 1 and 2 were increased to levels corresponding to those during high precipitation).

The ranges of surface movements recorded from the HI surveying in the treated section of Site 1 for Phases I and II are 0.07 to 0.74 in. (0.17 to 1.87 cm) and 0.12 to 0.63 in. (0.3 to

1.6 cm), respectively, and of Site 2 for Phases I and II are 0.06 to 0.12 in. (0.15 to 0.3 cm) and 0.01 to 0.25 in. (0.025 to 0.63 cm), respectively. As expected, the surface movements in the treated section at Site 1 are more compared to movements in the treated section at Site 2 during all seasons (Table 7.6). The difference in surface movements in the treated sections at Sites 1 and 2 was attributed to the high area ratio adopted for Site 2 (35%) when compared to Site 1 (25%). This confirms the fact that an increase in the area ratio increases the improvement effect by reducing the swell/shrink movements of the composite sections.

Results from the TS surveying show that the surface movements in the untreated section of Site 1 are in the ranges of 0.36 to 0.84 in. (0.91 to 2.1 cm) and 0.12 to 1.08 in. (0.3 to 2.74 cm), respectively, during Phases I and II of monitoring. For Site 2, the ranges are 0.12 to 0.84 in. (0.3 to 2.1 cm) and 0.36 to 0.78 in. (0.91 to 1.98 cm), respectively, during Phases I and II of monitoring. It should be noted here that movements in the untreated sections are higher when compared to the composite treated sections during all seasons of Phases I and II at Sites 1 and 2.

Overall absolute surface movement; i.e., the sum of the maximum shrinkage and swelling (shrink+swell) with respect to the initial position of the HI casing and/or elevation of the SP, of both the treated and untreated sections are also calculated and tabulated in Table 7.7. The untreated sections of Sites 1 and 2 have experienced vertical surface movements of over 1 in. (2.54 cm), whereas, the surface movements (from HI and SPs) between the DSM columns are < 1 in. Therefore, it can be expected that the movements of the treated sections when considered as whole, composite sections are less than those reported for the untreated section, as shown in Table 7.7. This again explains that the present DSM treatment has resulted in the decrease of the overall swelling and shrinking movements experienced in the untreated expansive soil sections.

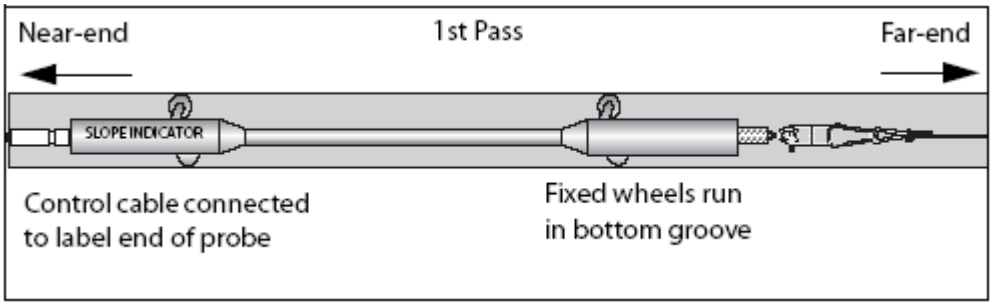

(a) 1st Pass

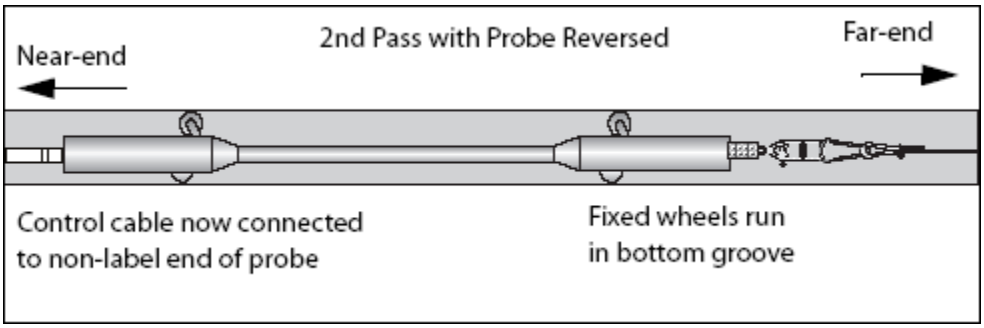

(b) 2nd Pass

Figure 7.7 Schematic showing the horizontal inclinometer survey (Slope Indicator 2004).

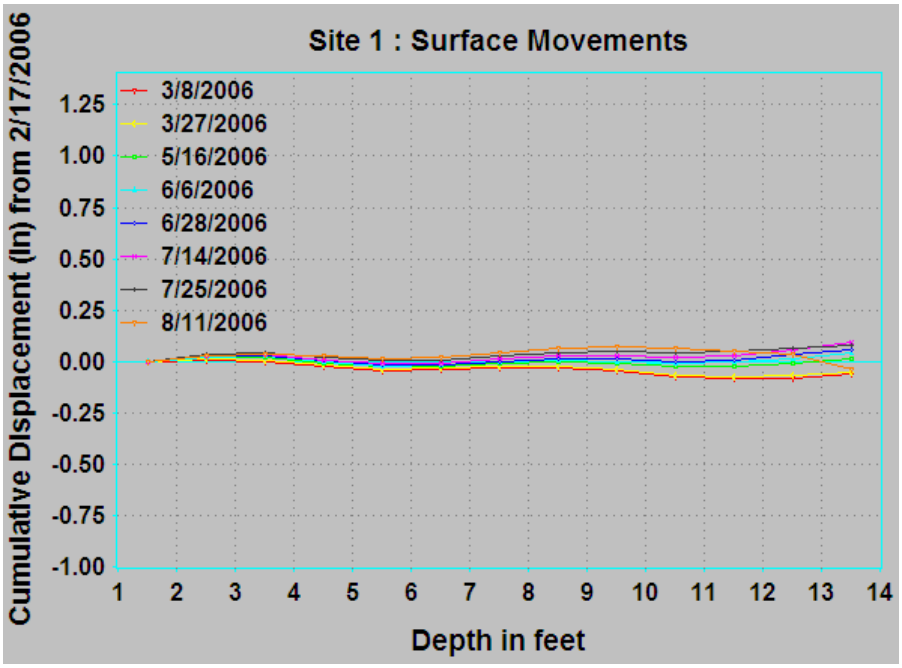

(a) Spring 2006 (Phase I)

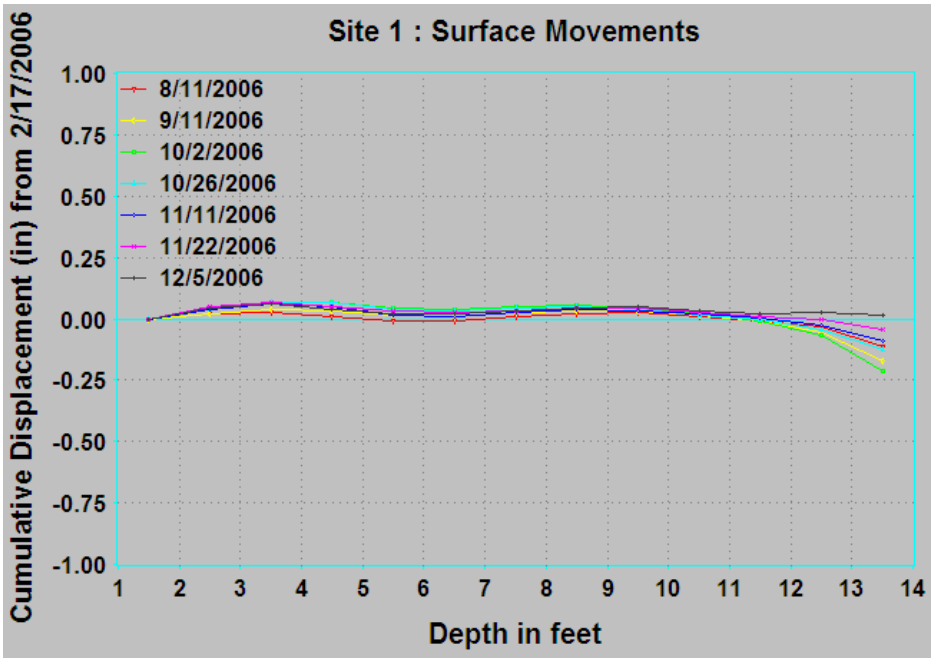

(b) Fall 2006 (Phase II)

Figure 7.8 Typical surface movements of east edge of treated section at Site 1 from horizontal inclinometer data.

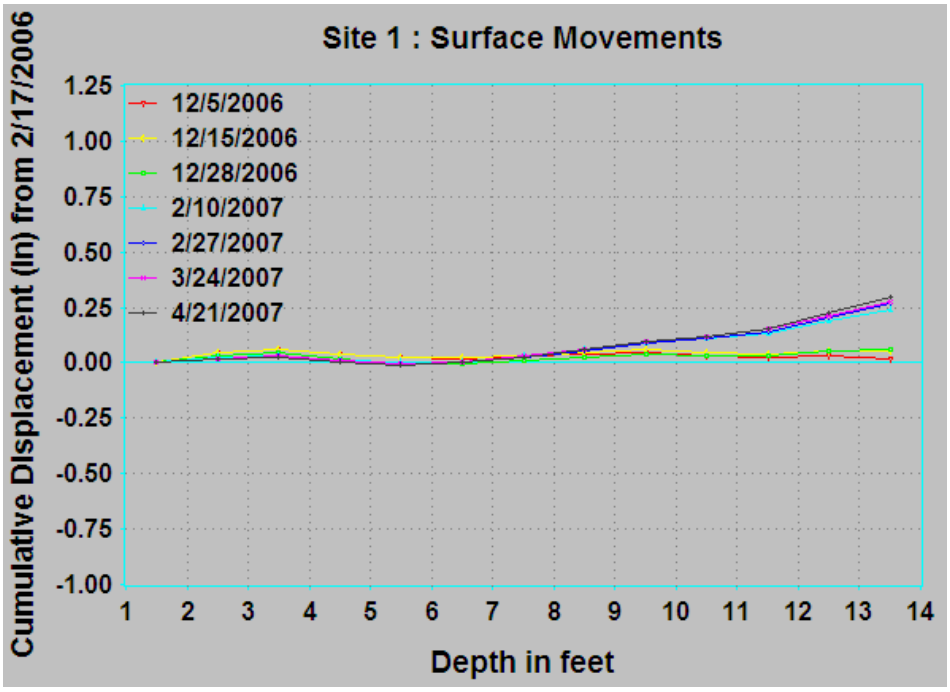

(c) Spring 2007 (Phase II)

Figure 7.8 Typical surface movements of east edge of treated section at Site 1 from horizontal inclinometer data (continued).

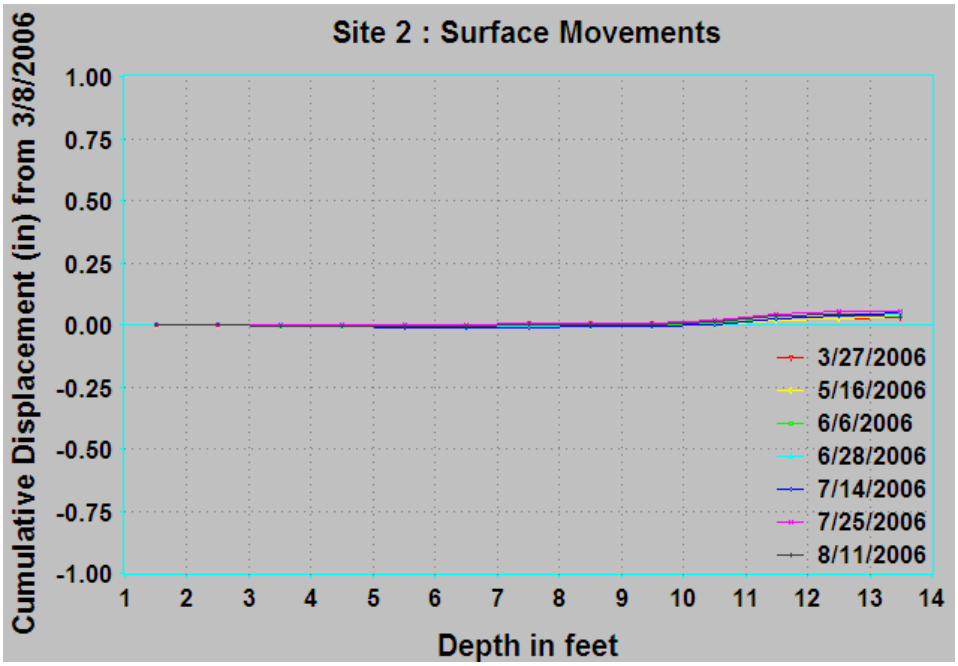

(a) Spring 2006 (Phase I)

Figure 7.9 Typical surface movements of east edge of treated section at Site 2 from horizontal inclinometer data.

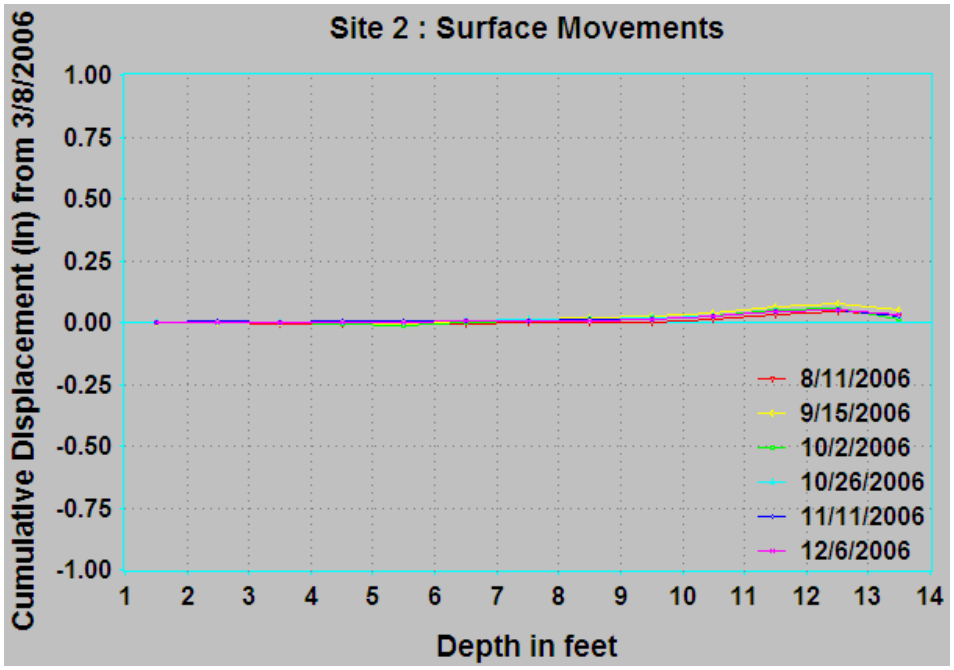

(b) Fall 2006 (Phase II)

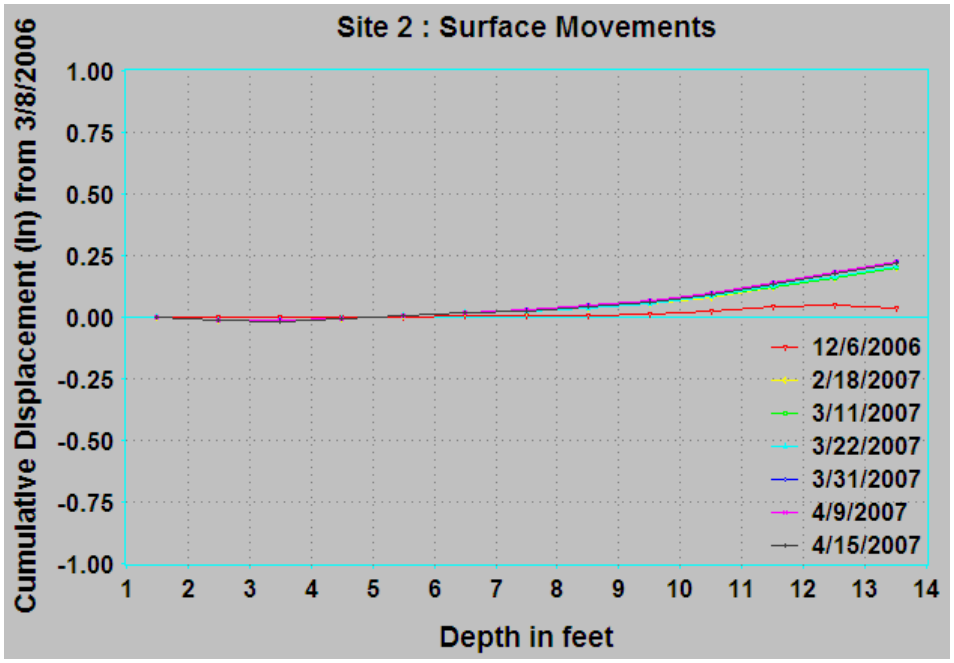

(c) Spring 2007 (Phase II)

Figure 7.9 Typical surface movements of east edge of treated section at Site 2 from horizontal inclinometer data (continued).

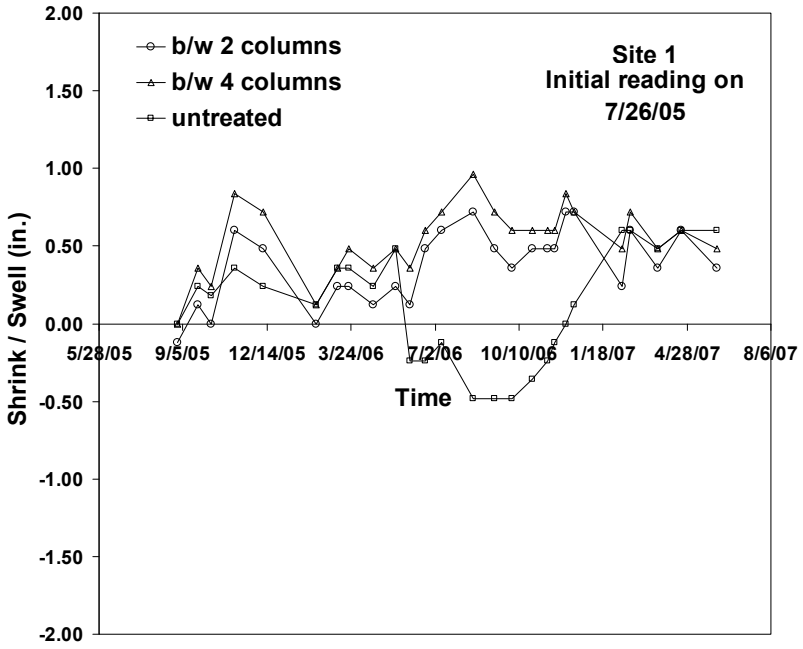

(a) Site 1

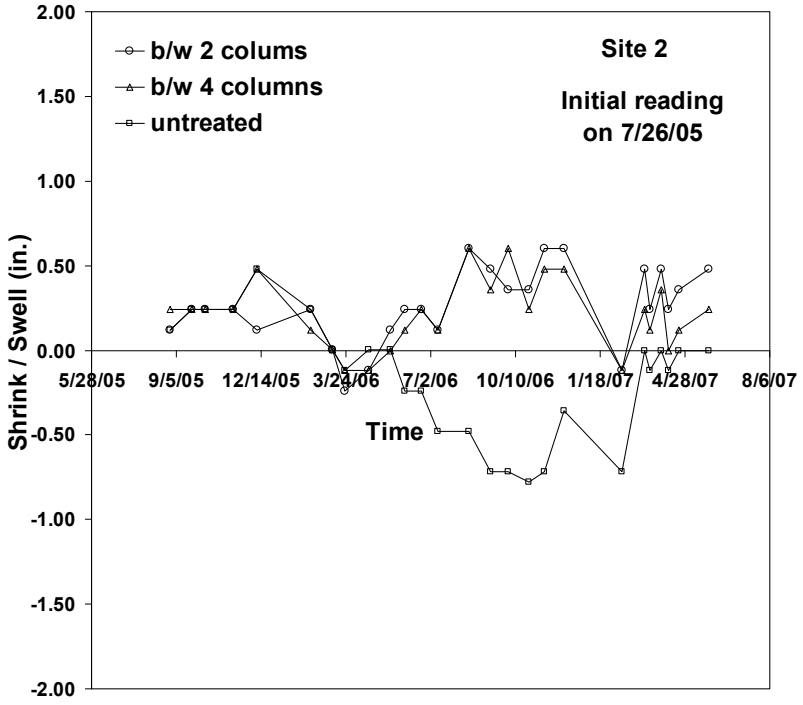

(b) Site 2

Figure 7.10 Typical results from total station surveying of settlement plates.

Table 7.6 Estimated vertical surface movements (in.) for each season / phase from HI and TS surveying data.

Season/Phase			Horizontal Inclinometer (HI) Surveying						Total Station (TS) Surveying					
			Center		East Edge		West Edge		b/w 4 columns		b/w 2 columns		untreated	
			Swell	Shrink	Swell	Shrink	Swell	Shrink	Swell	Shrink	Swell	Shrink	Swell	Shrink
SITE 1	Ph-I	F 2005	-	-	-	-	-	-	0.84	0.72	0.72	0.6	0.84	0.72
		Sp 2006	NR	0.7	0.24	0.74	0.17	0.07	0.36	0.12	0.24	0.12	0.36	0.72
	Ph-II	F 2006	0.5	0.12	0.63	0.25	0.26	0.25	0.6	0.36	0.6	0.36	1.08	0.36
		Sp 2007	0.38	NR	0.42	NR	0.26	NR	0.24	0.4	0.36	0.48	0.12	0.12
SITE 2	Ph-I	F 2005	-	-	-	-	-	-	0.48	NR	0.12	0.12	0.48	NR
		Sp 2006	0.12	NR	0.05	0.06	-	-	0.36	0.6	0.48	0.48	0.12	0.6
	Ph-II	F 2006	NR	0.02	0.01	0.04	-	-	0.48	0.36	0.48	0.72	0.42	0.78
		Sp 2007	0.15	NR	0.25	NR	-	-	0.48	0.6	0.6	0.24	0.72	0.36

Note: F – Fall; Sp – Spring; Ph – Phase and NR – not recorded

Table 7.7 Estimated absolute vertical movement during monitoring period from Fall 2006 to Spring 2007.

Site	Overall absolute movement (shrink+swell) with respect to initial elevations					
	Horizontal Inclinometer (HI) Surveying			Total Station (TS) Surveying		
	Center	East edge	West edge	b/w 4 columns	b/w 2 columns	untreated
1	0.87	0.55	1.05	0.96	0.84	1.32
2	0.25	0.25	-	0.72	0.84	1.26

7.2.3 Pressure Cell Data

A total of three vibrating wire (VW) type total pressure cells were installed for each site and the locations of the installation are depicted in Fig. 7.4. The orientation of the pressure cells was depicted in Fig. 5.32. Two pressure cells were oriented horizontally and one vertically against a DSM column. The locations of the horizontally oriented cells include the center of four columns and two DSM columns. Details about the VW type pressure cell and installation procedure are presented in an earlier chapter. After the installation of the pressure cells, the electrical cables projecting out from the cells were connected to a CR10x type data logger programmed to collect readings at an interval of one hour. Thus, pressure readings were collected continuously for every hour and stored in the data logger memory. The data stored in the memory were later transferred into the laptop computer using the LoggerNet software during regular site visits for inclinometer surveying.

The readings from the pressure cells are typically recorded in terms of frequency, as explained in section 5.5.2, in Hz. These readings are then converted into the pressure units (psi, kPa or kg/cm^2) using the following relationship developed by the manufacturers:

Pressure reading (P) = $Ax^2 + Bx + C$ (7.1)

where A, B and C are calibration factors and are different for each pressure cell and x is the recorded reading in Hz. The values of these factors are determined by the manufacturer by calibrating each pressure cell. In the present study, the calibration factors A, B and C for the pressure cells installed at Sites 1 and 2 are tabulated in Table 7.8.

Table 7.8 Calibration factors for pressure cells installed at both sites to obtain swell pressure in psi for Sites 1 and 2.

(a) Site 1

Pressure Cell	Calibration factors		
	A	B	C
Against DSM column	-2.7625×10^{-5}	-3.2014×10^{-4}	267.78
Center of 4 columns	-2.1186×10^{-5}	-1.4506×10^{-2}	239.04
Center of 2 columns	-2.3885×10^{-5}	8.9019×10^{-3}	201.35

(b) Site 2

Pressure Cell	Calibration factors		
	A	B	C
Against DSM column	-2.1076×10^{-5}	-8.0157×10^{-3}	217.57
Center of 4 columns	-2.4357×10^{-5}	1.1019×10^{-3}	521.94
Center of 2 columns	-2.0989×10^{-5}	2.5112×10^{-3}	190.91

In the present study, the recorded data were processed in a spreadsheet as per the Eq. 7.1 and the results are plotted against the time period in Julian (Calendar) days as depicted in Figs. 7.11 and 7.12 for Sites 1 and 2, respectively. The maximum vertical and lateral swell pressures experienced by the treated sections of Sites 1 and 2 due to the untreated soil around the DSM columns are estimated from the above figures and tabulated in Table 7.9. The swell

pressures experienced in Site 1 are more when compared to those at Site 2; this observation is similar to the one noticed with regard to vertical surface movements, which is explained in an earlier section. These higher values of swell pressure at Site 1 are attributed to a low area treatment ratio, a_r = 25%, and subsequent high surface movements experienced at Site 1.

The variations in swell pressures with time at Sites 1 and 2 are in accordance with the moisture changes reported in the following section and also with rainfall data presented in Table 6.6. As can be noticed, the swell pressures are more during Phase II of monitoring compared to those during Phase I for both Sites 1 and 2 due to the increased moisture contents within the treated sections from the site saturation process followed by high precipitation from March to July of Spring 2007 (Table 6.6). The ranges of maximum lateral and vertical swell pressures experienced in the treated sections are 0.3 to 3.0 psi (2.1 to 20.7 kPa) and 0.25 to 4.5 psi (1.7 to 31 kPa), respectively, for Site 1 and 0.25 to 2.1 psi (1.7 to 14.5kPa) and 0.2 to 1.4 psi (1.4 to 9.6 kPa), respectively, for Site 2. It is observed that these field pressures are very low compared to those estimated on the untreated soils in the laboratory environment (Table 7.10).

From the laboratory tests on the untreated soils from Sites 1 and 2, the expansive soils can be characterized as moderate swelling soils. After the DSM treatment, the field swell pressures around the DSM columns are reduced to 1/5 to 1/10 of the untreated swell pressures (Table 7.10). This indicates that the soil around the DSM column also improved to a certain degree due to migration of the chemical binder from the DSM and the effectiveness of the DSM treatment of expansive soils as a whole.

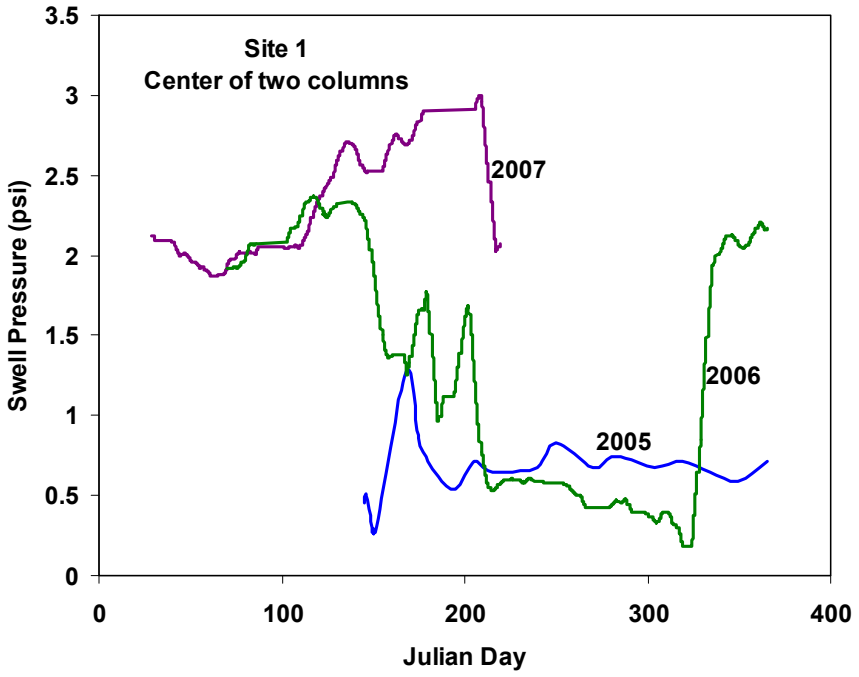

(a) Vertical swell pressures at the center of 2 DSM columns

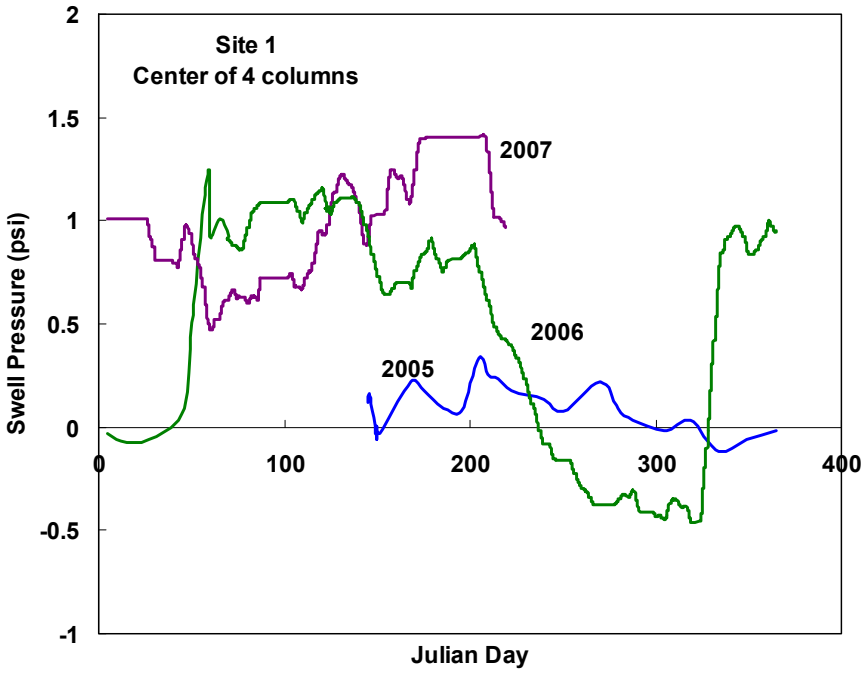

(b) Vertical swell pressures at the center of 4 DSM columns

Figure 7.11 Swell pressures obtained from VW pressure cells at Site 1.

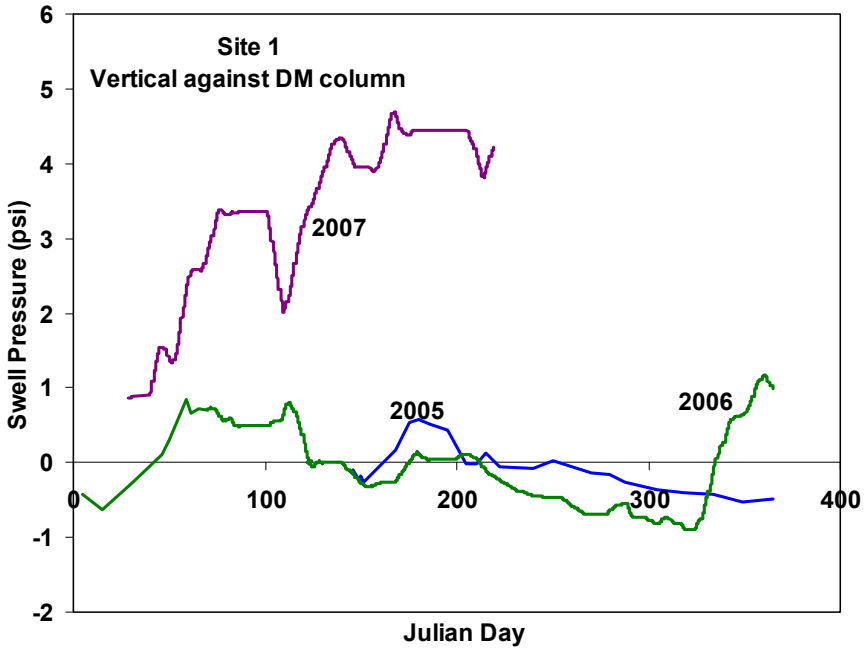

(c) Lateral swells pressure acting DSM column

Figure 7.11 Swell pressures obtained from VW pressure cells at Site 1 (continued).

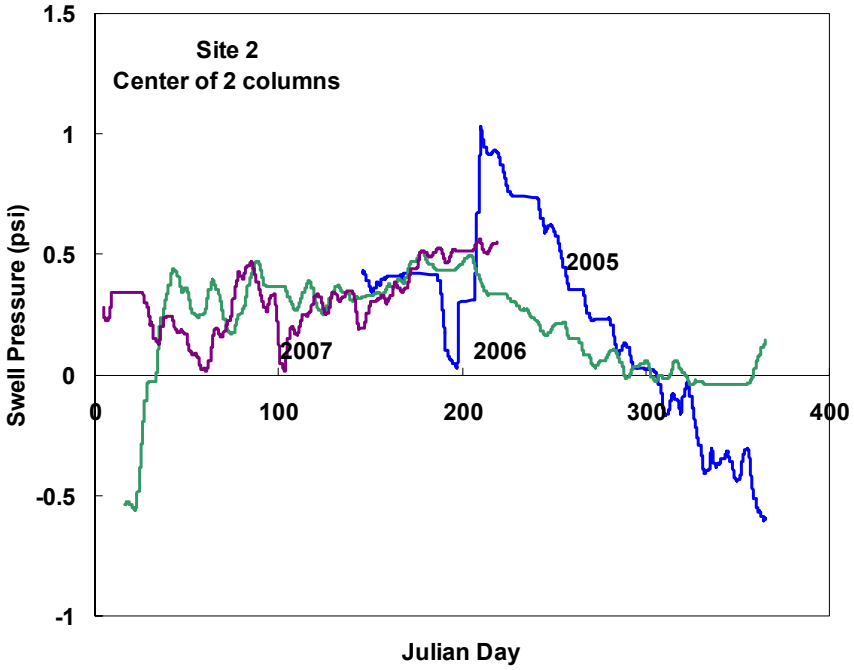

(a) Vertical swell pressures at the center of 2 DSM columns

Figure 7.12 Swell pressures obtained from VW pressure cells at Site 2.

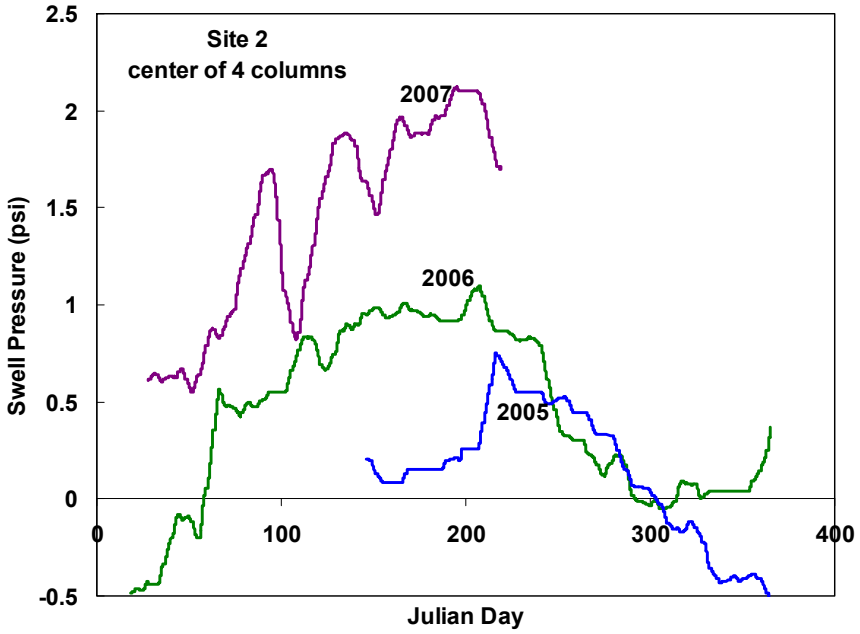

(b) Vertical swell pressures at the center of 4 DSM columns

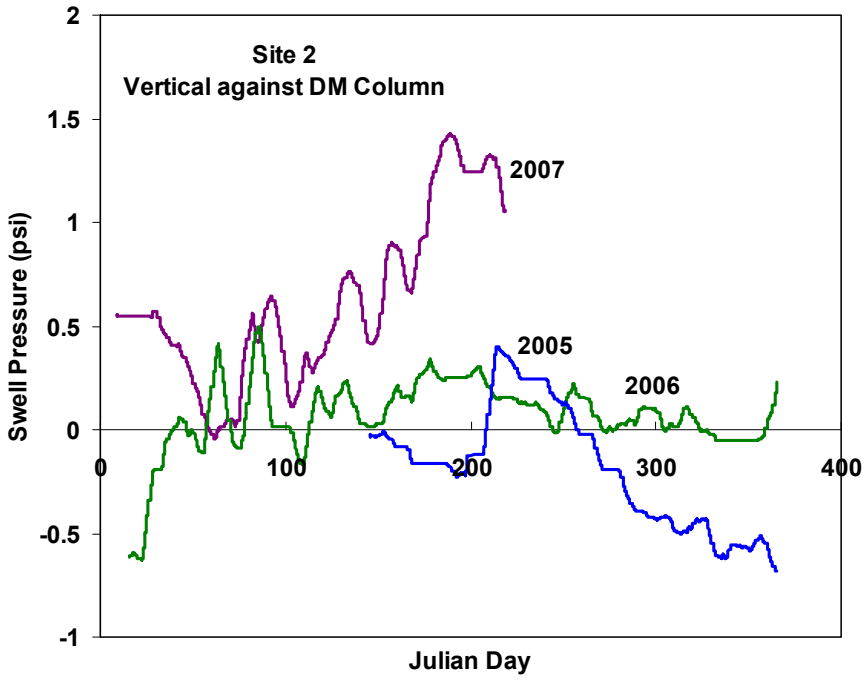

(c) Lateral swell pressures acting on DSM column

Figure 7.12 Swell pressures obtained from VW pressure cells at Site 2 (continued).

Table 7.9 Maximum swell pressures in psi recorded at Sites 1 and 2 during each phase.

Season		Site 1			Site 2		
		Lateral		Vertical	Lateral		Vertical
		b/w 2 columns	b/w 4 columns		b/w 2 columns	b/w 4 columns	
Ph-I	F 2005	1.25	0.3	0.25	1.0	0.75	0.4
	Sp 2006	2.4	1.25	0.9	0.5	1.05	0.5
Ph-II	F 2006	2.25	1.5	2.15	0.25	0.8	0.2
	Sp 2007	3.0	1.4	4.5	0.55	2.1	1.4

Table 7.10 Comparison of swell pressures estimated in laboratory and field conditions.

Site	Laboratory results		Max. pressures experienced in field from pressure cells	
	Untreated	Treated	Lateral	Vertical
1	11 to 28	< 0.1	0.3 to 3.0	0.25 to 4.5
2	16 to 28	< 0.1	0.25 to 2.1	0.2 to 1.4

7.3 Performance Evaluation Based on Non-Destructive Testing

After the initial non-destructive tests were carried out in June 2005, two series of annual tests with the downhole P-wave and the SASW methods were conducted at the two DSM sites in August 2006 and May 2007, respectively. The treated areas of the two sites, at least their top portions, were saturated during the 2007 testing. The goal of these tests was to monitor any losses in stabilization potential with time due to ground water flow and surface runoff from rainfall events in the sites and provide information for performance evaluation of the DSM systems. The tests performed and their codes are summarized in Table 7.11.

Table 7.11 Tests performed and their notation.

Test	Site 1 (Moderate PI)		Site 2 (High PI)	
	Code	Location	Code	Location
Downhole	S1-100	In a DSM column	S2-100	Untreated area
	S1-200	In a DSM column	S2-200	In a DSM column
	S1-300	Between 4 DSM columns	S2-300	Between 2 DSM columns
	S1-400	Between 2 DSM columns	S2-400	Between 4 DSM columns
	S1-500	Untreated area	S2-500	In a DSM column
SASW	Site 1a	Treated area	Site 2a	Treated area
	Site 1b	Treated area	Site 2b	Treated area
	Site 1c	Untreated area	Site 2c	Untreated area

7.3.1 Downhole Testing

For better results, the recording device used for the two series of downhole tests were a Tektronix 2630 Fourier Analyze instead of a SmartSeis S-24 seismograph system which was used in the initial tests. The impact source was located at the ground surface with a horizontal

offset of about 10 in. (25.4 cm) from the collar of each borehole. A sampling frequency of 20 kHz was adopted for all measurements, which resulted in a sampling interval of 0.02 milliseconds on each single time record. Readings were taken at a constant depth interval of 1 ft (0.3 m) in each borehole.

To analyze the downhole data obtained from each borehole, the time records or waveforms collected at different depths were assembled in an order with increasing depth to form a composite seismic record; i.e., waveforms are plotted against their respective depths. Since the reachable depths of all boreholes are less than 10 ft (3 m), certain corrections for the arrival times or travel paths, which are slant lines, are needed for the horizontal offset of the impact source from the collar of the boreholes (the amount of correction decreases as depth increases). This is an approximate way of converting the time spent traveling along the slant path to the time the signal would have taken if it had traveled at a vertical path down to the receiver.

As an example, the composite records from tests performed in August 2006 and May 2007 in Borehole S1-100, which is in a DSM column, are compared in Figure 7.13. In this figure, the first arrivals or transit times of the P-waves in each record are simply plotted as a straight line (it can be done by visual or least-square fit). The P-wave velocity is simply the slope of the line after the travel time or wave path corrections.

As another example, Figure 7.14 shows the composite records from the downhole tests performed in August 2006 and May 2007 in Borehole S1-400 which is located between two DSM columns. As shown in the figure, the average P-wave velocity of the material between the DSM columns was reduced significantly when the site was saturated (from 2780 ft/s or 834 m/s to 1060 ft/s or 318 m/s). Comprehensive results from the downhole P-wave tests performed at both of the sites in June 2005, August 2006 and May 2007 are summarized in Table 7.12 and Figure 7.15.

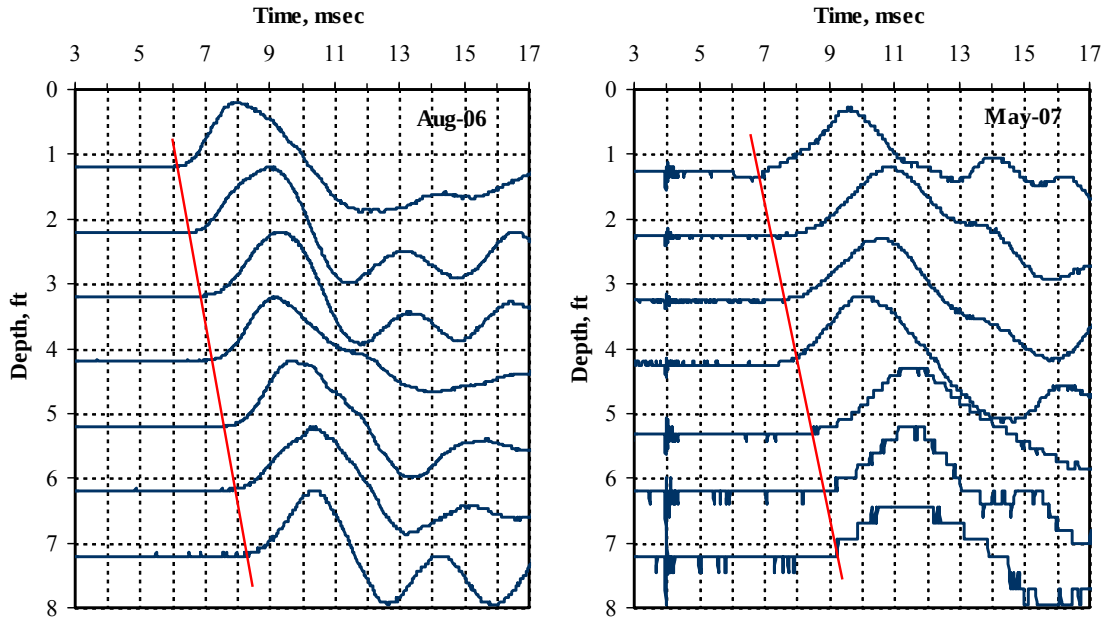

Figure 7.13 Composite seismic records from P-wave downhole tests in borehole S1-100 (in-column) in August 2006 and May 2007.

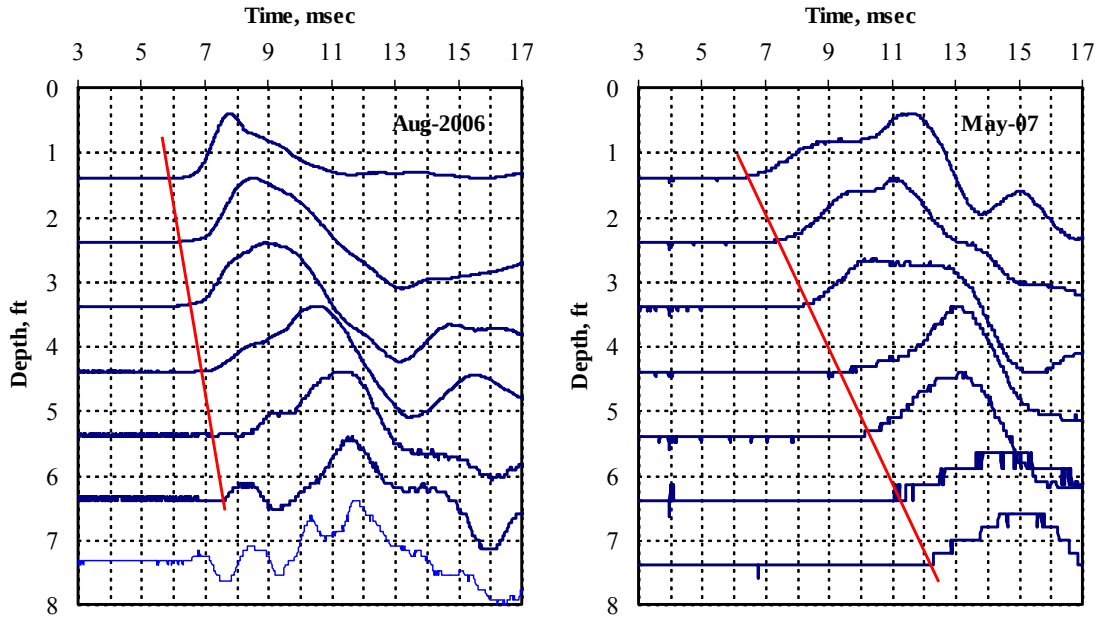

Figure 7.14 Composite seismic records from P-wave downhole tests in borehole S1-400 (center of 2 columns) in August 2006 and May 2007.

Table 7.12 Average P-wave velocities from downhole tests in different years.

Site 1				Site 2			
Borehole	P-Wave Velocity, ft/s			Borehole	P-Wave Velocity, ft/s		
	2005	2006	2007		2005	2006	2007
S1-100	3468	2817	2625	S2-100	2564	1956	1087
S1-200	3974	3089	2660	S2-200	3670	2640	2604
S1-300	3727	2363	2260	S2-300	2920	2809	2433
S1-400	4046	2781	1063	S2-400	3774	2697	2615
S1-500	NA	1634	1739	S2-500	4000	2800	2593

From Table 7.12 and Figure 7.15, it can be seen that the P-wave velocities from the downhole tests performed in years 2006 and 2007 in the DSM treated areas of both the test sections decreased considerably as compared with those from the initial tests performed in 2005. The magnitudes of the average P-wave velocities of the treated soil columns obtained from the downhole tests are about 3470 ft/s, 2820 ft/s and about 2630 ft/s in 2005, 2006 and 2007, respectively. Though the overall decrease is considerable, they are still higher than the untreated soil. However, the differences in the P-wave velocity between the two series of tests performed in 2006 and 2007 are quite small except for Borehole S1-400 (center of two DSM columns).

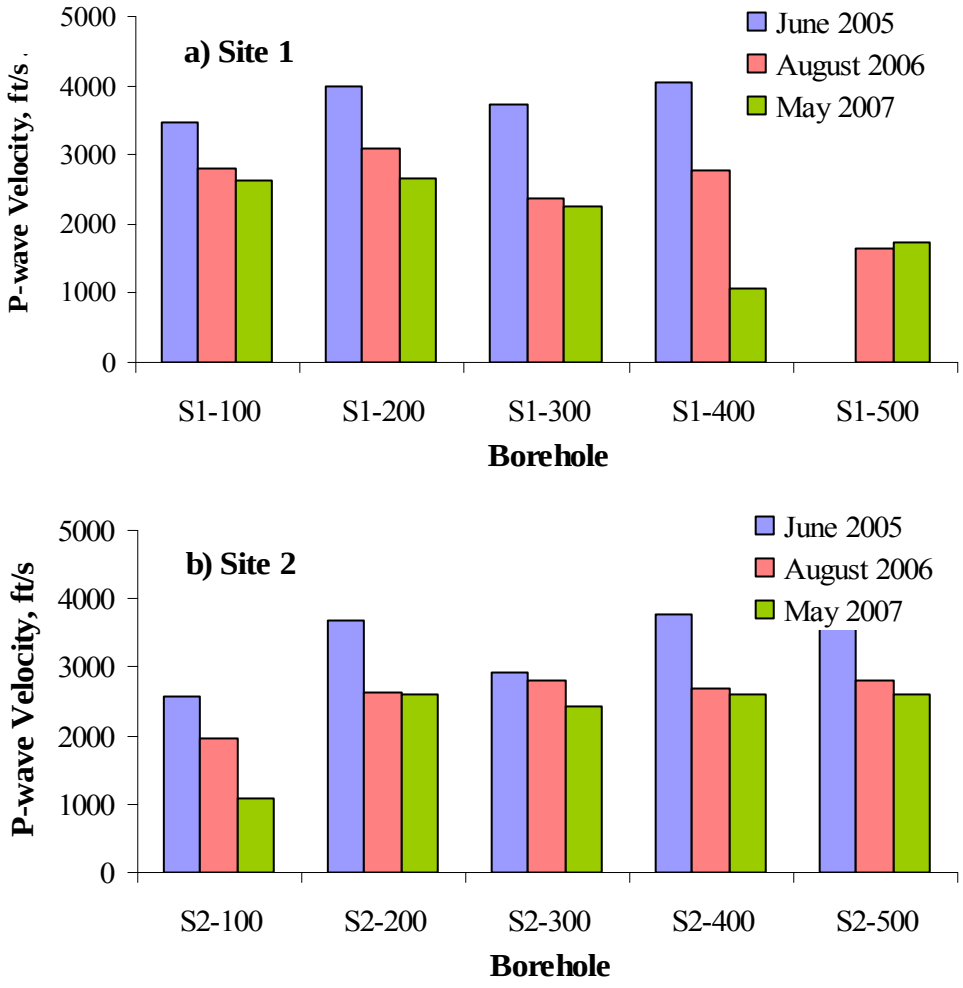

Figure 7.15 Composite seismic records from P-wave downhole tests in borehole S1-400 in 2005, 2006 and 2007.

Possible reasons for these decreases in P-wave velocities from year 2005 to subsequent tests in years 2006 and 2007 could be as follows:

- Noises from adjacent continuous trafficking,
- Unmatched impedance between the ground surface and the impact source system which may affect the dominant frequencies and energy transfer,
- Bad coupling between the PVC case and the surrounding soil,

- Refraction along the wall of the PVC case (P-wave velocity traveling in the PVC can be much faster than that in the soil), and
- Moisture variation at the time of these tests performed in each year. In particular tests in 2007 were done when the site was close to the saturation conditions.

7.3.2 SASW Testing

The equipment and field procedures used in these two series of tests were the same as those used in the initial tests except that the receiver spacing of 32 ft (9.6 m) was removed due to the traffic noise. With a largest spacing of 16 ft, the soil profiles down to a depth of about 12 ft (3.6 m) can be sampled. Another difference was the model used in data analysis: a six-layer model with fixed thickness for each layer was adopted for all SASW data sets. Representative dispersion curves (Site 1b and Site 2b) obtained from 2005, 2006 and 2007 tests in the treated areas of the two DSM sites are shown in Figure 7.16.

The dispersion curves obtained from 2006 and 2007 year tests are quite similar expect for the wavelengths less than 10 ft (3 m). They are considerably different from those obtained from the 2005 tests for both of the sites. Dispersion curves (Site 1c and Site 2c) obtained from the 2005, 2006 and 2007 year tests in the untreated areas of Sites 1 and 2 are shown in Figure 7.17.

For Site 1, the dispersion curves obtained from the 2006 and 2007 tests are very close to each other. The reason for the considerable difference between the results in years 2006 and 2007 and those obtained in 2005 at Site 1 is unknown. Though the exact reasons for this difference in results are difficult to point out, the difference was attributed to different testing locations in the untreated area in those years. The dispersion curves obtained from the three annual tests in the untreated area at Site 2 are very similar.

Shear wave velocity profiles derived from the dispersion curves are shown in Figs. 7.16 and 7.17 and are compared in Figs. 7.18 and 7.19, respectively. Shear wave velocities of the treated

sections derived from the SASW tests showed a decrease over the time period. The decrease in 2007 is expected since the measurements are made on the treated ground that was subjected to high saturation. The decrease in the shear wave velocities in year 2006 from those determined in year 2005 may be attributed to the selection of the testing location. The DSM treatment of the test sections in the present study is of an isolated column type; therefore location of the testing may be over the row of columns or between the column rows and it is difficult to find the column row after fill placement on the treated surface.

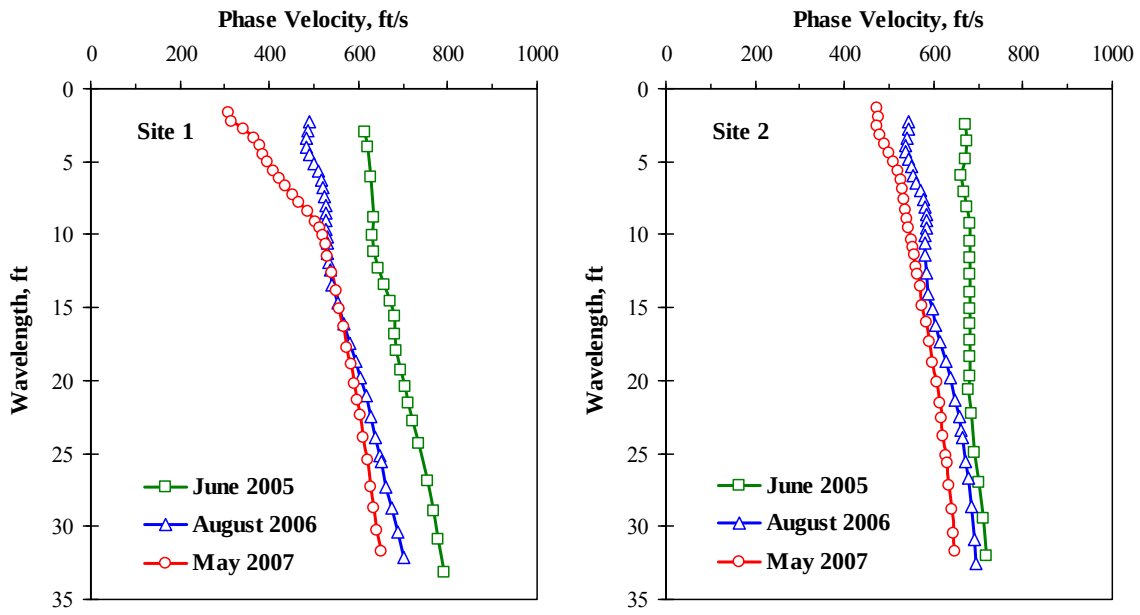

Figure 7.16 Comparison of representative dispersion curves obtained from 2005, 2006 and 2007 tests in treated areas.

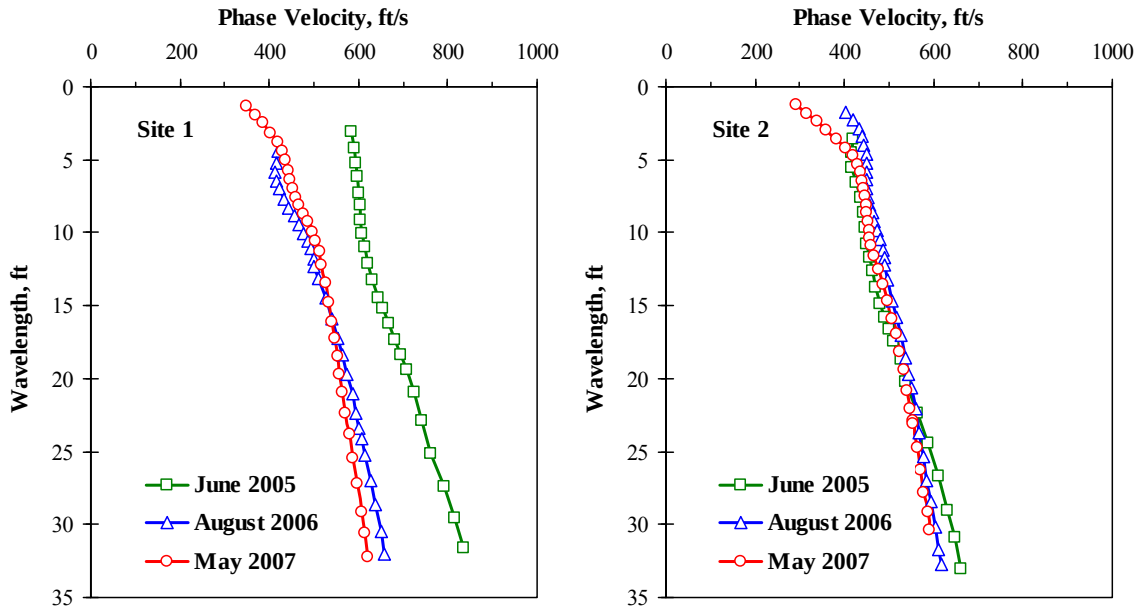

Figure 7.17 Comparison of representative dispersion curves obtained from 2005, 2006 and 2007 tests in untreated areas.

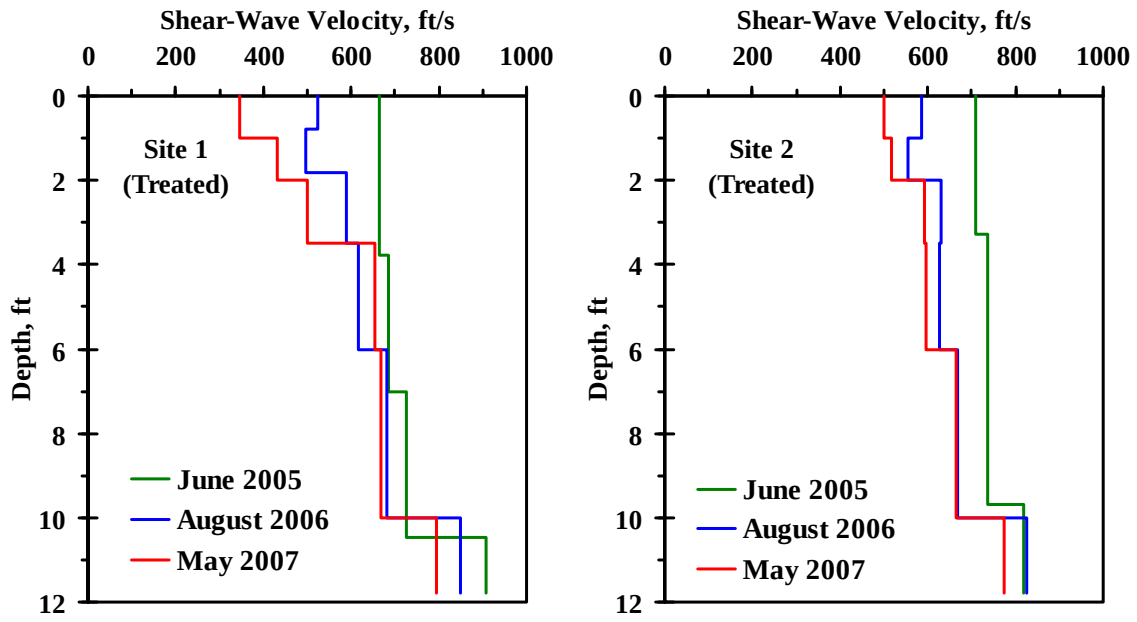

Figure 7.18 Comparison of shear-wave velocity profiles obtained from dispersion curves (treated sites).

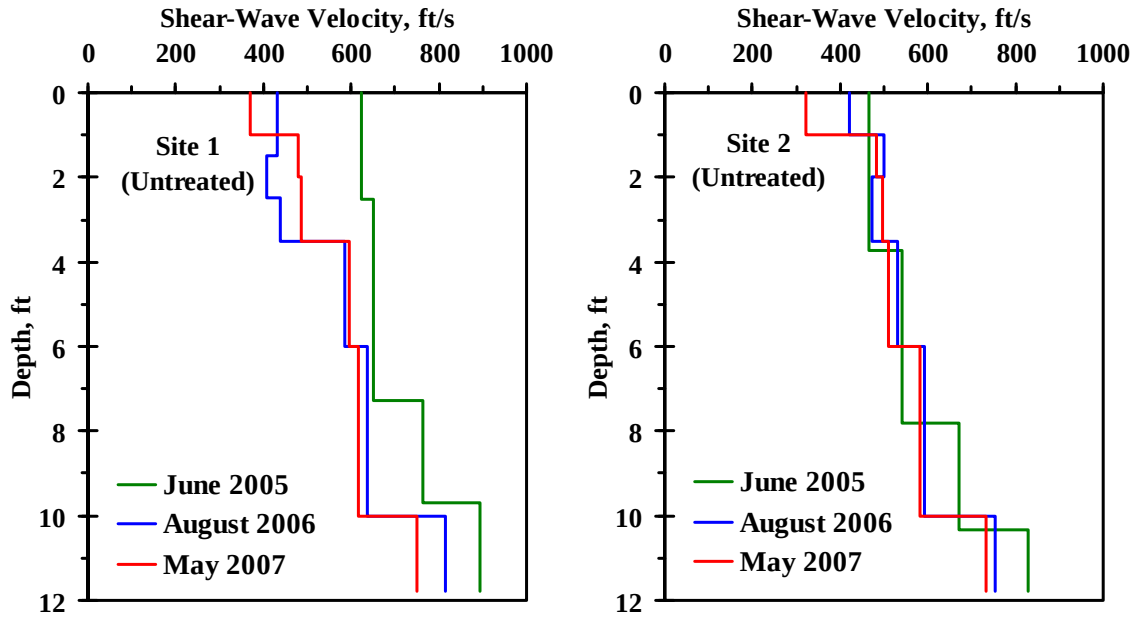

Figure 7.19 Comparison of shear-wave velocity profiles obtained from the dispersion curves (untreated sites).

7.4 Comparison of Field Data with Analytical and Numerical Simulation Studies

Vertical surface movements obtained from the horizontal inclinometers and settlement plates in the treated and untreated sections, respectively, are compared with estimations based on analytical formulations developed in Chapter 5. The governing Equations (5.1) and (5.5) for estimating heave of the untreated and treated sections are reproduced below in Eqs (7.1) and (7.2). For details of formulation and parameter definitions, it is recommended to refer to Chapter 5.

$$\Delta h = \sum_{i=1}^{n} \frac{C_{s,i} h_i}{1 + e_{o,i}} log \frac{p'_{f,i}}{p'_{s,i}} \tag{7.1}$$

$$\Delta h = \frac{C_{s,comp} h}{1 + e_o} \sum_{i=1}^{n} log \frac{p'_f}{p'_{s,comp}} \tag{7.2}$$

Fig. 7.20 depicts the comparison of the absolute vertical movements noticed in the treated and untreated sections with analytical estimations following the above equations. It can be noticed that the field observations are in good agreement with the analytical data for a suction range of 7 to 15 psi. The variations and distribution of field data that can be noticed in Fig. 7.20, is attributed to the variations in the soil properties between the locations at which the field observations were obtained. Based on the above observations, it can be concluded that the analytical model developed here appropriately predicts the amount of heave of the treated sections.

Numerical simulations of the DSM treated sections were also performed to understand the DSM column and surrounding untreated soil interaction. Modeling of the unsaturated DSM treated expansive soil is a complex problem to analyze. This is because the available material models were not applicable for modeling the expansive behavior of treated soils. However, simulations were carried out using a three dimensional PLAXIS 3D Foundation Version 1.5

finite element program. Limitation of the program is that the current version does not possess a material model that describes the behavior of expansive soils. Therefore, stress state (suction) changes related to moisture variations in the treated sections were mechanically simulated in the present study through unloading an applied load that is equivalent to the expected suction change.

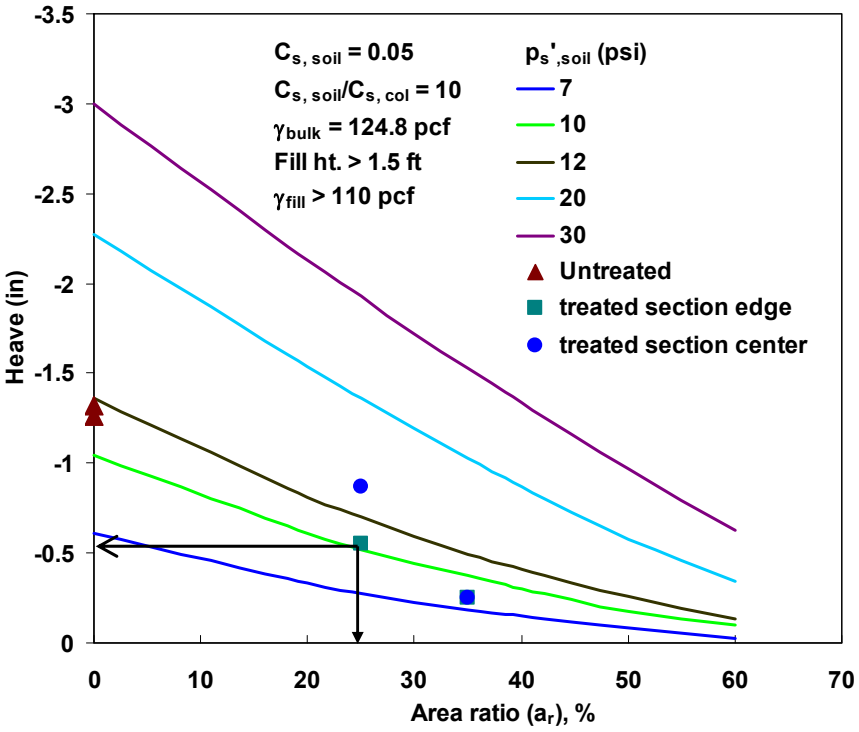

Figure 7.20 Comparison of field observations with analytical estimations.

During construction of the treated test sections, the DSM columns were arranged in a square pattern, as shown in Figs. 5.7 and 5.8. Based on results from previous studies, it was expected that each DSM column would influence an area around it and this area was assumed to be a square of size equal to the spacing of columns ($s_{c/c}$), as shown in Fig 7.20. This tributary area with a DSM column inside is considered as a unit cell and assumed to represent the behavior of the treated ground due to symmetry. For the simplification of 3D modeling in the

present study, a single DSM column with an effective square area of untreated soil around the column was considered for simulation (Fig. 7.21).

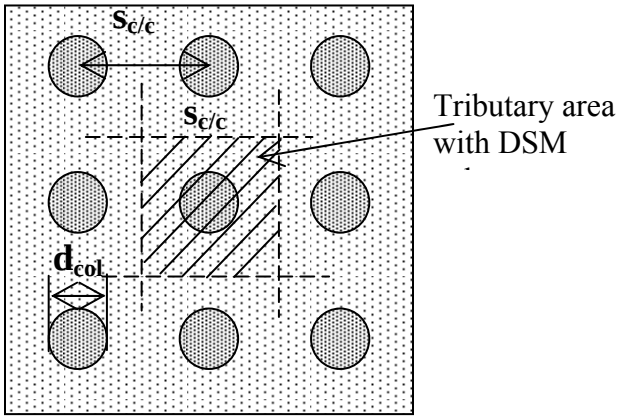

Figure 7.21 Definition sketch of unit cell.

A Soft Soil Creep (SSC) material model was considered for the untreated soil around the DSM column, whereas a Mohr-Coulomb material model was considered for the column. The properties used for both materials are tabulated in Table 7.13. During discretization of the geometry, a mesh with 15-node wedge elements was generated by default. In the present study, final state of the treated ground was modeled and the simulation was performed in two phases. In the first phase, gravitational stresses were generated and also the initial stress state of the treated ground was achieved by applying a load equivalent to expected swell pressure of the composite section. For this study, a load of 12 psi (82.7 kPa); i.e., the composite swell pressure of treated section, was applied based on results depicted in Fig. 7.20. In the second phase, unloading of the applied load was performed representing the release of swell pressure due to saturation of the treated ground. The final state is assumed to correspond to 100% saturation and stress state to account for the overburden stresses and any net changes in total stresses from either excavation or surcharge type loading. The typical results obtained from the numerical simulation for Site 1 treated section conditions are depicted in Fig. 7.22.

Table 7.13 Material details used in numerical simulation.

Details	DSM column	Untreated soil
Model type	Soft soil creep	Mohr-Coulomb
Unit weight (lb/ft^3)	124.8	106.1
C_c	0.2	NA
C_s	0.07	NA
E (lb/ft^2)	NA	208.8×10^4
Φ	5^0	25^0
ν	NA	0.2

It can be noticed from Fig. 7.22 that the untreated soil moved up relative to the column as expected. The maximum movement recorded at the surface was very small (0.007 mm) as compared to those obtained in the field and analytical calculations. This variation in magnitudes of the surface movements from the numerical simulation is attributed to several factors including the lack of physico-chemical behavior of the expansive soils in the model. However, the mechanism involved in surface movement of the treated sections is as expected. In order to encounter these movements from the untreated soil around the DSM column, a geogrid was placed at the top of the treated sections and anchored to the DSM columns, as shown in Fig. 5.12. As a result of surface movements from the untreated soil around DSM columns, the stresses in the geogrid get mobilized and in turn are transferred to the DSM columns, as shown in Fig. 7.23.

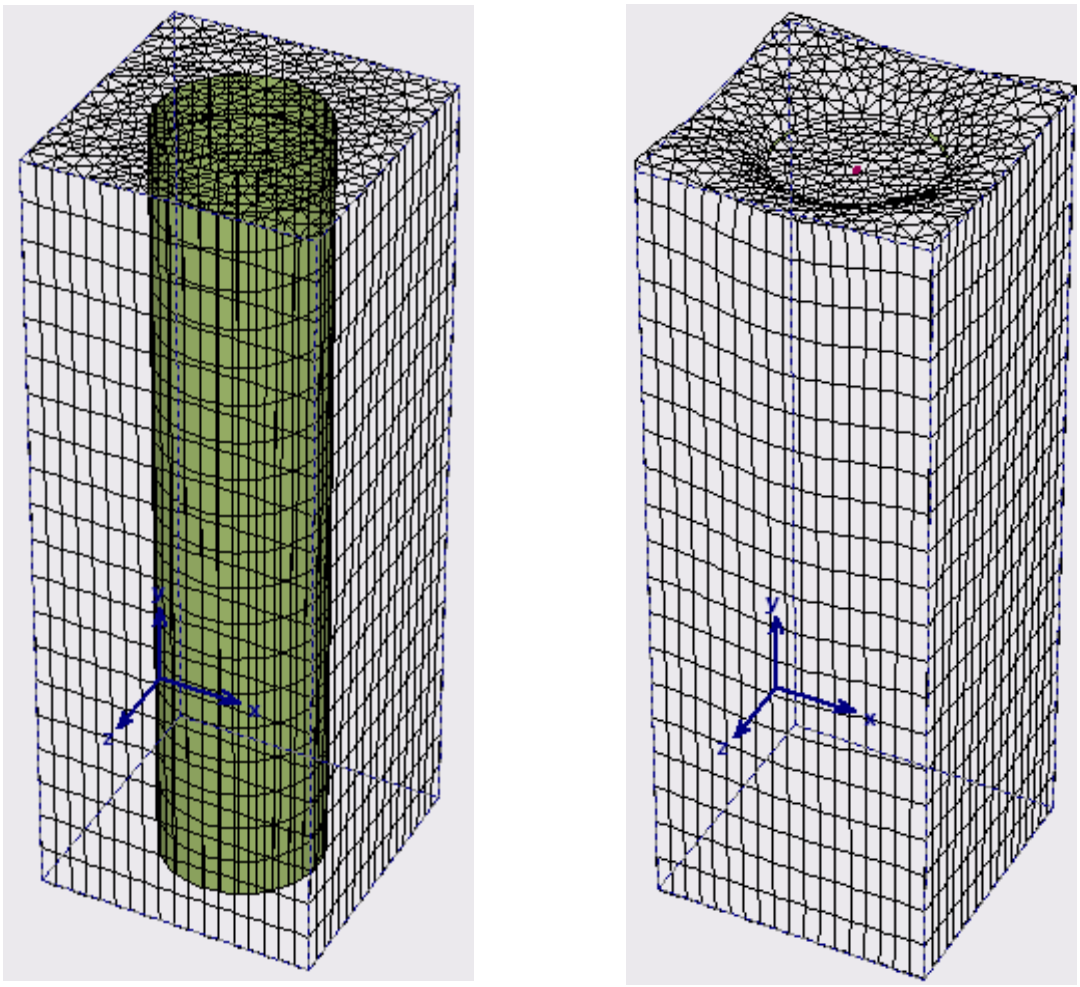

Figure 7.22 Typical numerical simulation results for a_r = 25%; (a) Original geometry and (b) Deformed geometry.

Considering the experience achieved from the numerical simulation studies, it is necessary that future research look into developing models that can simulate material models related to expansive soil problems considered in the present context. Studies related to understanding interaction between the DSM columns, surrounding untreated soil and geogrid are also necessary to make improvements in the design procedures.

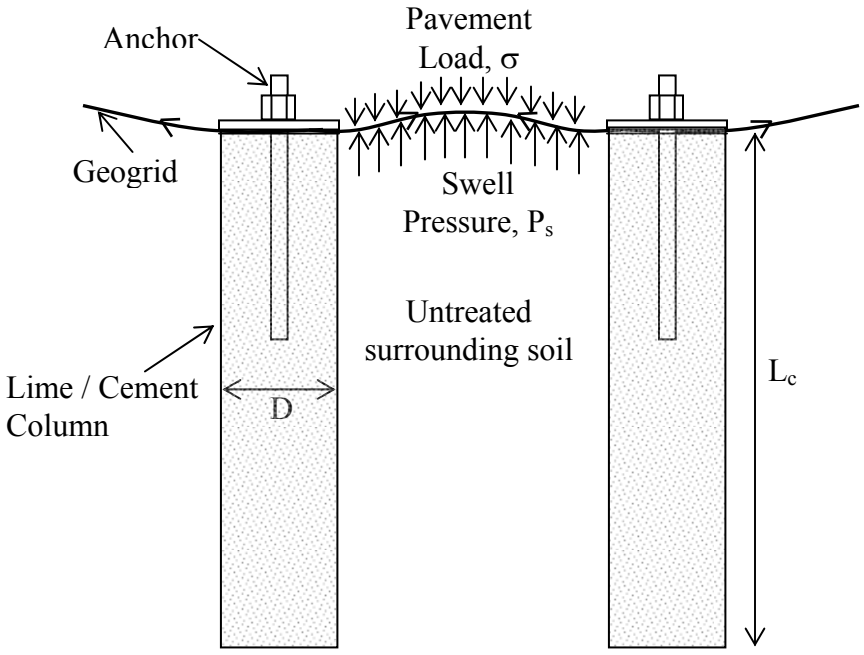

Figure 7.23 Schematic of hypothetical mechanism involved in DSM treated expansive soil sections.

7.5 Summary

This chapter presents the various details on data collected from the vertical (VI) and horizontal (HI) inclinometer surveys, pressure cells, moisture probes, settlement plates and non-destructive in situ testing of both the DSM treated and control test sections at Sites 1 and 2. The data were then analyzed to evaluate the effectiveness of the DSM treated test sections with respect to control sections in minimizing swell/shrink behavior. Overall, the vertical and horizontal inclinometer data showed low lateral movements but are considerable when compared to those obtained in the treated sections. Settlement plates installed in the untreated sections at Sites 1 and 2 reveal vertical surface movements of over 1 in. (2.54 cm) during the monitoring period, whereas in the treated sections the vertical surface movements recorded from HI are < 1 in. (2.54 cm).

Data from the pressure cells revealed that during Phase II of monitoring; i.e., at maximum moisture levels from saturation of the sites, lateral and vertical swell pressures at Sites 1 and 2 are more than those obtained during Phase I of the monitoring. But, these pressures are very low when compared to those obtained from the swell pressure tests on the untreated soils in the laboratory environment. Results from the SASW testing at Site 1 indicate slight improvement in the shear wave velocities compared to the untreated section but for Site 2 the improvement in shear wave velocities is considerable as compared to the untreated section.

In-column downhole testing showed consistent results during the monitoring period as compared to the testing in the untreated areas at Sites 1 and 2. However, downhole measurements of the composite DSM treated sections in years 2006 and 2007 showed a slight decrease as compared with those in year 2005. But, these measurements are high compared to the downhole measurements in the untreated sections for all years of monitoring. Considering the overall performance of the DSM treated sections compared to the untreated sections at Sites 1

and 2 based on the results discussed in this chapter it can be concluded that the DSM treatment is considerably successful in mitigating the shrink-swell movements related to moisture changes.

Finally, comparison of the field observations with the analytical calculations was presented and it is noticed that analytical formulations made appropriate predictions of the amount of heave of the treated sections. This was followed by the numerical simulation of a unit cell for an area ratio of a_r = 25%. Results from this study are not satisfactory but the expected behavior of the treated ground was noticed and this initiated the necessity of future research in this direction.

CHAPTER 8

SUMMARY AND CONCLUSIONS

8.1 General

Expansive soils are commonly present in many districts in Texas. Due to seasonal moisture fluctuations, shrink-swell related soil movements occur in the subgrade soils underneath pavements. These differential soil movements often cause pavement cracking and roughness problems resulting in poor performance and ride quality of the pavements. Common mass stabilization of the expansive soil with lime (shallow stabilization) is not considered for moderate to deep depths, since it is neither practical nor economical. Several other stabilization strategies were explored to stabilize expansive soils, but none of them are effective. Deep soil mixing was considered in this research for stabilization of expansive soils supporting the pavement infrastructure.

The effectiveness of the DSM treatment method was evaluated in pilot scale test sections that experienced less soil movements after DSM treatment at significant cost savings. Several binder types were used to treat the expansive soils in a laboratory investigation to select the appropriate binders for the field DSM studies.

Two test sections were designed and installed with DSM soil columns. Surcharge equivalent to loads from pavement structure base and surface layers was placed on top of the DSM test sections through a fill placement to simulate overburden pressures. These treated test sections along with control sections were instrumented and monitored. A successful completion of this research was demonstrated by considerably reducing the soil movements in both of the treated test sections. The final product of this research is the development of a DSM design methodology for stabilizing expansive soils up to considerable depths.

8.2 Summary and Conclusions

As the major objective of the research, both laboratory and field studies were planned to address the effectiveness of the deep soil mixing method for effectively mitigating expansive soil movements. The following sections describe major conclusions drawn from this research.

8.2.1 Laboratory Studies and QC/QA Studies

1. A stepwise procedure was formulated to simulate the field deep soil mixing process for expansive soils in the laboratory. Several laboratory related parameters including binder dosage, binder proportion and content, total water to binder ratio, curing time, and soil type were considered. This method resulted in the development of repeatable soil specimens with consistent bulk unit weights and low standard deviations. The standard deviation, $\overline{\sigma}$ values of the bulk unit weight data for linear shrinkage, free swell and UCS specimens were 0.36 to 0.66, 0.48 and 0.69 kN/m^3, respectively. These low $\overline{\sigma}$ values indicate consistent and homogenous specimen preparation with the proposed laboratory protocol for simulating deep soil mixing of moderately stiff to stiff expansive soils.
2. The linear shrinkage tests were performed at both molding water content and liquid limit of the soil-binder mixture. The $\overline{\sigma}$ of the unit weight at the molding water content and liquid limit is 0.66 and 0.36 kN/m^3, respectively. Overall, the low standard deviation at the liquid limit can be attributed to better workability and compaction of the soil-binder mix due to high moisture content.
3. Free swell and bar linear shrinkage potentials of the DSM treated soil specimens are less than 0.1% and 0.4%, respectively. This aspect was noted for all binder treatments and dosage levels used in this research.
4. A simplified linear ranking analysis was developed for selecting the appropriate binder proportion and dosage parameters from the laboratory data for implementing in the field

DSM studies. The analysis yielded a highest rank for the 100% cement binder treatment at dosage rates of 150 kg/m^3 and 200 kg/m^3. For the cement-lime treatment combination with 75% cement and 25% lime treatment, best enhancements were recorded at a binder dosage rate of 200 kg/m^3.

5. The procedure adapted for the soil specimen preparation from both the field DSM spoils and wet grab samples in the field conditions yielded specimens whose unit weights were close to those prepared in the laboratory conditions.
6. Quality assessment studies were conducted as a part of the present research by determining both unconfined compressive strength and small strain shear modulus, G_{max}, values of the field specimens and then comparing them with those determined from the laboratory prepared specimens. The near consistent results of stiffness and strength values with depth at Site 2 indicated a uniform mixing of soil and stabilizer in the field conditions.
7. Comparisons between the field and laboratory test results also indicated that the stiffness ratio $G_{max,field}/G_{max,lab}$ for Site 1 and Site 2 specimens varied between 0.43 to 0.67 and 0.56 to 0.65, respectively. The strength ratios ($q_{ucs,field}/q_{ucs,lab}$) for Site 1 and Site 2 varied from 0.67 to 0.70 and 0.83 to 0.86, respectively. Both stiffness and strength ratios indicate that the field stiffness and strength values are 40% and 20 to 30% lower, respectively, when compared to the laboratory treatments.

8.2.2. In Situ Non-Destructive Testing

1. The P-wave velocities of the treated soil column zones exhibited higher values than those recorded in the untreated soils. Also, the same measurements for the three consecutive yet different years showed a decrease in the P-wave velocities. The average P-wave velocities of the treated soil columns obtained from the downhole tests are about 3470 ft/s (1041 m/s), 2820 ft/s (846 m/s) and about 2630 ft/s (789 m/s) in 2005, 2006 and 2007, respectively.

Though the overall decrease is considerable, they are still higher than for the untreated soil. Possible reasons for these decreases could be traffic noises, bad coupling between the PVC tubes and the surrounding soil and the moisture levels at the time of testing. Nevertheless the velocities measured are high and are appropriate for the treated soils.

2. For Site 1, two dispersion curves from the SASW tests in the untreated areas in 2006 and 2007 are close to each other, which are different from the same curves measured in 2005. Though exact reasons for this difference are difficult to point out, the difference was attributed to different testing location in the untreated area in those years. The dispersion curves obtained from the three annual tests in the untreated area at Site 2 are very similar.
3. Shear wave velocities of the treated soils from the SASW tests showed a decrease in the shear wave velocities of the treated soils over the time period. The decrease in 2007 is expected since the measurements were made on the treated ground that was subjected to high saturation. The decrease in the shear wave velocities in year 2006 from those determined in year 2005 may be attributed to selection of the testing location. The DSM treatment of the test sections in the present study is of the isolated column type; therefore location of the testing may be over the row of columns or between the column rows as it is difficult to find the column row after fill placement on the treated surface.

8.2.3 Field Instrumentation and Monitoring Studies

1. Moisture probe readings and moisture content measurements from the soil samples collected immediately after saturation at each site clearly showed that the soils of depths up to 10 ft (3 m) or higher reached full saturation due to both simulated rain falls and higher natural precipitations recorded during that period. This implies that full heaving potentials up to active depths of 10 ft (3 m) or higher should have been realized during the saturation phase.

2. Vertical soil movements monitored from the horizontal inclinometers installed in the treated areas showed considerably less values than those monitored in the untreated soil sections utilizing elevation surveys. The reduction in the surface movement in the DSM treated sections was attributed to the improvement achieved through the DSM technique, thus, indicating effectiveness of the deep soil mixing method used in the present research.
3. Lateral soil movements recorded using the vertical inclinometers installed in both the treated and untreated sections were low. These low movements were due to lateral confinement due to overburden stresses. However, the DSM columns recorded negligible movements and around the columns the movements are considerably smaller than those recorded in the untreated section due both to swell and shrink cycles. This observation is valid in both sites. Again, the enhancements were attributed to the deep soil mixing method adapted in the field.
4. Swell pressures recorded from the pressure cells installed in the treated sections were considerably lower than those determined on the untreated soils from the laboratory tests. The maximum swell pressures recorded at both sites during Phases I and II were in the range of 1 to 4.5 psi (6.9 to 31 kPa) indicating that treated sections can be characterized as those sites with very low potential for swelling.
5. Swell pressures recorded during Phase II; i.e., saturation process associated with high precipitation were slightly more than those recorded during Phase I. Pressure cell results also revealed that the maximum lateral swell pressures in the range of 1.4 to 4.5 psi (9.6 to 31 kPa) were on DSM columns.

8.2.4 Comparison and Field and Analytical Data

1. Analytical predictions of the heave of the DSM treated composite test sections were in good agreement with the field observations of the vertical surface movements for both test sections. This indicated the proposed model accurately estimated the heave of the present

composite DSM sections. The design charts developed using this analytical model for various parameters will be useful in the design of DSM columns for other site conditions. Further validation with field measurements will enhance the confidence of practitioners in using these charts.

2. Numerical simulation studies performed using PLAXIS 3D Foundation finite element program did not produce satisfactory results due to the limitations of the software in modeling expansive soil behavior. However, expected behavior of the treated ground under final stress state corresponding to 100% saturation was noticed. This led to the necessity of 'future research' in understanding the interaction mechanism between the DSM columns, untreated soil surrounding the columns and geogrid anchored to the columns.

REFERENCES

[1] Ahnberg, H., Ljungkratnz, C., and Holmqvist, L. (1995). "Deep Stabilization of Different Types of Soft Soils." Proceedings of the 11th European Conference on Soil Mechanics and Foundation Engineering, Copenhagen, 28 May to 1 June, 167-172.

[2] Ahnberg, H., and Johansson, S. E. (2005). "Increase in Strength with Time in Soils Stabilized with Different Types of Binder in Relation to the Type and Amount of Reaction Products." *International Conference on Deep Mixing Best Practice and Recent Advances*, Deep Mixing, May 23 – 25, Stockholm, Sweden, 195-202.

[3] Ahnberg, H. (2006). "Strength of Stabilized Soils: A Laboratory Study on Clays and Organic Soils Stabilized with Different Types of Binder." *Doctoral Thesis*, Lund University, Lund, Sweden.

[4] Al-Omari, B., and Darter, M. I. (1992). "Relationship between IRI and PSI." *Report Number UIUL-ENG-92-2013*. Springfield, IL, Illinois Department of Transportation.

[5] Al-Tabba, A., Ayotamuno, M.J., and Martin, R. J. (1999). "Soil mixing of stratified contaminated sands." *Journal of Hazardous Materials*, Elsevier, 53–75.

[6] Arman, A., and G.A. Munfakh (1972). "Lime stabilization of organic soils." National Academy of Science. Highway Research. USA, 381.

[7] Asano, J., Ban, K., Azuma, K., and Takahashi, K. (1996). "Deep mixing method of soil stabilization using coal ash." *Proceedings of the 2nd International Conference on Ground Improvement Geosystems,* Grouting and Deep Mixing, 14-17 May, Tokyo, 1, 393-398.

[8] ASTM. (2000). *ASTM Book of Standards, Vol. 4.08,* ASTM, Philadelphia, Pennsylvania.

[9] Axelsson, K., Johansson, S. E., and Andersson, R. (2002). "Stabilization of Organic Soils by Cement and Pozzolanic Reactions: Feasibility Study." Report 3, Swedish Deep Stabilization Research Center, Linkoping, Sweden, 51 pages.

[10] Babasaki, R., Saito, S., and Suzuki, Y. (1984). "Temperature Characteristics of Cement Improved Soil and Temperature Analysis of Ground Improved using Deep Cement Mixing Method." Symposium on Strength and Deformation of Composite Ground. JSSMFE, 33-40

[11] Babasaki, R. M., Terashi, T., Suzuki, A., Maekaea, M., Kawamura, E., and Fukazawa. (1996). "JGS TC Report: Factors Influencing the Strength of Improved Soil." Grouting and Deep Mixing, *Proceedings of the 2nd International Conference on Ground Improvement Geosystems,* Grouting and Deep Mixing, 14-17 May, Tokyo, 2, 913-918.

[12] Baker, T. D. (1992). "Acceptance Criteria for Lime Slurry Injection." Proceedings of the 7th International Conference on Expansive Soils, Aug 3 – 5, Dallas, Texas, 343-346.

[13] Basma, A. A., Al-Rawas, A. A., Al-Saadi, S. N., and Al-Zadjali, T. F. (1998). "Stabilization of Expansive Clays in Oman." Environmental and Engineering Geoscience, IV (4), 503-510.

[14] Bergado, D.T., Anderson, L.R., Miura, N., and Balasubramaniam, A.S. (1996). "Soft Ground Improvement in Lowland and other Environments." *American Society of Civil Engineers (ASCE) Press*, New York, U.S.A.

[15] Bergado, D. T., and Lorenzo, G. A. (2005). "Economical mixing method for cement deep mixing." *Geotechnical Special Publication No. 136*., *ASCE*, CD ROM Proceedings, Austin, Texas.

[16] Bowles, J. E. (1996). "Foundation Analysis and Design." McGraw-Hill, New York.

[17] Broms, B., and Boman, P. (1979). "Lime columns – a new foundation method." *Journal of Geotechnical Engineering*, ASCE, Vol. 105, GT4, pp. 539-556, 1979.

[18] Bruce, D. (2001). "An introduction to the deep mixing methods as used in geotechnical applications. Volume III. The verification and properties of treated ground." *Report No. FHWA-RD-99-167*, US Department of Transportation, Federal Highway Administration, 2001.

[19] Bruce, D. (2002). "An introduction to deep mixing methods as used in geotechnical applications, Volume III: The verification and properties of treated ground." *FHWA-RD-99-167*. Federal Highway Administration, October 2001.

[20] Carey, W. N., and Irick, P.E. (1960). "The Pavement Serviceability Performance Concept." *Highway Research Board*, Bulletin 250, Washington, DC.

[21] Chen, F.H. (1988). "Foundations on Expansive Soils." Developments in Geotechnical Engineering, Vol.12, Elsevier Publications, Netherlands.

[22] Chen, X. L., Liu, Y.H., and Zhang, S. D. (1996). "Design methods of the cement soil retaining wall." Grouting and Deep Mixing, *Proceedings of the 2nd International Conference on Ground Improvement Geosystems*, Grouting and Deep Mixing, 14-17 May 1996, Tokyo, 1, 475-480.

[23] Coastal Development Institute of Technology. (2002). "The Deep Mixing Method – Principle, Design and Construction."

[24] Dong, J., Hiroi, K., and Nakamura, K. (1996). "Experimental study on behavior of composite ground improved by deep mixing method under lateral earth pressure." Grouting and Deep Mixing, *Proceedings of IS-Tokyo '96, The 2nd International Conference on Ground Improvement Geosystems*, 14-17 May 1996, Tokyo, Balkema, 585-590.

[25] Dunnicliff, J. (1988). "Geotechnical Instrumentation for Monitoring Field Performance." Wiley and Sons, NY.

[26] Enami, A., Yoshida, M., Hibino, S., Takahashi, M., and Akitani, K. (1985). "In Situ Measurement of Temperature in Soil Cement Columns and Influence of Curing Temperature on Unconfined Compressive Strength of Soil Cement." 20th Annual Meeting, JSSMFE, 1737-1740 (in Japanese).

[27] Esrig, M., Mac Kenna P., and Forte, E. (2003). "Ground Stabilization in the United States by the Scandinavian Lime Cement Dry Mix Process." ASCE, Geotechnical Special Publication No.120. *Proceedings of the 3rd International Conference on Grouting and Ground Treatment,* Vol. 1, pp. 501-514. Feb 10-12, 2003.

[28] EuroSoilStab. (1997). "Design and testing of mixtures of binder materials and organic soils." Project No. BRPR-CT97-0351, Report 2.1 and 2.2. "Development of design and construction methods to stabilize organic soils."

[29] EuroSoilStab. (2002). "Design guide soft soil stabilization." Project No. BE 96-3177, Ministry of Transport Public Works and Management.

[30] FEMA. (1982). Special Statistical Summary: Data, Injuries, and Property Loss by Type of Disaster 1970-1980. Federal Emergency Management Agency, Washington, DC.

[31] Fredlund, D. G., and Rahardjo, H. (1993). "An Overview of Unsaturated Soil Behavior." Unsaturated soils, *Geotechnical Special Publication No. 39*, ASCE, New York.

[32] Gay, D. A. (1994). "Development of a predictive model for pavement roughness on expansive clay." PhD dissertation, Department of Civil Engineering, Texas A&M University, College Station, Texas.

[33] Gotoh, M. (1996). "Study on soil properties affecting the strength of cement treated soils." Grouting and Deep Mixing, *Proceedings of IS-Tokyo '96, The 2nd International Conference on Ground Improvement Geosystems,* 14-17 May 1996, Tokyo, Balkema, 399-404.

[34] Gromko, G.J. "Review of Expansive Soils." Journal of the Geotechnical Engineering Division, June 1974.

[35] Halkola, H. (1999). "Keynote lecture: Quality control for dry mix methods." *Proceedings of the International Conference on Dry Mix Methods for Deep Soil Stabilization,* 13-15 October 1999, Stockholm, pp. 285-294. Balkema. 1999.

[36] Hampton, M.B., and Edil, T.B., (1998). "Strength gain of organic ground with cement-type binders." *Soil Improvement for Big Digs,* 135-148.

[37] Han, J. (2004). National Deep Mixing Workshop Presentation, Transportation Research Board Meeting, Washington, DC, January 2004.

[38] Hausmann, M. R. (1990). "Engineering Principles of Ground Modification." *McGraw Hill*, New York, 1990.

[39] Hebib, S., and Farrell, E. R. (1999). "Some Experience in Stabilizing Irish Organic Soils." *Proceedings of International Conference on Dry Mix Methods for Deep Stabilization*, 13-15 October, Stockholm, Sweden, 81-84.

[40] Hewayde E. H. (1994). "The Use of Lime Columns in Expansive Soil." MSc thesis, University of Technology, Baghdad, Iraq.

[41] Hewayde, E., El Naggar, H., and Khorshid, N. (2005). "Reinforced lime columns: A New Technique for Heave Control." *Ground Improvement*, 9 (2), 79-87.

[42] Hird, C. C., and Chan, C. M. (2005). "Correlation of Shear Wave Velocity with Unconfined Compressive Strength of Cement-Stabilized Clay." *International Conference on Deep Mixing Best Practice and Recent Advances*, Deep Mixing, May 23–25, Stockholm, Sweden.

[43] Holm, G., Bredenberg, H., and Broms, B. (1981). "Lime columns as foundations for light structures." Proceedings, 10th ICSMFE, Stockholm, Sweden, pp. 687-693.

[44] Holm, G. (1999). "Keynote lecture: Applications of Dry mix methods for deep soil stabilization." *Proceedings of the International Conference on Dry Mix Methods for Deep Soil Stabilization,* 13-15 October 1999, Stockholm, Balkema, 3-14.

[45] Hong, G. T., Aubeny, C. P., Bulut, R., and Lytton, R. L. (2006). "Comparative Design Case Studies of Pavement Performance on Expansive Soils." *Transportation Research Record*, 1967, TRB, 112-120.

[46] Horiuchi, N., Ito., M., Morita, T., Yoshihara, S., Hisano, T., Hanazono, H. and Tanaka, T. (1984). "Strength of Soil Mixtures under Lower Temperatures." 19th Annual Meeting, JSSMFE, 1609-1610.

[47] Hosoya, Y., Nasu, T., Hibi, Y., Ogino, T., Kohata, Y., and Makihara, Y. (1996). "JGS TC Report: An evaluation of the strength of soils improved by DMM." *Proceedings of the 2nd International Conference on Ground Improvement Geosystems,* Grouting and Deep Mixing, 14-17 May , Tokyo, 2, 919-924.

[48] Horpibulsuk, S., Miura, N., and Nagaraj, T.S. (2003). "Assessment of strength development in cement-admixed high water content clays with Abrams' law as a basis." *Geotechnique*, 53 (4), 439-444.

[49] Horpibulsuk, S., Miura, N., Koga, H., and Nagaraj, T.S. (2004). "Analysis of Strength Development in Deep Mixing: A Field Study." Ground Improvement, 8(2), 59-68.

[50] Horpibulsuk, Miura, N., and Nagaraj, T.S. (2005). "Clay–Water/Cement Ratio Identity for Cement Admixed Soft Clays." *Journal and Geotechnical and Geoenvironmental Engineering*, ASCE, 131 (2), 187-192.

[51] Huat, B. B. K. (2006). "Effect of Cement Admixtures on the Engineering Properties of Tropical Peat Soils." The Electronic Journal of Geotechnical Engineering, 11(B).

[52] Hudak, P.F. (1998). "Geologic Controls on Foundation Damage in North Central Texas." GeoJournal, 44, 159-164.

[53] Hudson, W. R. (1981). "Road Roughness: Its Elements and Measurements." *Transportation Research Record*, 836, TRB, Washington, DC, 1-7.

[54] Huttunen, E., and Kujala, K. (1996). "On the Stabilization of Organic Soils." *Proceedings of the 2nd International Conference on Ground Improvement Geosystems,* Grouting and Deep Mixing, 14-17 May, Tokyo, 1, 411-414.

[55] Injection for Expansive Clays Brochure: Injection Types, Purpose-Build Equipment, Benefits. 4 pgs / T16.

[56] Jacobson, Jesse. (2003). "Factors Affecting Strength Gain in Lime-Cement Columns and Development of a Laboratory Testing Procedure." *Master's Thesis*, Virginia Polytechnic Institute and State University, Blacksburg, Virginia.

[57] Janz, M., and Johansson, S. E. (2002). "The Function of Different Binding Agents in Deep Stabilization." Report 9, Swedish Deep Stabilization Research Center, Linkoping, Sweden, 46 pages.

[58] Japanese Geotechnical Society Standard. (2000). "Practice for Making and Curing Stabilized Soil Specimens Without Compaction." Vol. 5, Chapter 7. (JGS 0821-2000).

[59] Jayathilaka, R. (1999). "A Model to Predict Expansive Clay Roughness in Pavements with Vertical Moisture Barriers." *Doctoral Thesis*, Texas A&M University, College Station, Texas.

[60] Jones, D. E., and Jones, K. A. (1987). "Treating Expansive Soils." Civil Engineering Magazine, ASCE, 43 (11).

[61] Kadam, R. (2003). "Evaluation of low strain shear moduli of stabilized sulfate-bearing soils using bender elements." M.S Thesis, The University of Texas at Arlington, Arlington, Texas, 178 pages.

[62] Kamon, M., and Bergado, D. T. (1991). "Ground Improvement Techniques." *Proceedings of 9th Asian Regional Conference on Soil Mechanics and Foundation Engineering*, Bangkok, Thailand, 2, 526-534.

[63] Kamon, M. (1997). "Effects of Grouting and DMM on Big Construction Projects in Japan and the 1995 Hyogoken - Nambu Earth Quake." *Proceedings of IS-Tokyo '96, The 2nd International Conference on Ground Improvement Geosystems,* Vol. 2, 14-17 May 1996, Tokyo, Balkema/Rotterdam/Broolfield/1997, 807-823.

[64] Keller, E. A. (1996). Environmental Geology. Prentice Hall, Upper Saddle River, NJ.

[65] Kitsugi, K., and Azakami, H. (1982). "Lime Column Techniques for the Improvement of Clay Ground." Proceedings Symposium on Recent Developments in Ground Improvement Techniques, Bangkok, 105-115.

[66] Kujala, K., Makikyro, M., and Lehto, O. (1996). "Effects of Humus on the Binding Reaction in Stabilized Soils." *Proceedings of the 2nd International Conference on Ground Improvement Geosystems*, Grouting and Deep Mixing, Tokyo, 1, 415-420.

[67] Lambrechts, J., Ganse, M., and Layhee, C. (2003). "Soil Mixing to Stabilize Organic Clay for I-95 Widening, Alexandria, VA." ASCE Geotechnical Special Publication No.120. *Proceedings of the 3rd International Conference on Grouting and Ground Treatment,* Vol. 1, pp. 575-585. Feb 10-12, 2003.

[68] Little, D. N. (1995). "Handbook for Stabilization of Pavement Subgrades and Base Courses with Lime." National Lime Association, Kendall/Hunt Publishing Company, Dubuque, Iowa.

[69] Lorenzo, G. A., and Bergado, D. T. (2004). "Fundamental Parameters of Cement Admixed Clay – New Approach." JGGE, 130 (10), 1042-1050.

[70] Lorenzo, G. A., Bergado, D. T., and Soralump, S. (2006). "New and Economical Mixing Method of Cement Admixed Clay for DMM Application." *Geotechnical Testing Journal*, ASTM, 29 (11), 54-63.

[71] Lorenzo, G. A., and Bergado, D. T. (2006). "Fundamental Characteristics of Cement Admixed Clay in Deep Mixing." *Journal of Materials in Civil Engineering*, ASCE, 18 (2), 161-174.

[72] Lundy, Jr., H. L., and Greenfield, B. J. (1968). "Evaluation of Deep In Situ Soil Stabilization by High Pressure Lime Slurry Injection." Highway Research Record 235, Highway Research Board, Washington, DC, 27-35.

[73] Lytton, R.L, Bogges, R.L., and Spotts, J.W. (1976). "Characteristics of expansive clay roughness of pavements." Transportation Research Record, No. 568, Transportation Research Board, National Research Council, Washington, D.C., 9-23.

[74] Mattson, H., Larsson, R., Holm, G., Dannewitz, N., and Eriksson, H. (2005). "Downhole Technique Improves Quality Control on Dry Mix Columns." *International Conference on Deep Mixing Best Practice and Recent Advances*, Deep Mixing, May 23–25, Stockholm, Sweden, 581-592.

[75] McKeen, R. G. (1985). "Validation of procedures for pavement design on expansive soils." *Report DOT/FAA/PM-85/15,* U.S. Department of Transportation, Federal Aviation Administration, Washington, D.C.

[76] Mitchell, J. K., and Soga, K. (2005). "Fundamentals of Soil Behavior." 3rd Edition, John Wiley and Sons Inc., Hoboken, New Jersey.

[77] Miura, N., Horpibulsuk, S., and Nagaraj, T.S. (2001). "Engineering Behavior of Cement Stabilized Clay at High Water Content." *Soils and Foundations*, 41(5), 33-46.

[78] Montgomery, C. W. (1997). Environmental Geology. McGraw-Hill, Boston, MA.

[79] Moseley, M. P. (1993). Ground Improvement. Blackie Academic & Professional, Boca Raton, Florida.

[80] Nalbantoglu, Z., and Tuncer, E. R. (2001). "Compressibility and Hydraulic Conductivity of a Chemically Treated Expansive Clay." *Canadian Geotechnical Journal*, 38, 154-160.

[81] Nelson, J. D., and Miller, J.D. (1992). "Expansive soils: Problems and Practice in Foundation and Pavement Engineering." John Wiley and Sons, Inc., New York.

[82] Nyangaga, F. N. (1996). "Developing a Model to Predict Pavement Roughness Development on Expansive Soils." *Doctoral Thesis*, Texas A&M University, College Station, Texas.

[83] O'Neill, M. W., and Poormoayed, A. M. (1980). "Methodology for Foundations on Expansive Clays." *Journal of the Geotechnical Engineering Division*, ASCE, 106, 1345–1367.

[84] Okumara, T. (1996). "Deep Mixing Method of Japan." *Proceedings of IS-Tokyo '96, The 2nd International Conference on Ground Improvement Geosystems, Proceedings of IS-Tokyo '96, The 2nd International Conference on Ground Improvement Geosystems,* Vol. 2, 14-17 May 1996, Tokyo, Balkema/Rotterdam/Broolfield/1997, 879-888.

[85] Olive, W.W., Chleborad, A.F., Frahme, C.W., Schlocker, J., Schneider, R.R., and Schuster, R.L. 1989. "Swelling clays map of the conterminous United States." U.S. Geological Survey Miscellaneous Investigations Series Map IÐ1940.

[86] Paterson, W. D. O. (1986). "International Roughness Index: Relationship to Other Measures of Roughness and Riding Quality." Transportation Research Record, 1084, TRB, Washington, DC, 49-59.

[87] Petry, T. M., and Little, D. N. (2002). "Review of Stabilization of Clays and Expansive Soils in Pavements and Lightly Loaded Structures—History, Practice, and Future." *Journal of Materials in Civil Engineering*, ASCE, 14 (6), 447-460.

[88] Picornell, M., and Lytton, R. L (1989). "Field measurement of shrinkage crack depth in expansive soils." *Transportation Research Record 1219*. Transportation Research Board, National Research Council, Washington, D.C., 121-130.

[89] Pipkin, B. W., and Trent, D. D. (1994). Geology and the Environmental. West, Minneapolis, MN.

[90] Porbaha, A. (1998). "State-of-the-art in Deep Mixing Technology, Part I: Basic Concepts and Overview of Technology." *Ground Improvement*, 2, No. 2, pp.81-92. 1998.

[91] Porbaha, A. (2000). "State of the art in deep mixing technology: design considerations." *Ground Improvement*, 4 (3) 111-125.

[92] Pousette, K., Macsik, J., Jacobsson, A., Andersson, R., and Lahtinen, P. (1999). "Peat soil samples stabilized in the laboratory – Experiences from manufacturing and testing." Dry mix methods for Deep Soil Stabilization, Brendenberg, Holm, and Broms, eds. Balkema, Rotterdam. 85-92.

[93] Punthutaecha, K. (2002). "Volume change behavior of expansive soils modified with recycled materials." *Ph.D. thesis*, The University of Texas at Arlington, Arlington, Texas.

[94] Puppala, A. J. (2003). "Evaluation of in-situ method for quality assessment of deep mixing." Final Report, Project NDM 101a, National Deep Mixing Program.

[95] Puppala, A. J., Kadam, R., and Madhyannapu, Raja. S. (2006). "Small strain shear moduli of chemically treated sulfate bearing cohesive soils." *Journal of Geotechnical and Geoenvironmental Engineering*, ASCE, 132 (3), 322-336.

[96] Rajasekharan, G., and Rao, N. (1997). "Lime Stabilization Technique for the Improvement of Marine Clay." Soils and Foundations, Japanese Geotechnical Society, 37 (2), 97-104.

[97] Rao, R. R., Rahardjo, H., and Fredlund, D. G. (1988). "Closed-Form Heave Solutions for Expansive Soils." *Journal of Geotechnical Engineering*, ASCE, 114 (5), 573-588.

[98] Rao, S. M., and Venkataswamy, B. (2002). "Lime Pile Treatment of Black Cotton Soils." *Ground Improvement*, Thomas Telford Ltd., 6 (2), 85-93.

[99] Rathmayer, H. (1996). "Deep Mixing Methods for Soft Soil Improvement in the Nordic Countries." *Proceedings of the 2nd International Conference on Ground Improvement Geosystems,* Grouting and Deep Mixing, 14-17 May, Tokyo, 2, 869-877.

[100] Rauhut, B., and Lytton, R. L. (1984). "Serviceability Loss due to Roughness caused by Volume Change in Expansive Subgrades." *Transportation Research Record*, 993, TRB, 12-18.

[101] Rollings, M. P., and Rollings, R. S. (1996). "Geotechnical Materials in Construction." McGraw-Hill, New York.

[102] Saitoh, S., Nishioka, S., M., Suzuki, Y., and Okumara, R. (1996). "Required strength of cement improved ground." *Proceedings of the 2nd International Conference on Ground Improvement Geosystems,* Grouting and Deep Mixing, 14-17 May, Tokyo, 1, 557-562.

[103] Sayers, M. W., Gillespie, T. D., and Querioz, C. A. V. (1986). "The international road roughness experiment: establishing correlation and a calibration standard for measurements." *Technical Paper 45,* World Bank, Washington, D.C.

[104] Soralump, S. (1996). "Evaluation of design mix procedures for the soil-cement with and without additives for application to the reconstruction of the Bangna-Trad Highway improved with deep mixing method." *M.E. Thesis*, Asian Institute of Technology, Bangkok, Thailand.

[105] Shen, S. L. (1998). "Behavior of Deep Mixing Columns in Composite Clay Ground." *PhD Dissertation*, Saga University, Japan.

[106] Shen, S. L., Miura, N., and Koga, H. (2003a). "Interaction mechanism between deep mixing column and surrounding clay during installation." *Canadian Geotechnical Journal,* 40, 293-307.

[107] Shen, S. L., Huang, X. C., and Du, S. J. (2003c). "Laboratory studies in property changes in surrounding clays due to installation of deep mixing columns." *Marine Georesources and Geotechnology,* 21, Taylor and Francis Inc., 15-35.

[108] Shen, S.L., Han, J., and Miura, N. (2004). Laboratory evaluation of mixing energy consumption and its influence on soil-cement strength. *Journal of Transportation Research Board No.1868*. Transportation Research Board, National Research Council, Washington, D. C., 23-30.

[109] Shen, S. L., Han, J., and Hong, Z. S. (2005). "Installation Effects on Properties of Surrounding Clays by Different Deep Mixing Methods." *Geotechnical Special Publication No. 136*, ASCE, CD ROM Proceedings, Austin, Texas.

[110] Sherwood, P. T. (1993). "Soil Stabilization with lime and cement." Transport Research Laboratory State of the Art Review, HMSO, London.

[111] Sherwood, P. T. (1995). "Soil Stabilization with Cement and Lime." *HMSO Publications Center*, London, U.K., pp.14-55, 1995.

[112] Slope Indicator (1997). QC installation casing installation guide. Slope Indicator, Washington.

[113] Slope Indicator. (2000). Digitilt Inclinometer Probe. Slope Indicator Company, Mukilteo, Washington.

[114] Slope Indicator. (2004). Horizontal Digitilt Inclinometer Probe. Slope Indicator Company, Mukilteo, Washington.

[115] Steinberg, M. L. (1980). "Deep Vertical Fabric Moisture Seals." *Proceedings of the 4th International Conference on Expansive Soils,* Denver, Colorado, 1, 383-400.

[116] Steinberg, M. L. (1985). "Controlling Expansive Soil Destructiveness by Deep Vertical Geomembranes on Four Highways." Transportation Research Record, 1032, TRB, Washington, D.C., 48-53.

[117] Taki, O., and Yang, D. S. (1990). "Soil-cement mixed wall technique." ASCE, Geotechnical Engineering Congress, Denver, CO, pp. 298-309.

[118] Taki, O. (2003). "Strength Properties of Soil Cement Produced by Deep Mixing." *Geotechnical Special Publication*, ASCE, 120, 646-657.

[119] Thomann, J. G., and Hryciw, R. D. (1990). "Laboratory Measurement of Small Strain Shear Modulus under k_o Conditions." *Geotechnical Testing Journal*, 13 (2), 97-105.

[120] Tonoz, M. C., Gokceoglu, C., and Ulusay, R. (2003). "A Laboratory Scale Experimental Investigation on the Performance of Lime Columns in Expansive Ankara (Turkey) Clay." *Bulletin of Engineering Geology and the Environment*, Springer-Verlag, 62 (2), 91-106.

[121] Usui, H. "Quality Control of Cement Deep Mixing Method (Wet Mixing Method) in Japan." *International Conference on Deep Mixing Best Practice and Recent Advances*, Deep Mixing, May 23 – 25, Stockholm, Sweden, 635-638.

[122] Velasco, M.O., and Lytton, R.L. (1981). "Pavement roughness on expansive clays." *Research Report 284-2*, Texas Transportation Institute, The Texas A&M University System, College Station, Texas.

[123] Viggiani, G., and Atkinson, J. H. (1995). "Interpretation of Bender Element Tests." *Geotechnique*, 45 (1), 149-154.

[124] Wilkinson, A., Haque, A., Kodikara, J., Christie, D., and Adamson, J. (2004a). "Stabilization of Reactive Subgrades by Cementitious Slurry Injection – a review." *Australian Geomechanics Journal*, Vol. 39(4), pp. 81-93.

[125] Williams, H. F. L. (2003). "Urbanization Pressure Increases Potential for Soils-Related Hazards, Denton County, Texas." Environmental Geology, 44 (8), 933-938.

[126] Napat Intharasombat, "Studies on Compost Top Soil Amendments to Control Shrinkage Cracks in Expansive Shoulder Subgrades." *Ph.D Thesis*, The University of Texas at Arlington, Arlington, Texas.

[127] Wattanasanticharoen, E "Experimental Studies to Evaluate Volume Change Movements in Chemically Treated Sulfate Rich Soils." PhD Thesis, The University of Texas at Arlington, Arlington, Texas, August, 2004, 295 pages.

[128] Porbaha, A. and Roblee, C. (2001). "Challenges for Implementation of Deep Mixing in the USA." *Proceedings of International Workshop on Deep Mixing Technology*, Oakland, CA., National Deep Mixing Program, 2 volumes. 2001.

[129] Porbaha, A. (2002). "State of the Art in Quality Assessment of Deep Mixing Technology." *Ground Improvement, 6,* No. 3, pp. 95-120. 2002.

[130] Lambe W. T. and William, R. V. (2000). Soil Mechanics. John Wiley & Sons, New York.

[131] Tex-103-E. (1999). "Determining Moisture Content in Soil Materials" Soils and Aggregates Test Procedures, Texas Department of Transportation

[132] Tex-104-E. (1999). "Determining Liquid Limits of Soils" Soils and Aggregates Test Procedures, Texas Department of Transportation

[133] Tex-105-E. (1999). "Determining Plastic Limits of Soils" Soils and Aggregates Test Procedures, Texas Department of Transportation

[134] Tex-111-E. (1999). "Determining the Amount of Material in Soils Finer than the 75 m (No. 200) Sieve" Soils and Aggregates Test Procedures, Texas Department of Transportation

[135] Tex-113-E. (2004). "Laboratory Compaction Characteristics and Moisture-Density Relationship of Base Materials" Soils and Aggregates Test Procedures, Texas Department of Transportation

[136] Tex-145-E. (2005). "Determining Sulfate Content in Soils - Coloimetric Method" Soils and Aggregates Test Procedures, Texas Department of Transportation

[137] Tatsuoka, F. and Kohata, K. (1996). "Deformation and strength characteristics of cement treated soil." *Proceedings of IS-Tokyo '96, The 2nd International Conference on Ground Improvement Geosystems,* 14-17 May, Balkema, Tokyo, 453-459.

[138] Filz G. M., Hodges D.K., Weatherby D, E. and Marr, W. A. (2005). "Standardized definitions and laboratory procedures for soil-cement specimens applicable to the wet method of deep mixing," *Geotechnical Special Publication No. 136, ASCE*, CD ROM Proceedings, Austin, Texas

[139] Sridharan, A., Rao, A.S., and Sivapullaiah, P.V. (1986). "Swelling pressure of clays." Geotechnical Testing Journal. GTJODJ. Vol 9, No. 1. pp. 23-24

[140] Eades, J. L. and Grim, R. E. (1966). "A Quick test to determine lime requirements for lime stabilization." Highway Research Bulletin 139, pp 61-72.

[141] Das, B. M. (2002). Principles of Geotechnical Engineering. Brooks/Cole Pub. Co., Pacific Grove, California.

[142] Hayashi, H. and Nishimoto, S. (2005). "Strength characteristic of stabilized peat using different types of binders," *Proceedings of Deep Mixing 05,International Conference on Deep Mixing Best Practice and Advances,23-25 May 2005, Stockholm, Sweden*, 55-62.

[143] Tex-107-E. (1999). "Determining the bar linear shrinkage of soils." Soils and Aggregates Test Procedures, Texas Department of Transportation.

[144] Tex-110-E. (1999). "Particle size analysis of soils." Soils and Aggregates Test Procedures, Texas Department of Transportation.

[145] Tex-124-E. (1999). "Determination of potential vertical rise," Soils and Aggregates Test Procedures, Texas Department of Transportation.

[146] Puppala, A.J. and Porbaha, A (2004). "International Perspectives on Quality Assessment of Deep Mixing." Geo-Support 2004, *ASCE Geotechnical Special Publication*, Orlando, 2004, pp. 826-837.